Glioblastoma resistance to temozolomide : implication of $\alpha5\beta1$ integrin and p53 signalling pathways

Saidu Sani

UNIVERSITÉ DE STRASBOURG

ÉCOLE DOCTORALE DES SCIENCES DE LA VIE ET DE LA SANTE

Laboratoire de Bio-imagerie et Pathologies

UMR7021 CNRS

Faculté de Pharmacie

THESIS

To obtain the title of **Docteur de l'Université de Strasbourg**

Speciality: **Molecular and Cellular Biology Aspects**

By

Saidu SANI

Defended on **16 December 2020**

Glioblastoma resistance to Temozolomide: Implication of α5β1 integrin and p53 signalling pathways

Jury members

Docteur PINEL Sophie	Rapporteur externe
Professeur MORJANI Hamid	Rapporteur externe
Docteur GUENOT Dominique	Examinateur interne
Docteur DONTENWILL Monique	Directeur de thèse

Dedication

This thesis is dedicated to my late father. Mall. Sani Ahmadu, for his support in my quest for knowledge.

Acknowledgements

All gratitude is due to Allah; the Great, the Merciful, who bestows favours on His servants as He pleases. May the unending Love, Mercy and Blessings of Allah be on our noble Prophet Mohammad (S.A.W).

My gratitude further extends to my indefatigable supervisor Dr. Monique DONTENWILL who accepted me into her "Integrin team" in France and stood resolute to seeing the completion of this work through logical observations raised and constructive corrections. I am grateful for the scientific discussions that helped me understand the project and the extra hours she sacrificed for me and the support she gave me during the COVID-19 lockdown. Her encouragement and human qualities allowed me to make progress. For these strides, I will forever remain grateful for her stupendous contribution in my academic pursuit and I earnestly pray that the Almighty Allah grant her the best in this world and in the hereafter.

I would also like to express my gratitude to Dr. PINEL, Dr. GUENOT and Professor MORJANI for accepting to examine my thesis.

I would like to express my gratitude to late Madame Isabelle LELONG-REBEL who shared with me her scientific knowledge with great kindness and simplicity, and who encouraged me a lot when I felt bad.

I am grateful to Fanny who taught me a lot about the experimental techniques needed for my project. Her reliability and extreme rigor made her the ideal person to learn from or work with.

I am grateful to our collaborator, Luciana Marinelli who provided us with Compound 9.

I owe a lot to my team members who always encouraged me and share their enriching ideas and experiences with me.

-Laurence, for her availability, kindness, and advice.

-I am deeply grateful to Lionel, Mélissa and Nikita. I thank you very much for your endless help in the course of this work.

Natacha, for her kindness, and advice.

-Sophie Foppolo, who guide me through flow cytometry, Immunofluorescence and work had to make sure the cells are free of mycoplasma.

-Sophie Martin, who taught me a RT-qPCR, and was always available for any questions.

-Maxime, for his unique way of approaching scientific issues, for his freedom of thought, and for the several cups of coffee to revitalize our scientific thoughts.

-Many thanks to Marie-Cecile for her great help with understanding the basics of cell culture.

-Thank you Elisabete for our endless discussions on science, and for your encouragement and invaluable help on so many things.

Thanks to Ali, Aude, Basma, Cloé, Magalie, Marina, Ombline and Quentin for your kindness and friendship; I wish you good luck with your thesis in progress!

Thank you very much Tania, Micheal and Romain. It was a pleasure working with you.

Thank you Jérôme, Véronique and Rachel for your daily smiles and good mood.

Thank you, Ingrid, and Marlyse for your kindness and impeccable administrative work.

My sincere thanks goes to the funding body that financially supported my work. It is TETFund Nigeria and Alex Akwueme Federal University Ndufu-Alike Ikwo, Ebonyi State, Nigeria in partnership with Campus France.

Lastly, I wish to express gratitude to my family members who were supportive, morally, and financially during this program. To my mom and stepmom; Haj. Hadiza Sani and Mallama Fatima Sani, and my brothers and sisters; Mall. Sani Ibrahim, Mall. Sani Ismaila, Maj. Sani Labaran, Sani Saminu (PhD), Hauwa, Amina, Safiya, Musa, Asmau, Maimuna, Rabi, Bilyaminu, Atenae and Ahmad among others, I want to thank you all for taking care of my academic journey. Worthy of mention also is my little one (Hafsah) for her understanding of my busy schedule during this program. May Allah reward you all for the sacrifices made.

Saidu SANI

Glioblastoma resistance to Temozolomide: Implication of α5β1 integrin and p53 signalling pathways

Abstract

Résumé

Les glioblastomes sont les tumeurs cérébrales adultes les plus agressives pour lesquelles de nouvelles solutions thérapeutiques sont essentielles. Elles sont très résistantes aux thérapies et des récurrences sont observées dans la majorité des cas. Nous nous intéressons aux intégrines, en particulier l'intégrine α5β1, comme cibles thérapeutiques dans le glioblastome. Les travaux antérieurs ont montré que cette intégrine participait à la résistance à la chimiothérapie utilisée en clinique, le Témozolomide (TMZ) en inhibant l'activité du suppresseur de tumeurs p53. Dans cette thèse nous avons évalué une nouvelle option thérapeutique basée sur un traitement combiné d'antagonistes de l'intégrine α5β1 avec des activateurs de p53 dans des cellules de gliome U87MG et leurs congénères rendues résistantes au TMZ. Nous avons montré que la résistance au TMZ s'accompagne d'un grand réarrangement du répertoire des intégrines exprimées par les cellules et que l'intégrine α5β1 reste une cible dans les tumeurs résistantes. Ces cellules restent également sensibles à des inhibiteurs des complexes p53/mdm2 permettant de réactiver la signalisation p53-dépendante. Nos résultats sont en accord avec l'hypothèse d'un intérêt d'une combinaison inhibiteurs d'intégrine et activateurs de p53 pour traiter les glioblastomes récurrents.

Keywords : Glioblastoma, integrin, TMZ.

Résumé en anglais

Glioblastoma are the most aggressive adult brain tumours for which new therapeutic strategies are highly needed. They almost always recur due to resistance to radio-and chemotherapies. We are interested in integrins, in particular α5β1 integrin, as therapeutic targets in glioblastoma. Previous works showed that it participates to the Temozolomide (TMZ) chemotherapy resistance by partly inhibiting the tumour suppressor p53 pathway. Here we investigated a new therapeutic option based on the combination of p53 activators and α5β1 integrin inhibitors in naïve U87MG glioma cells and their TMZ-resistant counterparts. We showed that resistance to TMZ is accompanied by a huge rearrangement of integrin expressions and that α5β1 integrin remains a pertinent target for TMZ-resistant glioblastoma. In addition, TMZ-resistant cells proved sensitive to different blockers of p53/mdm2 complexes able to reactivate the p53 signalling pathways. Our data support the hypothesis that adding p53 activators together with integrin antagonists may represent a pertinent therapeutic strategy for recurrent glioma tumours.

Keywords: Glioblastoma, integrin, TMZ.

Table of Contents

List of Figures

List of tables

List of abbreviations

ABC	ATP-binding cassette
ADMIDAS	Adjacent to Metal ion-dependent adherent site
ADP	Adenosine diphosphate ribose
AIC	5-aminoimidazole-4-carboxamide
AKT	Serine-threonine protein kinase
AML	Acute myeloid leukemia
AMPK	Adenosine monophosphate activated protein kinase
ANGPTL4	Angiopoietin-like 4 protein
APAF1	Adapter protein apoptotic protease activating factor 1
APC/C	Anaphase-promoting complex/cyclosome
APNG	Alkylpurine-DNA-N-glycosylase
ARF	ADP-ribosylation factor
ATP	Adenosine triphosphate
ATRX	Alpha thalassemia / mental retardation syndrom X-linked
AVO	Acidic vesicular organelle
BAX	BCL-2 Associated X protein
BBB	Blood brain barrier
BCL-2	B-Cell Lymphoma 2
bFGF	Basic fibroblast growth factor
BH	Bcl-2 homology
c(RGDfV)	Cyclo(Arg-Gly-Asp-d-Phe-Val)
CAM	Chick chorioallontoic membrane
CAM-DR	Cell-adhesion mediated drug resistance
CAM-RR	Cell adhesion- mediated radio resistance
CARD	Caspase recruitment domain
CBP	CREB-binding protein
CDC20	Cell division cycle 20 homolog
Cdk	Cyclin-dependent kinase
CNS	Central nervous system
CpG	Cytosine - phosphate - guanine
CRISPR	Clustered Regularly Interspaced Short Palindromic Repeats

DAPI	4’, 6-diamidino-2-phenylindole
DAOY	Medulloblastoma
DBD	DNA-binding domain
DCE	Dynamic contrast enhanced
DDR	DNA damage response
DED	Death Effector Domain
DNA	Deoxyribonucleic acid
DSBs	Double stranded DNA breaks
DSC	Dynamic susceptibility contrast
EBRT	External beam radiation therapy
ECM	Extracellular matrix
EGF	Epidermal growth factor
EGFR	Epidermal growth factor receptor
ELISA	Enzyme linked immunosorbent assay
EMT	Epithelial to mesenchymal transition
ERK	Extracellular signal-regulated kinase
ESMO	European Society for Medical Oncology
FADD	Fas-associated death domain
FAK	Focal adhesion kinase
FDG	Fluoro-2-deoxy-D-glucose
FGF	Fibroblast growth factor
FMISO	Fluoromisonidazole
GBM	Glioblastoma multiform
GOF	Gain of function mutation
GSCs	Glioblastoma stem cells
GSH	Glutathione level
HDAC6/Hsp90	Histone Deacetylase 6/ Heat Shock 90kD Protein 1
HDM2	Human double minute 2 homolog
HDMX	Human double minute X homolog
HIF-1 α	Hypoxia-inducible factor 1-alpha
HTIC	Intracranial hypertension syndrome
HUVEC	Human umbilical vein endothelial cells
IBS	Integrin binding site
IBS1	Integrin binding site located in the talin head domain

IBS2	Integrin binding site located in the rod domain
IC50	Half maximal inhibitory concentration
IDH1	Isocitrate dehydrogenase 1
IGFBP	Insulin-like growth factor binding protein
ILK	Integrin-Linked Kinase
ILKAP	Integrin-linked kinase-associated serine/threonine phosphatase 2C
IMD	Integrin-mediated death
iMRI	Intraoperative magnetic resonance imaging
JMY	Junctional and regulatory protein
JNK	Jun amino-terminal kinase
(KLF) 8	Krüppel-like factor 8
KDM5A gene	Lysine (K)-specific demethylase 5A
Ktrans	Transfer coefficient
L1CAM	L1 cell adhesion molecule
LC3	Atg8 Orthologue light chain 3
LVD	Leucine-valine-aspartic acid
MAPK	Mitogen-activated protein kinase
MDM2	Mouse double minute 2 homolog
MGMT	O-6-methylguanine-DNA methyltransferase
MIDAS	Metal ion-dependent adherent site
miRNA	microRNA
MMP-2	Matrix metalloproteinases
MMR	DNA mismatch repair
MRI	Magnetic Resonance Imaging
mRNA	Messenger RNA
MTIC	3-methyl-(triazen-1-yl) imidazole-4-carboxamide
mTOR	Mammalian target of rapamycin,
NADP+ /NADPH	Nicotinamide adenine dinucleotide phosphate
NB	Normal brain
NCCN	National Comprehensive Cancer Network
NES	Nuclear export signal sequence
NF- KB	Nuclear Factor kappa B
NLS	Nuclear localization signal sequence
NOX	Phorbol-12-myrisate-13-acetate-induced protein 1

NSCLC	Non-small-cell lung cancer
NF-KB	Nuclear factor KB
O6-BG	O^6-benzyl guanine
P13K	Phosphoinositide-3-kinase
p53AIP1	p53-regulated Apoptosis-Inducing Protein 1
PAI-1	Plasminogen activator inhibitor-1
PAK4	Serine/threonine-protein kinase
PAR	Poly (ADP-ribose)
PARP-1	Poly (ADP-ribose) polymerase-1
RNA	Ribonucleic acid
PDAC	Pancreatic ductal adenocarcinoma
PDGFR	Platelet-derived growth factor receptor beta
PDH	Pyruvate dehydrogenase
PEA-15	Phosphoprotein enriched in astrocytes 15
PET	Positron emission tomography
PFS	Progression-free survival
PI3K	Phosphoinositid-3-kinase
PINCH1	Proteins such as the particularly interesting new cysteine-histidine-rich protein
pRb	Hypo-phosphorylated retinoblastoma gene
PS	Performing status
PSI	Plexin-semaphorin-integrin
PTEN	Phosphatase and tensin homolog
PUMA	p53-upregulated modulator of apoptosis
Raf	Serine/threonine-specific protein kinase
RAS	Rat Sarcoma
RB	Retinoblastoma protein
RE	Response elements
RGD	Arginine-glycine-aspartate
RITA	Reactivation of p53 and induction of tumour apoptosis
ROS	Reactive oxygen species
RS	Replicative senescence
RT	Radiotherapy
SA- β -gal	Senescent associated β-galactosidase

SASP	Senescence-associated secretory phenotype
Ser	Serine
SFKS	Src family kinases
SH2	Src-family kinase
Shc	Sch-transforming protein
SIPS	Stress-induced premature senescence
SOX2	Sex-determining region X2
Src	Proto-oncogenic tyrosine kinase 1
STAT3	Signal transducer and activator of transcription 3
TBS	Tris buffered saline
TCGA	The Cancer Genome Atlas
TD	Tetramerization domain
TGF-β	Transforming growth factor beta
TMZ	Temozolomide
TNF	Tumour necrosis factor
TNFR1	Death receptors such as type 1 TNF receptor
TP53	Tumour protein 53
TP53AIP1	p53-regulated apoptosis-inducing protein 1
TRADD	TNF receptor-associated death domain
TRAIL	TNF-related apoptosis-inducing ligand
ULK1	Kinase unc51- like kinase 1
VEGF	Vascular endothelial growth factor
WHO	World health organization
Wt	Wild type
ZEB1	Zinc finger E-box binding homeobox 1
α-KG	α-ketoglutarate
Hrs	Hours

Introduction

1. Gliomas

1.1. Definition

Gliomas are the most common malignant primary brain tumours of the central nervous system that arise from the excessive proliferation of glial cells (astrocytes, ependymocytes, oligodendrocytes and microglia cells). They account for about 1.35% of all cancer in adults, 2.2% of all cancer-related deaths, about 26.5% of all primary brain tumours and 80.7% of all brain malignancies (Louis et al., 2007; Ostrom et al., 2017). They have a general incidence of 2 to 3 cases per 100,000 inhabitants per year in the United States (Amirian et al., 2016).

Glioblastoma multiforme (GBM) is the most common and most aggressive brain and CNS malignancy that accounts for 54% of all gliomas, 45.2% of malignant primary brain and CNS tumours, and 16% of all primary brain and CNS tumours (Louis et al., 2007). The incidence is estimated at 2 to 3 new cases per 100,000 persons per year worldwide (Dolecek et al., 2012) and 4 cases per 100,000 population in France, or 2,000 new cases per year in France (Zouaoui et al., 2012). This increases by 1% per year, is due to the aging of the population and the improvement in access to healthcare and imagery. Glioblastoma is more common in adult male than female and its manifestation is generally at the median age of 64 but it can occur at any given age including during childhood (Wilson et al., 2014). Even though glioblastoma occur almost exclusively in the brain, it can also occur in the spinal cord, the cerebellum and the brainstem (Basu and Ghosh, 2019; Wilson et al., 2014). Glioblastomas are highly proliferative, invasive and resistant to therapy and are characterized with poor prognosis (Zhang et al., 2019). Currently there is no effective long-term treatment for this killer disease, but the standard of care which involves maximal surgical resection, followed by radiotherapy with concomitant and adjuvant temozolomide (TMZ) chemotherapy extend the median survival to 14.6 months (Stupp et al., 2005).

1.2. Epidemiologic risk factors

Several risk factors have been evaluated as potential contributors to glioblastoma. There are few rare family cases resulting from genetic alterations (Rajaraman et al., 2012). In addition, the risk of developing glioblastoma increases upon exposure to ionizing radiation and decreases for people having history of allergies or atopic disease (Ostrom et al., 2014). Other risk factors, such as exposure to chemical carcinogens or electromagnetic fields have been mentioned, but their implications in the development of brain tumours have not been confirmed (Ostrom et al.,

2014). The link between excessive cell phone use and the risk of developing brain tumour remains unclear (Hardell et al., 2007, 2008).

1.3. Diagnosis

The symptoms suggestive of gliomas are variable according to the cerebral localization and the volume of the tumour. They can appear in a silent and progressive manner, with nausea and vomiting, neurological deficit, cognitive disorders, and headaches resulting from an intracranial hypertension syndrome (HTIC), or suddenly with epileptic crises or relapses of HTIC. These clinical signs lead to further investigations (Batash et al., 2017), such as an MRI scan (gold standard) before the collection of biopsy or surgical attempt to remove the lesion (Batash et al., 2017).

1.4. Classification and origin of GBM

In 2016, the World health organization (WHO) classified glioblastoma into two main divisions, with one division having 90% Isocitrate Dehydrogenase (IDH)-wild type and the other 10% IDH mutants 1 and 2 (Louis et al., 2016). Compared to Isocitrate Dehydrogenase (IDH)-wild type, the presence of mutated IDH 1 and 2 improved prognosis of patients with glioblastoma (Carlsson et al., 2014; Van Meir et al., 2010; Weathers and Gilbert, 2015).

Primary glioblastoma belongs to the division of glioblastoma with Isocitrate Dehydrogenase (IDH)-wild type and occurs mainly in the elderly and the mean age at diagnosis is about 62 (Ohgaki and Kleihues, 2013). On the other hand, secondary GBM is found mainly in younger patients with mutant Isocitrate Dehydrogenase (IDH) (Ohgaki and Kleihues, 2013). Although both primary and secondary glioblastoma are clinically indistinguishable with common poor prognosis and key genetic mutations that affect pathways involved in proliferation, survival, invasion, and angiogenesis, they present different molecular features with the genomic profiles of each possessing a distinctly different transcriptional patterns and aberrations of recurrent DNA copy number (**Figure 1**) (Furnari et al., 2007; Ohgaki and Kleihues, 2013).

Accounting for 90% of all cases of GBM, primary GBM arises de novo, with no pre-existing histological evidence of cancer precursor and compared to secondary GBM, they are very lethal and are characterized by more genetic alterations (Ohgaki, 2005; Ohgaki and Kleihues, 2007). Unlike primary GBM, secondary GBM accounts for only 10% of all GBM cases and they originate from lower grade glioma. Found mainly in younger populations, the mean age at diagnosis is 45 years for secondary GBM (Ohgaki, 2005; Ohgaki and Kleihues, 2007).

Established onco-markers of primary GBM include amplification of epidermal growth factor receptor (EGFR), and mutations in the telomerase reverse transcriptase (TERT) promoter and phosphatase and tensin homolog (PTEN) tumour suppressor gene (Bush et al., 2017). On the other hand, secondary GBM are presented with mutations in isocitrate dehydrogenase 1 and 2 (IDH1/2), the p53 tumour suppressor protein (Bush et al., 2017), and Alpha Thalassemia/Mental Retardation Syndrome X-linked (ATRX) (Bush et al., 2017). Mutation in IDH1 is a predictor of a better prognosis (Bush et al., 2017; Parsons et al., 2008), and so far, preclinical research has been focused on the use of vaccine or selective inhibitors of the R132H protein such as AGI-5198 or (Rohle et al., 2013; Schumacher et al., 2014).

Amplification of the EGFR gene, occurring in the majority of primary GBM, contains a mutation that encodes a constitutively active variant of EGFR known as EGFR vIII, which is present in 50% of GBM (Aldape et al., 2015). TERT promoter mutations is present in 70- 80% of primary GBM (Bush et al., 2017). While patients with tumours having no IDH1/2 and TERT promoter mutations are associated with a worse survival outcome (Bush et al., 2017), those with IDH1/2 mutations and TERT promoter mutations may demonstrate increased survival (Bush et al., 2017).

Methylation of the O-6-methylguanine-DNA methyltransferase (MGMT) promoter that is located on chromosome 10q26, has been reported to demonstrate a better survival in patients treated with radiotherapy and TMZ (Stupp et al., 2005). This methylation, which is found in about 40% of primary GBM, causes reduced levels of MGMT, leading to increased sensitivity of tumour cells to alkylating agents (Bush et al., 2017). In addition to its role as a predictive maker, MGMT plays an import role as part of the decision making in the treatment of patients with glioblastoma (Batash et al., 2017; Hegi et al., 2005, 2019).

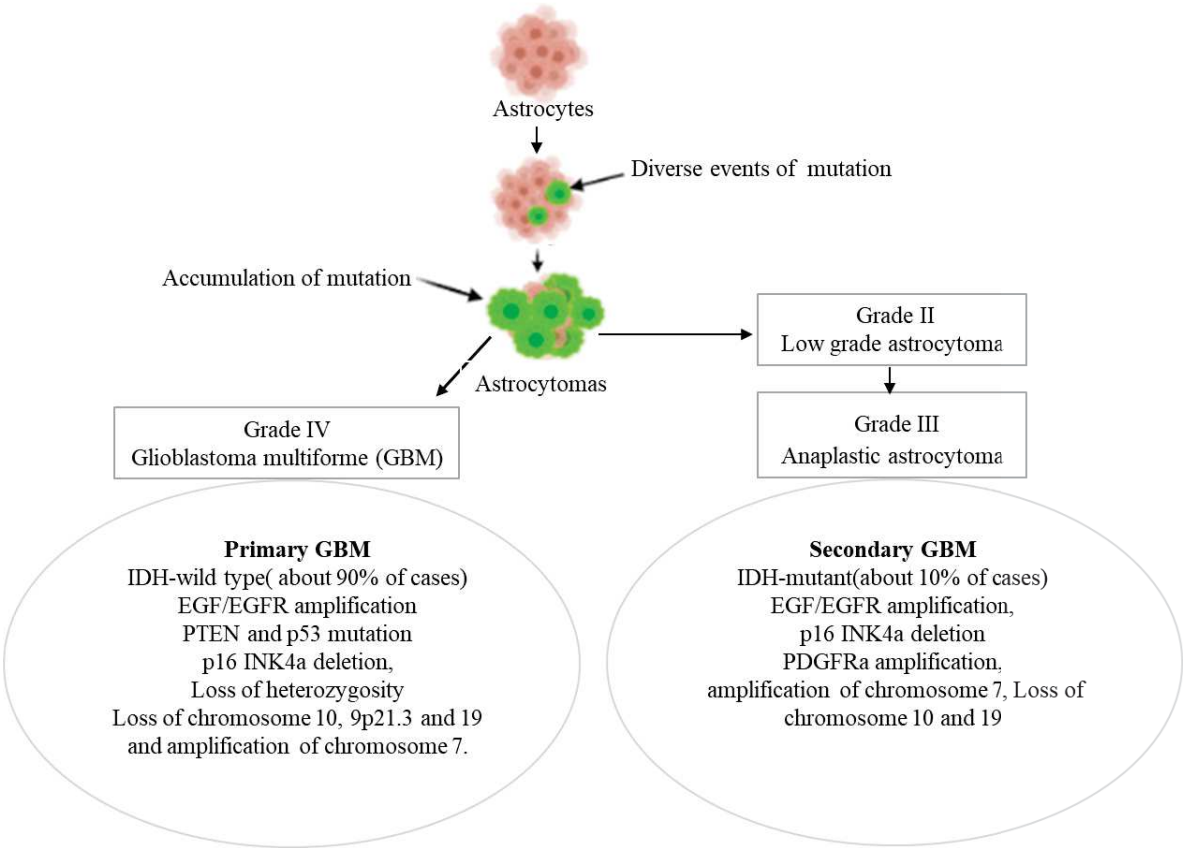

Figure 1.Origin and genetic changes in Primary and secondary GBM.
EGF/EGFR, epidermal growth factor/receptor; TP53, tumour protein p53; PTEN, phosphatase and tensin homolog; PDGFRα, platelet derived growth factor receptor alpha; IDH1/2, isocitrate dehydrogenase (NADP (+) 1 (Pawlowska et al., 2018).

Furthermore, The Cancer Genome Atlas (TCGA) classified GBM into four distinct molecular subtypes of classical, mesenchymal, proneural and neural, based on genomic data, gene expression, DNA mutation and gene copy (Kwon et al., 2015; Verhaak et al., 2010). This different subtypes respond differently to aggressive therapies (Verhaak et al., 2010), therefore, the need to tailored therapy at the molecular level to improve the life expectancy of patients with glioblastoma.

The discovery of multipotent neuronal stem cells (NSCs) in the brain has enabled researchers to have a better understanding of the origin of GBM cells. GBM cells originates from normal brain cells (also known as astrocytes) which accumulate mutations that induced their dedifferentiation, thus allowing them to acquire cancer phenotype (Visvader, 2011). Neuronal stem cells can generate both normal and cancer cells **Figure 2**. Tumour cells could be formed when mutations occur during the differentiation of neural stem cell. The differentiation of NSCs could result in either neural progenitor or glial progenitor cell. However, NSCs could instead

generate tumour-initiating cells (TICs) when they undergo transformation. While neural progenitors could undergo differentiation to form neuronal cells, the differentiation of glial progenitors leads to the formation of astrocytes. Tumour progenitor stem-like cells are formed when genetic aberrations occur in glial progenitor cells or via the differentiation of TICs. Finally, GBM are formed directly either from brain tumour progenitor-like cells, astrocytes, or oligodendrocytes (Uchida et al., 2000) (**Figure 2**).

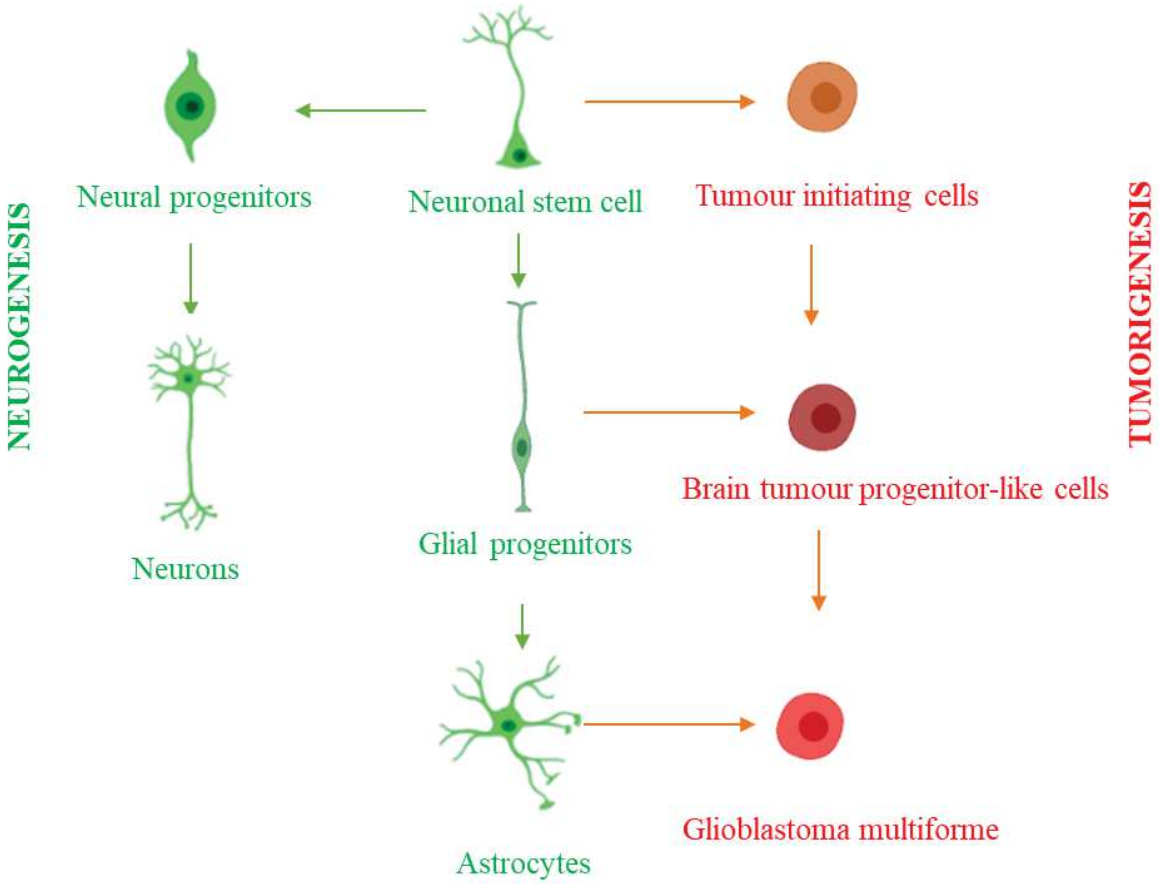

Figure 2.Differentiation of neural stem cells and cancer transformation.
NSCs can undergo transformation into tumour-initiating cells (TICs) and tumour progenitor-like cells or become neural progenitors upon differentiation (Pawlowska et al., 2018).

1.5. Treatment of GBM

Despite recent advances in science, the treatment of glioblastoma remains one of the most challenging task in clinical oncology due to the presence of blood brain barrier (BBB), location of the disease and its complex and heterogeneous biology (Kesari, 2011; Mrugala, 2013). The BBB, a highly selective semipermeable barrier that separates blood from the brain is made up of the endothelial cells of capillaries, astrocytes surrounding the capillary, and pericytes embedded in the capillary basal lamina. The BBB prevents about 98% of small molecule drugs from entering the central nervous system (CNS). However, the DNA alkylating agent TMZ, has been shown to cross the BBB and cause mismatches that initiate futile DNA repair cycles and subsequently DNA strand breaks resulting in cell death (Strobel et al., 2019).

The current standard of care for patients with high-grade gliomas is maximal surgical resection, followed by radiotherapy (RT) with concomitant and adjuvant chemotherapy using temozolomide (TMZ) as the first line chemotherapeutic agent (Stupp et al., 2005). In addition, the provision of an effective supportive care system that manages the various signs and symptoms of the disease including cerebral edema, seizures, gastrointestinal tract disturbances, osteoporosis, venous thromboembolism, cognitive impairment and mood disorders is of great importance (Van Meir et al., 2010).

1.5.1. Surgical resection

Maximal surgical resection is a principal component of standard care for the treatment of GBM. The extent of tumour resection is an important factor for improved survival and decreased requirement for steroids (Lacroix et al., 2001; Laws et al., 2003; Sanai and Berger, 2008). Maximal surgical resection is promising in the case of patients with newly diagnosed GBM. However, advanced age, and the anatomic structures invaded by the tumour could be an impending factor for maximal surgical resection. Recent advances in technology has helped optimize safe maximal surgical resection using improved surgical imaging techniques such as intraoperative magnetic resonance imaging (iMRI) and fluorescent-guided resection (Anton et al., 2012; Perry et al., 2012; Wilson et al., 2014). Fluorescent-guided resection uses a pharmacological agent that fluoresces only when exposed to tumour cell but not the surrounding normal brain, thus helped guide tumour resection by identifying tumour tissue that may otherwise appear normal (Anton et al., 2012; Pichlmeier et al., 2008). Unfortunately, almost all

glioblastomas recur due to extreme local invasiveness that cannot be completely cured by surgery; hence surgery alone is insufficient, and a combination treatment modality is required.

1.5.2. Radiotherapy

As part of the effort to eliminate the remaining tumour after surgical resection, surgical treatment is followed by radiotherapy and this approach has shown improved life expectancy for patients with glioblastoma (Scott et al., 2011). However, radiotherapy is associated with several risk factors such as radiation necrosis, radiation-induced permanent neuronal damage, radio-resistance of some tumours and invasive nature of GBM (Iacob and Dinca, 2009). Focal fractionated external beam radiation therapy (EBRT) applied at the cavity of surgical resection at about 2 cm margin at the surrounding brain tissue is the current standard of care for radiotherapy in glioblastoma (Aguilar et al., 2012). Particularly, radiotherapy is given at 2 Gy per day, 5 days a week, for a total dose of 60 Gy (Stupp et al., 2005). This ionizing radiation functions by inducing both a single-strand and double-strand DNA breaks in proliferating cells (Barani and Larson, 2015). Despite combined maximal surgical resection and radiotherapy, median survival of patients with glioblastoma is extend only by 12.1 month, a situation that has necessitated the need to include chemotherapy in this regimen. Currently, there is insufficient evidence to support re-irradiation as a therapy for recurrent gliomas. However it could be used as a palliative therapy for recurrent tumours (Batash et al., 2017).

1.5.3. Combination therapy

After surgical resection, TMZ is used as the standard of care in conjunction with radiotherapy. In a large randomized trial, Stupp et al., demonstrated that chemotherapy in addition to radiotherapy (TMZ/RT) followed by adjuvant Temozolomide significantly improved median survival to 14.6 months and 5-year survival rate of 10% (Stupp et al., 2005). The treatment algorithm (**Figure 3**) commences either with the ESMO guidelines which evaluates how fast the disease has developed or with the NCCN guidelines which uses the patient's age followed by performance status. Concurrent therapy was recommended for patients up to age 70 or patients with good performing status (PS) that are older than 70 years. The treatment includes 6 weeks of concomitant radiotherapy and TMZ 75 mg/m^2 after maximal surgical resection, followed by 6 months of adjuvant TMZ 150-200 mg/m^2 every 28 days. The concomitant radiotherapy and chemotherapy (TMZ) followed by adjuvant TMZ improve median survival (14.6 months) more than that of radiotherapy alone (12.1 months) (Stupp et al., 2005). In 2009 stupp et al., introduced a randomised phase III study on the effects of radiotherapy with

concomitant and adjuvant temozolomide versus radiotherapy alone on survival in glioblastoma in which the methylation status of the methyl-guanine methyl transferase gene, MGMT, was determined. The trial demonstrated that methylation of the MGMT promoter was the strongest predictor of outcome and benefits from TMZ chemotherapy (Stupp et al., 2009). Unfortunately, despite this intensive approach glioblastoma recur leading to progression of the disease in most patients. Second-line chemotherapy includes combination or monotherapy with procarbazine, lomustine, vincristine, cyclophosphamide, irinotecan, Temozolomide, and platinum-based regimens (Batash et al., 2017)

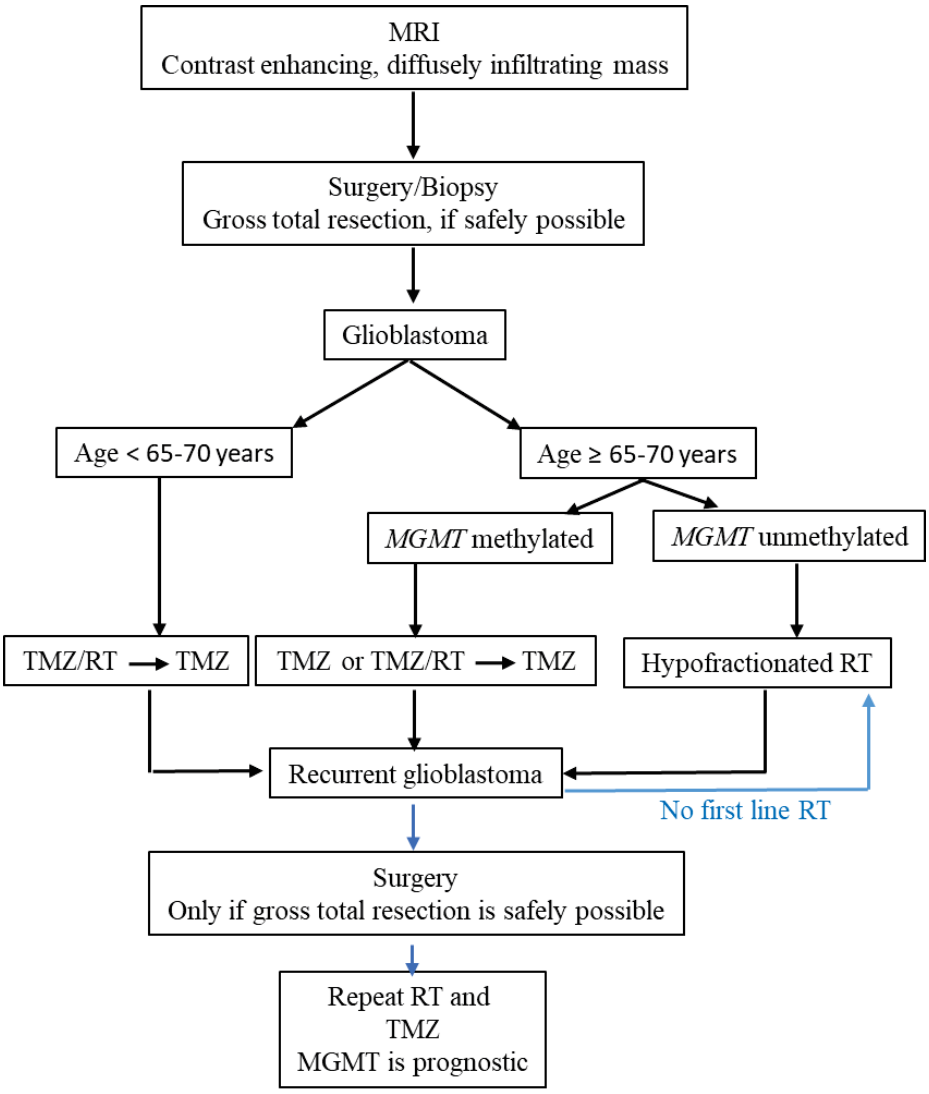

Figure 3.Therapeutic approach to glioblastoma.
MRI, magnetic resonance imaging; MGMT, O6-methylguanyl DNA methyltransferase gene promoter; TMZ, temozolomide 150–200 mg/m2 on 5/28 days; TMZ/RT, 30x2Gy = 60Gy with daily concomitant temozolomide at 75 mg/m2; hypofractionated RT, radiotherapy at 15x2.66 Gy = 40 Gy (Stupp et al., 2005).

2. Temozolomide resistance in GBM

2.1. Structure and activation of TMZ

The oral lipophilic molecule TMZ (**Figure 4A)** is an alkylating agent from the imidazotetrazine family with the capability to cross the blood brain-barrier due to its lipophilic nature (Lee, 2016a). As a prodrug TMZ is stable at acidic pH (pH <5) (a property which permits oral administration) but becomes labile in the systemic circulation (physiological pH>7) with a plasma half-life of 1.8 hours at pH 7.4 (Tsang et al., 1990; Zhang et al., 2012). Thus, TMZ is rapidly absorbed intact, but then undergoes spontaneous breakdown to form the active compound 3-methyl-(triazen-1-yl) imidazole-4-carboxamide (MTIC). Further hydrolysis of MTIC leads to the production of 5-aminoimidazole-4-carboxamide (AIC) and the highly reactive methyldiazonium cation. This unstable cation with a half-life of 0.4 seconds can transfer a methyl group to DNA to elicit the cytotoxic effect of TMZ (Friedman et al., 2000). The methyldiazonium cation methylate purine bases of DNA at the O^6 and N^7 positions of guanine and the N^3 position of adenine. The most frequent methylations are the N^7 and N^3 methylations which account for 80–85% and 8–18% of total alkylations, respectively (Zhang et al., 2012). Although the O^6 methylation accounts for only 5% of the total lesions caused by TMZ, it represents the main cause of cytotoxicity by TMZ (Drabløs et al., 2004). The process involved in the activation of the TMZ prodrug down to the transfer of methyl group usually occurs within a narrow pH window close to physiological pH. Compared to normal healthy tissue, brain tumours possess a more alkaline pH, a condition that favours the preferential activation of the prodrug within tumour tissue (Baer et al., 1993). Thus, the use of TMZ has registered significant therapeutic benefit for patients with glioblastoma.

2.2. Mechanisms of GBM resistance to TMZ

TMZ is currently the standard chemotherapeutic agent for the treatment of GBM (Stupp et al., 2005). However, GBM may harbour innate resistance or developed acquired resistance to TMZ during treatment thereby resulting in tumour progression and recurrence (Nakada et al., 2012). Therefore, understanding the mechanism of TMZ resistance could help overcome TMZ resistance and improve patient's survival. Studies have shown that several actors including the DNA repair system (e.g. MGMT, MMR and BER), β-catenin, MDM2, EGFR, the p53 protein, phosphatase and tensin homolog (PTEN), alteration in the expression profiles of certain microRNA (miRNA), GBM stem cells and processes such as autophagy and Epithelial to

mesenchymal transition (EMT), are involved in the development of GBM resistance to TMZ (Jiapaer et al., 2018; Messaoudi et al., 2015).

2.2.1. Role of DNA repair mechanisms in TMZ resistance

a. MGMT

The O^6-methylguanine DNA methyltransferase (MGMT) is a DNA repair system that represents the main mechanism of GBM resistance to TMZ. The 22 kDa protein MGMT can remove the methyl groups attached to the O^6 position of guanines (Kaina et al., 2007), allowing the direct repair of the lesion caused by TMZ and ultimately resulting in resistance and tumour recurrence (**Figure 4B**) (Park et al., 2012). MGMT acts as a suicide enzyme because it becomes inactivated upon the attachment of methyl group to the cysteine residue 145 located in its catalytic pocket (Tubbs et al., 2007). MGMT is not recycled but it is rather degraded by the proteasome (Xu-Welliver and Pegg, 2002). The MGMT gene is not frequently deleted or mutated and the levels of MGMT vary widely between and within tumours (Esteller et al., 2000). The expression of MGMT correlate well with the methylation profile of the MGMT promoter, and studies have demonstrated an inverse relationship between the level of MGMT and the density of the cysteine phosphate-guanine (CpG) methylation in CpG islands (Bhakat and Mitra, 2003). Hyper methylation of the CpG islands promoter leads to the silencing of the MGMT gene (Silber et al., 2012). Methylation of the MGMT promoter occurs in about 45% of patients with newly diagnosed GBM and they respond better to TMZ (Hegi et al., 2005). The use of the MGMT inhibitors O^6-benzyl guanine (O6-BG) and O^6-(4-bromothenyl) guanine preceding treatment with TMZ demonstrated promising results in vitro, in vivo, and in clinical trials by enhancing the activity of TMZ (Zhang et al., 2012). However, the high toxicity of this inhibitors against normal cells create a stumbling block to their use (Sancar et al., 2004).

b. MMR alteration

The DNA mismatch repair (MMR) system functions to correct nucleotide base mismatch errors that accumulates during DNA synthesis (Zhang et al., 2012). In the absence of MGMT that remove the methyl groups attached to the O^6 position of guanines, the O^6-MG mispaired with thymine, resulting in the formation of O^6-MG/T which is recognized and excise by MMR. Since only newly synthesized strands are excised by MMR, the O^6-MG remain intact. Repetition of this repair cycle upon the synthesis of another new strand results in futile cycles of insertion and excision of thymine leading to cell cycle arrest and apoptosis (Fu et al., 2012; Messaoudi et al., 2015; Zhang et al., 2012). Mutations in the MMR protein complexes can cause

impairment of the MMR pathway, resulting in inability of the MMR to recognize and repair O^6-MG adducts caused by TMZ. For this purpose, DNA replication occurs and allows the progression of the cell cycle and as a result TMZ becomes less effective and this results in resistance (Liu et al., 1996). Such mutations can be natural or acquired (Yip et al., 2009).

c. BER

The base excision repair (BER) system is involved in the repair of DNA damage caused by alkylating agents, oxidizing agents and ionizing radiation (Almeida and Sobol, 2007; Wood et al., 2005). The base excision repair (BER) system is made up of proteins and enzymes including the enzyme poly (ADP-ribose) polymerase-1 (PARP-1) which becomes activated in response to DNA damage. Upon activation PARP-1 binds to DNA and starts the synthesis of poly (ADP-ribose) (PAR) from NAD^+. This allows for DNA repair through the recruitment of BER complex proteins such as XRCC1, DNA polymerase, ligase and FEN-1 (Malanga and Althaus, 2005). The N^3 and N^7 methylations caused by TMZ are repaired by the BER pathway (Fu et al., 2012; Zhang et al., 2012). Unlike N^7 lesions, the N^3 lesions are lethal if not repaired (Zhang et al., 2012). Although the N^3 and N^7 methylations accounts for 90% of methylation caused by TMZ, these methylations are rapidly repaired by the BER. Mutations in one or more components of the BER could then results in the cytotoxic effect of TMZ. Despite the high level of N^7 and N^3 methylation as compared to O^6 methylation, the role of BER in TMZ resistance is less significant than either MMR or MGMT (Messaoudi et al., 2015).

2.2.2. p53, Mdm2 and PTEN

a. p53 and Mdm2

The transcription factor p53 is a tumour suppressor protein that plays a key role in DNA repair, cell cycle arrest, cellular senescence and apoptosis in response to cellular stress such as DNA damage (Fridman and Lowe, 2003; Shangary and Wang, 2009). The p53 protein is mutated in about 50% of all human cancer (Hainaut and Hollstein, 2000; Petitjean et al., 2007). Although the remaining 50% of cancer may express a wilde-type functional p53, its life cycle is strictly and frequently regulated by MDM2 which inhibit the tumour suppressive function of p53 by acting as an E3 ubiquitin ligase that mark and target p53 for proteasomal degradation (Shangary and Wang, 2009). Unfortunately, the MDM2 gene is frequently amplified in glioblastoma, where its overexpression results in the loss of functional p53 (Freedman et al., 1999). Mutation of the TP53 gene and the loss of functional p53 to MDM2 results in the promotion of tumour

growth (Burton et al., 2002) and the development of resistance to chemotherapy (**Figure 5)** (Shchors et al., 2013). Given the significance of p53 deficiency in the development of resistance to chemotherapeutic drugs, several strategies including gene therapy and p53–Mdm2 inhibitors such as Nutlin-3a have been developed to restore p53 function (Hong et al., 2014).

b. PTEN

The Phosphatase and Tensin homolog (PTEN) gene are tumour suppressor gene frequently mutated in a wide range of cancers including glioblastoma. It regulates a variety of biological processes, including maintenance of genomic stability, cell survival, proliferation, migration, and metabolism. Mutations and/or decrease in the level and activity of PTEN is associated with enhanced tumour cell proliferation (Hill et al., 2017; Kato et al., 2000; Knobbe et al., 2002). Studies have shown that, decreased in the level of PTEN resulting from increased level of miR-181a is as an important contributor to the development of endometrial cancer in non-obese patients (Geletina et al., 2018). PTEN inhibit PI3K and the transcription of Mdm2, thereby preventing the inactivation and degradation p53 wild-type (Mayo et al., 2002). The p53 protein can increase the activity of PTEN, since PTEN is a p53 target gene. Binding of p53 to PTEN leads to p53 stabilization and increase in p53 activity (Stambolic et al., 2001). Restoration of wild-type PTEN in tumours lacking PTEN or tumours having mutated PTEN has been reported to suppresse tumorigenicity, thereby sensitizing cells to chemotherapy by promoting apoptosis (Lee et al., 2018; Mayo et al., 2002; Tanaka et al., 2000). Therefore, restoration of wild-type PTEN and wild-type p53 could enhance the sensitivity of tumour cells to anticancer drugs such as TMZ (**Figure 5**).

A

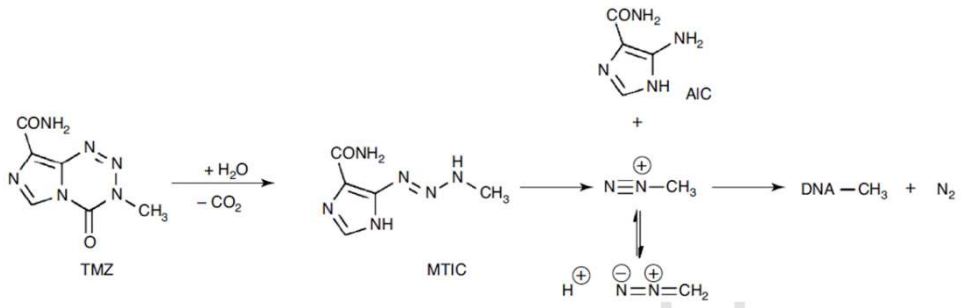

B

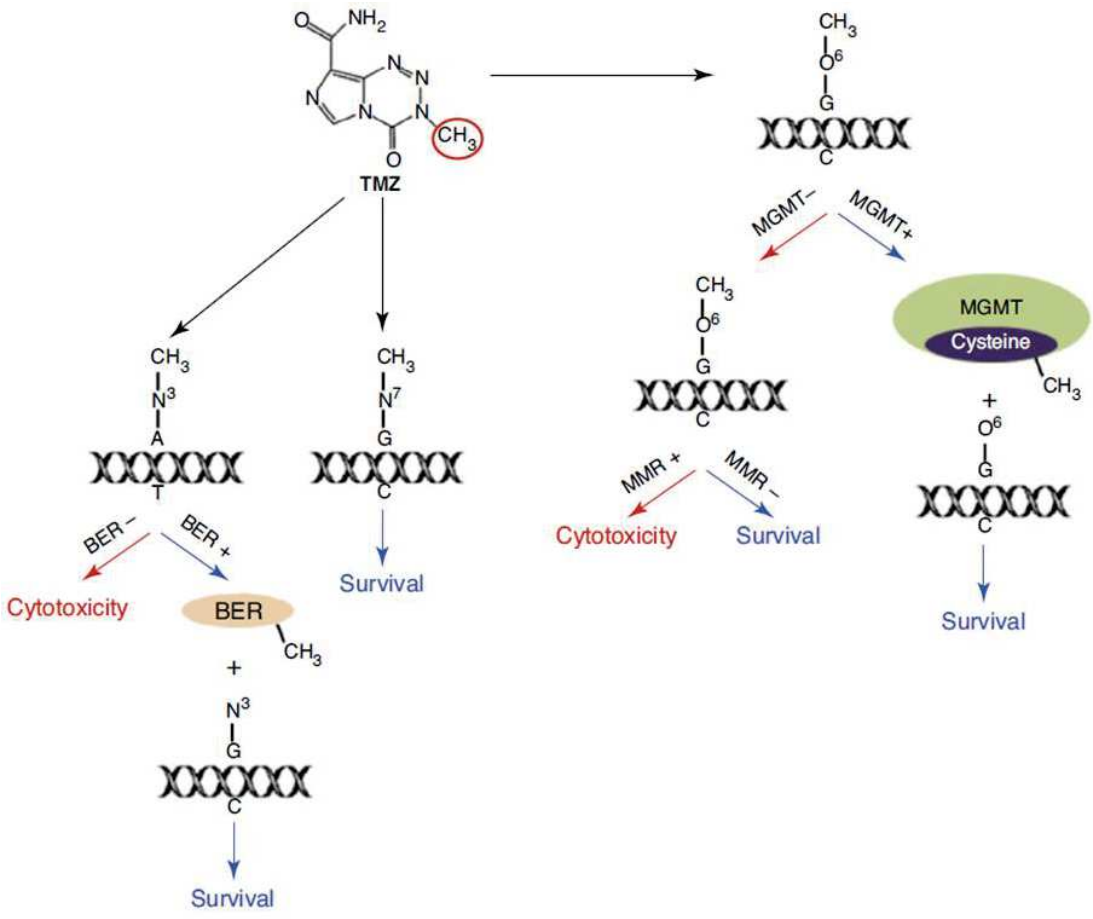

Figure 4.TMZ mechanism of action and resistance.
Structure and activation of TMZ to produce the active compound imidazole-4-carboxamide (MTIC). **B.** TMZ modifies DNA at N^7 and O^6 sites on guanine and the N^3 on adenine by the addition of methyl groups. The methylated sites can remain mutated, be fixed by DNA mismatch repair (MMR), be removed by base excision repair (BER) by the action of a DNA glycosylase such as, alkyl purine-DNA-N-glycosylase (APNG), or deakylated by the action of a demethylating enzyme such as O^6-methylguanine methyl transferase (MGMT). Cells are TMZ sensitive when MMR is expressed and active. When MGMT, APNG, and BER proteins are expressed, GBM cells are resistant to TMZ (Messaoudi et al., 2015).

2.2.3. miRNAs

MicroRNAs (miRNAs) are small, non-coding, endogenous RNAs that regulate gene expression at the post-transcriptional level (Babashah and Soleimani, 2011; Castro-Magdonel et al., 2020). They play an essential role as a novel class of tumour suppressor genes or oncogenes, where they regulate a variety of biological process including proliferation, differentiation and apoptosis (Babashah and Soleimani, 2011). Dysregulation of miRNA expression has been reported to affect the sensitivity of GBM to TMZ (Mizoguchi et al., 2013). For example, the upregulation of miR-21, miR-195, miR-455-3p and miR-10a* (Shi et al., 2010; Ujifuku et al., 2010) and the downregulation of miR-145 and miR-1268a have been reported in TMZ-resistant glioblastoma cells (Yang et al., 2012) (**Figure 5**). Using RNA-seq analysis, Li et al., showed that miR-1268a modulates TMZ-resistance in GBM cells by targeting ABCC1. ABCC1 is part of the C subfamily of ATP-binding cassette (ABC) family, that has been reported to contribute to cancer drug-resistance by extruding various anticancer drugs from the cell, thereby reducing their bioavailability (Cole, 2014). The overexpression of ABCC1/ MRP1 in various tumours including lung cancer, esophageal cancers, classical Hodgkin lymphoma, colorectal cancer and GBM has been associated with resistance to a variety of anticancer drugs including TMZ (Cole, 2014; Greaves et al., 2012). Furthermore, studies have shown that the overexpression of ABCC1 in GBM cells enhance chemo-resistance by increasing drug efflux (Tivnan et al., 2015). The expression of ABCC1 is negatively regulated by several miRNAs, such as miR-7 in small cell lung cancer, miR-326/miR-134 in breast cancer cell, miR-1291 in pancreatic carcinoma cell, embryonic kidney cell and miR-1268a in GBM (Castro-Magdonel et al., 2020). Given the emerging evidence on the tumour suppressive and oncogenic roles of miRNAs in cancer, it is thought that manipulating the expression level of miRNA could be a potential therapeutic strategy for newly diagnosed and recurrent GBM(Castro-Magdonel et al., 2020).

2.2.4. Overexpression of EGFR

The epidermal growth factor receptor (EGFR) (170 kDa) is an effector of several signalling cascades that plays an important role in tumour growth and development by stimulating cell angiogenesis, proliferation, migration, metastatic spread, and cell resistance to chemotherapy (Brennan et al., 2013; Huang et al., 2009). The receptor tyrosine kinase EGFR can bind ligands to activate signalling pathways such as Ras/Raf/MAPK (Guha et al., 1997) and PI3K/AKT/mTOR (Narita et al., 2003). The strong activation of these signalling pathways in glioblastoma that leads to inhibition of autophagy and apoptosis results in decreased efficiency

of TMZ (**Figure 5**) (Furuta et al., 2004). EGFR is frequently amplified and overexpressed in 40% of glioblastoma (Ekstrand et al., 1991). Therapeutic molecules such as Cetuximab1, Gefitinib1 and Erlotinib1 have been developed to inhibit the EGFR signalling pathway. The monoclonal antibody Cetuximab1 for example, has been shown to specifically binds to EGFR and inhibit its downstream signalling pathways resulting in the inhibition of cell proliferation in vitro (Weiner et al., 2010).

2.2.5. β-catenin

β-catenin, is a subunit of the protein complex cadherin, that serves as a major mediator of the Wnt signalling pathway. The Wnt/ β-catenin signalling pathway, one of the most significantly activated functions in TMZ-resistant cells (Cai et al., 2020), has been shown to regulate cell viability, growth, invasion, and apoptosis in several types of cancer including glioma (Hong et al., 2015; Ma et al., 2015). Nuclear β-catenin, the hallmark of active Wnt/β-catenin signalling (Peifer et al., 1991), has been reported to contribute to glioblastoma development, progression and resistance to chemotherapy (Figure 4) (Liu et al., 2011; Zhang et al., 2009). In addition, it is positively correlated with the grade and prognosis of glial neoplasms (Ma et al., 2015). The Wnt/β-catenin pathway induce chemotherapy resistance in various type of cancer via regulation of the MGMT gene expression (Wickström et al., 2015). However, in U87MG glioma cells lacking MGMT, activation of the Wnt/β-catenin pathways has been reported to cause chemotherapy resistance by inducing epithelial-to-mesenchymal transition-like changes in the phenotype and characteristic proteins (Yi et al., 2016). Several studies have reported the development of glioma resistance to TMZ via modulation of the wnt/ β-catenin signalling. For example, Yu et al., showed that the overexpression of the transcription factor Krüppel-like factor 8(KLF8) activates β-catenin to induce TMZ-resistance in U87MG glioblastoma cells (Yu et al., 2016). Moreover, knockdown of KLF8 combined with TMZ treatment inhibited both total and nuclear β-catenin levels in U87 GBM cells (Yu et al., 2016). Furthermore, Schnell et al., showed that KLF8 plays a critical role in tumour development, and its expression is positively associated with the different grades of glioma (Schnell et al., 2012). Similarly, Xu et al., showed that FoxO3a, a Forkhead box O (FoxO) protein member of the Forkhead family, renders GBM cells resistant to TMZ by regulating the nuclear accumulation of β-catenin (Xu et al., 2017). Rrecent findings showed that the overexpression of the sex-determining region X2 (SOX2) contributes to TMZ resistance in GBM cells by promoting the maintenance of GSC stemness via activation of the Wnt/β-catenin signalling pathway (Garros-Regulez et al., 2016; Luo et al., 2019). SOX2 is a member of the SOX family of transcription factors that is

characterized by highly conserved mobility group of DNA-binding domains. On the one hand, activation of this family of transcription factors control several important functions and processes involved in the maintenance of stem cell properties in several tissues during embryonic development and adulthood. On the other hand, its genetic inactivation induces stem cell differentiation. The overexpression of SOX2 has been correlated with tumour aggressiveness and poor prognosis in glioblastoma (Ben-Porath et al., 2008; Garros-Regulez et al., 2016). Therefore, inactivation of the Wnt/β-catenin signalling pathway via targeting either KLF8, FoxO3a or SOX2 could be a promising strategy to overcome TMZ resistance in GBM.

2.2.6. Glioma stem cells

Glioma Stem Cells (GSCs) are highly tumorigenic cells with remarkable cellular heterogeneity and hierarchy. They are endowed with high capacity for extensive self-renewal, differentiation, potential to drive malignant growth, and resistance to chemotherapy and radiotherapy (Bao et al., 2006; Lathia et al., 2015; Yamada and Nakano, 2012). Established molecular makers for GSCs include CD15, CD133, nestin, and stage-specific embryonic antigen-1 (SSEA1). Oberstadt et al., demonstrated that the development of chemo-resistance resulting from GSCs was associated with the diversity of GSCs and drug efflux transporter (ATP-binding cassette, ABCG2)(Oberstadt et al., 2013). In GBM the bulk of the tumour is made up of several heterogenetic GSC phenotypes based on distinct genomic profiles (Oberstadt et al., 2013). The high self-renewal and poor differentiation capacity of GSCs enable them to survive under treatment conditions, thereby resulting in the development of resistance and tumour recurrence. While modulation of GSC by the tumour microenvironment could cause phenotypic changes leading to the formation of different type of GBM cell lines, differentiated GBM cells are capable of transforming into GSCs when subjected to therapeutic doses of TMZ, both scenario are important factors in the development of TMZ resistance (**Figure 5**) (Safa et al., 2015). Tsai et al., showed that the expression and secretion of the angiopoietin-like 4 protein (ANGPTL4) leads to TMZ resistance via an EGFR/AKT/4E-BP1 cascade-mediated stemness enrichment in GBM (Tsai et al., 2019). Furthermore, studies have shown that the presence of intrinsic or acquired resistance to TMZ in GBM could result from the promotion of stemness and enhance upregulation of MGMT in GSCs by the hypoxia-inducible factor 1-alpha (HIF-1a) (Hombach-Klonisch et al., 2018; Sciuscio et al., 2011; Yuen et al., 2016). Therefore, therapeutic strategies that eliminate both GSCs and the entire tumour bulk could be promising in the fight against TMZ resistance in GBM.

2.2.7. Autophagy

Autophagy is a complex physiological process in which cells maintain homeostasis via the degradation and recycling of cellular proteins, organelles, and other cellular components. It is regulated by cellular stress such as starvation, hypoxia, pathogens, radiation, toxic agent, and DNA damage (Jiapaer et al., 2018). Depending on the cellular context and treatment conditions, the activation of autophagy in cancer, can either promote the survival of cancer cells (Cytoprotective autophagy), or contribute to the death of cancer cells (cytotoxic/nonprotective autophagy) (Russo and Russo, 2018). The reduced activity of autophagy observed in cancer cells compared to normal cells is a self-defence mechanism that allow cancer cells to activate cytoprotective autophagy in response to radiation or chemotherapeutic agent such as TMZ (Kanzawa et al., 2004; Ogier-Denis and Codogno, 2003). In GBM cells TMZ induced high rate of autophagy with no apoptosis (Kanzawa et al., 2004; Zou et al., 2014) or very few apoptotic cells (Hirose et al., 2001). The highly protective autophagy in GBM resulting from treatment with TMZ is considered an important mechanism of chemo resistance (Sui et al., 2013; Thorburn et al., 2014). Studies have shown that TMZ-induced autophagy via the ATM/AMPK pathway could result in the induction of acidic vesicular organelle (AVO) formation and Atg8 Orthologue light chain 3 (LC3) aggregation both of which are essential for autophagosome and lysosome interaction, thus facilitating cytoprotective autophagy and cell survival (**Figure 5**) (Jiapaer et al., 2018; Zou et al., 2014). Furthermore, inhibition of adenosine monophosphate activated protein kinase (AMPK) has been shown to augments the cytotoxic effect of TMZ in GBM cells, thus signifying the vital role of autophagy in the cytotoxic effect of TMZ (Zou et al., 2014). AMPK is an initiator of autophagosome formation that can interact with mammalian autophagy initiating kinase unc51- like kinase 1 (ULK1) (**Figure 5**) (Sanchez et al., 2012; Zou et al., 2014). Although combine therapy using TMZ and an inhibitor of autophagy seems promising in combatting highly resistant glioma, the varied role played by different autophagy inhibitors at different steps of the process of TMZ induced autophagy, has been reported to induce different results. For example, the autophagy inhibitor, Bafilomycin A1, which inhibits autophagosome and lysosome fusion to blocked TMZ-induced cytoprotective autophagy at the late stage caused a more effective apoptotic cell death as compared with either TMZ or Bafilomycin A1 treatment alone. On the other hand, combination therapy using TMZ and the autophagy inhibitor 3-methyladenine (3-MA), which inhibit TMZ-induced autophagy at the early stage showed reduced TMZ cytotoxicity (Kanzawa et al., 2004).

2.2.8. Epithelial to mesenchymal transition

Epithelial to mesenchymal transition (EMT), a process in which epithelial cells are transformed into mesenchymal cells leading to increased motility and invasion has been reported to play an important role in tumour progression, metastasis and resistance to therapy (Yi et al., 2016; Zeisberg and Neilson, 2009). EMT is one of the most significantly activated functions in TMZ-resistant cells (Cai et al., 2020). It is associated with loss of epithelial characteristics, gain of mesenchymal properties, decrease in the expression of epithelial cell biomarkers (such as E-cadherin and β-catenin) and an increased expression of mesenchymal cell biomarkers (such as N-cadherin, Slug, Snail, and zinc finger E-box binding homeobox 1/2 (ZEB 1/2)) (Kashiwagi et al., 2018). Elevated expression of the anaphase-promoting complex/cyclosome (APC/C)-associated protein CDC20 (cell division cycle 20 homolog) induce EMT-like changes to cause TMZ-resistance in GBM (Wang et al., 2017). Siebzehnrubl et al., showed that the epithelial to mesenchymal transition pathway participate to chemo-resistance in GBM cells via a mechanism in which the transcription factor zinc finger E-box binding homeobox 1 (ZEB1) regulates MGMT expression via miR-200c and c-MYB (Siebzehnrubl et al., 2013). The expression of ZEB1 in GBM patients is a predictor of short-term survival and poor response to TMZ (Siebzehnrubl et al., 2013). However, in GBM cells lacking MGMT, TMZ resistance could arise from EMT-like changes caused by activation of Wnt/β-catenin and Akt signalling (Yi et al., 2016).

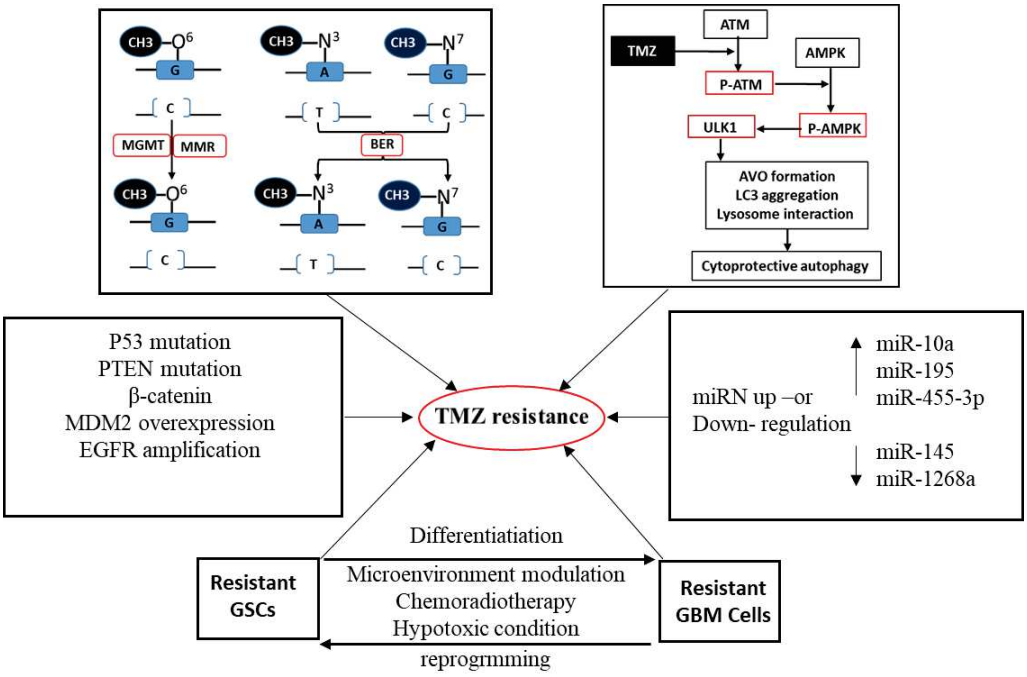

Figure 5.Different actors involved in TMZ induced resistant glioblastoma cells.

2.3. Generation of acquired TMZ-resistance in glioblastoma

2.3.1. Treatment protocols for the generation of TMZ-resistant cells

TMZ is the primary and most promising therapeutic drug for the treatment of GBM (Liu et al., 2017). However, the presence of innate or acquired TMZ-resistance in GBM that leads to tumour relapse, progression and poor prognosis represents a major clinical challenge in the effective use of TMZ for the treatment of GBM (Zeng et al., 2017). To overcome glioma resistance to TMZ, a representative model of TMZ-resistance is required to decipher the molecular events involved in the development of glioma resistance to TMZ.

Over the years, several studies have shown that the generation of acquired TMZ-resistant GBM cells can be achieved by subjecting either established GBM cell lines (Ma et al., 2002; Wu et al., 2020) or cells isolated from primary tumours to varying doses of TMZ for different time points (Bredel et al., 2006; Chien et al., 2019). Acquired TMZ resistant GBM cells have been successfully generated from known TMZ sensitive GBM cell lines such as U87, U251, U373, U343, A172, SNB-19, LNT 229, LN 308, SF188 and D45 as reviewed in Lee et al. (Lee, 2016). Other studies have reported the generation of TMZ-resistant cells from known TMZ-resistant glioblastoma cell lines such as LN-18 and T98G (Happold et al., 2012; Wang et al., 2017). Several approach have been employed to generated TMZ-resistant U87MG cells (**Table 1**), for example, Xu et al. generated TMZ-resistant U87MG cells by subjecting U87MG cells that were originally sensitive to TMZ to repeated treatment with 400 µM TMZ, every 24 h for 5 consecutive days, followed by exposure to fresh TMZ every 3 days for a total of 3 weeks (**Table 1**). This leads to a significantly reduced cellular proliferation and survival at the beginning, but the small population of cells that survived eventually recovered and proliferate profusely (Xu et al., 2017).

In most studies, the establishment of TMZ-resistant GBM cells, is usually confirmed by either the lack of sensitivity of the generated cells to TMZ or by the fold increase in the IC50 values of the cells to TMZ compared to the parental cells (Cheng et al., 2017; Happold et al., 2012; Wu et al., 2020). The acquired TMZ-resistant GBM cells can be maintained by culturing in medium containing the maximum concentration of TMZ used (Zeng et al., 2017) or by culturing in TMZ-free medium (Wang et al., 2017). Once developed, acquired TMZ-resistant glioma cells are expected to display a fold increase in the IC50 value and should have the capacity to

proliferate at a similar rate in the presence or absence of TMZ (Happold et al., 2012; Yamashiro et al., 2020). The IC50 values could vary between different Laboratories, and between the methods used in determining the IC50 value. For example, while Auger et al reported an IC50 value of 101µM when TMZ was used to treat TMZ-resistant SNB-19 cells, Zhang et al., reported 280 µM for the same cells (Auger et al., 2006; Zhang et al., 2010). This variation could have resulted from the differences in the original responses of the parental cells to TMZ in the two laboratories: 1.03 µM (Auger et al., 2006) as compared to 36 µM (Zhang et al., 2010). Concerning variation in the IC50 based on the method used, Kohsaka et al., reported a 4 fold increased in IC50, from 40 µM to 150 µM, for TMZ on acquired TMZ resistant U87 cells, 3 weeks post low doses of TMZ, when measured with growth inhibition assay, but a 40 fold increase, from 10µM to 400µM, when measured using clonogenic assay (Kohsaka et al., 2012). In most cases the derived resistant cells remain insensitive to TMZ even after multiple cycles of freeze thawing and culturing in medium without TMZ, implying that genetic alteration could be into play.

Other studies have reported the generation of acquired TMZ-resistant GBM cells from known TMZ-resistant glioblastoma cell lines such as LN- 18. For example, Happold et al generated TMZ-resistant LN 18 by subjecting TMZ insensitive LN 18 cells to repetitive pulse exposure to TMZ (24 hours exposure for 2 weeks), followed by increasing concentration of TMZ for 6 months based on the median effective concentration (EC50 values) (Happold et al., 2012). This lead to a 2-fold increase in the IC50 (IC50 of parental TMZ- resistant LN-18: ~400 µM to ~800 for acquired TMZ- resistant LN-18 (Happold et al., 2012).

2.3.2. Mechanisms of Acquired TMZ-resistance in GBM cells

At the molecular level, differences could exist between acquired TMZ-resistant GBM cells and their parent cells. In fact, several studies have reported, an increase in the protein expression levels of MGMT a known TMZ resistance molecules in acquired TMZ resistant SF188, LN-18, U87, U251, and primary tumour derived GBM cells as reviewed in Lee et al (Lee, 2016). However, no alteration in MGMT protein expression was reported in acquired TMZ resistant SNB-19, LNT-229, U251, U343 and U373 cell (Lee, 2016a). Alteration of other molecules known to participate in TMZ resistance have also been reported. For example, down-regulation of MSH6 and upregulation of the BER gene NTL1 (Zhang et al., 2010) in acquired TMZ-resistant SNB-19 cells, down-regulation of DNA mismatch-repair protein in acquired TMZ-resistant LNT-229 cells (Happold et al., 2012), upregulation of STAT3/p-STAT3 (Zhang et al.,

2010), up-regulation of microRNA (Ujifuku et al., 2010), decreased remodelling of the mitochondria electron transport chain and mitochondrial DNA copy number (Oliva et al., 2010) in acquired TMZ-resistant U251. Other alterations reported in acquired TMZ resistant GBM cells include activation of JNK (Ueno et al., 2015), increased histone demethylase KDM5A gene expression (Banelli et al., 2015) and up-regulated metabolisms of glucose, citrate, and isocitrate (St-Coeur et al., 2015).

In TMZ-resistant U87 MG cells (**Table 1**), several molecular alterations have been reported, including decreased MSH2, MSH6 (McFaline-Figueroa et al., 2015), downregulation of DHX9, HNRNPR, RPL3, HNRNPA3, SF1, DDX5, EIF5B, BTF3, RPL8 (Yi et al., 2018), collagen I, fibronectin, laminin, CD44 (Zeng et al., 2017) miR-29b (Xu et al., 2020) and the tumour suppressor candidate 3 (TUSC3) (Cheng et al., 2017) , and upregulated expression of DRD4, Akt, mTOR, β-catenin, CDK6, NF-kB, Erk1/2 (Wen et al., 2019), FoxO3a (Xu et al., 2017), MGMT, STAT3(Kohsaka et al., 2012), ATP-binding cassette transporters (ABCB1, ABCC and BCRP) (Zeng et al., 2017) and miR-132 (Cheng et al., 2017).

Depending on the duration of exposure to TMZ, variation could also exist between resistant cells derived from the same parental cells. For example, Yamashiro et al demonstrated that TMZ-resistant U87 MG cells derived from TMZ-sensitive parental cells subjected to longer exposure (over 6 months) showed minimal G2 arrest as compared to those derived from the same parental cells by shorter exposure (4 months) to TMZ (Yamashiro et al., 2020).

Table 1. Generation and molecular characterization of TMZ-resistant U87MG cells.

S	TMZ-resistant U87MG cells Selection and maintenance method	Molecular events in acquired TMZ-resistant U87MG cells	Reference
1	Cells were cultured for 3 weeks with a low dose of TMZ	Upregulation of MGMT and STAT3	(Kohsaka et al., 2012)
2	Cells were first cultured with 20 μM TMZ and the surviving fraction with 40 μM TMZ	TMZ resistance is correlated with decreased mismatch repair (MMR) activity such as MSH2 and MSH6	(McFaline-Figueroa et al., 2015)
3	Cells were treated with 200 μM TMZ for 1 week	Downregulation of the proteins DHX9, HNRNPR, RPL3, HNRNPA3, SF1, DDX5, EIF5B, BTF3, and RPL8 which were significantly associated with poor prognosis of GBM patients and mainly involved in ribosome and spliceosome pathway	(Yi et al., 2018)
4	Long-term culture in 100 μM TMZ and maintained by continuous culture in 100 μM TMZ	Increased expression of CD133, Bmi-1, and SOD2. SOD2 in resistant cells functionally determined the cell fate by limiting TMZ-stimulated superoxide reaction and cleavage of caspase-3.	(Chien et al., 2019)
5	After initial dose–response evaluation (100 to 1000 μM), TMZ-resistant (TR) cells were established by continuous exposure to the IC50 of TMZ for ~6 months	Up-regulation of DRD4, Akt, mTOR, β-catenin, CDK6, NF-kB and Erk1/2 expression	(Wen et al., 2019)
7	TMZ treatment (400 μM) was repeated every 24 hours for 5 consecutive days, and the cells were then exposed to fresh TMZ every 3 days for a total of 3 weeks.	-Upregulation of FoxO3a and β-catenin. FoxO3a renders GBM cells resistant to TMZ treatment, via regulation of nuclear accumulation of β-catenin	(Xu et al., 2017)
8	Cell were treated with TMZ for 3 hours at 10 μM → 25 μM → 50 μM → 100 μM → 200 μM every 2 weeks, and surviving cells were maintained with repetitive TMZ administration at 200 μM/2 weeks and TMZ-resistant clones were maintained in TMZ for 4 months and at least 6 months	Unlike TMZ-resistant clones with short exposure (4 months), TMZ-resistant clones with long exposure (>6 months) showed minimal G2 arrest and reduced expression of MSH6	(Yamashiro et al., 2020)
9	Cells were exposed to increasing concentration of TMZ (0-100 μM) for 3 days and subsequently maintained in 50 μM TMZ for 6-8 generation	-Downregulation of miR-29b expression and increased protein levels and phosphorylation of STAT3	(Xu et al., 2020)
10	Parental cells were cultured in gradually increasing doses (2-20 μM) of TMZ for 4 months	Upregulation of PomGnT1 (in U87-TR cells) which subsequently regulates the expression of factors in epithelial-mesenchymal transition signalling including TCF8, vimentin, β-catenin and Slug	(Liu et al., 2017)
11	Repetitive pulse exposure of cells to TMZ (48 hours every 2 weeks), followed by increasing concentration of TMZ for 6 months. TMZ-resistant cells were then maintained in 500 μM TMZ	-Dysregulation of several lncRNAs and mRNAs, -Upregulated expression of ATP-binding cassette transporters (ABCB1, ABCC and BCRP) and MGMT, -Decreased protein expression of collagen I, fibronectin, laminin and CD44	(Zeng et al., 2017)

3. Integrin

The name “integrin” which refers to protein complex that linked extracellular matrix to the actin-based cytoskeleton was first proposed by Tamkun et al., in 1986 (Tamkun et al., 1986). The integrins are transmembrane, heterodimeric cell surface receptors that mediate cell adhesion to the extracellular matrix and encourage cell-cell interaction in different physiological and pathological conditions (Alday-Parejo et al., 2019; Ellert-Miklaszewska et al., 2020; Janouskova et al., 2012a). The integration of the cytoskeleton to the extracellular matrix by integrins transmit a two-way signal; an inside out signalling and outside in signalling. This enable the integrins to participate in the regulation of a wide array of cellular activity, including cell proliferation, migration, survival, tissue invasion and innate immunity (Ellert-Miklaszewska et al., 2020; Hynes, 2002). All integrins are heterodimers composed of non-covalently linked α and β subunit (Ruoslahti and Pierschbacher, 1987) and the de-regulation of integrin function often contributes to the development of various diseases, including cancer (Ellert-Miklaszewska et al., 2020).

3.1. Integrin family

The integrin family is made up of at least 24 different heterodimers with distinct ligand recognition and tissue distribution profiles. In mammalian cells, there are 18α and 8β distinct integrin subunits that can non-covalently combine in variously ways to form 24 different heterodimers (**Figure 6**) (Alday-Parejo et al., 2019).

Natural integrin ligands are important components of the extracellular matrix (ECM), such as fibronectin, laminin, collagen and vitronectin. The sequence arginine-glycine-aspartate (RGD), in fibronectin was originally identified as an integrin-binding pattern (Pierschbacher and Ruoslahti, 1984). Based on ligand specificity, integrins can be classified into four groups, i.e., collagen, laminin, RGD motif-binding integrins and leucocyte-specific receptors (**Figure 6**). Collagen receptors are composed of α1, α2, α10 and α11 subunits forming heterodimers with β1 subunit. In laminin receptors, α3, α6 and α7 subunits pair mostly with β1(Anderson et al., 2014; Takada et al., 2007). Arginine-glycine-aspartic acid (RGD) motif binding integrins include αIIbβ3, α5β1 and α8β1 and other integrins derived from the association of αv with either β1, β3, β5, β6 or β8 subunit. Fibronectin, vitronectin, fibrinogen, tenascin and osteopontin are common examples of integrin ligands containing the RDG motif (Nieberler et al., 2017)**.**

Leukocytes binding integrins consist of integrin heterodimers formed between the association of one of several α subunit counterparts αL, αM, αX, and αD with β2 subunit. Cell-to-cell

interactions in innate and adaptive immunity is regulated by these integrins. Leucine-valine-aspartic acid (LVD) binding integrins are made up of integrin heterodimers formed due to interaction of α4 and α9 subunits with β1 and β7 subunits. Leucine-valine-aspartic acid (LVD) binding integrins share similar ligands to leucocyte-specific integrins, for example vascular cell adhesion molecules (VCAM) and intracellular adhesion molecules (ICAM) (Anderson et al., 2014; Takada et al., 2007).

The integrins are further subdivided into two groups of subunits based on structural similarity. These include subunits containing I-domain, such as α2, α10, α11, αL, αM, αX, αD and αE and subunits with no I-domain, such as α3, α4, α5, α6, α7, α8, α9, αV and αIIb. The I-domains play a central role in ligand binding and intercellular adhesion (Liddington, 2014; Takada et al., 2007).

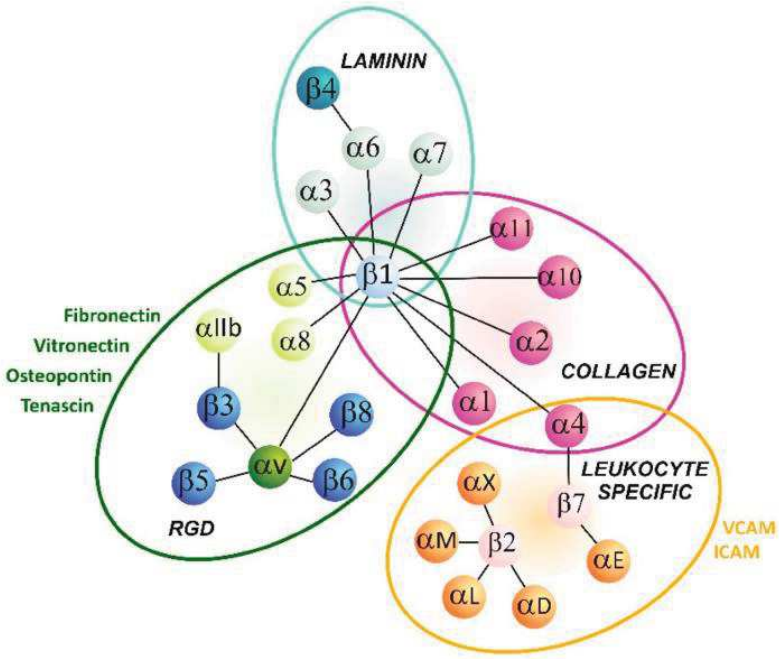

Figure 6. Overview of the main integrin heterodimers and their ligands.
There are at least 18α and 8β subunits in humans, that can non-covalently combine in various ways to form 24 heterodimeric integrins. Integrin subunits that bind to each other to form a heterodimer are connected by solid lines. Each integrin has distinct ligand-binding specificity and tissue and cell distribution (Ellert-Miklaszewska et al., 2020).

3.2. Integrin structure

The α and β integrin subunits are distinct from each other with no homology between them. The different α subunits have similarities among themselves, just as there are conserved regions in the different β integrin subunits (Barczyk et al., 2010). The sequence identity is about 30%

and 45% for α and β respectively. All integrin heterodimers share a conserved architecture, with each subunits consisting of a large extracellular region known as ectodomain (Xiong et al., 2009), a dimeric transmembrane region known as TM domain (Lau et al., 2009; Yang et al., 2009) and a short intracellular largely unstructured cytoplasmic domain (Anthis and Campbell, 2011) (**Figure 7b**). The size of each subunit varies within the integrin members, but typically α subunit contains around 1000 amino acids and β subunit around 750 amino acids (Barczyk et al., 2010; Luo et al., 2007).

The extracellular domain of α subunit is composed of a 7-bladded β propeller connected to a thigh, a calf-1, and -2 domains **(Figure 7a)**. Although the amino acid sequence of α and β subunits are conserved across species, in vertebrate, a subset of integrin α subunits consisting of half of the 18 mammalian α subunits contains additional ~200 amino acid inserted between blades 2 and 3 of the β propeller (Kadry and Calderwood, 2020; Larson et al., 1989). This inserted region, also known as an αI domain or an αA domain (due to its similarity to the A-domain of von Willebrand factor), contains the metal ion-dependent adherent site (MIDAS) and is responsible for ligand binding (Kadry and Calderwood, 2020; Lee et al., 1995). It is found in integrins that bind collagen and in some laminin binding integrins, where it is the major site of ligand binding (Calderwood et al., 1997; Emsley et al., 2000). Even though the α cytoplasmic domains are highly divergent, integrins containing α-I domain have a high homology in their α-I domains (Takada et al., 2007). The β subunit contains 7 domains consisting of a plexin-semaphorin-integrin (PSI) domain, a hybrid domain, a β-I- domain and 4 cysteine-rich epidermal growth factor (EGF) repeats (Lee et al., 1995) **(Figure 7a)**. Present in the βI domain is a Mg^{2+} coordinating MIDAS and ADMIDAS (a site adjacent to MIDAS) binding an inhibitory Ca^{2+} ion. The binding of ADMIDAS site to Mn^{2+} ion leads to a conformational change which results in integrin activation (Chamberlain et al., 2012; Humphries et al., 2003). In the cytoplasmic chain, the β integrins share homology in their NPX / Y motifs that allow them to bind proteins containing PTB domains (Moser et al., 2008).

The major role of the α subunit is in determining integrin ligand specificity. The ligand binds to the integrin through the β propeller domain of the α subunit and the β-l domain (in non-αI containing integrins). If the α-I domain is present, it forms the ligand-binding domain. The ligand binding to α-l domain causes its conformational changes, which in turn affect the conformation of the β subunit (Barczyk et al., 2010)**.**

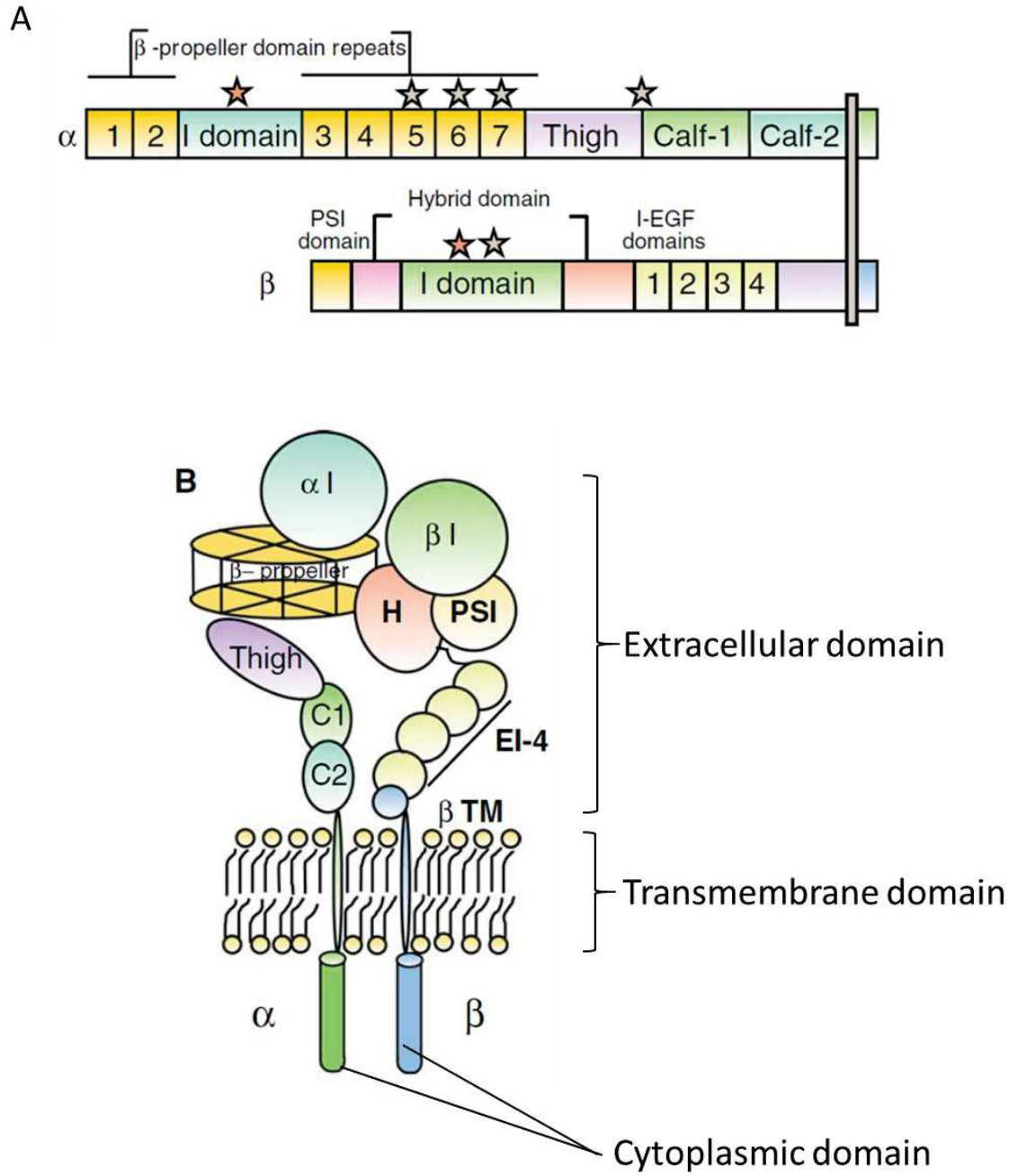

Figure 7. Structure of integrin.

A. Domain organization of α and β integrin subunit (Nine out of the 18 integrin α chains contains an α-I domain (stars denotes divalent cation-binding sites). **B**. schematic structure of αI-domain-containing integrin (Barczyk et al., 2010).

3.3. Integrin activation

Integrin activation enable cells to regulate integrin function by modulating the ligand affinity of integrins. The modulation of integrin affinity for extracellular ligands is tightly regulated through a multistep activation process that consists of several major stages: intracellular adaptor

recruitment and conformational activation, ECM ligand engagement, clustering/focal adhesion assembly, and finally, integrin inactivation (Kadry and Calderwood, 2020).

Crystal structures of integrins revealed that integrins can exist in three main conformations; inactive bent conformation with a low affinity for the ligand, extended with closed headpiece and extended with an open headpiece (**Figure 8**) (Takada et al., 2007). Interactions in the TM region is responsible for maintaining integrins in the inactive state. When in the inactive state, the integrin ectodomain adopts a bent conformation, such that there is a ‘‘knee’’ in the α subunit between the thigh domains and Calf-1, and in the β subunit between the EGF1 and Hybrid domains **(Figure 7a).** In addition, the head group of integrin in the bent form points inwards towards the cell surface and has low affinity for ligands (Mould and Humphries, 2004).

The integrins can transmit signal in bidirectional way via either “inside-out signalling” or “outside-in signalling”. In “inside-out signalling”, regulatory intracellular adaptors such as talin binds directly to β-integrin cytoplasmic tails using either the integrin binding site located in the rod domain (IBS2) of talin or the one located in the talin head domain (IBS1). Talin binding destabilizes the association of the α and β tails close to the membrane leading to disruption of intramembrane interactions between the transmembrane helices of α and β integrin subunits. This in turn may result to substantial conformational changes in the heterodimer, from bent to an extended form of the integrin, leading to inside-out activation and increased affinity for extracellular ligands (Shattil et al., 2010). This process is known to regulate cell adhesion, migration and invasion (Kadry and Calderwood, 2020; Shattil et al., 2010).

In “outside-in signalling”, extracellular ligands bind to integrins and induce integrin clustering in the membrane which causes a further conformational change in the cytoplasmic tails of integrin that promote linkage to the actin cytoskeleton, focal complexes formation, and subsequent downstream signal transduction through their cytoplasmic domain (mostly via β subunit) by activation of kinases (such as Focal Adhesion Kinase (FAK) and Integrin-Linked Kinase (ILK)) or Rho-GTPases (Ginsberg, 2014; Morse et al., 2014)**.** The activation of this signal cascade leads to intracellular signals, which regulate cell polarity, survival, migration, changes in cytoskeleton and gene expression. Unligated integrins can activate caspase-8, and as a consequence, induce apoptosis through a process known as integrin-mediated death (IMD) (Cheresh and Stupack, 2002).

.

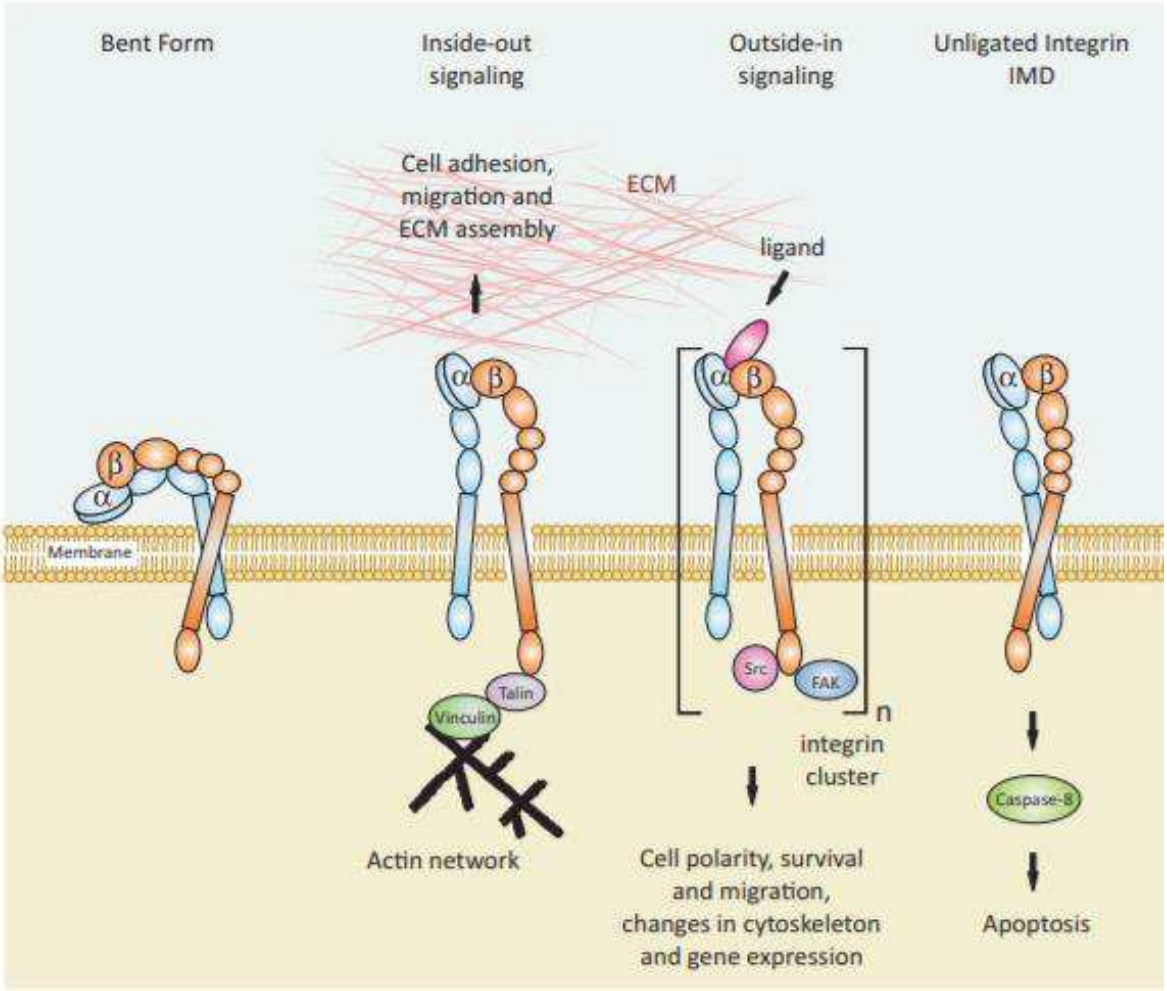

Figure 8.Schematic representation of integrin activation.
Integrin can be activated in two ways: through inside-out signalling, where intracellular activators such as talin and kindlin, interact with the cytoplasmic tail of β integrin subunit to induce conformational changes and increase integrin affinity for extracellular ligands or through outside-in signalling where the binding of integrin to extracellular ligands changes the conformation of the integrin and contributes to integrin activation and clustering (Mas-Moruno et al., 2010).

3.4. Integrin signalling

Integrins are bi-directional signalling transmembrane receptors that are involved in outside-in and inside-out signalling. The inside-out signalling serves mainly to bring the integrin into the active conformation. As previously mentioned, integrin activation can be regulated by regulatory intracellular adaptors such as talins and kindlins. Upon ligand binding, integrins undergo conformational changes leading to outside-in signalling and subsequent activation of

cell-specific and complex signalling events depending on other signalling receptors and signalling systems present in the cell (Kadry and Calderwood, 2020; Kim et al., 2000). The formation of integrin-based adhesion sites such as focal adhesion kinase (FAK) generates a series of dynamic events, known as mechano transduction. This leads to rapid changes in cellular mechanics and affect the adaptation of cells to the surrounding microenvironment in the long-term by releasing biochemical signals (Anderson et al., 2014).

Since integrins lack an intrinsic catalytic activity, extracellular signals are transmitted into the cell via activation of integrin-associated proteins and the formation of focal adhesions with non-receptor tyrosine kinases: with the adaptor SRC Homologous and the enzyme Focal Adhesion Kinase (FAK) as the key components, or via direct or indirect interactions of integrins with other cell surface proteins such as caveolin (Ellert-Miklaszewska et al., 2020) (**Figure 9)**. The non-receptor protein tyrosine kinase FAK (Focal adhesion kinase) is the most extensively studied kinase that is activated by integrin (Hanks et al., 1992)**.** FAK is linked either directly to the β cytoplasmic tail or indirectly through talin or paxillin. Upon integrin binding, FAK is activated by auto-phosphorylation at Tyr397 (Ellert-Miklaszewska et al., 2020; Schaller et al., 1994). Phosphorylated FAK acts as a scaffold, which serves as a high affinity binding site for SH2 domains of Src family kinases (SFKS) (Schaller et al., 1994)**.** Src bound to this site to mediate the phosphorylation of additional tyrosine residues of FAK, and activates several downstream partners, leading to the activation of Jun amino-terminal kinase (JNK) and Nuclear factor KB (NF-KB) molecules (Brunton and Frame, 2008; Guo and Giancotti, 2004; Playford and Schaller, 2004). FAK also activates Phosphoinositide-3-kinase (P13K) and Extracellular signal-regulated kinase/Mitogen-activated protein kinase (ERK / MAPK). FAK has been demonstrated to play an important role in integrin-mediated cellular events, such as cell migration, cell proliferation, and cell death (Guo and Giancotti, 2004; Hu and Luo, 2013)**.**

In addition to the role of the Src family kinases (SFKS) as cofactors of FAK, they can be activated independent of FAK where they interact directly with β cytoplasmic tail of integrins (Arias-Salgado et al., 2003) to mediate the phosphorylation of the adapter Shc, which then activate the Ras-ERK / MAPK pathway. The signalling pathways activated by integrin-SFKS are enough to induce cell migration and protect the cells from apoptotic cell death (Guo and Giancotti, 2004). Integrin like kinase (ILK), a serine/threonine kinase, is another component that was reported to be essential in integrin outside-in signalling (Hannigan et al., 1996). ILK directly binds to the cytoplasmic tail of integrin. ILK signalling up-regulates the activity of

serine/threonine-specific protein kinase AKT, and thus promotes cell survival (MacDonald et al., 2001).

Generally, integrins can activate four main signalling pathways relevant to cancer initiation, progression, angiogenesis, metastasis, and inflammation: the phosphoinositid-3-kinase (PI3K)-AKT, the Rat Sarcoma (RAS)-mitogen activated protein kinases (MAPKs), the Rho-family GTPases, and the Nuclear Factor kappa B (NF- B) pathways (Alday-Parejo et al., 2019).

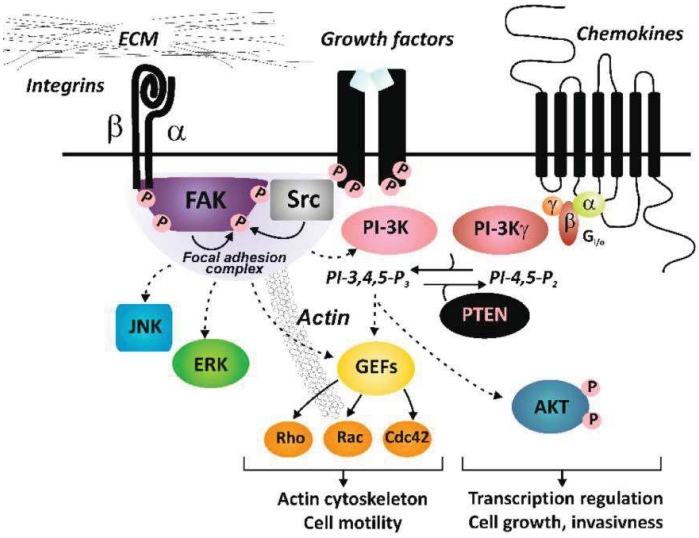

Figure 9.Integrin signalling.
Generally, the integrins activate four main signalling pathways relevant to cancer initiation, progression, angiogenesis, metastasis, and inflammation: the phosphoinositid-3-kinase (PI3K)-AKT, the Rat Sarcoma (RAS)-mitogen activated protein kinases (MAPKs), the Rho-family GTPases, and the Nuclear Factor kappa B (NF- B) pathways (Ellert-Miklaszewska et al., 2020).

3.5. Integrins expression in glioblastoma

Since integrins are rarely mutated in tumours, they do not function as oncogenes. However, they can cooperate with oncogenes to promote tumorigenesis, either by post-translational modifications, overexpression of certain integrins in tumours compared to normal tissues, or through integrin recycling.

First identified as an attractive therapeutic target in GBM, αvβ3 and αvβ5 integrin are overexpressed in both tumour-associated ECM and GBM cells as compared to normal brain cells (Gladson et al., 1995; Roth et al., 2013). In addition, the ECM ligands fibronectin (Serres et al., 2014) and vitronectin (Gladson et al., 1995) have also been reported to be upregulated in GBM. Comparative immunohistochemistry staining of both GBM and normal tissues shows

the overexpression of α2, α3, α4, α5, α6 and β1 as well as of αvβ3, αvβ5, αvβ8 and α6β1 integrins (Delamarre et al., 2009; Gingras et al., 1995), and more recently α7 (Haas et al., 2017) and α10β1 integrins (Munksgaard Thorén et al., 2019) in glioblastoma as compared to normal tissues.

In a recently published paper, Ellert-Miklaszewska et al., compared the expression patterns of major integrin subunits in glioblastoma, lower grade gliomas (WHO grade II and III) and normal brain samples using transcriptomic RNAseq data from The Cancer Genome Atlas (TCGA). The Heat-map showed upregulation of α5 and α3 integrins only in WHO grade IV GBM (Ellert-Miklaszewska et al., 2020) (**Figure 10**). The expression levels of α7, αvβ3, αvβ5 and αvβ8 integrins were also positively correlated with higher grade glioma (Haas et al., 2017; Roth et al., 2013; Schittenhelm et al., 2013; Zhou et al., 2015). The overexpression of αvβ3, α3β1, α5 and α3 at the protein level were positively associated with poor prognosis in GBM (Ducassou et al., 2013; Janouskova et al., 2012; Zhou et al., 2015). In addition, the overexpression of β1, β3, α3, α5 integrins were associated with decreased overall survival of primary GBM patients subgroup treated with standard chemoradiation (Weller et al., 2014).

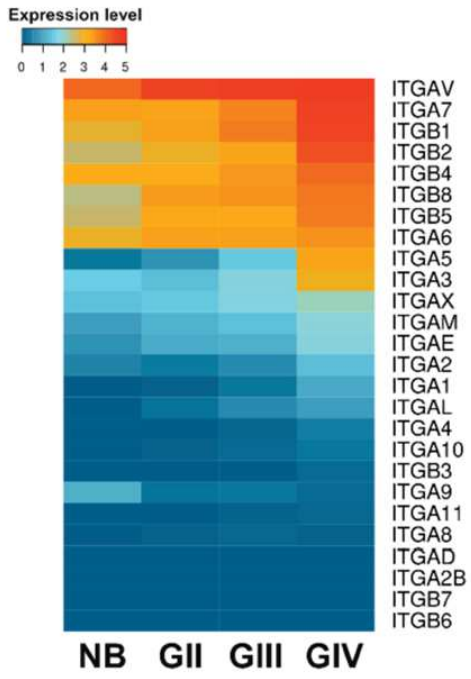

Figure 10.Expression profile of major integrin subunits.

Data from 5 normal brain (NB) samples, 248 WHO grade II (GII), 261 WHO grade III (GIII) and 160 glioblastoma (GBM) WHO grade IV (GIV) tumour samples were acquired from TCGA RNAseq repository as FPKM values, quantile normalized and log2 transformed (Ellert-Miklaszewska et al., 2020).

3.5.1. Integrin in glioblastoma proliferation, migration, and invasion

Integrins promotes the proliferation of tumour cell mainly through interaction with components of the extracellular matrix and the maintenance of cell adhesion to substrate (Paolillo and Schinelli, 2017; RUSSO et al., 2012). Studies have demonstrated that, the interaction of α5β1 integrin with either Anosmin-1 (Choy et al., 2014) or Rap1A Rho-GTPase (Sayyah et al., 2014) promote the proliferation of glioblastoma cells, and functional inhibition of this integrin, reduces glioblastoma cell proliferation (Maglott et al., 2006). The interaction of β4 integrin with the extracellular ligand netrin-4 has also been reported to participate in the sustenance of proliferation in glioblastoma cell (Hu et al., 2012). **Table 2** summarizes the different integrins and their role in GBM proliferation, migration, and invasion.

The contribution of integrins to cell adhesion, migration and invasion has been extensively studied in glioblastoma. Studies have shown that αvβ3 and αvβ5 integrin can directly bind to the extracellular matrix protein such as fibronectin, vitronectin, osteopontin or periostin to activate intracellular signalling pathways that promotes migration and invasion of glioblastoma cells (Malric et al., 2017; Mikheev et al., 2015; Serres et al., 2014). For example, both αvβ3 and αvβ5 integrins can either trigger FAK, which controls cytoskeletal organization, force generation and survival, or activate additional pathways such as Shc/MAP-Kinases, Rho-GTPases and Src Family Kinases to promotes migration and invasion (Hehlgans et al., 2007; Lawson and Burridge, 2014). Integrin αvβ3 has been shown to promote glioblastoma cell invasion by activating MMP-2 at the plasma membrane and the subsequent degradation of complex ECM (Wu et al., 2008). Interestingly, the inhibition of αvβ3/αvβ5 in murine models reduced glioblastoma cell migration and invasion (Scaringi et al., 2012). Delamarre et al., demonstrated that the expression of α6β1 integrin in U87 glioblastoma cell line promote cell invasion both in vitro and in vivo (Delamarre et al., 2009), through cooperation with extracellular-signal-regulated kinase (ERK) and N-cadherin (Velpula et al., 2012). The association of β1 with α3, α5 or α9 and β8 has recently been shown to promote glioblastoma cell migration and invasion, although the mechanisms are yet to be properly define (Malric et al., 2017). While α5β1 may act by interacting with matrix metalloproteinases (MMP-2) (Kesanakurti et al., 2013), αvβ8 may act through the modulation of Rho-GTPases activities (via RhoGDI1) to promote cell proliferation in glioblastoma (Reyes et al., 2013). Therefore,

targeting specific integrins in glioblastoma may reduce tumour cell proliferation, invasion, and aggressiveness.

3.5.2. Integrins in glioblastoma angiogenesis

Neoangiogenesis, the process by which new blood vessels are formed from existing vasculature, is critical for tumour growth and invasion (Avraamides et al., 2008). Interactions of endothelial cells with surrounding ECM proteins, which are mediated by integrins, are important for vessel formation and maturation. Several integrins including α1β1, α2β1, αvβ3, α3β1 and α5β1 that are expressed on endothelial cells promote angiogenesis by regulating proliferation and migration of endothelial cells (Avraamides et al., 2008; Ellert-Miklaszewska et al., 2020; Garmy-Susini et al., 2005). The compensatory effect of integrin family members and the complex interplay between various integrins involved in the regulation of angiogenesis was demonstrated in Lewis Lung carcinoma and B16-F10 melanoma cells where deletion of αvβ3, αvβ5 in mice did not reduce angiogenesis (Murphy et al., 1999).

Although poorly expressed in resting endothelial cells, α5β1 and αvβ3/5 integrins are highly upregulated on endothelium cells during tumour angiogenesis in GBM. The expression of αvβ3/αvβ5 in endothelial cells provide survival signals and traction for invading cells both of which are important mechanisms required for angiogenesis (Roth et al., 2013). Angiogenesis associated with αvβ3 and αvβ5 integrins are usually dependent on the secretion of basic fibroblast growth factor (bFGF)/TNFα and Vascular endothelial growth factor (VEGF) respectively by tumour cells through an amplification loop that results in the overexpression of αvβ3/αvβ5 on endothelial cells. These integrins allow the formation of new vessels (Chung et al., 2002; Roth et al., 2013). When overexpressed, αvβ3/αvβ5 modulate adhesive interactions with ECM proteins such as vitronectin, fibronectin, fibrinogen, osteopontin, and von Willebrand factor (Friedlander et al., 1995; Malric et al., 2017). Also involved in glioblastoma angiogenesis is β1, which can associate with other α-subunits, such as α9, to support endothelial cells-mediated angiogenesis (Walsh et al., 2012). The upregulation of α5β1 by fibroblast growth factor (FGF) on tumour endothelium during angiogenesis, promotes the survival and migration of endothelial cells (Lee et al., 2014). Furthermore, overexpressed α4β1 favour blood vessel maturation and stabilization in pericyte-dependent angiogenesis (Avraamides et al., 2008). When overexpressed on glioblastoma cells, αvβ8 promote vessel formation and remodelling through an autocrine transforming growth factor beta (TGF-β)-dependent differential control of angiogenesis (Tchaicha et al., 2011). These integrins therefore, could

serve as interesting targets in highly vascularized GBM that is dependent on angiogenesis for growth.

3.5.3. Integrins in glioblastoma survival and resistance to therapy

The mediation of cell adhesion to the ECM by the integrin allows the transmission of both chemical and mechanical signals into the cell. In GBM, different mechanisms could deregulate integrin signalling to strengthen uncontrol proliferation and the ease to survive in foreign microenvironments after invasion (Cooper and Giancotti, 2019). The appearance of unligated-integrins that activate caspase-8 to trigger apoptosis through a mechanism known as "integrin mediated death" (IMD) may be lacking in cancer to promote survival (Lotti et al., 2010; Zutter, 2007). The inhibition of integrin in GBM have been shown to induced a TGFβ-dependent cell death known as anoikis (Silginer et al., 2014). In addition, both the cytoskeleton regulatory kinase PAK4 and αvβ3 have been shown to mediate a p21-dependent senescence evasion in glioblastoma (Franovic et al., 2015).

Exposure to either chemotherapy or radiotherapy in glioblastoma is associated with alterations of integrin-linked pathways. For example, αvβ3 is up-regulated in U87 cells upon irradiation, and α2β1, α3β1 and α5β1 were overexpressed in multidrug resistant human glioma cells (Hikawa et al., 2000), thus suggesting the role of integrins in glioblastoma resistance upon chemotherapy and radiotherapy. Tumours can become resistant to either chemotherapy (cell-adhesion mediated drug resistance) or radiotherapy (cell adhesion- mediated radio resistance) through cell adhesion to the ECM that is mediated by integrin ligation.

In the case of cell-adhesion mediated drug resistance (CAM-DR), GBM harbours resistance to TMZ due to the presence of β1 and β4 integrins (Han et al., 2014; Li et al., 2013). A negative crosstalk between α5β1/p53 has been demonstrated to modulate two anti-apoptotic proteins: Phosphoprotein enriched in astrocytes 15 (PEA-15) and Survivin. Therefore, glioblastoma patients with α5β1- overexpression may benefit from targeted therapies associating survivin repressors and integrin antagonists (Renner et al., 2016a). Using RNA-sequencing, Meyer et al., showed an up-regulation of αv integrin and a downregulation of α7 integrin in TMZ resistant clones as compared to TMZ sensitive clones (Meyer et al., 2015).

Unlike cell-adhesion mediated drug resistance (CAM-DR), cell adhesion- mediated radio resistance (CAM-RR) is more documented in glioblastoma. The expression of αvβ3/αvβ5 in U87 cells, confer radio resistance through an ILK/RhoB pathway and specific inhibition of

αvβ3 by Cilengitide or ILK blockade leads to a significant increase in radiosensitization in vitro (Monferran et al., 2008). Concomitant radiotherapy and chemotherapy with Cilengitide in U251 cells xenograft rats showed survival advantage compared to treatment with radiotherapy alone. Sensitization of these cells to radiotherapy correlated with an increase in radiation-induced apoptosis (Mikkelsen et al., 2009).

β1 participate in cell-adhesion mediated drug resistance by activating the pro-survival pathway transduced by Akt, paxillin, p130Cas and JNK (Cordes et al., 2006). Simultaneous inhibition of β1 and JNK radiosensitized GB-initiating cells in vitro and in vivo (Vehlow et al., 2017). A number of data suggest that , the induction of survival pathways such as PI3K/ Akt, NFKB, Bcl2, JNK etc or inhibition of pro-apoptotic pathways (p53), through activation of FAK, could sensitize glioblastoma cells to radiotherapty (Hehlgans et al., 2007; Lim et al., 2008; Matter and Ruoslahti, 2001). Irradiation has been shown to induce the anti-apoptotic protein, survivin (Guvenc et al., 2013), which modulate the radiotherapy-induced mitotic cell death in U87 cell via the integrin-linked kinase (ILK)/HIF-1α/survivin pathway (Lanvin et al., 2013). In addition to ILK/ FAK, other focal adhesion proteins such as PINCH1 and ILKAP also contribute to radioresistance in glioblastoma (Hausmann et al., 2015). Cell adhesion- mediated radio resistance (CAM-RR) in glioblastoma is also mediated by interaction of integrins with the growth factor pathways and simultaneous inhibition β1 and EGFR can sensitize tumour cells to radiotherapy (Eke et al., 2015).

Taken together, these observations suggest that several integrins including αvβ3, αvβ5, α5β1 and β4 are potential targets in glioblastoma that can be combine with ionizing radiations for radiosensitizing strategies.

Table 2. Summary of integrin involved in glioblastoma (Malric et al., 2017).

INTEGRINS	ROLES IN GLIOBLASTOMA
αvβ4, α5β1	Proliferation
αvβ3, αvβ5, α3β1, α5β1, α9β1	Migration
αvβ3, αvβ5, αvβ8, α3β1, α5β1, α6β1	Invasion
αvβ3, αvβ5, αvβ8, α9β1	Angiogenesis
αvβ3, α5β1	Survival
αvβ3, αvβ4, αvβ5, α5β1	Therapy resistance
αvβ3, α3β1	Prognostic marker
α3β1, α6β1	Stemness

3.6. Interfering with integrin signalling as a therapeutic strategy against GBM

The discovery of Arg-Gly-Asp (RGD) sequence as the main integrin (α5β1 and αv) binding motif for fibronectin, coupled with the important roles of these integrins in vascular biology and angiogenesis has led several researchers to target this sequence in search of anticancer agents (Avraamides et al., 2008). Early studies showed that inhibition of integrins containing the RGD binding motif would efficiently sensitized GBM cells to radiotherapy (Lomonaco et al., 2011; Mikkelsen et al., 2009). This initial exciting finding has led to the development of a variety of integrin ligands that can now be grouped as: Antibodies, Natural ligands, RGD-derived peptides, Non-RGD-derived peptides and Small molecules RGD-mimetics as potential anticancer agents. The specificity, selectivity, and activity of this integrin ligands are further discussed in detail on the attached article on page 174.

3.6.1. Antibodies

a. Intetumumab (CNTO 95)

CNTO 95 is a fully human monoclonal antibody that recognise the αv family of integrins. CNTO 95 binds to purified αvβ3 with a Kd of approximately 200 pM and to αv integrin–expressing human cells with a Kd of 1–24 nM (Trikha et al., 2004). CNTO 95 has been shown to inhibit adhesion, migration and invasion of human melanoma cell in vitro (Trikha et al., 2004). In preclinical studies, CNTO 95 demonstrated potent antitumor and antiangiogenic properties in vivo in human melanoma xenograft model in nude mice (Trikha et al., 2004). In breast tumour, CNTO 95 inhibited tumour cell adhesion, migration, and invasion in vitro via interruption of αv integrin mediated focal adhesions and cell motility signals (Chen et al., 2008). CNTO 95 significantly inhibited both tumour growth and metastasis of MDA-MB-231 cells to the lungs in an orthotopic breast tumour xenograft model in vivo (Chen et al., 2008). CNTO 95 showed a good safety profile in phase 1 clinical trials of patients with advanced refractory solid tumours (Mullamitha et al., 2007) and metastatic malignant melanoma and angiosarcoma (O'Day et al., 2012).

c. Volociximab (M200)

Volociximab is a high-affinity chimeric (82% human, 18% murine) IgG4 monoclonal antibody with high specificity for α5β1 integrin. Volociximab showed affinity for α5β1 integrin by ELISA (EC50= 0.2nM), Biacore (Kd= 0.1- 0.4nM) and inhibition of fibronectin binding (IC50=

2-3nM) (Ramakrishnan et al., 2006). Ramakrishnan et al., demonstrated that Volociximab potently inhibited proliferation of human umbilical vein endothelial cells (HUVEC) (IC50= 0.2-0.5nM) and potently inhibited angiogenesis in vitro in HUVEC tube formation assay. Furthermore, functional inhibition of α5β1 integrin by volociximab induced apoptosis of actively proliferating endothelial cells and potently inhibited neovessel formation in vivo in cynomolgus model of choroidal revascularization (Ramakrishnan et al., 2006). This preclinical finding demonstrated that volociximab has therapeutic potential in diseases in which new vessel formation is a component of the pathology. Intravenous administration of volociximab significantly inhibited the growth of tumours growing subcutaneously or intramuscularly in syngeneic rabbit VX2 carcinoma model (Bhaskar et al., 2008). Volociximab is well tolerated when administered intravenously at 15 mg/kg per week in patients with advanced solid malignancies (Ricart et al., 2008). Although weekly administration of volociximab was well tolerated in phase II clinical trials, it was clinically ineffective in patients with refractory tumours (Bell-McGuinn et al., 2011). Furthermore, several nonrandomized Phase II clinical trials have evaluated the efficacy of volociximab as a single-agent or in combination with conventional chemotherapeutic agents, and promising results were obtained for patients with renal cell carcinoma, pancreatic cancer, malignant melanoma, and lung cancer (Almokadem and Belani, 2012). Volociximab was well-tolerated and showed preliminary evidence of efficacy as a single agent or when combined with carboplatin or paclitaxel in phase 1b clinical trials for advanced untreated non-small-cell lung cancer (NSCLC) (Besse et al., 2013).

3.6.2. Natural Ligands

a. Echistatin

Echistatin is an RGD cyclic peptide (**Figure 11**) that has been shown to effectively inhibit platelet aggregation and platelet-fibrinogen interaction (Gan et al., 1988). Its isolation from snake venom was first described by Gan et al (Gan et al., 1988). In a competitive enzyme linked immunosorbent assay (ELISA), using the immobilized natural integrin ligand and the soluble purified integrins, Kapp et al., showed that echistatin possess a broad spectrum of activity with low half maximal inhibitory concentration (IC50)-values for αvβ3 (0.46 ± 0.14 nM),α5β1 (0.57 ± 0.19 nM), αIIbβ3 (0.9 ± 0.24 nM), αvβ5(1.4± 0.2), αvβ6 (13.7 ± 0.3) and αvβ8 (12.8 ± 2.5) (Kapp et al., 2017). This broad and high affinity pattern displayed by echistatin, makes it an ideal candidate to be included as a positive control in cell-free integrin binding tests. Echistatin dose-dependently inhibited the proliferation, migration, invasion, and adhesion of 143B-LM4

osteosarcoma cells over-expressing αvβ3 integrin in vitro (Tome et al., 2016a). It significantly inhibits tumour angiogenesis of the high-metastatic variant 143B-LM4 cells in chick chorioallontoic membrane (CAM) model. Furthermore, echistatin has been shown to inhibit experimental lung metastasis of 143B-LM4 cells in nude mice, and in combination with doxorubicin, it inhibits orthotopic tumour growth and increased survival (Tome et al., 2016).

3.6.3. RGD-derived peptides

a. Cilengitide

Cilengitide (c(RGDf(NMe)V)) is an RGD based and the most active cyclic pentapeptide inhibitor of αvβ3 integrins described so far (**Figure 11**). Developed through systematic N-methylation scan, it is the first anti-angiogenic small molecule drug candidate (Mas-Moruno et al., 2010b). In man, it has a half-life of approximately four hours and does not undergo enzymatic degradation (Becker et al., 2015). In a competitive enzyme linked immunosorbent assay (ELISA), using the immobilized natural integrin ligand (fibronectin or vitronectin) and the soluble purified integrins (α5β1 and αvβ3 integrins respectively), cilengitide demonstrated an extraordinarily low IC50-value for αvβ3 integrin (0.058nM) (Dechantsreiter et al., 1999), 0.54±0.12nM (Merlino et al., 2018) and 0.61 nM(Kapp et al., 2017)), and a higher, but still significant IC50-value for α5β1 (15.4± 3.4nM(Merlino et al., 2018) and 14.9 nM(Kapp et al., 2017)). Taga et al., demonstrated that cilengitide potently inhibited angiogenesis, tumour growth and induced apoptosis in DAOY (medulloblastoma) and U87MG cells expressing αvβ3 integrin via inhibition of αvβ3 integrins interaction with vitronectin (Taga et al., 2002). Cilengitide efficiently blocked tumour growth of melanomas expressing αvβ3 integrin in a dose and time dependent manner in vivo (Mitjans et al., 2000). It demonstrated anti-angiogenic and anti-tumour activity in DAOY and U87MG orthotopic nude mice in vivo (MacDonald et al., 2001). In amelanotic hamster melanoma A-Mel-3, cilengitide significantly reduced functional vessel density and decreased tumour growth and metastasis in vivo (Buerkle et al., 2002). In experimental breast cancer bone metastases, cilengitide caused a pronounced antiresorptive and antitumor effects (Bäuerle et al., 2011). Under hypoxic conditions, cilengitide significantly and dose dependently decreased the intracellular level of the hypoxia-inducible factor 1 α (HIF-1 α) in U87MG and SF763 glioblastoma cells (Skuli et al., 2009). As a single agent, cilengitide has completed phase I clinical trials for metastatic solid tumours, advanced solid tumours, pediatric brain tumours, and in recurrent and newly diagnosed glioblastoma as reviewed in Mas-Moruno et al., (Mas-Moruno et al., 2011). Even though, the phase II clinical trials of cilengigitide as a single agent for recurrent glioblastoma and in combination with standard TMZ

chemotherapy in newly diagnosed glioblastoma demonstrated antitumor activity (Stupp et al., 2010), it fails to improve patient's outcome in phase III clinical trials (Stupp et al., 2014). Despite this failure, recent findings suggest that integrins including α5β1, remain a potential treatment target for GBM (Ellert-Miklaszewska et al., 2020).

3.6.4. Non-RGD-derived peptides

a. ATN-161

The non-RGD linear pentapeptide, ATN-161 (AcPHSCN-NH2) (**Figure 11**) is a non-competitive inhibitor of the fibronectin synergy domain (PHSRN sequence), in which the original arginine residue was replaced by a cysteine residue along with peptide acetylation and amidation. This results in a capped peptide (AcPHSCN-NH2) with increased stability, bioactivity and acceptable pharmaceutical properties (Livant et al., 2000). In a competitive enzyme linked immunosorbent assay (ELISA), using the immobilized natural integrin ligand (fibronectin or vitronectin) and the soluble purified integrins (α5β1 and αvβ3 integrins respectively), Kapp et al., demonstrated that ATN-161 possess high selectivity for α5β1integrin with a low IC50 value of 4.2 ± 0.5nM but inactive for αvβ3, αvβ5, αvβ6, αvβ8 (Kapp et al., 2017). The design of ATN-161 is not based on RGD sequence (Livant et al., 2000), therefore it does not inhibit integrin-dependent adhesion to extracellular matrix and does not cause cell detachment, but may rather inhibit integrin dependent signalling as part of its mechanism of action(Khalili et al., 2006). The formation of disulphide between the free cysteine thiol in ATN-161 and the β subunits of integrin, blocks the disulphide interchange that mediate integrin activation thereby suppressing integrin function (Cianfrocca et al., 2006). ATN-161 has been shown to inhibit the migration and angiogenesis of human choroidal endothelial cells in vitro. Although ATN-161 has no effect on proliferation of human choroidal endothelial cells in vitro, it significantly decreased the proliferation of these cells in vivo (Wang et al., 2011). In preclinical studies, a combination therapy with ATN-161 and continuous-infusion of 5-FU significantly reduced tumour burden, metastases, cell proliferation, increased tumour cell apoptosis and improved survival of mice with murine colon cancer (Stoeltzing et al., 2003). ATN-161 significantly inhibited tumour growth and metastasis in MDA-MB231 human breast cancer cells in vivo, thus providing a rationale for the clinical development of ATN-161 for the treatment of breast cancer (Khalili et al., 2006). ATN-161 was well tolerated in Phase 1 clinical trials of adult patients with advanced solid tumours (Cianfrocca et al., 2006) and is currently in Phase II clinical trial in combination with Carboplatin in adult patients with recurrent intracranial malignant glioma.

3.6.5 Small molecules RGD-mimetics

a. GLPG0187

GLPG0187 is a nonpeptide antagonist of αv integrin receptors (**Figure 11**). In a solid-phase binding assay Van der horst et al., demonstrated that GLPG0187 possess selectivity for several RGD integrin receptors with the following IC50: 1.3 nM for αvβ1, 3.7 nM for αvβ3, 2.0 nM for αvβ5, 1.4 nM for αvβ6, 1.2 nM for αvβ8 and 7.7 nM for α5β1(van der Horst et al., 2011). In preclinical models, GLPG0187 significantly inhibits angiogenesis, osteoclastogenesis, bone loss, de novo formation and progression of bone metastases in prostate cancer (van der Horst et al., 2011). Pharmacological inhibition of αvβ3 by GLPG0187 caused GL-261 and SMA-560 glioma cells to uniformly detached and formed large cell clusters (Silginer et al., 2014). In MDA-MB-231 cells, GLPG0187 inhibits cell invasion, migration and the progression of bone metastasis in mouse xenografts of breast cancer (Li et al., 2015). Silginer et al., demonstrated that pharmacological inhibition of αvβ3 and αvβ5 integrin by the non-peptidic molecule GLPG0187, not only inhibit angiogenesis, but also block AhR- and TGF-β-controlled features of malignancy in human glioblastoma (Silginer et al., 2016). In addition, GLPG0187 significantly reduced the number of prostate tumour cells homing to bone in vivo and reduced migration and proliferation in vitro (Reeves et al., 2015). Although, GLPG0187 was well tolerated upon continuous infusion in phase I clinical trials for adult patients with progressive high-grade glioma and other advanced solid malignancies, continuous infusion of GLPG0187 failed to show signs of monotherapy efficacy (Cirkel et al., 2016).

b. K34C

K34C is a non-peptidic integrin antagonist (**Figure 11**) that was named 34c in the original publication (Heckmann et al., 2008). It is a highly active ligand with a good selectivity for α5β1 integrin over αvβ3 integrin (Heckmann et al., 2008). In a competitive enzyme linked immunosorbent assay (ELISA), using immobilized natural integrin ligand (fibronectin or vitronectin) and soluble purified integrins (α5β1 and αvβ3 integrins respectively), Heckmann et al., demonstrated that K34C possess the lowest IC50-value for the integrin subtype α5β1 (3.1nM) and is inactive against αvβ3 (IC50:1624nM) (Heckmann et al., 2008). Functional inhibition of α5β1 integrin in U87MG cells by K34C inhibited single cell migration(Ray et al., 2014) and partially inhibited clonogenic cell survival (Renner et al., 2016). K34c decreased chemotherapy-induced premature senescence and facilitates cell apoptosis by modulating the p53 pathway in U87MG p53 wild type cells (Martinkova et al., 2010).

Fr248

Fr248 is a non-peptidic, integrin antagonist from the same series of compounds as K34c (**Figure 11**), named 44b in the original publication (Heckmann et al., 2008). It is a highly active ligand with a good selectivity for α5β1 integrin over αvβ3 integrin (Heckmann et al., 2008). In a competitive enzyme linked immunosorbent assay (ELISA), using immobilized natural integrin ligand (fibronectin or vitronectin) and soluble purified integrins (α5β1 and αvβ3 integrins respectively), Heckmann et al., demonstrated that Fr248 possess the lowest IC50-value for the integrin subtype α5β1 (0.86 nM) and is inactive against αvβ3 (IC50: 9600nM) (Heckmann et al., 2008). Fr248 decreased cell migration in U87MG cells overexpressing α5 integrin (Ray et al., 2014).

a. SJ749

SJ749 (SJ749 ((S)-2-[(2,4,6-trimethylphenyl) sulfonyl] amino-3-[7-benzyloxycarbo nyl-8-(2-pyridi nylaminomethyl)-1-oxa-2,7-diazaspiro-(4,4)-non-2-en-3-yl] carbonylamino] propionic acid)**)** is the first highly selective nonpeptidic α5β1 integrin antagonist (Pitts et al., 2000; Smallheer et al., 2004). In a competitive enzyme linked immunosorbent assay (ELISA), using the immobilized natural integrin ligand (fibronectin or vitronectin) and the soluble purified integrins (α5β1 and αvβ3 integrins respectively), Smallheer et al., demonstrated that SJ749 possess an extraordinarily low IC50-value for the integrin subtype α5β1 (0.18nM) and a higher, but significant IC50-value for αvβ3(49nM) (Smallheer et al., 2004). Martinkova et al., showed that inhibition of α5β1 integrin by SJ749 decreased chemotherapy-induced premature senescence and facilitates cell apoptosis by modulating the p53 pathway in U87MG p53 wild type cells (Martinkova et al., 2010a). SJ749 significantly reduced clonogenic survival and transmigration of U87MG cells (Martin et al., 2009). Furthermore, it dose-dependently inhibited adhesion, proliferation and anchorage-independent growth of A172 and U87MG cells without inducing apoptosis (Maglott et al., 2006).

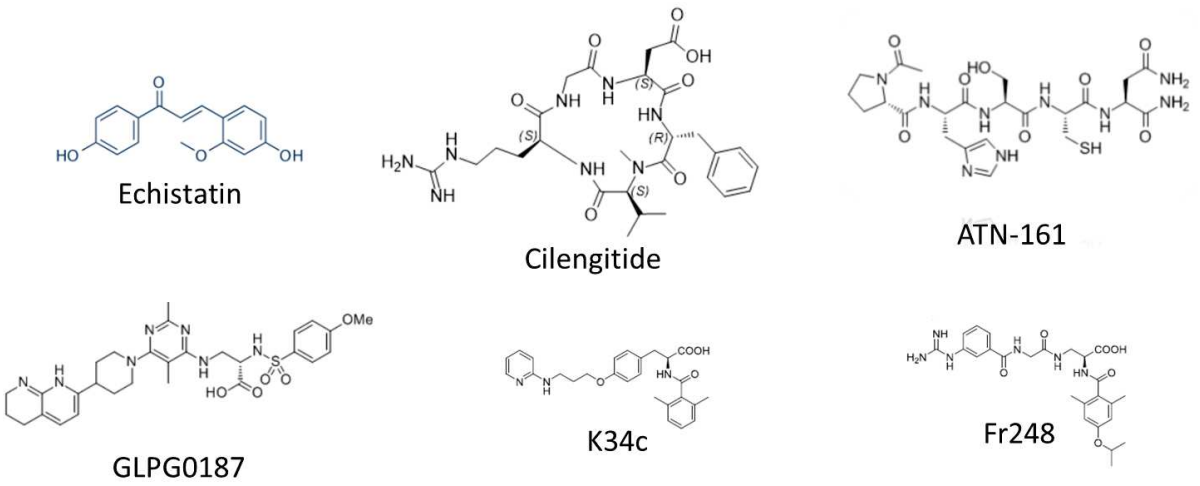

Figure 11. Structures of integrin antagonists.

Echistatin, Cilengitide, GLP0187 and ATN-161 were adapted from selleckchem database. K34c and Fr248 (Heckmann et al., 2008)

4. The p53 protein

The human p53 protein is a nuclear phosphoprotein encoded by TP53 gene located on human chromosome 17p13.1 (Isobe et al., 1986). It belongs to a family of three members consisting of p53, p63 and p73 (Kaghad et al., 1997; Schmale and Bamberger, 1997). Although these proteins are structurally and functionally related, p53 is involved in the prevention of tumour development, whereas p63 and p73 proteins play a crucial role in normal developmental biology (Irwin and Kaelin, 2001). Functional p53 is a homotetramer that adapts a dimer-of-dimers topology (Jeffrey et al., 1995; Rajagopalan et al., 2011). Mutations of the p53 protein are the most common alterations in human cancer (Hainaut and Hollstein, 2000; Kastenhuber and Lowe, 2017). p53 protein plays a central role in maintaining genome integrity by regulating cell cycle and apoptosis. Under a variety of cellular stresses such as DNA damage, p53 becomes activated and promotes cell cycle arrest, senescence and apoptosis to prevent damaged cells from propagation (Kastenhuber and Lowe, 2017). Other roles of the p53 protein include regulation of cellular metabolism, stemness, autophagy, invasion and metastasis (Bieging et al., 2014; Brennan et al., 2013; Kastenhuber and Lowe, 2017). Because p53 is implicated in those processes, its role as a potential target to cure malignant cancer has been investigated over the past years.

4.1. Structure of p53 protein

The tumour suppressor protein p53 consisting of 393 amino acids, can be divided into four major structural and functional domains: the transactivation and a proline-rich domain (residues 1 to 43 and 61 to 94, respectively) located at the N-terminus, the central DNA-binding domain (DBD) (residues 110 to 286), and a nuclear localization signal sequence (NLS), 3 nuclear export signal sequence (NES), tetramerization (oligomerization) domain (TD) and regulatory domain (residues 326 to 355 and 363 to 393, respectively), located at the C-terminus (residues 301-393) **Figure 12** (Bai and Zhu, 2006; Slee et al., 2004).

The transactivation domain is required for transcriptional activity and it interacts with many proteins, including MDM2 and acetyltransferases. The proline-rich region is involved in the regulation of p53 stability, transcriptional activity, and the induction of transcription independent apoptosis. Depletion of this region makes p53 more susceptible to MDM2 mediated degradation. The central DNA-binding domain (DBD) required for sequence-specific DNA binding is highly conserved, and missense mutations in this region account for the majority of p53 mutations found in cancers. The tetramerization domain allows the oligomerization of the p53 and the formation of a tetrameric complex that represents the active conformation of p53. The formation of tetrameric complex is such that the monomer, which consists of a β strand and an α-helix, associates with a second monomer across an antiparallel beta sheet and an antiparallel helix-helix interface to form a dimer. Two of these dimers associate across a second and distinct parallel helix-helix interface to form the tetramer. Oligomerization plays an essential role in p53 activation. Tetrameric p53 binds to its DNA response elements (RE) 100-times more tightly than monomeric core domain, and this tetrameric p53 is required for transactivation of p53 target genes (Jeffrey et al., 1995; Rajagopalan et al., 2011). Studies have shown that the C-terminus is a negative regulator that bind and lock the DNA binding domain as a latent conformation. Disruption of the interaction between the C-terminus and the core DNA binding domain by posttranslational modification such as phosphorylation activate the DNA binding domain and induce enhanced transcriptional activity (Bai and Zhu, 2006).

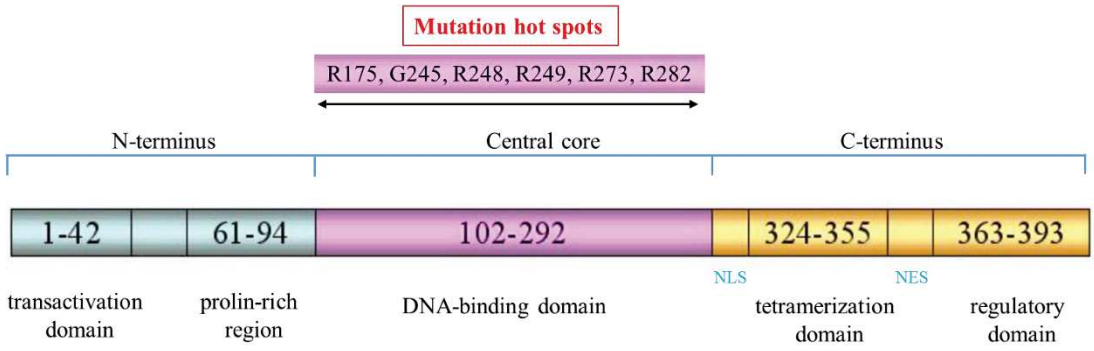

Figure 12. Schematic representation of p53 structure.

(Bai and Zhu, 2006).

4.2. Functions of p53: regulation of gene expression

The transcription factor p53 is implicated in tumour growth suppression and in induction of apoptosis and its transcriptional activity modulate genes involved in DNA repair, cell cycle arrest, apoptosis, and senescence. The p53 protein can mediate several of its downstream effects by repressing or activating its target genes. The significance of these activities for p53 function was demonstrated in a study in which the loss of growth inhibitory activity in mice results from the substitution of a gene encoding a transcriptionally inactive mutant p53 for the wild-type gene. In addition, the downstream effects of p53 such as induction of apoptosis are regulated by transcriptionally independent activities of the p53 protein (Yamada and Yoshida, 2019). The mechanisms governing these p53 functions include the trafficking of death receptors to the cell surface (Bennett et al., 1998), a direct role for p53 in the mitochondria (Marchenko et al., 2000) and the ability of p53 to regulate translation by directly binding to the 5′ untranslated region of certain mRNAs (Riley and Maher, 2007; Tournillon et al., 2017).

Studies have identified several p53-dependent target genes that play key role as downstream effectors for each p53 function (Vogelstein et al., 2000). The cyclin dependent kinase inhibitor p21Waf1/Cip1, for example, is a direct p53 target gene whose deletion significantly decreased the cell cycle arrest response to p53 (el-Deiry, 1998). Since apoptosis is preferred over cell

cycle arrest and senescence, upon the reactivation of p53, it becomes important to identify the target genes implicated in p53-triggered apoptosis. Although several studies demonstrated that the p53 protein can activate the expression of several genes that could participate in the apoptotic response, no single key effector has been identified. The p53 protein can induce the expression of proteins that target both intrinsic and extrinsic apoptotic pathways (Ke et al., 2016). The p53 protein can mediate the induction of mitochondria localized proteins such Bax, PUMA, NOXA, and p53AIP1, to trigger the permeabilization of the outer mitochondria membrane and the subsequent release of cytochrome c and the activation of Apaf-1/caspase-9 apoptosome (Hong et al., 2014; Ke et al., 2016). In addition, the p53 protein can also induces the expression of death-domain-containing protein PIDD and death receptors, such as Killer/DR5, Fas, which participate in the extrinsic apoptotic pathway (Ke et al., 2016). PERP a member of the PMP-22/gas3 family of proteins mainly localized to the endoplasmic reticulum and Golgi apparatus is another potential mediator of p53-induced apoptotic response (Attardi et al., 2000).

4.3. Keeping p53 under control

Being a potent inhibitor of cell growth and proliferation, the function of the p53 protein must be tightly regulated to allow for normal growth and development. This regulation is achieved through several mechanisms such as regulation of p53 transcription, translation, stability, subcellular localization and activity (Woods and Vousden, 2001). Most cellular stress cause rapid induction of p53 function through post-translational mechanisms that leads to p53 stabilization and activation.

4.3.1. Regulation of p53 stability

The MDM2 protein is one of the main regulators of p53; it can inhibit the transcriptional activity of p53 by acting as an E3 ubiquitin ligase that target p53 for proteasomal degradation. The ability of MDM2 to ubiquitinates both p53 and itself, results in rapid turnover of both proteins (Woods and Vousden, 2001). Since MDM2 is a transcriptional target of p53, increase in p53 activity results in increase in the expression of MDM2 the negative regulator of P53, thus generating an autoregulatory feedback loop (**Figure 13**). The significance of this regulatory loop was demonstrated in a study where the loss of MDM2 expression in mice, leads to an early embryonic lethality due to abnormally high p53-driven apoptosis. In addition, the normal development of MDM2 null mice in the absence of p53, demonstrates the importance of MDM2 as a negative regulator of p53 during development (de Rozieres et al., 2000). The induction of

p53 in response to cellular stress is usually through the inhibition of MDM2 function, via several independent pathways, based on the stress signal (Woods and Vousden, 2001). Mechanisms involved in the regulation of p53 degradation induced by MDM2 include post-translational modification of MDM2 and p53, regulation of the subcellular localization of p53 or MDM2, expression of proteins that inhibit MDM2 function and the direct repression of MDM2 expression. For instance, studies have shown that the DNA-damage-induced Checkpoint kinases(Chk1 and Chk2) phosphorylates a region in the amino terminus of p53 (**Figure 13**), resulting in a modification that prevents the interaction between p53 and MDM2, thereby preventing the degradation of p53 and ultimately stabilizing the p53 protein (Chehab et al., 2000; Shieh et al., 2000). On the contrary, stabilization of the p53 protein as a result of aberrant proliferation due to oncogene activation is independent of p53 phosphorylation, but requires the activation of ADP-ribosylation factor (ARF) protein, which can directly bind and inhibit MDM2 (Song et al., 2018). Defects in pathways that allow stress induced stabilization of p53 have been identified in several types of cancer expressing wild-type p53 (Dai and Gu, 2010; Woods and Vousden, 2001). Although, deregulations of the pathways that allow p53 stabilization can lead to tumour development, the finding that defects in response to stress signal such as oncogene activation may not stop the activation of p53 in response to a different signal such as DNA damage provides a bases for therapeutic intervention in a subset of human tumours (Hong et al., 2014).

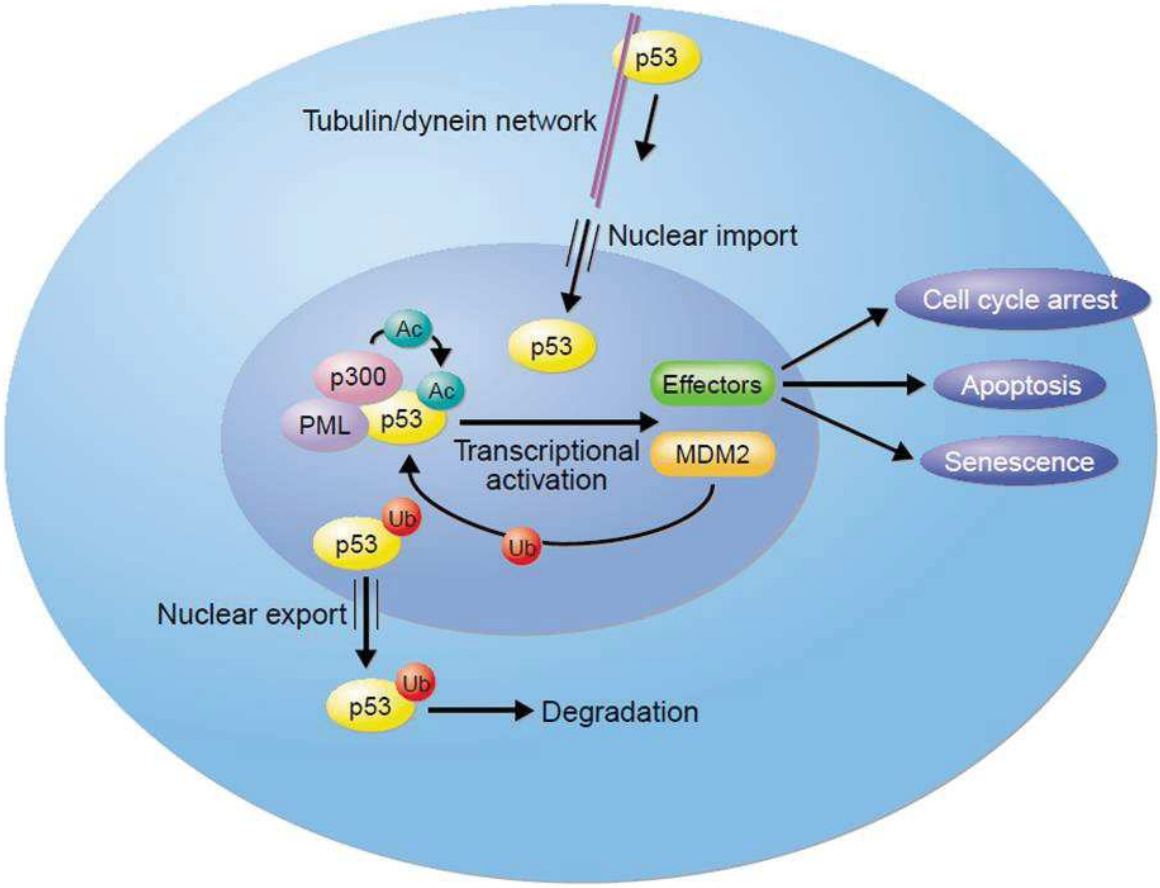

Figure 13.Regulating p53 subcellular localization, stability, and transcriptional activity. Although some degree of p53 degradation occur in the nucleus, nuclear export via ubiquitination is required for efficient p53 degradation (Ryan et al., 2001).

4.3.2. Regulation of p53 protein localization

Nuclear localization of p53 plays an important role in its function (**Figure 13)** and the main determinants of p53 nuclear localization; p53 nuclear import and nuclear export are tightly regulated (Vousden and Vande Woude, 2000). In nuclear import, p53 interacts with the molecular motor dynein and microtubule network, and it is actively transported towards the nucleus, where nuclear localization signals within the carboxyl terminus of p53 allow efficient nuclear import (**Figure 13**) (Giannakakou et al., 2000). Although the p53 protein also contain a nuclear export signal within its carboxyl terminus, efficient export of p53 from the nucleus to the cytoplasm is highly dependent on the ubiquitin ligase activity of MDM2 (Boyd et al., 2000). MDM2 ubiquitinates p53 within the carboxyl terminus of the p53 protein (**Figure 13)** (Rodriguez et al., 2000) and mutation of the lysine residues in the carboxy terminus have been shown to inhibits MDM2-dependent nuclear export of p53 (Nakamura et al., 2000; Ryan et al.,

2001). This ubiquitination which take place in the nucleus (Yu et al., 2000), may impact on the oligomerization status of p53 to activates its nuclear export to the cytoplasm (**Figure 13**) (Roth et al., 1998). Studies have shown that the loss of p53 activity in several tumour expressing wild-type p53 is associated with failure of p53 to accumulate in the nucleus. These could results from proteasomal degradation or cytoplasmic sequestration, due to interactions with the glucocorticoid receptor (Sengupta et al., 2000). Therefore, the restoration of nuclear localization of p53 represent a therapeutic potential in tumours expressing wild-type p53 (Lu et al., 2000).

4.3.3. Regulation of p53 activity

The binding of p53 to DNA which enable it to function as a transcription factor is regulated by posttranslational modification (Zhu, 2017). Posttranslational modifications including phosphorylation (Meek, 1999), sumoylation (Rodriguez et al., 1999) and acetylation (Gu and Roeder, 1997) which occur within the carboxyl terminus of p53 have been shown to enhance p53 sequence-specific DNA binding and transcriptional activities in response to cellular stress (**Figure 13**). Acetylation can regulate p53 activity via three main mechanism: (i) it promotes p53 stabilization by excluding ubiquitination on the same site, (ii) it inhibits the formation of HDM2/HDMX repressive complexes on target gene promoters, and (3) it recruits cofactors for the promoter-specific activation of p53 transcriptional activity (Zhu, 2017).

Studies have correlated p53 acetylation to p53 activation during DNA damage response (Zhu, 2017). Histone acetyltransferases, such as p300/CBP and pCAF can binds within the amino terminus of p53 to mediate the acetylation of lysine in its carboxyl terminus (Gu and Roeder, 1997; Liu et al., 1999). Enhanced p53 activity is obtain when phosphorylation within the amino terminal region of p53 increases its interaction with acetyltransferases, to generate a phosphorylation/acetylation cascade (Sakaguchi et al., 1998). Comparatively, p53 function is inhibited by reduction in p53 acetylation, which could result from either direct binding of p53 to a deacetylase complex (Luo et al., 2007) or MDM2-mediated inhibition of the acetyltransferases (Kobet et al., 2000). ARF activates p53 by preventing the inhibition of p53 acetylation by MDM2 (Ito et al., 2001). The localization of this protein to nuclear bodies with p53 and CREB-binding protein (CBP), results in the phosphorylation and acetylation of p53 at the amino-terminal and carboxy-terminal, respectively.

In addition to complete regulation of p53 transcriptional activity, post-translational modification of p53 is also involved in defining the choice of cellular responses resulting from

p53 activation. Although this choice is tightly regulated by the cell environment, cell type and genetic alterations, differential activation of distinct groups of p53 target genes by p53 participates in the choice to induce either apoptosis or cell cycle arrest (Vousden and Vande Woude, 2000).

Although, p53 phosphorylation at Ser46 induced the expression of the apoptotic target gene p53AIP1, leading to apoptotic cell death, the function of p53 in cell cycle arrest is not dependent on p53 phosphorylation at Ser46 (Oda et al., 2000b). Phosphatase Wip1, a transcriptional target of p53 inhibits p53-mediated apoptosis by attenuating UV-induced p38-MAPK (mitogen-activated protein kinase) mediated phosphorylation of Ser46 in p53 (Takekawa et al., 2000). The presence of transcription factors, such as NF-κB (Ryan et al., 2000), and co-activators, such as Junctional and regulatory protein (JMY) (Shikama et al., 1999), may allow discrimination in the choice of activating apoptosis or cell cycle arrest.

Cell cycle and apoptotic responses can also be independently regulated through regulation of transcriptional repression by p53. The interaction of p53 with mSin3a and histone deacetylases leads to transcriptional repression that favours apoptotic activity (Murphy et al., 1999). The MDM2 protein directly inhibits both transcriptional activation and repression by p53, upon its binding to the amino-terminal transactivation domain of p53. In addition retinoblastoma protein (pRB), a tumour suppressor protein can form trimeric complex with p53 and MDM2, to prevent the degradation of p53 (Hsieh et al., 1999).

4.4. Cellular response induced by p53

4.4.1. Cellular senescence

Definitions and biochemical properties

First described in 1961 (Hayflick and Moorhead, 1961), cellular senescence is a process that prevent most cells from undergoing continuous division (Lundberg et al., 2000). It is a stable form of cell cycle arrest in which cells lack the ability to reinitiate the cell cycle in response to external stimuli, such as growth factors except after transformation (Cristofalo et al., 1989; Wang, 1995). Despite their non-proliferative state, senescent cells remain metabolically active and viable (Matsumura et al., 1979).

Basically, there are two types of cellular senescence: replicative senescence (RS) and stress-induced premature senescence (SIPS) (de Magalhães and Passos, 2018). Replicative senescence is spontaneously achieved by somatic cells and it depends on the number of completed cell divisions by the cell. This type of senescence is an unavoidable consequence of genome duplication that is controlled by telomere shortening (Martens et al., 2000; Wang et al., 2019). On the other hand, stress-induced premature senescence is the type of senescence that is caused by cellular stress such as DNA damage, cytotoxic drugs, oncogene activation, and oxidative stress (**Figure 14**). Although stress-induced premature senescence shares several molecular and functional features with replicative senescence, it is independent of telomere status (Goligorsky and Hirschi, 2016; Wang et al., 2019).

Currently, there is no single specific biomarker for senescent cells because they do not express one specific biomarker. However, some features and molecular markers, which represents the hallmarks of senescence, have been used to identify senescent cells. Senescent cells are usually enlarged with flattened morphology and display positive staining for β-galactosidase activity at pH 6 (Dimri et al., 1995). The β-galactosidase (SA- β -gal) produced by senescent cells can catalyse the substrate X-Gal at pH 6, to form a dark blue product, which can easily be observed using optical microscope. Studies have associated the inability of senescent cells to proliferate in a pro-mitogenic environment with increased expression of cell cycle inhibitors such as p21WAF1/CIP1, p16INK4a, and hypo-phosphorylated retinoblastoma gene (pRb) (Childs et al., 2015; Lundberg et al., 2000). In addition, senescent cells display high plasminogen activator inhibitor-1 (PAI-1), expression of p19ARF, p53 as well as chronic DNA damage response with DNA damage foci (Hewitt et al., 2012) and senescence-associated secretory phenotype (SASP) (Wang et al., 2019).

Several studies have shown that cellular stress such as telomere erosion, certain DNA lesions and reactive oxygen species (ROS) can induce cellular senescent in vitro via activation of DNA damage response (DDR), a signalling pathway in which ATM or ATR kinases block cell-cycle progression via transcriptional activation of the cyclin-dependent kinase (Cdk) inhibitor p21 and the stabilization of p53 (Nardella et al., 2011; Sedelnikova et al., 2004; von Zglinicki, 2002). In addition, activated oncogenes such as Ras acts via the suppression of nucleotide metabolism and overexpression of cell division control protein 6 (Cdc6) to cause aberrant DNA replication, leading to the formation of double stranded DNA breaks (DSBs) and the activation of DNA damage response pathway (Di Micco et al., 2006; Noushmehr et al., 2010). These cellular stress acts through the activation of p53 and p16Ink4a. Upon activation, p53 induces

p21, which inhibit cyclin E–Cdk2 to induce a temporal cell-cycle arrest. On the other hand, p16Ink4a inhibits cell-cycle progression by targeting cyclin D–Cdk4 and cyclin D–Cdk6 complexes. Both p16Ink4a and p21 act by preventing the inactivation of Rb, thus resulting in continued repression of E2F target genes required for S-phase onset (Wang et al., 2019). The type of stress that activate p53 through DNA damage response signalling are indicated with grey text and arrows. Upon severe cellular stress (red arrows), cells undergoing cell cycle arrest transition into senescent cells. While cells exposed to mild damage that can be successfully repaired resume normal cell-cycle progression, cells exposed to moderate stress that is chronic in nature or that leaves permanent damage resume proliferation through reliance on stress support pathways (green arrows). This phenomenon termed assisted cycling is achieved through p53-mediated activation of p21. Suggesting that the p53–p21 pathway can either synergize or antagonize with p16Ink4a in senescence depending on the type and level of stress (Wang et al., 2019).

On the contrary senescence due to E2F3 activation or c-Myc inhibition is independent of DNA damage response but rather it involves p19Arf and p16Ink4a (Lazzerini Denchi et al., 2005; Nardella et al., 2011). BRAF(V600E) is also independent of DNA damage response and induces senescence through a metabolic mechanism involving upregulation of mitochondrial pyruvate dehydrogenase (PDH). Furthermore, inactivation of the tumour suppressors RB, PTEN, NF1 and VHL have been reported to trigger cellular senescent (Nardella et al., 2011; Shamma et al., 2009). RB inactivation is dependent on DNA damage response. However inactivation of PTEN, NF1 and VHL are independent of DDR and act through p19Arf and p16Ink4a (Shamma et al., 2009).

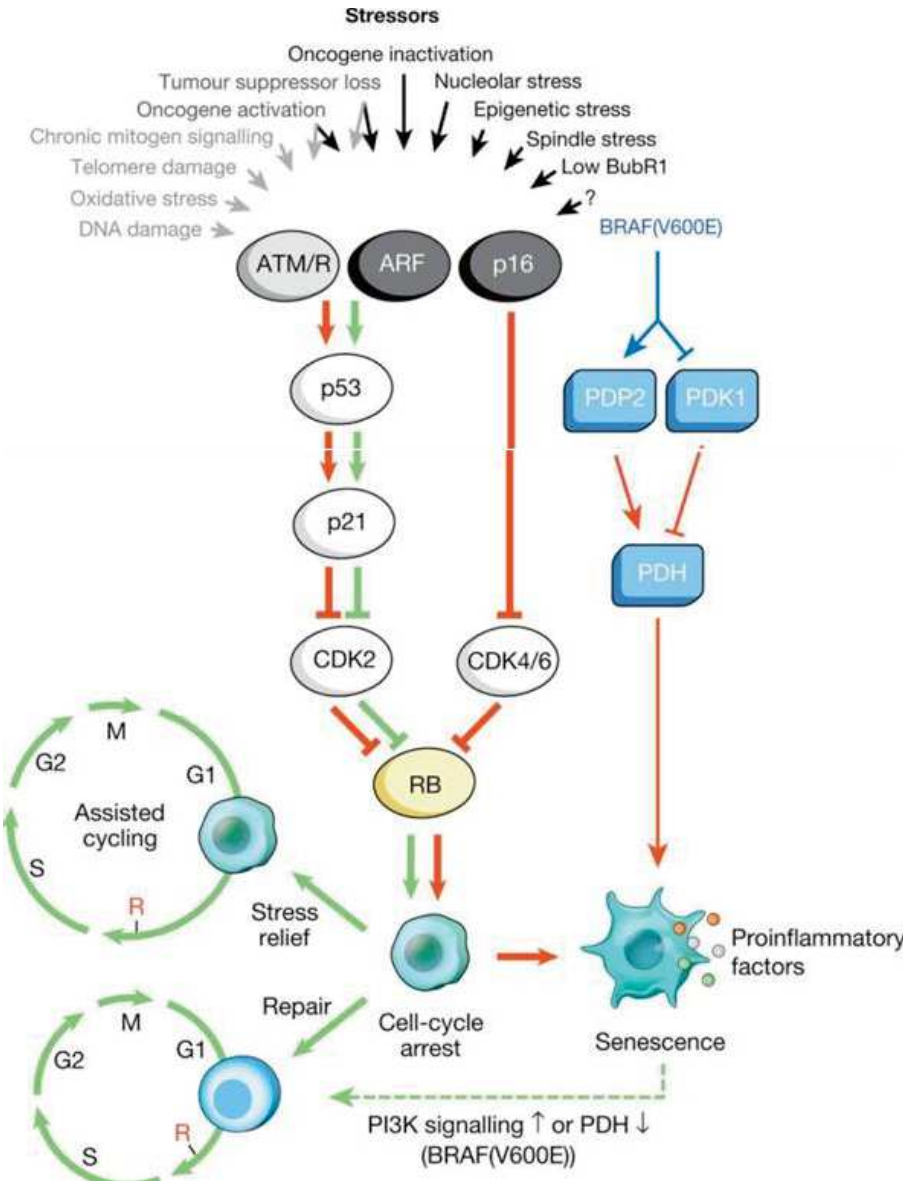

Figure 14. Schematic representation of senescence-inducing stimuli and main effector pathways.

Cells undergoing senescence induce an inflammatory transcriptome regardless of the senescence inducing stress (coloured dots represent various SASP factors). Red and green connectors indicate 'senescence-promoting' and 'senescence-preventing' activities, respectively, and their thickness represents their relative importance. The dashed green connector denotes a 'senescence-reversing' mechanism (Wang et al., 2019).

4.4.2. Apoptosis

First used in 1972 to describe a morphologically unique type of cell death (Kerr et al., 1972). Apoptosis is now known as a programmed or controlled cell death in which the cellular contents are not spilled into the surrounding environment. The activation of cysteine-aspartic proteases (caspases) initiates the apoptotic process. These caspases are of two types: the initiator caspases and the executioner caspases (Elmore, 2007). Upon cellular damage, inactive procaspases are activated into the initiator caspases (caspases 8 and 9) which proceed to activate the executioner caspases (caspases 3, 6 and 7). Upon activation, the executioner caspases initiate a cascade of events leading to DNA fragmentation as a result of activation of endonucleases, crosslinking of proteins, expression of ligands for phagocytic cells and the formation of apoptotic bodies (Poon et al., 2014).

Generally, apoptosis is different from other types of cell death based on its incidence, biochemistry, and morphology. Specific alterations in the morphology of apoptotic cells include nuclear condensation and fragmentation, cell shrinkage, dynamic membrane blebbing, and loss of adhesion to neighbouring cells and the extracellular matrices. Biochemical alterations in apoptosis include chromosomal DNA cleavage into internucleosomal fragments, activation of a family of proteases known as caspases and phosphatidylserine externalization (Ouyang et al., 2012). Apoptosis can be initiated when the cell detects damage via several intracellular sensors (the intrinsic pathway of apoptosis) or may occur as a result of the interaction between a damaged cell and a cell of the immune system (extrinsic pathway of apoptosis) (Oppenheim et al., 2001). An estimated 1×10^9 cells in human body undergo apoptosis per day (Elliott and Ravichandran, 2010).The two distinct but converging, pathways to apoptosis (intrinsic and extrinsic pathways of apoptosis) work synergistically to ensure good health in multi-cellular organisms through removal of defective cells from the body. Failure in the regulation of apoptosis may result in pathological conditions. In the degenerative diseases Alzheimer for example, neuronal death is initiated by the activation of important caspases that are involved in apoptosis (Dickson, 2004). However, insufficient apoptosis, can lead to uncontrolled growth and cell division as seen in cancer (Goldar et al., 2015). One of the most important roles of the p53 protein is its ability to activate apoptosis via both transcription-dependent and transcription-independent ways. The tumour suppressor protein p53 is a cellular gatekeeper and a key player in apoptosis where it is involved in both the intrinsic and extrinsic pathways of apoptosis. It can initiate apoptosis through mitochondrial depolarization and sensitization of cells to inducers of apoptosis (Hofseth et al., 2004).

a. Intrinsic apoptotic pathway

The intrinsic apoptotic pathway also known as the mitochondrial or stress pathway is mainly regulated by a family of proteins known as B-cell lymphoma 2 protein (BCL-2) family (BCL 2), which control the release of cytochrome c from the mitochondria (Monian and Jiang, 2012). The Bcl-2 family of proteins is made up of 25 pro-apoptotic and antiapoptotic members and the maintenance of good cell health depends on the balance between the pro apoptotic and anti-apoptotic Bcl-2 proteins (**Figure 15).**

The Bcl-2-family members usually have one or more Bcl-2 homology (BH) domains. Members containing the BH1, BH2, BH3, BH4 BCL-2 homology domains (BCL-2, BCL-XL, BCL-w, MCL-) and A1 are anti-apoptotic and their anti-apoptotic function depends on their ability to directly bind and inhibit pro-apoptotic proteins via protein-protein interactions (Czabotar et al., 2014). The pro-apoptotic family members are subdivided into two subgroups, based on the presence of BH1, BH2 and BH3 BCL-2 homology domains into effector proteins BAK, BAX or the presence of only the BH3 domain, including BID, BIM, PUMA, NOXA, BIK, BAD, HRK, and BMF (Chipuk et al., 2004; Czabotar et al., 2014). Furthermore, members of the BH3-only are subdivided based on their ability to interact with either the anti-apoptotic BCL-2 proteins or both the effectors and anti-apoptotic proteins. The BH3-only proteins such as BAD, BIK, NOXA that binds only to anti-apoptotic proteins are known as sensitizer, while other BH3-only proteins such as BID and BIM that bind both anti-apoptotic members and effectors (BAX and BAK), to induce the oligomerization of BAK and BAX are known as direct activators (Chipuk and Green, 2008; Haupt et al., 2003). While some studies categorized PUMA as sensitizer (Kuwana et al., 2005), others have demonstrated that PUMA can directly activate BAX (Cartron et al., 2004; Gallenne et al., 2009).

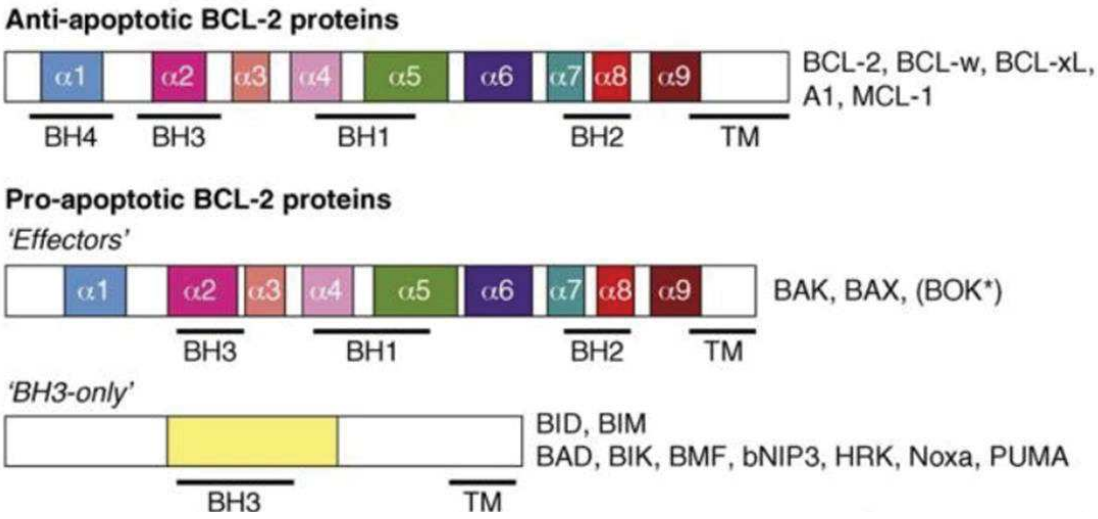

Figure 15. BCL-2 related
The BCL-2 family is divided into three groups according to their homology in BCL-2 domains. Known α-helical transmembrane regions are indicated. The anti-apoptotic members such as BCL-2, BCL-X_L, BCL-w, MCL-1 and A1 comprise four BCL-2 homology domains(BH1, BH2, BH3 and BH4).The pro-apoptotic members termed as effectors including BAX and BAK, contain BH1, BH2 and BH3 domains. The BH-only pro-apoptotic proteins, such as BID, BIM,BAD, BIK, NOXA, PUMA and others, contain only BH3 domain (Chipuk and Green, 2008).

The initiation of cell death in BCL-2-regulated apoptotic pathway is usually through transcriptional and/or posttranscriptional upregulation of the pro-apoptotic BH3-only members of the BCL-2 protein family such as PUMA, BAD, NOXA, BIM, BID, BMF, BIK and HRK which bind and inhibit the pro-survival BCL-2 proteins such as BCL-2, BCLXL, MCL-1, BCL-W and A1/BFL1, thus resulting in the release of the cell death effectors BAX and BAK. Some BH3-only proteins have been reported to directly activate BAX/BAK (Green, 2005; Youle and Strasser, 2008). BAX and BAK can undergo homo-oligomerize into proteolipid pores upon activation, leading to increased permeability of the outer mitochondrial membrane and subsequent release of cytochrome c and other mitochondrial proteins such as endonuclease G, apoptosis-inducing factor (AIF) , Smac/DIABLO and serine protease (Omi/HtrA2) (Acehan et al., 2002; Chipuk et al., 2006). Cytochrome c binds to the WD domain of APAF1 monomers, to induce conformational change in APAF1 that expose its nucleotide binding domain, oligomerization domain, caspase recruitment domain (CARD domain) and oligomerization domains which allows several APAF1 to form a complex called apoptosome (Acehan et al., 2002). Several exposed CARD domains in the open centre of the apoptosome recruit and

activate several procaspase 9 proteins. The activated initiator caspase-9 catalyse the proteolytic maturation of effector caspases such as caspase 3, 6, and 7, which can fully induce apoptosis in the form of active caspase 3 (**Figure 16**) (Cain et al., 2002).

P53-mediated induction of apoptosis involves transcriptional activation of multiple pro-apoptotic target genes. The P53 protein can transactivates pro-apoptotic BCL-2 related proteins such as BAX (Miyashita and Reed, 1995), PUMA (Nakano and Vousden, 2001) NOXA (Oda et al., 2000), and BID (Sax et al., 2002) all of which are important molecules in the intrinsic pathway. In addition, the p53 protein can also activate the expression of adapter protein apoptotic protease activating factor 1 (APAF1), the scaffold protein for caspase-9 activation (Moroni et al., 2001)**.** The genes Puma and Noxa are both direct p53 targets and they encode the pro-apoptotic BH3- only proteins (Han et al., 2001; Nakano and Vousden, 2001; Oda et al., 2000a). The p53 protein can directly upregulate these genes. The over of expression these genes in cell lines results in rapid apoptosis while knockdown protects against cytotoxic stimuli that trigger apoptosis in a p53-dependent manner. For example, studies using gene-targeted mice demonstrated that PUMA and to a lesser extent NOXA are important for p53- mediated apoptosis in different cell types (Nakano and Vousden, 2001; Oda et al., 2000a) The p53 protein has been demonstrated to trans-repress BCL-2 anti-apoptotic genes such as MCL-1 (Pietrzak and Puzianowska-Kuznicka, 2008) and BCL-2(Wu et al., 2001). In addition, BCL-2 non-related anti-apoptotic proteins expression can also be repressed by p53. An example is the repression of the negative regulator of apoptosis survivin by p53 (Hoffman et al., 2002). The p53 protein triggers apoptosis by inducing the transcription of DR-5, BAX, BAK, NOXA, PUMA and through the inhibiting the transcription of anti-apoptotic genes such as Bcl-2 and survivin. The cytoplasmic interaction of p53 with the anti-apoptotic Bcl-2 family proteins in the mitochondria induces the release of apoptogenic factors such as cytochrome c from the mitochondrial outer membrane. Furthermore, the p53 protein can directly interact with BAX and/or BAK resulting in their activation. Activated BAX and BAK undergo homo-oligomerize into proteolipid pores, that results in increased permeability of the outer mitochondrial membrane and subsequent release of cytochrome c (Goldar et al., 2015)

b. Extrinsic death receptor pathway

In the extrinsic apoptotic pathway, signalling is initiated by the attachment of extracellular ligands, such as Fas ligand (Fas-L), tumour necrosis factor (TNF), and TNF-related apoptosis-inducing ligand (TRAIL) to death receptors such as type 1 TNF receptor (TNFR1), Fas (also

called CD95/Apo-1) and the TRAIL receptors (**Figure 16**) (Guicciardi and Gores, 2009; Jin and El-Deiry, 2005). The death receptor becomes activated upon binding of ligand and it can bind to a corresponding protein motif in adapter proteins such as Fas-associated death domain (FADD) and TNF receptor-associated death domain (TRADD) via its intracellular death domain. The protein interaction domain known as the Death Effector Domain (DED) is also present in these adaptor proteins. The DED in pro-caspase-8 and 10 can interacts with the DED of FADD (Khosravi-Far and Esposti, 2004) to generate a death inducing signalling complex (DISC), that results in the auto-catalytic activation of procaspase-8 and 10 (Boatright et al., 2003). The active caspase-8 and 10 further activates effector/executioner caspases such as caspase 3,6 and 7, which can fully induce apoptosis in the form of active caspase 3 (Jin and El-Deiry, 2005). The extrinsic apoptotic pathway is also regulated by p53 but the overall contribution of this regulation to p53-mediated cell death is poorly understood. The p53 protein activates this pathway through the stimulation of genes transcription of transmembrane proteins such as FAS (Müller et al., 1998). In addition, the overexpression of p53 has been reported to enhances the levels of FAS in the cell membrane by promoting trafficking of the FAS receptor from Golgi apparatus (Bennett et al., 1998).

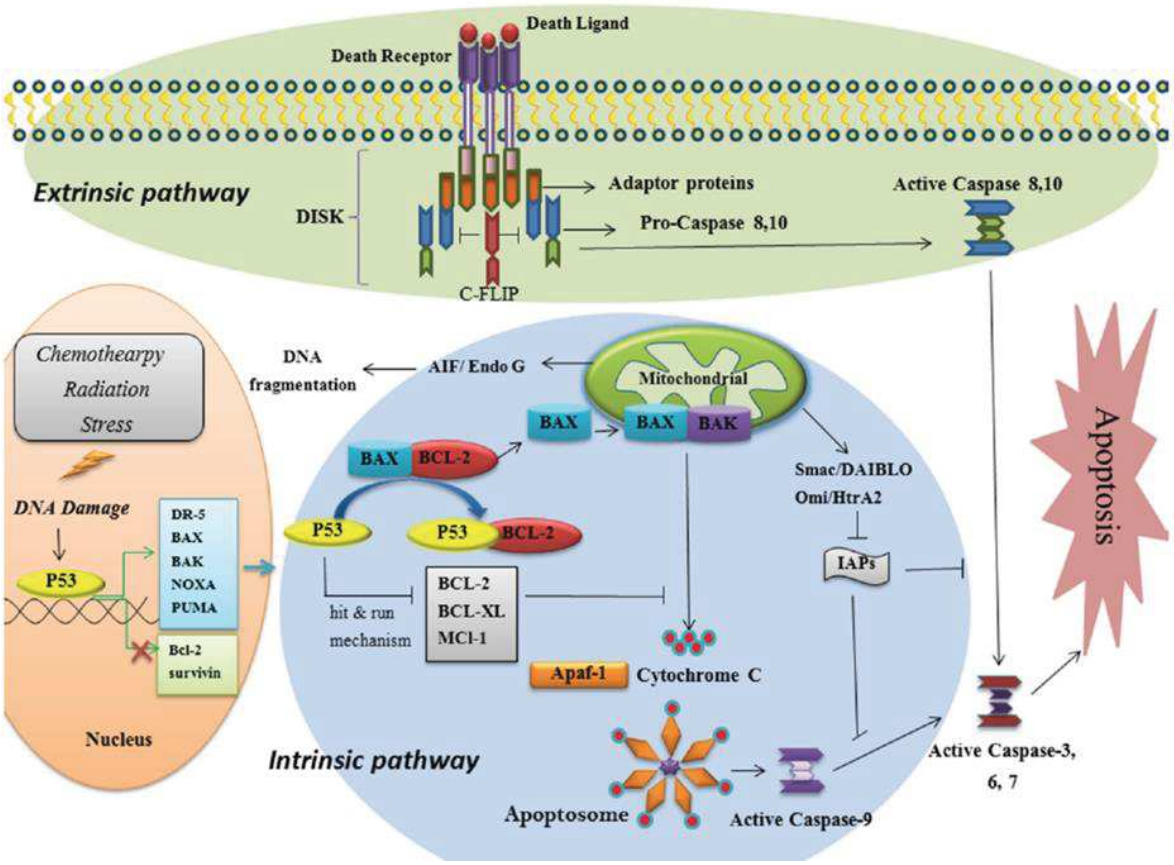

Figure 16. Diagrammatic representation of the intrinsic, extrinsic apoptotic pathways.

Apoptosis is executed through two central apoptotic pathways, the extrinsic and the intrinsic pathways. The two pathways converge on the same execution caspase. The extrinsic pathway is initiated upon the attachment of extracellular ligands to the extracellular domain of transmembrane receptors, the intrinsic apoptotic pathway is initiated by several intracellular stimuli (Goldar et al., 2015).

4.5. The role and deregulation of p53 in glioblastoma

4.5.1. P53 is implicated in GBM progression

In normal cells, the p53 protein is present at low concentration but accumulate in the nucleus and becomes activated in response to cellular stress such as oxidative stress, nutrient deprivation, hypoxia, DNA damage, telomere attrition, oncogene expression, and ribosomal dysfunction (**Figure 17**) (England et al., 2013). Upon activation, the p53 protein exerts its tumour suppressor activity primarily by altering the expression of several genes involved in cell cycle arrest, apoptosis, stem-cell differentiation (Leroy et al., 2013) and cellular senescence (Lin et al., 2005). These responses depend on the cell type and cellular stress, for example, DNA damage might result in growth arrest to allow for repair of the damage cells, or permanent removal of these cells from the organism by apoptosis (Leroy et al., 2013). Either responses would prevent damaged cells from proliferating and passing mutations to the next generation (Vousden and Lu, 2002). TP53 mutation in glioblastoma is oncogenic in nature (Zheng et al., 2008) and is associated with glioblastoma progression (Krex et al., 2003). Inactivation of p53 has been correlated with a phenotype that is more proliferative, more invasive, more stem-like and less apoptotic (England et al., 2013; Zhang et al., 2018; Zheng et al., 2008).

4.5.2. The p53 pathway is frequently deregulated in GBM

The tumour suppressor p53 is a transcription factor that is mutated in 50% of all tumours, where its mutation contribute to tumour progression (Lane and Benchimol, 1990). However, in many other tumours including glioblastoma, the p53 protein is present in its wild-type form, but this wild type p53 may also be inactivated by deletion of one or both p53 alleles, nonsense or splice site mutations in the OD, amplification of the MDM2 gene, deletion of the ARF gene, or mis localization of p53 to the cytoplasm (Lane and Benchimol, 1990). Dysregulation of the p53 pathway in glioblastoma, is found in 85.3% of primary glioblastoma, with 27.9%, 57.8% and 15% caused by missense mutations or homozygous deletion of p53, deletion of cyclin-dependent kinase inhibitor 2A (CDKN2A) and amplification of mouse double minute homologs respectively (Brennan et al., 2013).

4.5.2. MDM2 and MDM4 are amplified in glioblastoma and negatively regulate p53

MDM2 and its homologue MDM4 act as oncogenic inhibitors of the tumour suppressor protein p53 by targeting it for proteasomal degradation (Crespo et al., 2015; England et al., 2013). P53 induced the transcription of MDM2, creating a p53-MDM2 negative feedback loop that regulate

the expression of MDM2 and the activity of p53 (Crespo et al., 2015). Overexpression of MDM2 in a variety of human tumours, including glioblastoma, impairs p53 wild-type function and deregulates the p53-MDM2 feedback loop, leading to loss of several tumour suppressor functions of p53, including growth arrest, apoptosis, DNA repair, and senescence (England et al., 2013; Verreault et al., 2016). Targeting the p53-MDM2 complex is considered a promising treatment approach to reactivate the p53 pathway in tumours harbouring p53 wildtype (Klein and Vassilev, 2004). Studies on the assessment of chromosomal imbalance using array comparative genome hybridization and whole genome amplification-DNA from two to five separate tumour areas of 14 primary glioblastomas, showed a list of genetic alterations including amplifications in 1q32.1(MDM4) and12q15(MDM2), that were common to all tumour areas analysed (Sumihito et al., 2010). MDM2 is frequently amplified in glioblastoma cell lines expressing p53 wild type (He et al., 1994) and data from TCGA showed that, MDM2 and MDM4 amplifications occurs in 14% and 7% of glioblastoma, respectively (Crespo et al., 2015).

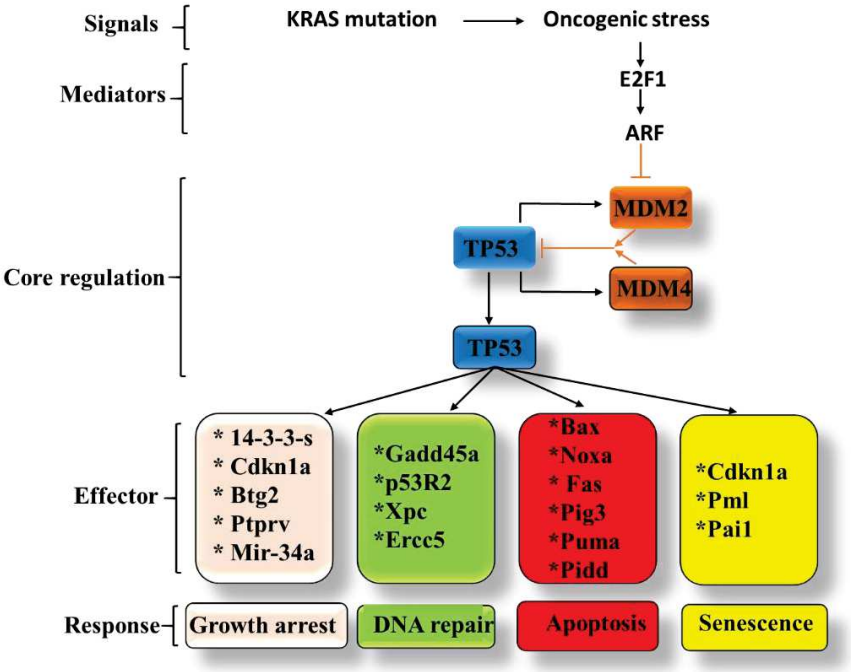

Figure 17. The p53-ARF-MDM2/4 pathway.

In response to cellular stress and/or DNA damage, pathway mediators, such as ARF, are activated. MDM2 and MDM4 mark p53 for degradation and are subsequently degraded when upstream mediators are activated. This releases p53 from degradation, and leads to increased cell cycle arrest, apoptosis, DNA Repair, and cellular senescence (Leroy et al., 2013).

4.6. P53-targeted therapies

The frequent dysregulation of the p53 pathway and the vital role it plays in various cancer including glioblastoma underscore the importance of reactivating the p53 pathway (either by reactivating wildtype p53 or restoring the wild type p53 function of mutant p53) for cancer therapy (Muller and Vousden, 2014; Vassilev, 2004). Generally, the diverse p53 activators can be grouped into two main categories depending on the mechanism of action: molecules that activate wild-type p53 and molecules that restore wild-type function of mutant p53 or degrade mutant p53 (**Figure 18).**

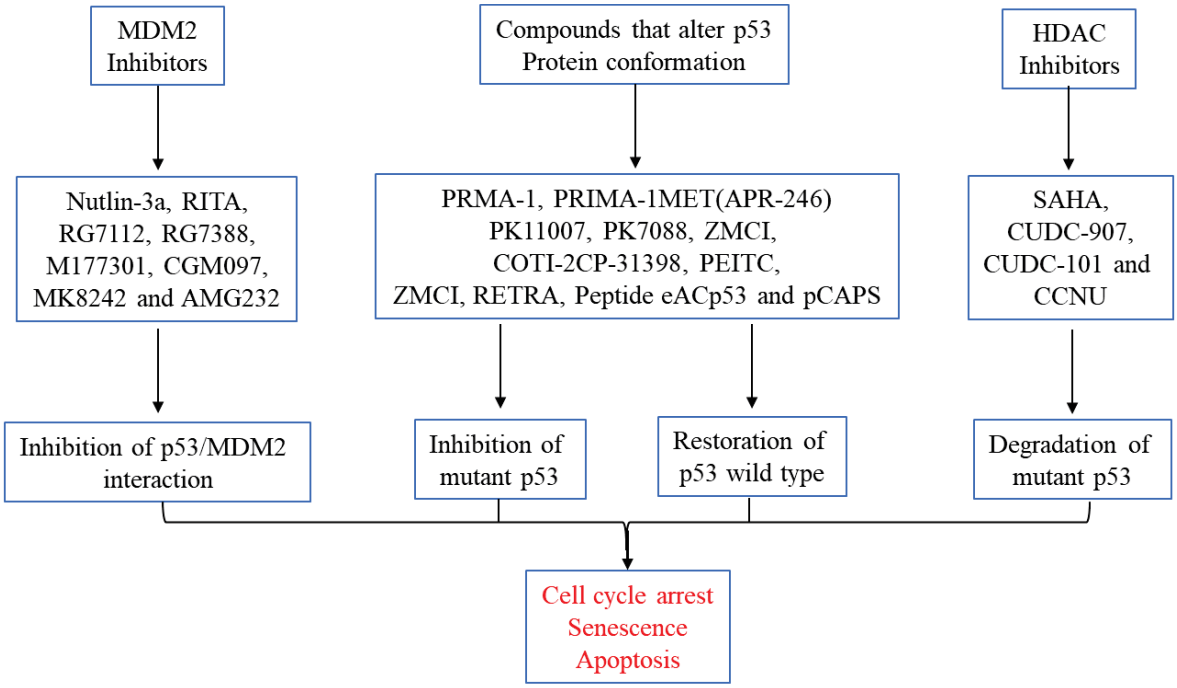

Figure 18. Summary of selected strategies for the therapeutic targeting of p53 in GBM. Approaches include restoration of wild type p53 activity or degradation of mutant p53 (Zhang et al., 2018).

4.6.1. Small molecule wild type p53 activators

One of the earliest strategies in the treatment of tumours expressing wild type p53 is the search for MDM2 inhibitors that interact with the p53-binding pocket of MDM2 to prevent degradation of p53 by MDM2 (Chène, 2003). MDM2, a zinc finger nuclear phosphoprotein is an E3 ubiquitin ligase that controls the cellular levels of p53. In unstressed conditions, MDM2

maintains low levels of p53 by targeting it for proteasomal degradation. However, in response to cellular stress, both MDM2 and p53 undergo post-translational modifications that impair their interaction, allowing p53 to accumulate and exert its tumour-suppressive functions (Gupta et al., 2019). The frequent overexpression of mdm2 gene in glioblastoma results in p53 inactivation, cancer cell proliferation and survival (Crespo et al., 2015; England et al., 2013; Gupta et al., 2019; Verreault et al., 2016).

Several efforts have been made to develop small molecule inhibitors of the p53-MDM2 interaction. A high-throughput screening of a library of synthetic compounds, lead to the discovery of the first specific and potent small-molecule inhibitor of MDM2, Nutlin-3a which bind the hydrophobic p53-binding pocket of MDM2 at nanomolar concentrations to block the p53-MDM2 interaction (Gupta et al., 2019; Vassilev, 2004). Treatment with Nutlin-3a induced a non-genotoxic stabilization of p53 protein and subsequent activation of the p53 pathway in cancer cells expressing wild-type p53 (Klein and Vassilev, 2004). Optimization of this novel imidazolines through chemical modifications that replaced the methoxy group with a tert-butyl group, results in the Nutlin-3a analogue RG7112, a more potent MDM2 inhibitor with improved metabolic stability and good pharmacologic characteristics (Tovar et al., 2013). A preclinical evaluation, showed that RG7112 restored p53 activity, crossed the blood–brain, reduced tumour growth and increased animal survival in MDM2-amplified TP53 wild-type glioblastoma xenografts (Verreault et al., 2016). RG7112 was the first small-molecule p53−MDM2 inhibitor in clinical trials (Ding et al., 2013; Vu et al., 2013). The discovery of RG7388 (Idasanutlin), was reported, shortly after the development of RG7112 (Ding et al., 2013). Idasanutlin, is a p53-MDM2 inhibitor, with similar activation of the p53 pathway as RG7112, but with far more potency, selectivity, and better pharmacokinetic profile. RG7388 activates p53 at a significantly reduced concentration than RG7112 in both in vitro and in vivo condition (Ding et al., 2013). The approval of Idasanutlin, for a phase III clinical study to compare its combination with cytarabine or cytarabine alone in patients with relapsed or refractory AML (NCT02545283), makes it the first small molecule p53 activator that has progressed the furthest in a clinical trial setting (Khurana and Shafer, 2019). This success story served as a proof of principle that rational design of MDM2 inhibitors is an attractive and viable option for cancers harbouring p53 wild type (about 50% of all cancer) (Zhang et al., 2018). To date, several other chemical classes of MDM2 inhibitors have been developed (**Figure 18**).

Activation of p53 wild type can also be achieved using small molecules such as RITA, that directly binds to p53 and disrupt p53-MDM2 interaction (Issaeva et al., 2004). RITA

(reactivation of p53 and induction of tumour cell apoptosis) is a thiophene derivate, identified in a screen for compounds with growth-suppressive effects in cancer cells expressing wtp53 (Issaeva et al., 2004). RITA has been reported to prevent p53-MDM2 interaction in vitro and in vivo, induced expression of p53 target genes and massive apoptosis in various tumour cell lines expressing wild-type p53 (Weilbacher et al., 2014). Although both Nutlin-3a and RITA target the p53/MDM2 interaction, the effects on p53 activity are different. While RITA-activated p53 mainly affects genes related to apoptosis, Nutlin-3a mainly induce cell cycle regulators and functions only in cells expressing p53 wild type. Unlike Nultin-3, RITA can induce apoptosis through p38 and JNK/SAPK not only in tumour cells harbouring p53 wild type but also in p53 mutant and in p53-null cells (Weilbacher et al., 2014).

4.6.2. Targeting mutant p53 for therapy

Several strategies have been explored to target mutant p53 for cancer therapy. While some strategies use small molecules that directly target mutant p53, to induce its degradation or restore its wild type function, other strategies exploits tumour addiction to mutant p53 gain of function targeting pathways, induced by gain-of-function p53 mutants.

4.6.2.1. Restoration of p53 wild type conformation and function

TP53 mutations in glioblastoma are mostly point mutations that lead to high expression of gain of function (GOF) oncogenic variants of the p53 protein (Zhang et al., 2018). Efforts to rescue mutant p53 is directed towards the development of drugs that promote conformational change in mutant p53 folding, thereby restoring the wild type p53 function of mutant p53 (Pitolli et al., 2019). A wide range of compounds have been developed for the restoration of wild type p53 function of mutant p53 in various cancers, including glioblastoma (Zhang et al., 2018). Functional screening of NCI drug library in cancer cells based on their capacity to restore wild type function from select p53 missense mutants, lead to the discovery of PRIMA-1. It is one of the most efficient molecules for p53 restoration, it interact with the cysteine residues of mutant p53 protein causing it to refold into a wild type p53 conformation (Lambert et al., 2009). PRIMA-1, also restored the wild type p53-like transcriptional activity and induce the expression of the p53 target genes BAX, NOXA and PUMA (Lambert et al., 2009), leading to cell cycle arrest and apoptosis (Zhang et al., 2018). The more potent and less toxic methylated analogue of PRIMA-1, PRIMA-1^{Met} (APR-246) have been shown to inhibit cell growth and stemness and induce apoptosis in glioblastoma (Patyka et al., 2016). Both PRIMA-1 and PRIMA-1^{MET} (APR-246) have been shown to inhibit tumour growth in mouse models of GBM (Zache et al.,

2008). Phase I/IIa clinical trial for PRIMA-1^{MET} (APR-246) has been completed in patients with prostate cancer and haematological malignancies (Zhang et al., 2018). Peptides that bind to different p53 regions to restore wild type function of mutant p53, have also been developed. For example, the peptides, pCAPs, restored normal p53 conformation and function, and showed tumour regression in mouse xenografts of colorectal, ovarian, and breast cancer (Tal et al., 2016).

4.6.2.2. Degradation of Mutant p53

Compare to wild type p53, Mutant p53 are highly stable due to interaction with the Histone deacetylase 6/ Heat Shock 90kD Protein 1 (HDAC6/Hsp90) chaperone complex that prevent its degradation mediated by MDM2 E3 ubiquitin ligase (Alexandrova and Moll, 2017; Li et al., 2011). To promote mutant p53 degradation, compounds are being developed to disrupt the HDAC6/HSP90 complex. For example, the HDAC inhibitor SAHA is able to promote proteasome-dependent degradation of mutant p53 (Alexandrova et al., 2015; Li et al., 2011; Pitolli et al., 2019).

4.6.2.3. Targeting mutant p53 GOF

Gain of function mutation (GOF) acquired by mutant p53 proteins contribute to tumour development and progression by activating cell migratory pathways capable of stimulating migration, invasion, and metastasis. The inhibition of downstream pathways triggered by mutant p53 GOF is a promising strategy for effective treatment of p53-mutant cancers (Zhang et al., 2018). For example, mutant p53 has been implicated in promoting invasion and metastasis in a mouse model of pancreatic ductal adenocarcinoma (PDAC), by enhancing platelet-derived growth factor receptor beta (PDGFR) signalling. Interestingly, inhibition of PDGFR signalling by imatinib, effectively impaired cell invasion and metastasis in p53-mutant pancreatic cancers (Weissmueller et al., 2014).

Objectives

Glioblastoma (GBM) is the most common and most aggressive primary brain tumour in adults (Bush et al., 2017; Geraldo et al., 2019) that is characterized by high proliferation, invasion, poor prognosis, and resistance to therapy (Martin et al., 2012). Currently, there is no effective long-term treatment for GBM, but the standard of care is maximal surgical resection, followed by radiotherapy with concomitant and adjuvant chemotherapy with temozolomide (TMZ) as the first line chemotherapeutic agent (Stupp et al., 2005). TMZ is currently the most effective chemotherapeutic agent that has been confirmed to significantly prolong the overall survival of patients with GBM. However, the development of acquired TMZ resistance in GBM usually leads to chemotherapy failure and tumour recurrence. This indicates a need to develop novel therapeutic strategies to overcome acquired TMZ resistance in GBM.

Previous studies from my laboratory showed that 1) p53-induced activation by genotoxic drugs triggered senescence rather than apoptosis in GBM (Martinkova et al., 2010), 2) antagonists of α5β1 integrin channelled TMZ-treated cells from senescence toward apoptosis while modulating the p53 pathway (Martinkova et al., 2010), 3) a negative crosstalk exists between α5β1 integrin and p53wt implicated in TMZ resistance (Janouskova et al., 2012), 4) α5 integrin gene overexpression is associated with decreased survival in patients with high-grade glioma (Janouskova et al., 2012), 5) inhibition of α5β1 integrin in association with Nutlin-3a (an antagonist of the MDM2-p53 relation) triggered strong apoptosis in glioma cells expressing a functional p53 and revealed a negative crosstalk between integrin and p53 pathways (Renner et al., 2016) and 7) PEA15 and survivin, two anti-apoptotic proteins respectively in the integrin and the p53 pathways, may be considered as synthetic lethal partners (Renner et al., 2016). MDM2 seemed to be at the crossroad of both pathways.

Here, our objectives are:

I. To compare the effect of different p53 activators in U87MG cells
II. To explore the role of α5β1 integrin in the p53/MDM2 pathway
III. To determine the role of α5β1 integrin in GBM resistance to TMZ
IV. To explore new combination therapies for TMZ resistant GBM cells

Materials and Methods

1. Materials

1.1. Treatment agents

Temozolomide (TMZ), 8-carbamoyl-3-methylimidazo[5,1-d]-1,2,3,5-tetrazin(3H)-one 5 (Sigma-Aldrich), was prepared as 100mM stock solution in DMSO and stored at 4°C until use.

Nutlin-3a (4-[4,5-bis-(4-chlorophenyl)-2-(2-isopropoxy-4-methoxy-phenyl)-4,5-dihydro-imidazole-1-carbonyl]-piperazin-2-one), the active enantiomer, was from Cayman chemical company (Interchim, France). Nutlin-3a was prepared as 10mM stock solution in ethanol and stored at -20°C until use.

Idasanutlin (also known as RG7388 ($C_{31}H_{29}Cl_2F_2N_3O_4$)) was from MedChem Express. Idasanutlin was prepared as 10mM stock solution in DMSO and stored at -20°C until use.

RITA (5,5'-(2,5-furandiyl) bis-2 thiophenemethanol), was from Cayman chemical company (Interchim, France). RITA was prepared as 10mM stock solution in ethanol and stored at -20°C until use.

K34c (2-(S)-2,6 dimethylbenzamido)-3-[4-(3-pyridin-2-ylaminoprooxy)-phenyl] propionic acid), first synthesized by the group of Professor Kessler (Munchen, Germany); here was synthesized by a chemical company according to the procedure described in (Heckmann et al., 2008). K34C was prepared as 10mM stock solution in DMSO and stored at 4°C until use.

Fr248 was synthesized by the group of Professor Kessler (Munchen, Germany) (Heckmann et al., 2008b) (Heckmann et al., 2008) and was kindly given as gift to the laboratory. Fr248 was prepared as 10mM stock solution in DMSO and stored at 4°C until use.

ATN-161 (1-Acetyl-L-prolyl-L-histidyl-L-seryl-L-cysteinyl-L-aspartamide, Ac-Pro-His-Ser-Cys-Asn-NH2, PHSCN (Modifications: Pro-1 = N-terminal Ac, Asn-5 = C-terminal amide), Ac-PHSCN-NH2), was from Sigma-Aldrich. ATN-161 was prepared as 10mM stock solution in H_2O and stored at -20°C.

Compound 9 was from Luciana Marinelli, our collaborator from Napoli, Italy. Compound 9 was prepared as 10 mM stock solution in DMSO and stored at 4°C.

1.2. Antibodies

Table 3. List of antibodies.

Antibody	Reference	Blocking solution	Dilution
Anti-α5 integrin H104(Santa Cruz	SC-10729	5% milk/1xTBS/0.1%Tween -20	1/1000
Anti-β1 integrin Ts2 (Millipore)	AB1952	5% milk/1xTBS/0.1%Tween -20	1/1000
Anti-αv integrin (Millipore)		5% BSA/1xTBS/0.1%Tween -20	1/1000
Anti-p53(BD Bioscience)	554293	5% milk/1xTBS/0.1%Tween -20	1/1000
Anti-pp53ser15(Cell signalling)	9284S	*5% BSA/1xTBS/0.1%Tween -20	1/1000
Anti-GAPDH (Millipore)	MAB374	5% milk/1xTBS/0.1%Tween -20	1/5000
Anti-p21(Cell signalling)	2946S	5% milk/1xTBS/0.1%Tween -20	1/1000
Anti-MDM2 (Calbiochem)	OP466100UG	5% milk/1xPBS/0.1%Tween -20	1/1000
Anti-p16 (Cell signalling)	SC-56330	5% milk/1xPBS/0.1%Tween -20	1/200
Mouse HRP-conjugated secondary antibody (PROMEGA)	W4028	5% milk/1xTBS/0.1%Tween -20	1/10000
Rabbit HRP-conjugated secondary antibody (PROMEGA)	W4018	5% milk/1xTBS/0.1%Tween -20	1/10000
Purified NA/Le mouse anti-human CD49e	555614	3% PBS-BSA	1/100
Purified anti-human CD29	303002	3% PBS-BSA	1/100
Alexa fluoro@647 goat anti-mouse IgG	A21236	3% PBS-BSA	1/200
Alexa fluoro@488 goat anti-mouse IgG	A11029	3% PBS-BSA	1/200

* Membrane was blocked in milk; the primary antibody was incubated in BSA and the secondary antibody in milk.

1.3. Cell culture

U87MG (p53 wild type), U373 (p53 mutant) was from American Type Culture Collection (LGC Standards Sarl, Molsheim, France). LN443 was a kind gift from Monika Hegi (Lousaune). U87MG R50 and U87MG OFF R50 cell were developed from the parent U87MG GBM cells as described under methods. Cell lines were routinely cultured in MEM (Minimum Essential Medium Eagle) supplemented with 10% heat-inactivated fetal bovine serum, 1% Na pyruvate and 1% Non-essential amino acid at 37ºC in a humidified atmosphere containing 5% CO_2. All cells were authenticated by Multiplexion GmbH, and periodically tested for the presence of mycoplasma. Except otherwise stated, all treatments were carried out in 2% FBS containing medium.

2. Methods

2.1. Generation of TMZ-resistant GBM cells

U87MG cells (500,000) were seeded in T25 cm^2 cell culture flask, containing Eagle's minimal essential medium supplemented with 10% serum, 1% Na pyruvate and 1 % Non-essential amino acid. Cells were allowed overnight (24h) to adhere and the medium was replaced with a fresh medium containing 50µM TMZ. Cell treatment was repeated twice a week for several weeks resulting in a sub-population of stable TMZ-resistant cells. Resistance to TMZ was confirmed in a cell confluence assay, using the IncuCyte live-cell analysis system. The sub-population of resistant cells generated were continuously cultured in medium containing temozolomide (U87MG R50) or medium without temozolomide (U87MG OFF R50).

2.2. Generation of U87MGα5KO cells

U87MGα5KO cells were generated by deleting the gene coding for α5 integrin using the gene editing technology known as Clustered Regularly Interspaced Short Palindromic Repeats associated nuclease 9 (CRISPR Cas 9) and the deletion of this integrin was confirmed by genomic and western blot analysis.

2.3. Cell viability assay

Cell viability was determined by Trypan blue exclusion method. Cells were plated (100 000 cells per well) into six well plates and treated for 96hrs with solvent or drugs in 2% FBS containing medium. Viable cells were counted with the TC20 cell counter (Bio-Rad, Marnes La Coquette, France).

2.4. IncuCyte live cell confluence assay

Cells were plated (2,000 cells in 100µl per well) into 96-well culture plates and allowed at ambient temperature (15 minutes) to ensure homogenous settling. The appropriate solvent control or drugs at 2x concentration in 100µl of 2% FBS containing medium was added to the already prepared wells of the 96-well plate. The cell plates were placed into the IncuCyte live-cell analysis system and allowed to warm at 37°C for 30 minutes prior to standard scanning with 4x objective. Imaging was performed using the IncuCyte Zoom Live-Cell Imaging System from Essen Bioscience. Cell confluence was calculated using IncuCyte Zoom software (2018) by phase-contrast images. Cells were scanned every three hours from 0 to 96 hrs post treatment.

2.5. Senescence assay

The β-galactosidase activity at pH 6 was determined using the Senescence Cells Histochemical Staining Kit (Sigma) according to the manufacturer's instruction. Briefly, cells were plated (2,000 cells/200µl) into a 96 well plate for 72 hours. The cells were washed twice with 1xPBS and fixed with 1x fixation buffer for 7 minutes at room temperature. The fixation buffer was aspirated, and wells rinsed thrice with 1x PBS. After washing the cells were covered with staining mixture and incubated at 37ºC without CO_2. After 12 hours of staining light microscopy was used to identify senescent (blue stained) cells.

2.6. Western blotting

Cells were plated (200,000 cells per well) into 6-well culture plates and treated with the appropriate solvent control or drugs. Cells were lysed with Laemmli sample buffer (Biorad) on ice and lysates heated at 95^0C for 10 minutes. Proteins were separated on precast gradient 4-20% SDSPAGE gels (Bio-Rad) and transferred to PVDF membrane (GE Healthcare, Velizy, France). After 1 hour of blocking at room temperature, membranes were probed with primary antibodies against αv, α5 and β1integrins, MDM2, p21, p16 p53, pp53ser15 and GAPDH overnight at 4ºC. Membranes were subsequently incubated with antirabbit or anti-mouse antibodies conjugated to horseradish peroxidase (Promega, Charbonnieresles- Bains, France), developed using chemoluminescence (ECL, Bio-Rad) and visualized with Las4000 image analyser (GE Healthcare). Quantification of non-saturated images was done using ImageJ software (National institutes of Health, Bethesda, MD, USA). GAPDH was used as the loading control for all samples.

2.7. Real-time qPCR

RNA was extracted using RNeasy minikit (Qiagen) according to the manufacturer's instruction. The extracted RNA was quantified using Nanodrop One (ThermoScientific) and was transcribed into cDNA using high capacity cDNA kit (Applied Biosystems). Real-time quantitative PCR was carried out using the ABI7000 SYBRGreen PCR detector with the following probes (Invitrogen) listed in **Table 4**. Relative levels of mRNA gene expression were calculated using the $2^{-\Delta\Delta Ct}$ method.

Table 4. List of primers.

Gene	Primer (Forward 5'-3')	Reverse 3'-5'
P21	GGCAGACCAGCATGACAGATT	TGTGGGCGGATTAGGGCT
MDM2	AGACCCTGGTTAGACCAA	TGGCCAAGATAAAAAAGAACCTCT
Fas	5CCCTCCTACCTCTGGTTCTTACG	AGTCTTCCTCAATTCCAATCCCTT
Survivin	TGACGACCCCATAGAGGAACA	CGCACTTTCTCCGCAGTTTC
α5 integrin	AGCAAGAGCCGGATAGAGGA	TCAGGGCATTCTTGTCACCC
hGAPDH	GTCACCAGGGCTGCTTTTAACTCT	GGAATCATATTGGAACATGTAAACCAT

2.8. Confocal microscopy and Image Analysis

Coverslips were coated with fibronectin (20 µg/mL-1 in DPBS) and 25 000 cells were seeded in 10% serum containing medium and cultured for 24 hours. Cells were then fixed in 4% (v/v) paraformaldehyde for 12 minutes, and permeabilized with 0.1% Triton-X100 for 2 min. After 1-hour of blocking step in 3% bovine serum albumin (BSA)-PBS solution, cells were incubated with primary antibodies against integrin α5 (clone IIA1 Pharmingen, 1µl/100µl in 3% PBS-BSA) and β1 integrin (purified anti human CD29, Clone:TS2/16, 1µl/100µl in 3% PBS-BSA) overnight at 4 °C. Cells were rinsed in 1xPBS and incubated with appropriate secondary antibodies (Alexa fluor@ 647 goat anti-mouse (A21236)1µl/200µl in 3% PBS-BSA and Alexa fluor@ 688 goat anti-mouse 1µl/200µl in 3% PBS-BSA) and 4', 6-diamidino-2-phenylindole (DAPI) (1µl/2000µl in 3% PBS-BSA was added for nuclei staining) for 45 min. Samples were mounted on microscope slides using fluorescence mounting medium (Dako). Images were acquired using a confocal microscope (LEICA TCS SPE II, 63× magnification oil-immersion). For each experiment, identical background subtraction and scaling was applied to all images. Mean gray values of 10-12 images (4-5 cells per images) from 3 independent experiments were calculated using JACoP plugin ImageJ software.

For 3D spheroid microscopy, microtissues (3D spheroids) of U87MG, U87MG R50 and U87MG OFF R50 cells were collected from hanging drops after 6 days of culture and were embedded in Tissue-Tek, frozen at -20°C and sectioned (10µm) using a cryostat (Leica, CM3000). Serial sections were rinsed with PBS and fixed for 10 min with 4%

paraformaldehyde at 4°C. After three washes with 1xPBS for 5 minutes each at room temperature, sections were incubated for 30 minutes at room temperature in a blocking solution of 1% BSA and 0.1% Triton X100 and then incubated overnight at 4°C with the primary antibodies against integrin α5 (clone IIA1 Pharmingen, 1µl/100µl in 1% PBS-BSA) and β1 integrin (purified anti human CD29, Clone:TS2/16, 1µl/100µl in 1% PBS-BSA) overnight at 4 °C (1µl/100µl each in 1% PBS-BSA). After three washes with 1xPBS, sections were incubated with the appropriate secondary antibodies (Alexa fluor@194(A21203) and Alexa Fluor 488 (A11001)). Nuclei were stained with 4', 6-diamidino-2-phenylindole (DAPI, Euromedex, Souffelweyersheim, France). Negative controls were performed either omitting the primary antibody or using normal goat serum (NGS). After 3 additional washes in PBS, slides were mounted in fluorescence mounting medium (Dako, Trappes, France) and observed with a fluorescence microscope (Leica DM4000B).

2.8. RNA-sequencing

RNA-Seq libraries were generated from 400 ng of total RNA using TruSeq Stranded mRNA Library Prep Kit and TruSeq RNA Single Indexes kits A and B (Illumina, San Diego, CA), according to the manufacturer's instructions. Briefly, following purification with poly-T oligo attached magnetic beads, the mRNA was fragmented using divalent cations at 94°C for 2 minutes. The cleaved RNA fragments were copied into first strand cDNA using reverse transcriptase and random primers. Strand specificity was achieved by replacing dTTP with dUTP during second strand cDNA synthesis using DNA Polymerase I and RNase H. Following addition of a single 'A' base and subsequent ligation of the adapter on double stranded cDNA fragments, the products were purified and enriched with PCR (30 sec at 98°C; [10 sec at 98°C, 30 sec at 60°C, 30 sec at 72°C] x 12 cycles; 5 min at 72°C) to create the cDNA library. Surplus PCR primers were further removed by purification using AMPure XP beads (Beckman-Coulter, Villepinte, France) and the final cDNA libraries were checked for quality and quantified using capillary electrophoresis. Libraries were then sequenced on an Illumina HiSeq4000 system as single-end 1x50 base reads. Image analysis and base calling were performed using RTA 2.7.7 and bcl2fastq 2.17.1.14. Reads were preprocessed using cutadapt (Martin, 2011) version 1.10 in order to remove adapter, polyA and low-quality sequences (Phred quality score below 20), reads shorter than 40 bases were discarded for further analysis. Reads mapping to rRNA were also discarded (this mapping was performed using bowtie (Langmead and Salzberg, 2012) version 2.2.8). Reads were then mapped onto the hg38 assembly of human genome using STAR (Dobin et al., 2013) version 2.5.3a (--twopassMode Basic). Gene expression was quantified

using htseq-count (Anders et al., 2015) version 0.6.1p1 and gene annotations from Ensembl release 99. Statistical analysis was performed using R 3.3.2 and DESeq2 (Love et al., 2014).

Gene expression data obtained with DESeq2 was used to generate the heatmaps and dendrogram with R. Only genes expressed in all condition (defined if normalized reads count divided by median of transcripts length in kb is greater than 1 for gene across all nine libraries) were taken into account for visualization. Hierarchical clustering method was performed according to pairwise complete-linkage method and using Pearson correlation for row clustering and Spearman correlation for column clustering. The biological significance of differentially expressed genes (DEGs) obtained were explored using ReactomePA, an R/Bioconductor package for reactome pathway analysis and visualization (Yu and He, 2016). |Log2(fold change) | > 2 (|log2FC|>2) and an adjusted false discovery rate (FDR) < 0.05 (using Benjamini-Hochberg correction) were used as the cut-off criteria of DEGs samples.

Results

Results Part 1: Effect of different p53 activators and role of α5β1 integrin in p53/MDM2 pathway

1. Comparison of different modes of p53 activation in U87MG cells

Restoration of p53 activity by inhibition of the p53−MDM2 interaction is considered an attractive approach for the treatment of cancer. We explored the impact of p53 reactivation by Nutlin-3a, Idasanutlin and RITA. Nutlin-3a is a non-genotoxic drug, known to inhibit the p53-mdm2 negative feedback regulatory loop through binding to mdm2 to impair the mdm2-dependent degradation of p53 resulting in direct activation of p53(Tovar et al., 2013). Like Nutlin-3a, Idasanutlin also binds to MDM2 to disrupt the p53-MDM2 interaction, however this second generation of MDM2 inhibitor, is highly potent and selective (Ding et al., 2013). RITA is another non-genotoxic p53 activator that has been described. Unlike Nutlin-3a and Idasanutlin, RITA binds to p53 to impair the p53-mdm2 interaction resulting in p53 stabilization and activation (Issaeva et al., 2004). The effects of these p53 activators on cell confluence, viability, and activation of the p53 signalling pathway were compared using the Incucyte technology, trypan blue exclusion assay and western blots, respectively.

1.1. Effect of p53 activators on cell confluence and morphology of U87MG cells

To investigate whether Nutlin-3a, Idasanutlin and RITA repress cell confluence in U87MG cells, we treated U87MG cells with Nutlin-3a 1μM, Idasanutlin 1μM and RITA 1μM and cell confluence was dynamically detected and calculated using IncuCyte Zoom software based on phase-contrast images obtained in real time. Nutlin-3a, Idasanutlin and RITA all significantly decreased cell confluence in U87MG cells (**Figure 19A**). No difference was observed between treatment with Nutlin-3a and RITA. However, the p53 activator, Idasanutlin more efficiently decreased cell confluence than either treatment with Nutlin-3a or RITA. In addition, phase contrast images obtained from the IncuCyte in real time revealed that treatment with Nutlin-3a 1μM, Idasanutlin 1μM and RITA 1μM all decreased cell number and confluence 72hrs post treatment (**Figure 19B**). Compared to Nutlin-3a or RITA, treatment with Idasanutlin 1μM more effectively decreased cell number and confluence of U87MG cells.

These results suggest that treatment with Nutlin-3a, Idasanutlin and RITA all suppressed cell confluence of U87MG cells. Compared to Nutlin-3a and RITA, Idasanutlin is the most efficient.

A.

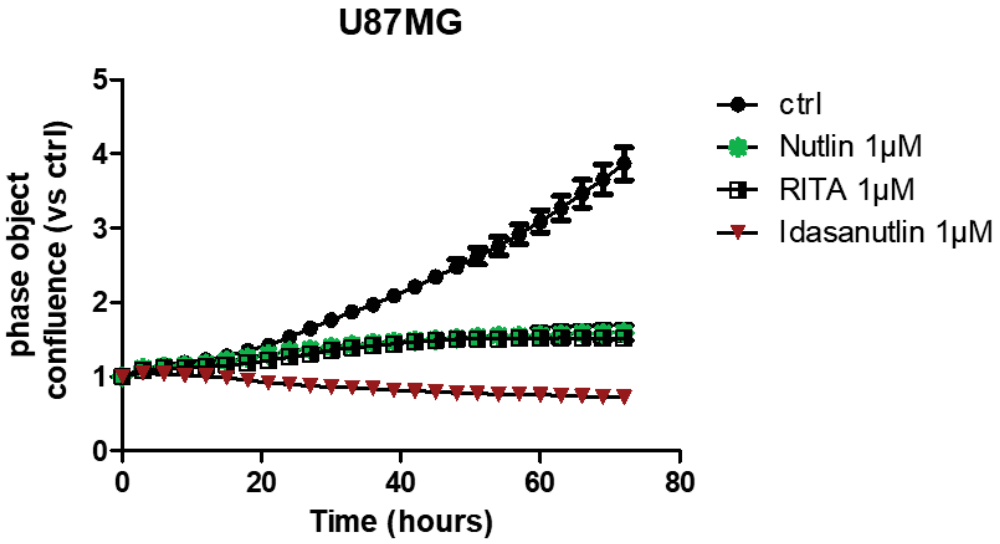

B.

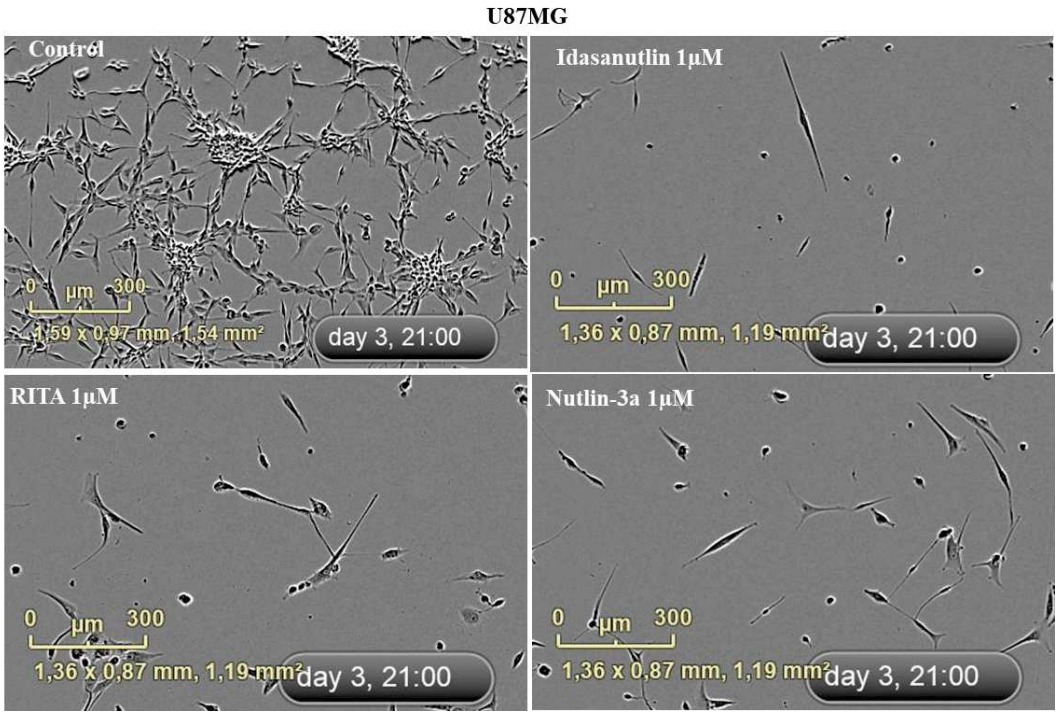

Figure 19. Effect of p53 activators on cell confluence and morphology of U87MG cells. (**A**) Cell confluence was calculated using IncuCyte Zoom software based on phase-contrast images of U87MG cells from 0 hr to 72 hrs treated with Nutlin-3a 1µM, RITA 1µM and Idasanutlin 1µM. Each data point represents mean ± S.E.M. of at least three independent experiments. (**B**) Representative phase contrast images from the IncuCyte showing the cellular morphology of U87MG cells 72hrs post treatment with Nutlin-3a 1µM, Idasanutlin 1µM and RITA 1µM. Scale bar, 300µm.

1.2. Dose dependent effect of p53 activators on the viability and confluence of U87MG cells

To study the effect of Nutlin-3a and RITA on cell viability in vitro, U87MG cells were treated with increasing concentrations of Nutlin-3a (1 and 5μM) and RITA (0.1, 0.5 and 1μM) for 72 hrs, at the end of the experiment, trypan blue exclusion assay was used to detect the cell survival. Trypan blue exclusion assay revealed that both Nutlin-3a and RITA dose dependently decreased cell viability of U87MG cells (**Figure 20A**). No statistically significant difference was observed between treatment with Nutlin-3a (1μM) and RITA (1μM).

We next treated U87MG cells with increasing concentrations of Idasanutlin (0.05, 0.1, 0.2, 0.4, and 0.8 μM) and cell confluence was dynamically detected and calculated using IncuCyte Zoom software based on phase-contrast images obtained in real time. Treatment with Idasanutlin, dose dependently decreased cell confluence in U87MG cells even at the lowest concentration of 0.05 μM (**Figure 20B**).

These results suggest that treatment with Nutlin-3a, Idasanutlin and RITA suppressed cell confluence and viability in U87MG cells with Idasanutlin been the most efficient.

A.

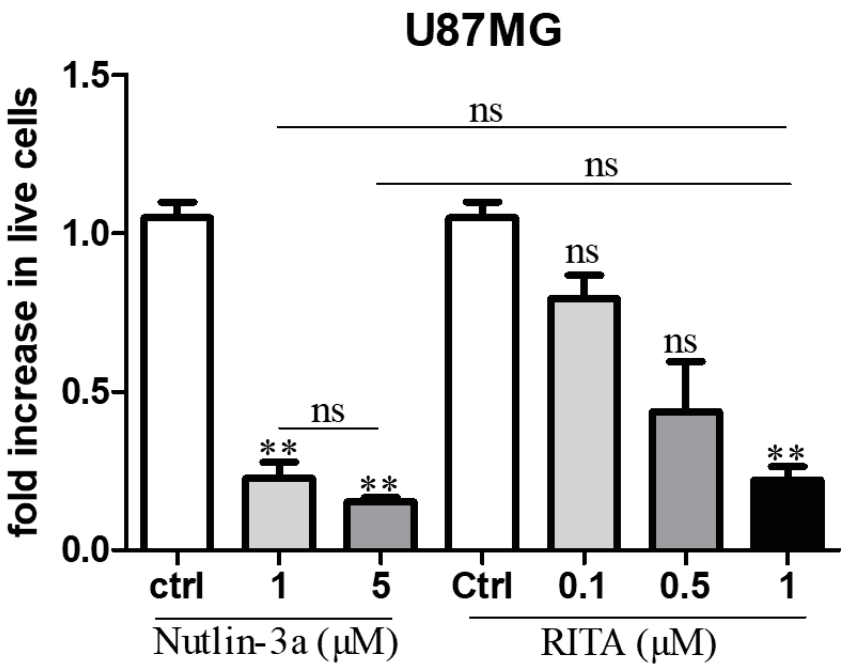

B.

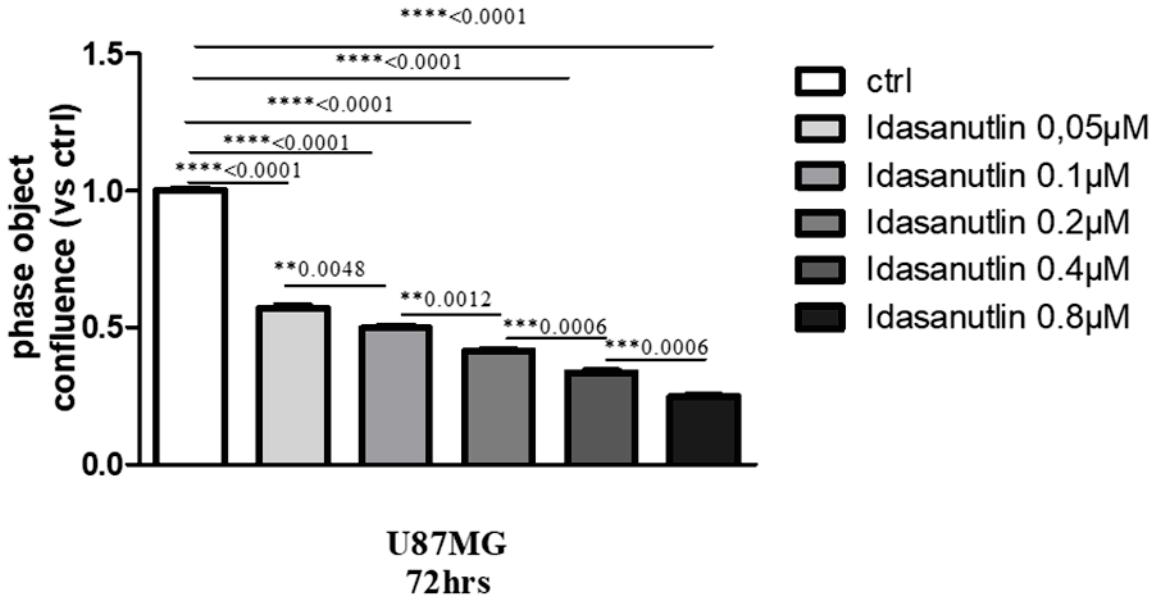

Figure 20. Effect of p53 activators on cell viability and confluence of U87MG cells.
(**A**) Dose dependent effect of Nutlin-3a (1 and 5μM) and RITA (0.1, 0.5 and 1μM) on U87MG cell. Data are reported as fold increase in live cells at 72 hrs of treatment as compared with plated live cells at time 0. Histograms represent the mean± S.E.M. of two independent experiments. (**B**) Cell confluence was calculated using IncuCyte Zoom software based on phase-contrast images of U87MG cells from 0 hr to 72 hrs treated with increasing concentrations of Idasanutlin. For all panels: mean± S.E.M. of at least three independent experiments with *, $p<0.05$; **, $p<0.01$; ***, $p<0.001$; ns, non-significant.

1.3. The effect of p53 activators on cell confluence is dependent on the p53 status of the cells

We demonstrated that Nutlin-3a, Idasanutlin and RITA decreased cell confluence in U87MG cells expressing p53 wild type. In the course of this work, we generated TMZ-resistant U87MG cells (U87MG OFF R50 cells) from U87MG cells. We wondered whether the p53 activators would impact these cells as was observed in the parental cells. To confirm this point, we treated TMZ-resistant U87MG OFF R50 cells with Nutlin-3a 1µM, Idasanutlin 1µM and RITA 1µM, and cell confluence was dynamically detected and calculated using Incucyte Zoom software based on phase-contrast images obtained in real time. As expected, Nutlin-3a, Idasanutlin and RITA all significantly decreased cell confluence in TMZ-resistant U87MG OFF R50 cells. Idasanutlin was the most efficient, while RITA appeared to be the least efficient in decreasing cell confluence in these cells (**Figure 21A**). Moreover, phase contrast images revealed that treatment with Nutlin-3a 1µM, Idasanutlin 1µM and RITA 1µM all decreased cell number and confluence 72hrs post treatment (**Figure 21B**). Similarly, Idasanutlin was the most efficient, while RITA appeared to be the least efficient in decreasing cell number and confluence of these cells.

Based on these results, we wondered whether the observed effects of p53 activators on cell confluence is dependent on the p53 status of the cells. To confirm this point, we treated U373MG cells expressing mutant p53 with Nutlin-3a 1µM and Idasanutlin 0.1µM and the cell confluence was dynamically detected and calculated using IncuCyte Zoom software based on phase-contrast images obtained in real time. In these cells, treatment with Nutlin-3a 1µM and Idasanutlin 0.1µM did not inhibit cell confluence (**Figure 22A**). No observable difference in the cellular morphology of U373 MG cells treated with either Nutlin-3a or Idasanutlin as compared to the control was observed (**Figure 22B)**.

These results confirmed that the suppression of cell confluence by p53 activators is dependent on the p53 status of the cells and that p53 mutant cells will not be affected.

A.

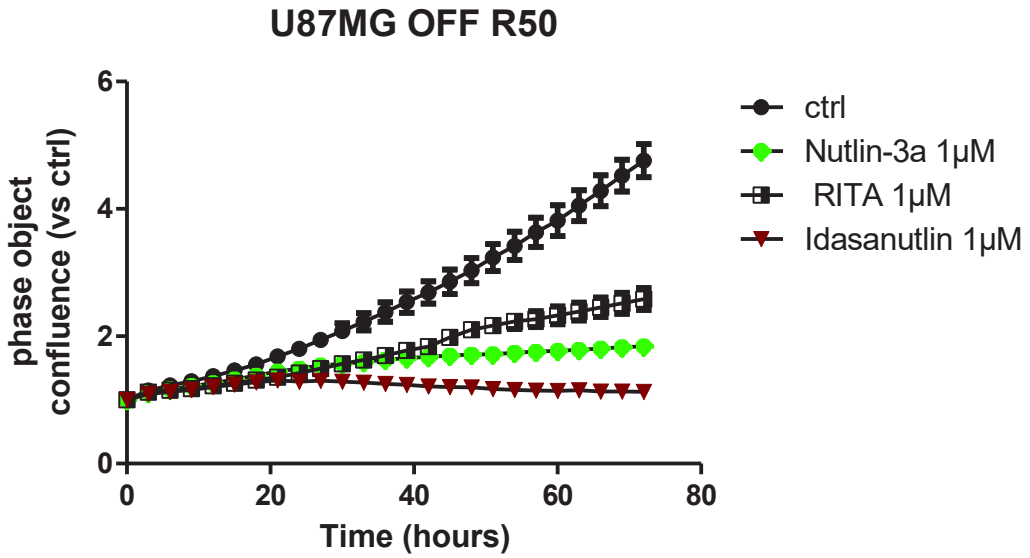

B.

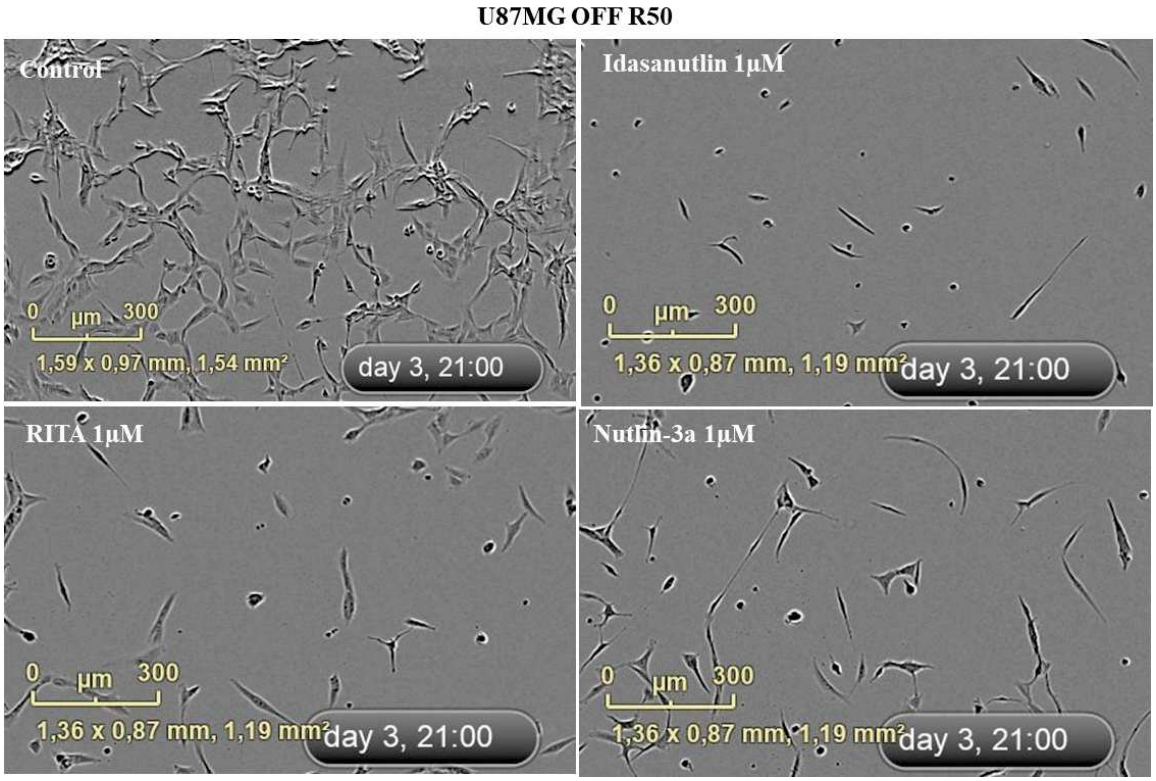

Figure 21. Effect of p53 activators on cell confluence and morphology of TMZ-resistant U87MG OFF R50 cells.

(**A**) Cell confluence was calculated using IncuCyte Zoom software based on phase-contrast images of TMZ-resistant U87MG OFF R50 cells from 0 hr to 72 hrs treated with Nutlin-3a 1µM, RITA 1µM and Idasanutlin 1µM. Each data point represents mean ± S.E.M. of at least three independent experiments. (**B**) Representative phase contrast images from the IncuCyte showing the cellular morphology of TMZ-resistant U87MG OFF R50 cells 72hrs post treatment with Nutlin-3a 1µM, Idasanutlin 1µM and RITA 1µM. Scale bar, 300µm.

A.

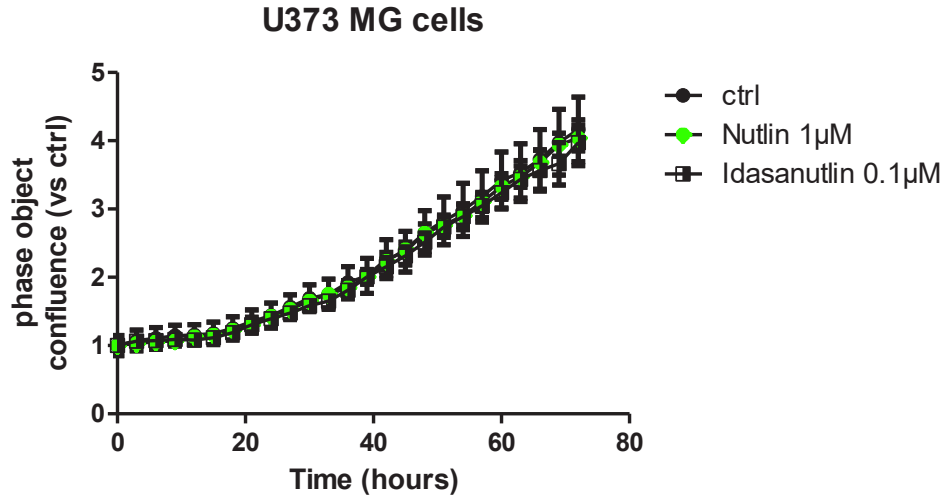

B.

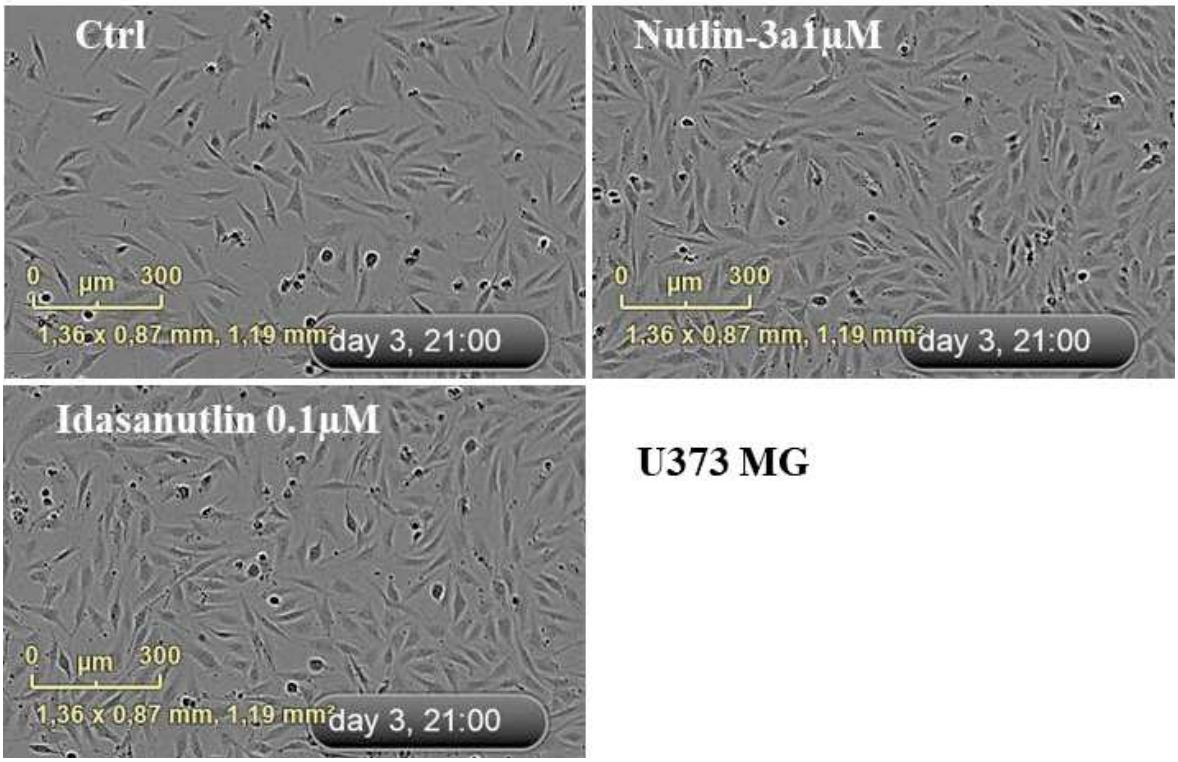

Figure 22. Effect of p53 activators on cell confluence and morphology of U373MG cells (mutant p53).

(**A**) Cell confluence was calculated using IncuCyte Zoom software based on phase-contrast images of U373MG cells (mutant p53) from 0 hr to 72 hrs treated with Nutlin-3a 1µM and Idasanutlin 0.1µM. Each data point represents triplicate wells. (**B**) Representative phase contrast images from the IncuCyte showing the cellular morphology of U373MG cells (mutant p53) 72hrs post treatment with Nutlin-3a 1µM and Idasanutlin 0.1µM. Scale bar, 300µm.

1.4. Effect of Nutlin-3a, RITA and Idasanutlin on the p53 pathway

To explore the impact of p53 reactivation by Nutlin-3a, RITA and Idasanutlin, we assessed the reactivation of the p53 pathway by evaluating p53 protein stability and activity in U87MG cells 24 and 48hrs post treatment with increasing concentrations of Nutlin-3a (1 and 5 μM) and RITA (0.1, 0.5 and 1μM). Western blot analysis showed that treatment with Nutlin-3a significantly and dose dependently increased p53 protein stability in U87MG cells at both 24, and 48hrs post treatment (**Figure 23)**. MDM2 protein expression was also significantly and dose dependently increased by Nutlin-3a at all the time points tested. Furthermore, Nutlin-3a at 5μM (but not 1μM) significantly decrease the protein levels of α5 integrin in these cells 24hrs post treatment. This decrease was time dependent as treatment with Nutlin-3a at both 1μM and 5μM significantly decreased the protein levels of the integrin 48hrs post treatment (**Figure 23**). To substantiate the activation of p53 in GBM by Nutlin-3a, we treated U87MG R50 and U87 MG OF R50 cells both of which are model of TMZ-resistant GBM, with Nulin-3a and evaluated the effects on p53 stability and MDM2 expression by western blot. Interestingly, treatment with Nutlin-3a dose dependently increased p53 stability/activity and MDM2 expression in both U87MG R50 and U87 MG OF R50 cells (**Figure 24**). Like Nutlin-3a, Idasanutlin dose dependently increased p53 protein stability (**Figure 25**). In addition, Idasanutlin proved to be more potent than Nutlin-3a, as it efficiently stabilized p53 at a lower concentration of 0.1μM.

Taken together, we demonstrated that Nutlin-3a, RITA and Idasanutlin all stabilized the p53 protein, with Idasanutlin been the most efficient. Additionally, stabilization of the p53 protein was accompanied by a decrease in the level of α5 integrin.

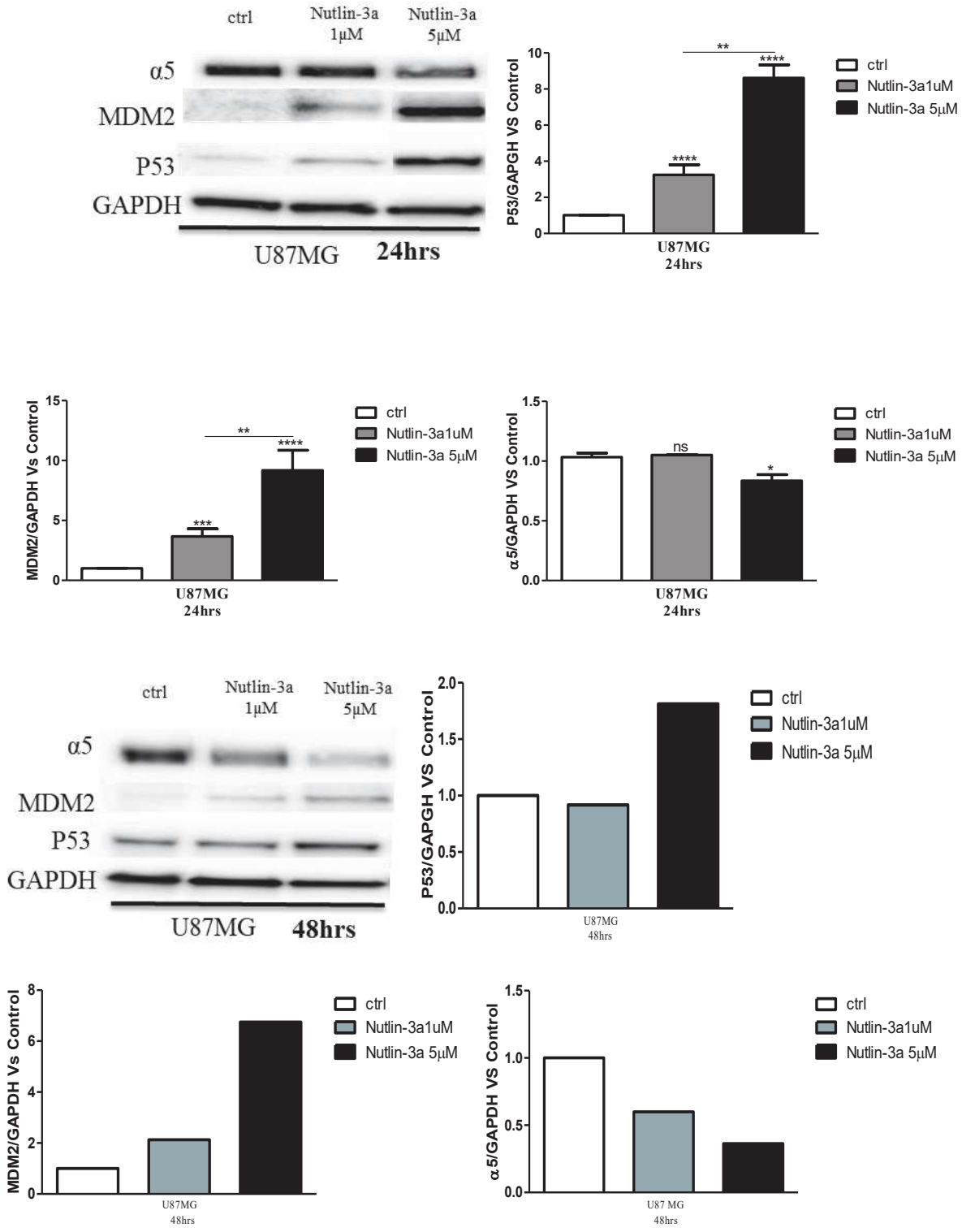

Figure 23. Effect of increasing concentrations of Nutlin-3a on p53 stability/ activity and MDM2 expression.

A representative western blot showing dose dependent effect of Nutlin-3a (1 and 5μM) on p53 stability and MDM2 expression 24 and 48hrs post treatment. GAPDH was used as the loading control. For experiments in upper panel: mean± S.E.M. of at least three independent experiments with *, $p<0.05$; **, $p<0.01$; ***, $p<0.001$; ns, non-significant. Experiment in lower panel was made once

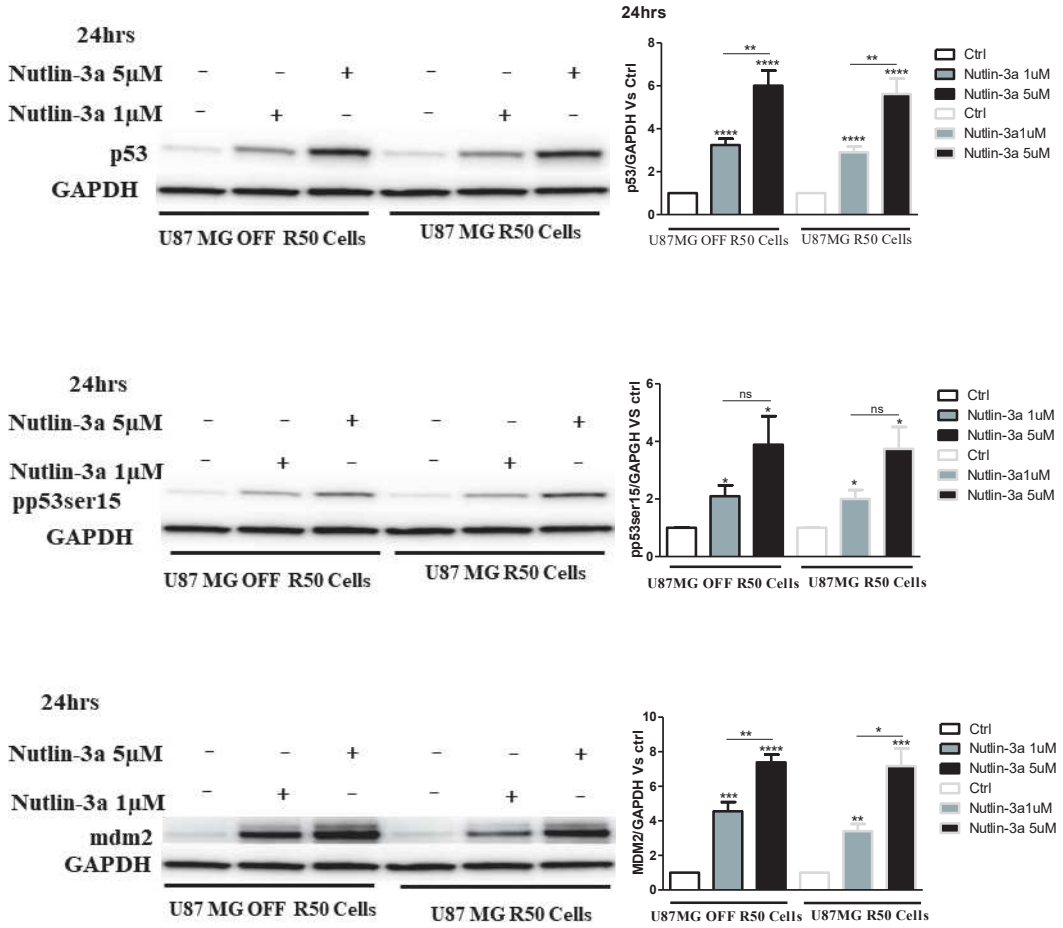

Figure 24. Nutlin-3a stabilized p53 and increased MDM2 expression in TMZ-resistant cells in a dose dependent fashion.

A representative western blot showing dose dependent effect of Nutlin-3a 1μM on p53 stability and MDM2 expression 24hrs post treatment. GAPDH was used as the loading control. For all panels: mean± S.E.M. of at least three independent experiments with *, $p<0.05$; **, $p<0.01$; ***, $p<0.001$; ns, non-significant.

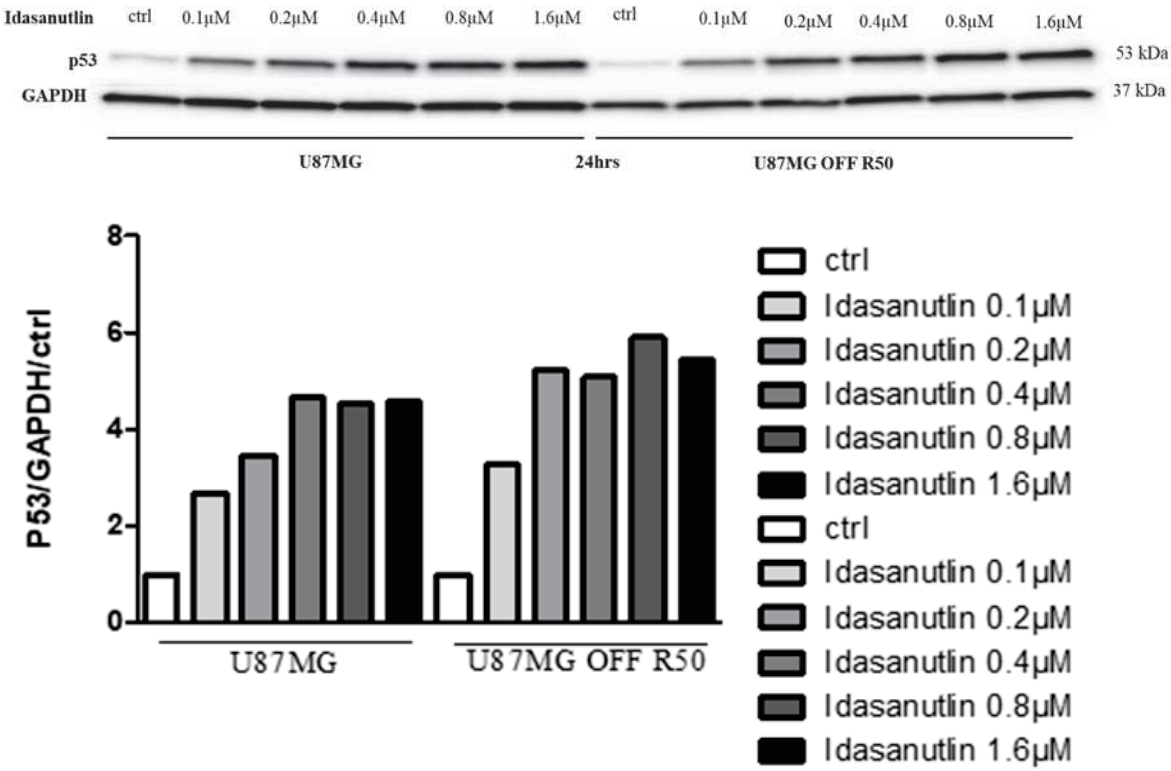

Figure 25. Dose dependent effect of Idasanutlin on p53 stability in U87MG cells.
Western blot showing dose dependent effect of Idasanutlin on p53 protein stability 24hrs post treatment. GAPDH was used as the loading control. Experiment was made once.

To compare Nutlin-3a (which binds to MDM2) and RITA (which binds to p53), we treated U87MG cells with increasing concentrations of RITA (0.1, 0.5 and 1μM) and evaluated the effects on the p53 pathway by western blot. Western blot analysis showed that RITA, significantly and dose dependently increased p53 protein stability in U87MG cells both at 24 and 48 hrs post treatment (**Figure 26**). Unlike Nutlin-3a, RITA had no effect on MDM2 protein stability and the expression of α5 integrin in U87MG cells at all concentration tested both at 24 and 48hrs (**Figure 26**). Furthermore, treatment with Nutlin-3a (1μM) is more efficient in increasing p53 protein stability as compared to RITA (1μM) (**Figure 27**).

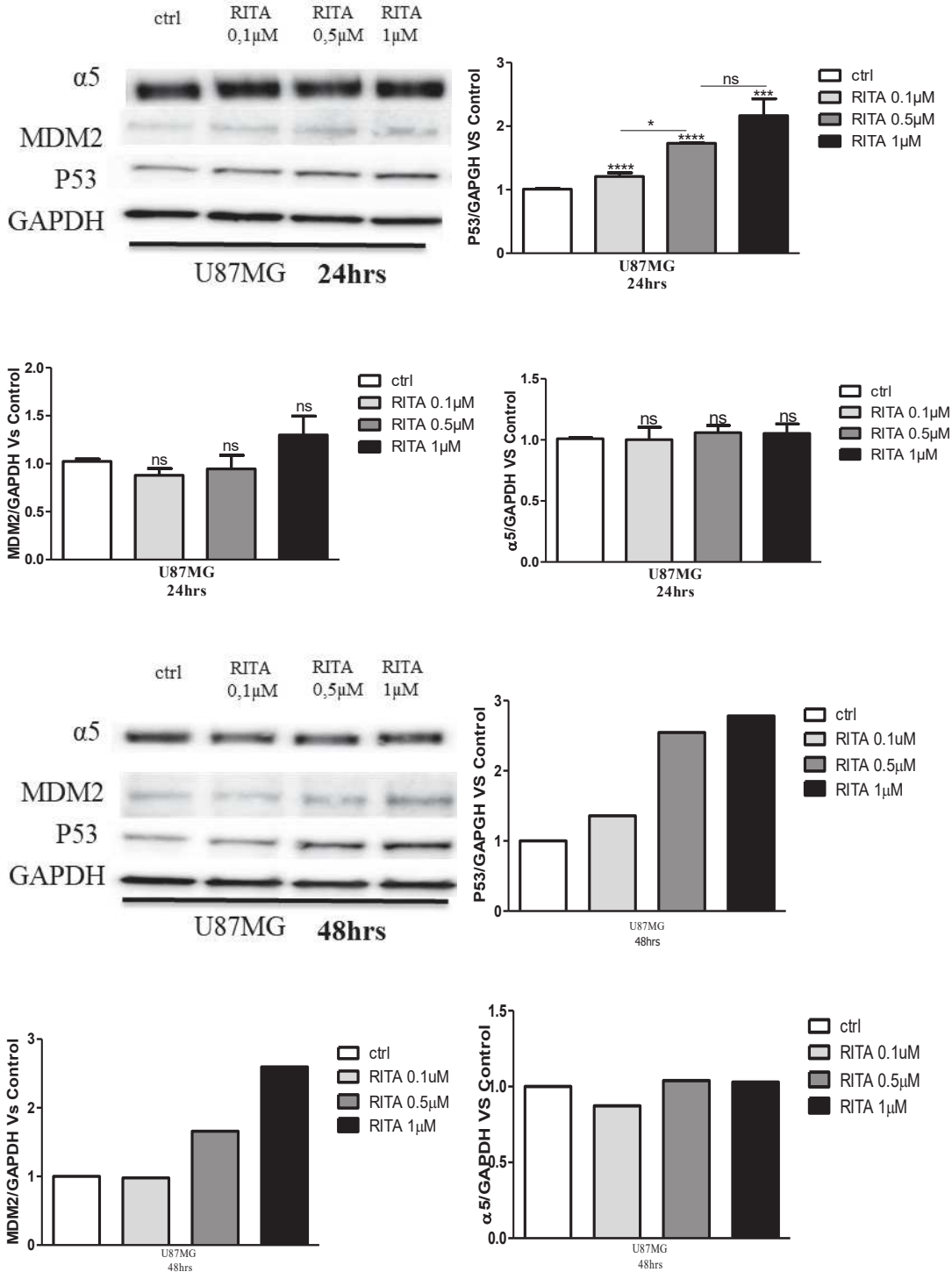

Figure 26. Effect of increasing concentrations of RITA on p53 stability/ activity and MDM2 expression.

A representative western blot showing dose dependent effect of RITA (0.1, 0.5 and 1μM) on p53 stability and MDM2 expression in U87MG cells 24 and 48 hrs post treatment. GAPDH was used as the loading control. For experiments in upper panel: mean± S.E.M. of at least three independent experiments with *, $p<0.05$; **, $p<0.01$; ***, $p<0.001$; ns, non-significant. Experiment in lower panel was made once.

We next investigated the transcriptional activity of p53 by evaluating the expression of the p53 target genes: MDM2, a physiological inhibitor of p53 and its main transcriptional target; p21, a cell cycle inhibitor; Fas, a gene product required for p53-mediated apoptosis; and birc5/survivin an anti-apoptotic protein. RT-qPCR analysis showed that, the transcription of the p53 induced genes p21, fas and MDM2 were significantly increased by both Nulin-3a and RITA, confirming the activation of the p53 pathway (**Figure 27B)**. The repressible p53-target gene, birc5, was significantly decreased after treatment with Nutlin-3a and RITA. Compared to RITA, Nutlin-3a is more efficient in increasing the transcription of MDM2 and decreasing the transcription of birc 5 (**Figure 27B)**.

These results confirmed that at 1µM, Nutlin-3a is more efficient than RITA in reactivating the p53 pathway in U87MG cells 24 hrs post treatment.

A.

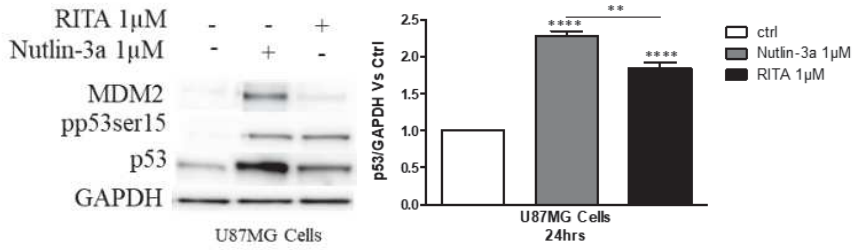

B.

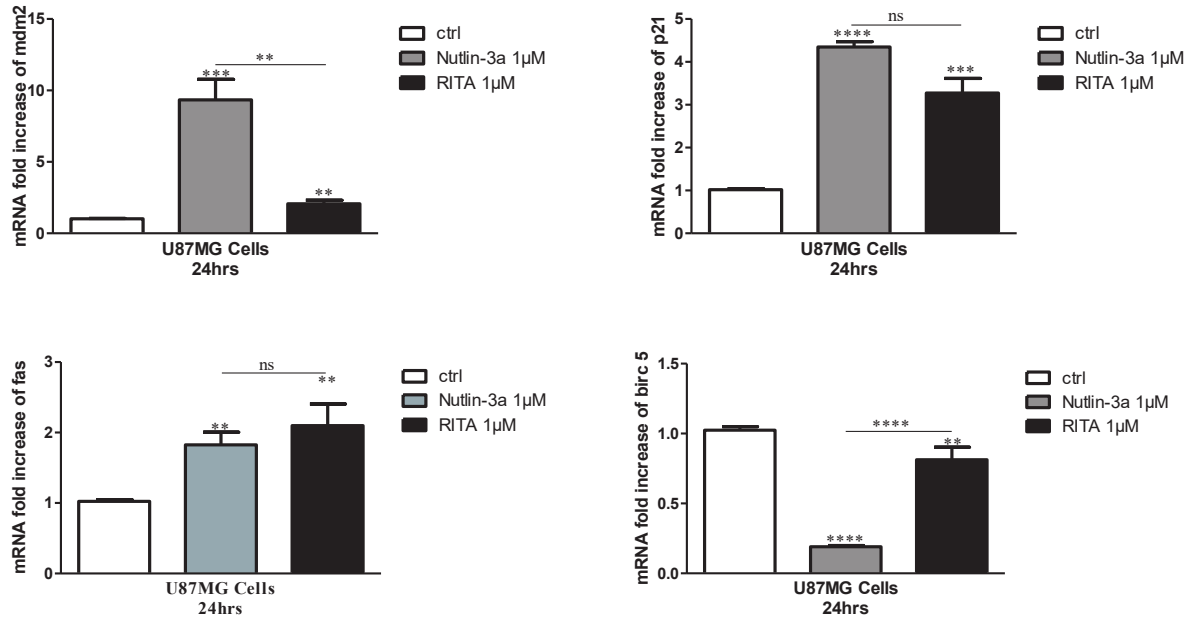

Figure 27. Nutlin-3a and RITA reactivates the p53 pathway in U87MG cells.
(**A**) p53 stabilization/activation and MDM2 expression were detected by western blot analysis of total p53, p53 phosphorylated at ser15 (pp53ser15) and total MDM2. A representative western blot of U87MG cells treated during 24hrs with Nutlin-3a 1µM and RITA 1µM. Histograms represent the mean ± S.E.M. of at least three independent experiments. GAPDH was used as the loading control. (**B**) qPCR analysis of p53 target genes p21, MDM2, Fas and birc5 in U87MG cells 24hrs post treatment with Nutlin-3a 1µM and RITA 1µM. Histograms show the fold increase in mRNA expression normalized to GAPDH levels. For all panels: mean± S.E.M. of at least three independent experiments with *, $p<0.05$; **, $p<0.01$; ***, $p<0.001$; ns, non-significant.

2. Role of α5β1 integrin in the p53/MDM2 pathway

Previous studies suggested that α5 integrin expression inhibited p53 activation by in part impacting on MDM2 stability (Renner et al., 2016a). To explore this point, we used U87MG cells in which the gene for α5 integrin was deleted using the CRISPR/Cas9 technology (U87MGα5KO) in comparison with U87MG cells expressing the integrin.

We checked the effects of Nutlin-3a and RITA in a kinetic study on p53 stability and activity and on MDM2 stability. Treatment with Nutlin-3a leads to rapid and strong induction of p53 stability and activity already at 3hrs post treatment in both U87MG and U87MGα5KO but the induction of p53 protein stability and activity by RITA was delayed and was apparent only after 24hrs post treatment (**Figure 28**). No differences could be seen between the two cell lines at the p53 level.

Concerning the MDM2 protein expression, the kinetic studies revealed that at earlier time points, α5 integrin expression led to a sustained stabilisation of MDM2 by Nutlin-3a treatment from 6 to 12 hours whereas in U87MG-α5KO cells its level decreased rapidly (**Figure 29**). Results suggested that this integrin might modulate MDM2 expression in certain situations. To confirm this point, we treated U87MG cells firstly with Nutlin-3a to increase MDM2 level and secondly with K34c, an antagonist of the integrin. We expected to see a decrease in MDM2 level with the antagonist with no change in p53. However, results indicated that both MDM2 and p53 proteins were affected by the combined treatment at 6 hours (**Figure 29**). This part of the project was rendered difficult to conclude, as MDM2 seems to be decreased by an integrin antagonist it is also increased by the activation of p53 by Nutlin-3a as a p53 target gene. The respective part of both effects needs further investigations.

We decided to turn our investigations on TMZ-resistant GBM cells, as it was shown in the literature that some recurrent GBM over-express α5 integrin. We thus decided to develop an in vitro model of resistant cells to explore if p53 activation combined with integrin antagonists may be a valuable strategy to target them.

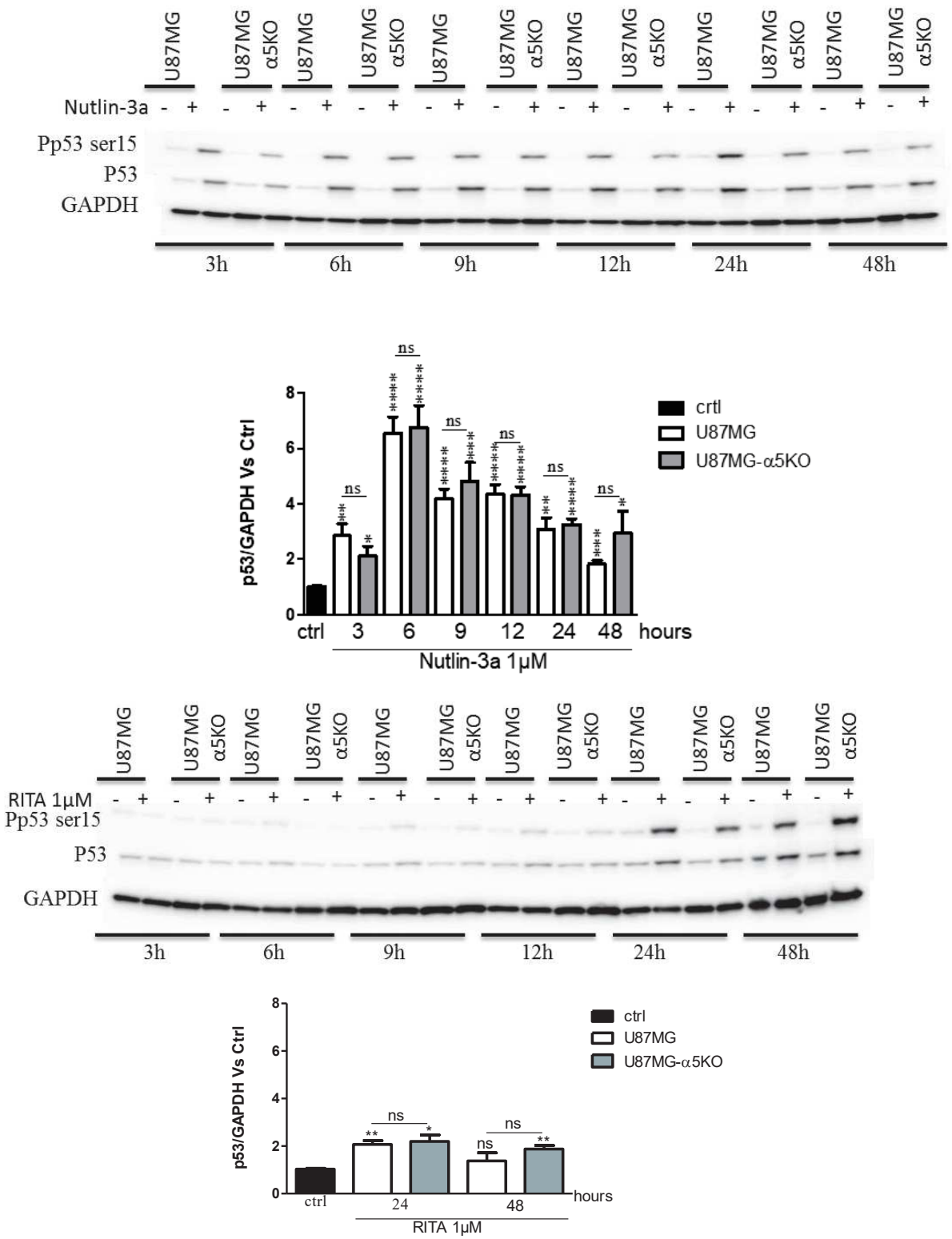

Figure 28. Time dependent effect of Nutlin-3a and RITA on p53 stability and activity.
A representative western blot showing a time course of p53 stability and activity in U87MG Cells and U87MG-α5KO cells after treatment with Nutlin-3a and RITA. GAPDH was used as the loading control. For all panels: mean± S.E.M. of at least three independent experiments with *, p<0.05; **, p<0.01; ***, p<0.001; ns, non-significant.

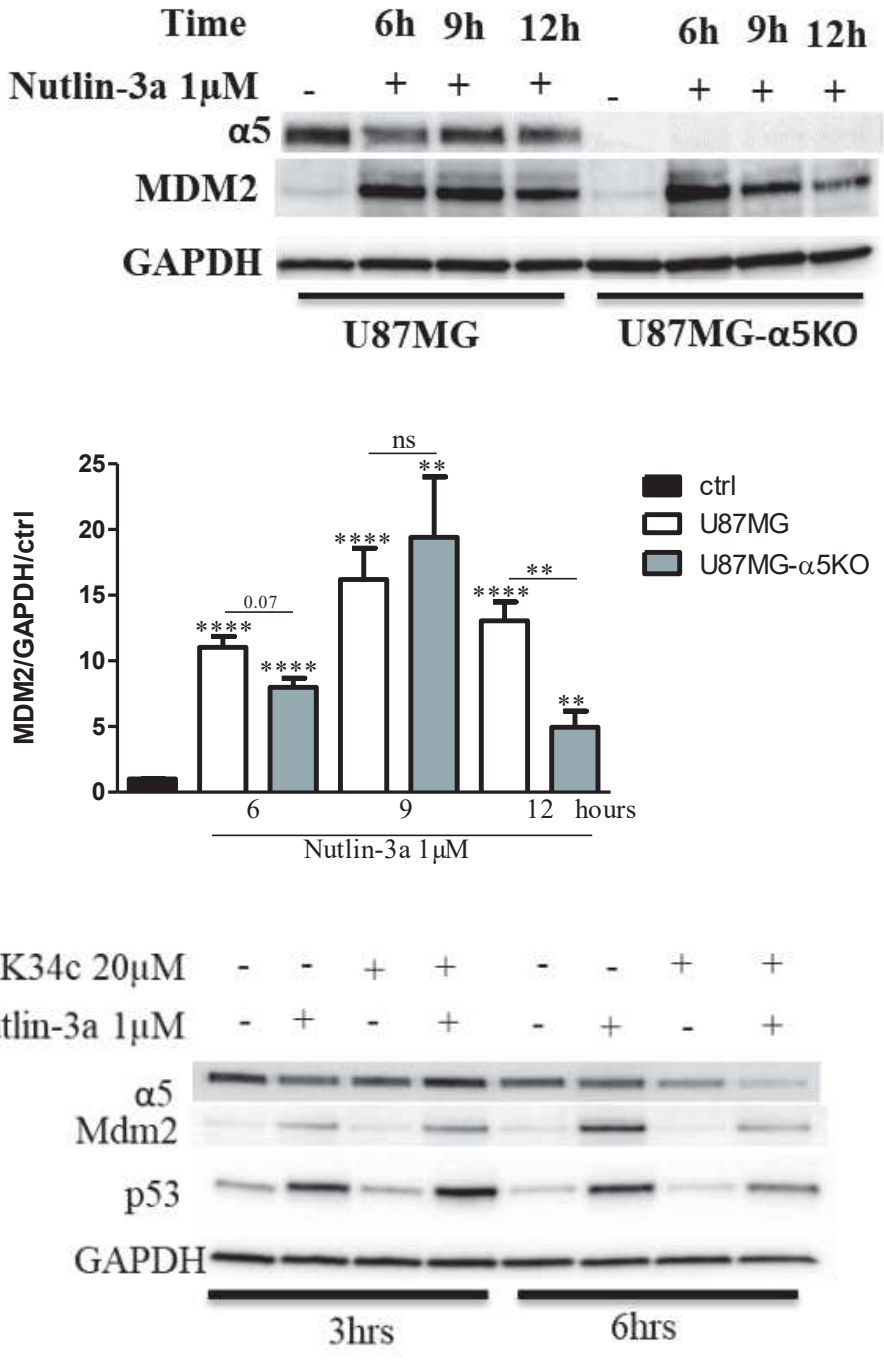

Figure 29. Modulation of p53/MDM2 pathway by α5β1 integrin.
A representative western blot showing the time course of MDM2 expression in U87MG Cells and U87MG-α5KO cells after treatment with Nutlin-3a. GAPDH was used as the loading control. For experiments in upper panel: mean± S.E.M. of at least three independent experiments with *, $p<0.05$; **, $p<0.01$; ***, $p<0.001$; ns, non-significant. Experiment in lower panel was made once.
.

Discussion

Disruption of the MDM2-P53 protein-protein interaction leading to restoration of the tumour suppressor function of wild-type p53 is considered an attractive therapeutic strategy to treat cancers including glioblastoma. Several small molecule inhibitors of the p53-MDM2 complex have been developed with some already in clinical trials. Here, we sought to compare the p53 activators Nutlin-3a, Idasanutlin and RITA. Nutlin-3a and Idasanutlin both functions to increase p53 activity by binding to MDM2 to inhibiting the MDM2-p53 protein-protein interaction. Nutlin-3a, a cis-imidazoline compound is the first selective MDM2 inhibitor developed (Klein and Vassilev, 2004). However, the large hydrophobic protein-protein interaction interface on MDM2 that compromises its potency and pharmacokinetic profiles, led to the discovery of Idasanutlin, a pyrrolidine compound with superior potency and selectivity (Ding et al., 2013). We compared the effect of Nutlin-3a and Idasanutlin in our cell lines. Consistent with earlier findings, our data demonstrated that the clinically evaluated p53 activator, Idasanutlin is more efficient in decreasing cell confluence and in stabilizing the p53 protein than Nutlin-3a. We demonstrated that the effect of both Nutlin-3a and Idasanutlin on cell confluence is dependent on the p53 status of the cells. We found that both drugs had effect on cells expressing wild-type p53 but had no effect on the confluence of U373MG cells expressing mutant p53. Our results are in line with those described by Renner et al. and Ding et al. in which cells expressing wild-type p53 are responsive to Nutlin-3a (Renner et al., 2016b) and Idasanutlin (Ding et al., 2013), but cells expressing mutant p53 are not responsive.

We further compared Nutlin-3a (which binds to mdm2) and RITA (which binds to p53) both drugs functions to increase p53 activity by inhibiting the MDM2-p53 protein-protein interaction. We found no observable difference on cell viability or cell confluence between treatment with Nutlin-3a and RITA on U87MG cells. In contrast to Nutlin-3a, RITA did not decrease the expression of α5 integrin when both were tested at equal concentration (1μM) but did at higher concentration confirming other works (Janouskova et al., 2012). Additionally, a less efficient induction of p53 with no increase in MDM2 expression was observed with RITA compared to Nutlin-3a. The observed findings mirrored those of previous studies that compared the effect of Nutlin-3a and RITA on colon cancer (Janouskova et al., 2012). There are several possible explanations for these results. For example, our data suggest that the activation of p53 below a threshold value, as obtained with RITA, is insufficient to affect the expression of α5 integrin. More recently, a similar threshold mechanism was described to mediates p53 cell fate

decision between cell cycle arrest and apoptosis (Kracikova et al., 2013). Another possible explanation for this is that MDM2 is released unmodified upon the binding of RITA to p53, whereas the binding of Nutlin-3a to MDM2, might cause alteration in the binding site of MDM2 that allow it to bind to other proteins such as α5 integrin besides p53. These results provide further support on the important role of α5 integrin in GBM and the need to continue with the task of developing selective inhibitors for this integrin.

On cell survival and the induction or repression of p53 target genes, different outcome has been described. For example, while RITA preferentially induced apoptosis, Nutlin-3a more commonly push cells to cell cycle arrest (Enge et al., 2009). We demonstrated that, in comparison to Nutlin-3a, RITA is less efficient to either increase p53 target genes or decrease the antiapoptotic protein birc5. In contrast to the above discussed differences, however, no difference was observed on the effect of Nutlin-3a and RITA on cell survival after 72 hours. In line with this, It is possible that p53 activation by RITA may surpass activation by Nutlin-3a over prolong period, since treatment with RITA does not significantly affects MDM2 expression, the negative regulator of p53 as compared to treatment with Nutlin-3a.

A negative crosstalk between α5β1 integrin and the p53 protein was described (Janouskova et al., 2012) and overexpression of this integrin was shown to stabilized the MDM2 protein (Renner et al., 2016b). Both α5β1 integrin (Janouskova et al., 2012) and the MDM2 protein (Ene et al., 2020) contribute to tumour aggressiveness and resistance to therapy. Targeted elimination of key drivers of tumour aggressiveness might impact positively on treatment outcome. We hypothesized that upon treatment with Nutlin-3a, a functional MDM2 with altered conformation to bind other proteins including α5 integrin is expressed, and that functional or pharmacological inhibition of this integrin could inhibit MDM2 expression thereby preventing the proteasomal degradation of p53, leading to sustained p53 stabilization and activation. We found that treatment with Nutlin-3a led to increased expression of MDM2 in U87MG cells expressing α5 integrin but a decreased release of MDM2 in cells in which the gene for α5 integrin was deleted between 9 to 12 hours. This interesting finding has opened a short therapeutic window within which an α5 integrin antagonist could be used in combination with a p53 activator to increase p53 stabilization/activity by modulating the level of MDM2. However, the results when Nutlin-3a was combine with the integrin antagonist K34c were not very encouraging 6 hours post treatment, as both MDM2 and the 53 protein were affected. This part of the project was rendered difficult to conclude, as the MDM2 expressed due to treatment with Nutlin-3a is decreased by an integrin antagonist, as a p53 target gene it is also increased

by the activation of p53 by Nutlin-3a. In the same vain, as p53 is activated by Nurlin-3a, its is degraded by MDM2, consistent with a feedback regulation exerted by a reactivated p53. The respective part of both effects needs further investigations. In future investigations, it might be possible to use a different model in which the expression of MDM2 due treatment with Nutlin-3a is replaced by the transfection of U87MG cells with cDNA clone of the gene for MDM2 to create a stable cell line overexpressing MDM2.

Conclusion

Returning to the question posed at the beginning of this study, it is now possible to state that Idasanutlin is the most potent of the p53 activators tested. One of the more significant findings to emerge from this study is that our data have added more evidence to existing data supporting the important role of α5β1 integrin in GBM. It was also shown that inhibition of this integrin led to depletion in the level of the MDM2 protein. In line with previous findings from our Laboratory (Martinkova et al., 2010; Renner et al., 2016), this finding suggest that, the use of targeted therapies to repress the expression or inhibit the function of this integrin could sensitise GBM to conventional chemotherapeutic drugs.

Results part 2: Integrin α5β1 as a target in TMZ resistant cells

Modulation of integrins in Temozolomide-resistant U87MG glioblastoma cells. Integrin α5β1 as a target.

Saidu SANI[a,b], Mélissa MESSE[a], Nikita PALLAORO[a], Isabelle LELONG-REBEL[a], Ezzeddine HARMOUCH[c], Horst KESSLER[d], Jean-Pierre GIES[a], Lionel THOMAS[e], Patrice LAQUERRIERE[e], Sophie FOPPOLO[a], Damien REITA[a,f] and Monique DONTENWILL[a,*]

In memoriam of Isabelle Lelong-Rebel deceased in 2019.

a) Laboratoire de Bioimagerie et Pathologies (LBP), UMR CNRS 7021, Université de Strasbourg, Faculté de Pharmacie, 74 route du Rhin, CS 60024, 67401 Illkirch cedex, France. Institut Thématique Interdisciplinaire InnoVec, Université de Strasbourg.

b) Cancer and Diabetic Research Group, Department of Biochemistry and Molecular Biology, Faculty of Science, Alex Ekwueme Federal University Ndufu-Alike Ikwo, P.M.B 1010, Abakaliki, Ebonyi State. Nigeria.

c)

d)

e) Institut Pluridisciplinaire Hubert Curien (IPHC), UMR CNRS 7178, Université de Strasbourg, 67000 Strasbourg, France.

f) Department of Oncobiology, Laboratory of Biochemistry and Molecular Biology, University Hospital of Strasbourg, France

* corresponding author; monique.dontenwill@unistra.fr

Abstract

Glioblastoma are the most aggressive adult brain tumours for which new therapeutic strategies are highly needed. They almost always recur due to resistance to radio-and chemotherapies. We are interested in integrins, in particular α5β1 integrin, as therapeutic targets in glioblastoma. Previous works showed that it participates to the Temozolomide (TMZ) chemotherapy resistance by partly inhibiting the tumour suppressor p53 pathway. Here we investigated a new therapeutic option based on the combination of p53 activators and α5β1 integrin inhibitors in naïve U87MG glioma cells and their TMZ-resistant counterparts. We showed that resistance to TMZ is accompanied by a huge rearrangement of integrin expressions and that α5β1 integrin remains a pertinent target for TMZ-resistant glioblastoma. In addition, TMZ-resistant cells proved sensitive to different blockers of p53/mdm2 complexes able to reactivate the p53 signalling pathways. Our data support the hypothesis that adding p53 activators together with integrin antagonists may represent a pertinent therapeutic strategy for recurrent glioma tumours.

Keywords: Glioblastoma, integrin, Temozolomide.

Introduction

Glioblastoma (GBM) is the most common and most aggressive malignant brain tumour in adult that is characterized by high proliferation, invasion into normal brain tissue and resistance to therapies (Geraldo et al., 2019; Omuro, 2013). Currently there is no effective long-term treatment for this killer disease, but the standard of care is maximal surgical resection, followed by radiotherapy with concomitant and adjuvant temozolomide (TMZ) chemotherapy (Stupp et al., 2005). However, the prognosis of patients with glioblastoma remains poor and has not improved despite numerous clinical trials on new therapeutic propositions. Therefore, there is an urgent need for novel therapeutic strategies which may be underlined by a deep understanding of GBM and surrounding microenvironment crosstalk.

Primary and acquired resistance are the major challenges for the clinical use of standard and targeted therapies in GBM (Hombach-Klonisch et al., 2018; Yi et al., 2019). The main mechanism of glioblastoma resistance to TMZ involves O^6-methylguanine DNA methyl transferase (MGMT), a suicide enzyme that allows the direct repair of the lesion caused by TMZ, through removal of methyl group in position O^6 of guanine (Park et al., 2012). Previous studies have shown that cellular accumulation of the tumour suppressor protein p53 downregulates the expression of MGMT (Grombacher et al., 1998; Harris et al., 1996). The p53 protein is mutated in about 30% of glioblastoma (Brennan et al., 2013) although a subtype of glioblastoma expressing mostly wild type p53 has been identified in an integrated genomic analysis (Verhaak et al., 2010). But even if wild type p53 is expressed in 70% of GBM, its functions is frequently suppressed by MDM2/MDM4, E3 ubiquitin ligases that mark and target p53 for proteasomal degradation (Crespo et al., 2015; England et al., 2013; Vassilev, 2004). MDM2, a zinc finger nuclear phosphoprotein and negative regulator of the p53 protein, is often overexpressed in GBM and has been implicated in cancer cell proliferation and survival (Her et al., 2018; Reifenberger et al., 1993; Verreault et al., 2016). Inhibition of the p53-MDM2 interaction can rescue p53 degradation and restore p53 transcriptional activity, leading to p53-mediated induction of tumour cell apoptosis, thus making p53-MDM2 complex a promising target for glioblastoma expressing wild type p53 (England et al., 2013; Vassilev, 2004). The discovery of the p53-MDM2 inhibitor Nutlin-3a represented a breakthrough in the development of p53-activators (Vassilev, 2004). The more recent development of RG7388 (Idasanutlin), a second-generation MDM2 inhibitor with greater potency, selectivity, bioavailability and

effective p53 activating ability leading to p53-mediated induction of tumour cell apoptosis, is promising for cancers including GBM (Berberich et al., 2019; Fishlock et al., 2018).

Integrins have become the subject of numerous studies in the past 20 years, because of the vital role they play in tumour progression. The integrins are transmembrane heterodimeric cell surface receptors that mediate cell adhesion to the extracellular matrix (ECM) and support cell–cell interactions in multiple physiological and pathological conditions (Ellert-Miklaszewska et al., 2020; Malric et al., 2017). The frequent deregulation of integrin expressions and pathways in cancer cells underscores specific integrin major contributions in tumour growth and resistance to therapies. The disruption of the integrin signalling pathways by integrin antagonists has been shown to inhibit tumour growth and sensitize tumours to therapies in preclinical contexts. Cilengitide was the first integrin αvβ3/β5 antagonist reaching the clinic but clinical trials with cilengitide in combination with the standard of care (Stupp protocol) were unsuccessful (Stupp et al., 2010, 2014). Several reasons may explain these failures as reviewed in (Tucci et al., 2014). However, knowledge on integrin expressions and functions in glioblastoma merit further investigations to adapt integrin-based therapies to specific subpopulations of patients. In this way, expression of α5 integrin is enhanced in the mesenchymal subgroup of glioblastoma patients as compared to the others (Ellert-Miklaszewska et al., 2020; Janouskova et al., 2012) presumably conferring to these patients a better sensitivity to anti-α5 integrin therapy.

We and others (Janouskova et al., 2012; Renner et al., 2016) showed previously that α5β1 integrin is an interesting therapeutic target for GBM. Its overexpression at the mRNA (Lathia et al., 2014) or protein (manuscript submitted) levels define populations of patients with worse prognostic. In preclinical experiments it was shown that this integrin is involved in survival, migration, resistance to therapies and neoangiogenesis, all being hallmarks of GBM (Hynes, 2002; Janouskova et al., 2012; Murphy et al., 2015; Ray et al., 2014). In particular, we demonstrated the existence of a negative cross-talk between α5β1 integrin and p53 pathways supporting an implication in glioma resistance to chemotherapies (Janouskova et al., 2012; Martin et al., 2012). We also showed that inhibition of the integrin concomitantly with p53 activation with Nutlin-3a in α5-overexpressing cells led to a huge increase of cell apoptosis (Renner et al., 2016).

Integrin expressions in GBM vary after therapies (Malric et al., 2017). As an example, it was shown that in tumours recurring after bevacizumab treatment, α5β1 integrin was overexpressed in a subpopulation of patients (Delay et al, 2012). In this study, we aimed to investigate if

Temozolomide treatment may affect the integrin repertory in glioma cells taking as an example the U87MG cell line. Temozolomide-resistant cells were obtained that conserve the resistance even after removal of the drug. Transcriptomic analysis of non-treated U87MG cells and resistant cells cultured in the presence or absence of TMZ showed a high variation in the level of integrins. Interestingly, α5β1 integrin expression decreases in the presence but recovers after removal of the drug suggesting that it may represent a therapeutic target for recurrent glioblastoma. We also investigated if treatment of these recurrent TMZ-resistant cells may be sensitive to a combination of integrin antagonists and p53 reactivators. Our results may add new therapeutic perspectives for recurrent glioblastoma expressing high level of α5β1 integrin.

2. Materials and Methods

2.1 Drugs

Temozolomide (TMZ), 8-carbamoyl-3-methylimidazo[5,1-d]-1,2,3,5-tetrazin(3H)-one 5 (Sigma-Aldrich), was prepared as a 100mM stock solution in DMSO and stored at 4°C until use. Nutlin-3a, (4-[4,5-bis-(4-chlorophenyl)-2-(2-isopropoxy-4-methoxy-phenyl)-4,5-dihydro-imidazole-1-carbonyl]-piperazin-2-one), the active enantiomer, was from Cayman chemical company (Interchim, France). Nutlin-3a was prepared as a 10mM stock solution in ethanol and stored at -20°C until use. Idasanutlin also known as RG7388 ($C_{31}H_{29}Cl_2F_2N_3O_4$) was from Euromedex (MedChemExpress, France). Idasanutlin was prepared as a 10mM stock solution in DMSO and stored at -20°C until use. RITA (5,5'-(2,5-furandiyl) bis-2 thiophenemethanol), was from Cayman chemical company (Interchim, France). RITA was prepared as a 10mM stock solution in ethanol and stored at -20°C until use. K34c (2-(S)-2,6 dimethylbenzamido)-3-[4-(3-pyridin-2-ylaminoprooxy)-phenyl] propionic acid), first synthesized by the group of Pr Kessler (Munchen, Germany) here it was synthesized by a chemical company according to the procedure described in (Heckmann et al., 2008). Fr248 was synthesized in Kessler's Laboratory. K34C and Fr248 were prepared as a 10mM stock solution in DMSO and stored at 4°C until use. ATN-161 was from Sigma-Aldrich. ATN-161 was prepared as a 10mM stock solution in H_2O and stored at -20°C.

2.2 Cell culture

U87MG glioblastoma cell line (p53 wild type) was from American Type Culture Collection (LGC Standards Sarl, Molsheim, France). Cell lines were routinely cultured in MEM (Minimum Essential Medium Eagle) supplemented with 10% heat-inactivated foetal bovine

serum, 1% Na pyruvate and 1% Non-essential amino acid at 37ºC in a humidified atmosphere containing 5% CO_2. All cells were periodically authenticated by Multiplexion GmbH and tested for the presence of mycoplasma.

2.3 Generation of temozolomide-resistant glioblastoma cells

U87MG cells (500,000) were seeded in T25 cm^2 cell culture flask, containing EMEM (Eagle's minimal essential medium) supplemented with 10% serum, 1% Na pyruvate and 1 % Non-essential amino acid. The cells were allowed to adhere and after 24 hours the medium was replaced with a fresh medium containing 50 µM TMZ. Cell treatment was repeated twice a week for several weeks resulting in a sub-population of stable TMZ-resistant cells. The sub-population of resistant cells generated were continuously cultured in medium containing TMZ and named U87MG R50. After two months, a subpopulation of U87MG R50 cells was cultured in medium without TMZ and named U87MG R50 OFF.

2.4 IncuCyte cell confluence assay

Cells were plated (2,000 cells in 100 µl per well) into 96-well culture plates and the appropriate control solvent or drugs at 2x concentration in 100 µl of 2% FBS containing medium was added to the appropriate wells. To monitor cell growth, the plates were placed into the IncuCyte live-cell analysis system and allowed to warm at 37°C for 30 minutes prior to standard scanning with 4x objective every 3 hours for at least 96 hours. The captured phase contrast images were analysed using the incuCyte ZOOM software 2018.

2.5 Senescence assay

The β-galactosidase activity at pH 6 was determined using the Senescence Cells Histochemical Staining Kit (Sigma) according to the manufacturer's instructions. Briefly, cells were plated (2,000 cells/200µl) into a 96 well plate and the cells were washed twice with 1xPBS and fixed with 1x fixation buffer for 7 minutes at room temperature. The fixation buffer was aspirated, and wells rinsed thrice with 1x PBS. After washing, the cells were covered with staining mixture and incubated at 37ºC without CO_2. After 12 hours of staining, light microscopy was used to identify senescent (blue stained) cells.

2.6 Western blotting

Cells were plated (200,000 cells per well) into 6-well culture plates and treated with the appropriate control solvent or drugs. For the basal level values of proteins of interest cells were used 24h after plating. Proteins were extracted from adherent and floating cells after lysis with Laemmli sample buffer (Biorad) on ice and lysates heated at 95^0C for 10 minutes. Proteins were separated on precast gradient 4-20% SDSPAGE gels (Bio-Rad) and transferred to PVDF membrane (GE Healthcare, Velizy, France). After 1 hour of blocking at room temperature, membranes were probed with appropriate primary antibodies (**table 1**) overnight at 4ºC. Membranes were subsequently incubated with anti-rabbit or anti-mouse antibodies conjugated to horseradish peroxidase (Promega, Charbonnieresles- Bains, France), developed using chemoluminescence (ECL, Bio-Rad) and visualized with Las4000 image analyser (GE Healthcare). Quantification of non-saturated images was done using ImageJ software (National institutes of Health, Bethesda, MD, USA). GAPDH was used as the loading control for all samples.

2.7. Real-time qPCR

RNA was extracted using RNeasy minikit (Qiagen) according to the manufacturer's instructions. The extracted RNA was quantified using Nanodrop One (ThermoScientific) and was transcribed into cDNA using high capacity cDNA kit (Applied Biosystems). Real-time quantitative PCR was carried out using the ABI7000 SYBRGreen PCR detector with the probes (Invitrogen) listed in **Table 2**. Relative levels of mRNA gene expression were calculated using the $2^{-\Delta\Delta Ct}$ method.

2.9 RNAseq data

RNA-Seq libraries were generated from 400 ng of total RNA using TruSeq Stranded mRNA Library Prep Kit and TruSeq RNA Single Indexes kits A and B (Illumina, San Diego, CA), according to manufacturer's instructions. Briefly, following purification with poly-T oligo attached magnetic beads, the mRNA was fragmented using divalent cations at 94°C for 2 minutes. The cleaved RNA fragments were copied into first strand cDNA using reverse transcriptase and random primers. Strand specificity was achieved by replacing dTTP with dUTP during second strand cDNA synthesis using DNA Polymerase I and RNase H. Following addition of a single 'A' base and subsequent ligation of the adapter on double stranded cDNA fragments, the products were purified and enriched with PCR (30 sec at 98°C; [10 sec at 98°C, 30 sec at 60°C, 30 sec at 72°C] x 12 cycles; 5 min at 72°C) to create the cDNA library. Surplus PCR primers were further removed by purification using AMPure XP beads (Beckman-Coulter,

Villepinte, France) and the final cDNA libraries were checked for quality and quantified using capillary electrophoresis. Libraries were then sequenced on an Illumina HiSeq4000 system as single-end 1x50 base reads. Image analysis and base calling were performed using RTA 2.7.7 and bcl2fastq 2.17.1.14. Reads were preprocessed using cutadapt (Martin, 2011) version 1.10 in order to remove adapter, polyA and low-quality sequences (Phred quality score below 20), reads shorter than 40 bases were discarded for further analysis. Reads mapping to rRNA were also discarded (this mapping was performed using bowtie (Langmead and Salzberg, 2012) version 2.2.8). Reads were then mapped onto the hg38 assembly of human genome using STAR (Dobin et al., 2013) version 2.5.3a (--twopassMode Basic). Gene expression was quantified using htseq-count (Anders et al., 2015) version 0.6.1p1 and gene annotations from Ensembl release 99. Statistical analysis was performed using R 3.3.2 and DESeq2 (Love et al., 2014) 1.16.1 Bioconductor library.

Gene expression data obtained with DESeq2 was used to generate the heatmaps and dendrogram with R. Only genes expressed in all condition (defined if normalized reads count divided by median of transcripts length in kb is greater than 1 for gene across all nine libraries) were taken into account for visualization. Hierarchical clustering method was performed according pairwise complete-linkage method and using Pearson correlation for row clustering and Spearman correlation for column clustering. The biological significance of differentially expressed genes (DEGs) obtained were explored using ReactomePA, an R/Bioconductor package for reactome pathway analysis and visualization (Yu and He, 2016). |Log2(fold change) | > 2 (|log2FC|>2) and an adjusted false discovery rate (FDR) < 0.05 (using Benjamini-Hochberg correction) were used as the cut-off criteria of DEGs samples.

2.10 Confocal microscopy and Image Analysis

Coverslips were coated with fibronectin (20 µg/mL-1 in DPBS) and 25 000 cells were seeded in 10% serum containing medium and cultured for 24 hours. Cells were then fixed in 4% (v/v) paraformaldehyde for 12 minutes, and permeabilized with 0.1% Triton-X100 for 2 min. After 1-hour of blocking step in 3% bovine serum albumin (BSA)-PBS solution, cells were incubated with primary antibodies against integrin α5 (clone IIA1 Pharmingen, 1µl/100µl in 3% PBS-BSA) and β1 integrin (purified anti human CD29, Clone:TS2/16, 1µl/100µl in 3% PBS-BSA) overnight at 4 °C (1µl/100µl each in PBS-BSA 3%). Cells were rinsed in 1xPBS and incubated with appropriate secondary antibodies (Alexa fluor@ 647 goat anti-mouse (A21236)1µl/200µl in 3% PBS-BSA and Alexa fluor@ 688 goat anti-mouse 1µl/200µl in 3% PBS-BSA) and 4', 6-

diamidino-2-phenylindole (DAPI) (1µl/2000µl in 3% PBS-BSA was added for nuclei staining) for 45 min. Samples were mounted on microscope slides using fluorescence mounting medium (Dako). Images were acquired using a confocal microscope (LEICA TCS SPE II, 63× magnification oil-immersion). For each experiment, identical background subtraction and scaling was applied to all images. Mean gray values of 10-12 images (4-5 cells per images) from 3 independent experiments were calculated using JACoP plugin ImageJ software.

For 3D spheroid microscopy, microtissues (3D spheroids) of U87MG, U87MG R50 and U87MG OFF R50 cells were collected from hanging drops after 6 days of culture and were embedded in Tissue-Tek, frozen at -20°C and sectioned (10µm) using a cryostat (Leica, CM3000). Serial sections were rinsed with PBS and fixed for 10 min with 4% paraformaldehyde at 4°C. After three washes with 1xPBS for 5 minutes each at room temperature, sections were incubated for 30 minutes at room temperature in a blocking solution of 1% BSA and 0.1% Triton X100 and then incubated overnight at 4°C with the primary antibodies against integrin α5 (clone IIA1 Pharmingen, 1µl/100µl in 1% PBS-BSA) and β1 integrin (purified anti human CD29, Clone:TS2/16, 1µl/100µl in 1% PBS-BSA) overnight at 4 °C (1µl/100µl each in 1% PBS-BSA). After three washes with 1xPBS, sections were incubated with the appropriate secondary antibodies (Alexa fluor@194(A21203) and Alexa Fluor 488 (A11001)). Nuclei were stained with 4', 6-diamidino-2-phenylindole (DAPI, Euromedex, Souffelweyersheim, France). Negative controls were performed either omitting the primary antibody or using normal goat serum (NGS). After 3 additional washes in PBS, slides were mounted in fluorescence mounting medium (Dako, Trappes, France) and observed with a fluorescence microscope (Leica DM4000B).

Results

1. Long term exposure of U87MG cells to TMZ generates persistent resistant cells

To generate TMZ-resistant cells, we subjected U87MG cells to 50 µM TMZ for several weeks resulting in a sub-population of stable TMZ-resistant U87MG cells. The sub-population of resistant cells were either continuously cultured in medium containing 50 µM TMZ (U87MG R50) or, after 2 months in presence of TMZ, cultured in medium without TMZ (U87MG OFF R50). We confirmed that the parental cells were sensitive to 50 µM TMZ and that the U87MG R50 cells were insensitive to TMZ up to 96 hours (**Figure 1A**). Interestingly, TMZ resistance was maintained in U87MG OFF R50 cells (**Figure 1A**). Furthermore, while the parental cells

were dose dependently sensitive to TMZ, the U87MG R50 and U87MG OFF R50 cells remained insensitive to varying concentrations up to 100 μM TMZ (**Supplementary Figure S1**).

Phase-contrast images obtained from the IncuCyte (**Figure 1B**), showed that the cellular morphology of U87MG R50 cells differed from its parental cells by having a more spread, enlarged, and flattened morphology. However, the U87MG OFF R50 cells displayed a mixed morphology with some cells presenting the morphology of U87MG R50 cells while the others present the morphology of the parental cells. TMZ treatment for 3 days produced a profound change in the cellular morphology of the parental cells, causing extensive branching, reduction in total cell number and confluence (**Figure 1B**). On the contrary, both the U87MG R50 cells and U87MG OFF R50 cells appeared healthy with no obvious morphological changes 72 hrs post TMZ treatment (**Figure 1B**). Overall, these results demonstrated that a fraction of the U87MG cells that survived prolonged exposure to TMZ, developed acquired TMZ-resistance which remains even after withdrawal of TMZ.

2. TMZ induces senescence in U87MG cells

Since the resistant cells showed the morphological features of senescent cells, we next tested the senescence marker SA-βGAL. Upon short incubation in 50 μM TMZ, remaining cells were all positive for SA-βGAL staining. Positive cells were maintained in the U87MG R50 cells but largely decreased in U87MG OFF R50 cells (**Figure 2A**). Accordingly, a significant increase in the expression of proteins p16 and p21, known to be involved in senescence, was observed in U87MG R50 cells as compared to the parental cells. Increase in p16 but not in p21 was recorded in U87MG R50 OFF cells (**Figure 2B**). The capacity to fill the culture wells was slightly decreased for U87MG R50 cells as compared to parent and U87MG OFF R50 cells (**Figure 2C**). Altogether, results suggest that TMZ triggers senescence in U87MG cells as already reported (Li et al., 2013; Martinkova et al., 2010) which is decreases after TMZ removal.

3. Extracellular matrix organization and integrins are affected by TMZ

We used RNAseq to compare the three cell lines. Analysis of global gene variations by unsupervised hierarchal clustering showed that profound changes occurred during TMZ treatment with the biggest differences between U87MG and U87MG R50 cells (**Figure 3A**). U7MG R50 OFF were more closely related to the U87MG non treated cells. The most

significant genes were subjected to reactome pathway analysis. Biological pathways mostly impacted by long term Temozolomide treatment (R50 versus control cells) are Extracellular matrix organisation, O-linked glycosylation and Integrin cell surface interactions (**Figure 3B**). Focusing on the integrin genes, profound rearrangements of integrin subunit expression levels were observed (**Figure 3C**). Four main clusters may be underlined. Cluster 1 corresponds to integrins expressed in U87MG control cells but repressed in R50 cells and with intermediary expression in R50 OFF cells (Integrins α2, α3, α4, α5, α10, α11, αv, β1, β3). Cluster 2 involves integrins overexpressed in U87MG R50 OFF cells as compared to the two other cell lines (α6, β6 and β8) of which α6 and β8 are described as markers of glioma stem cells (Lathia et al., 2010; Malric et al., 2019). Cluster 3 corresponds to integrins repressed in U87MG R50 OFF cells (α7, α9, αx, αD, β5, β7). Cluster 4 includes integrins overexpressed in U87MG R50 cells (α1, αL, αM, β2, β4) including some leucocyte specific integrins. Data confirm that integrin expressions are subjected to specific variations during the time course of chemotherapy with Temozolomide.

As we demonstrated previously that integrin α5β1 is involved in TMZ resistance (Janouskova et al., 2012), we next focused on this integrin and examined its expression at the protein level in the parent and TMZ-resistant cells lines. We observed a clear decrease of the α5 subunit in U87MG R50 cells without significant change in that of the β1 subunit. Interestingly, α5 integrin level increases after removal of TMZ in the U87MG R50 OFF cells reaching the level seen in non-treated cells and β1 integrin level became slightly higher than in the non-treated cells (**Figure 4A**). By contrast, αv integrin (another integrin largely involved in glioblastoma aggressiveness) level did not change between the 3 cell lines. As a confirmation we also addressed the changes of expression of α5β1 integrin by immunohistochemistry. As can be seen in **Figure 4B**, the expression of either α5 or β1 integrin is reduced in U87MG R50 but both reappear after removal of TMZ in U87MG R50 OFF cells. These results were confirmed in cells grown as spheres (**suppl. Figure 2**). To further confirm the effect of TMZ on α5β1 integrin expression, we evaluated the long-term effect of TMZ on U373 and LN443 glioma cells. Interestingly, TMZ significantly decreased the basal expression of α5 integrin in U373 cell line but removal of TMZ did not increase its expression. No effect on the expression of α5 integrin was observed in LN443 cells (**Figure 4C**). We checked the effect of TMZ in the two cell lines and observed that U373 cells were sensitive but LN443 cells were insensitive (**suppl. Figure 3).** These results suggest that α5β1 integrin expression in GBM is decreased under the pressure of TMZ in TMZ-sensitive cell lines.

Other integrins were evaluated to confirm the RNAseq data. Experiments in way

4. Effects of α5β1 antagonists on the U87MG parental and TMZ resistant cells.

We next aimed to compare the effects of three α5β1 antagonists on cell morphology and confluence by the Incucyte technology. We used K34c, FR248 and ATN161. The two former are RGD-like integrin ligands able to inhibit the cell adherence to fibronectin as shown in our previous works (Ray et al., 2014). ATN161 has been designed to target the fibronectin synergy site for α5β1 integrin and is unable to disturb cell adherence (Khalili et al., 2006). As shown in the **figure 5A**, K34c proved able to decrease the cell adherence for all three cell lines inhibiting the cell spreading and forming some sphere-like structures particularly in U87MG and U87MG R50 OFF cells. FR248 is less efficient to inhibit cell spreading than K34c and particularly ineffective in U87MG R50 cells. Lastly, ATN161 was unable to inhibit cell adherence as expected in all cell lines. Quantification of cell confluence after 3 days of treatments confirmed these morphological observations (**Figure 5B**). FR248 which is more selective than K34c for α5β1 than for αvβ3 integrin (Heckmann et al., 2008) is inactive in U87MG R50 cells in accordance with the low level of α5β1 integrin in these cells. Data suggest that U87MG and U87MG R50 OFF cells may be similarly sensitive to α5β1 integrin antagonists at least for inhibition of cell adherence and confluence.

5. p53 signalling pathway in U87MG and TMZ-resistant cells.

TMZ is known to activate the p53 pathway (Martinkova et al., 2010b; Renner et al., 2016b)**.** In order to compare the p53 stabilisation and activation in the 3 cell lines we evaluated the expression of p53 and MDM2 proteins in basal conditions of culture. In U87MG R50 cells as well as in the U87MG R50 OFF cells, p53 is stabilised and its target gene MDM2 is increased as compared to the parental cell line. MDM2 and p21 mRNA levels showed that both were increased in the presence of TMZ but only MDM2 mRNA remained higher in U87MG R50 OFF cells as compared to control U87MG cells (**Figure 6A**). Results suggest that p53 activation is sustained in the presence of TMZ but that activation of target genes MDM2 and p21 may differ after removal of the drug.

As reactivation of p53 by small molecules inhibiting the MDM2/p53 interaction and p53 degradation may represent an alternative therapeutic option than chemotherapy in p53 wild type tumours (Renner et al., 2016), we next aimed to see if such drugs are able to affect p53 signalling in control and resistant cells. Three different p53 activators were used: Nutlin-3a and

Idasanutlin that bind to the MDM2 part and RITA that bind to the p53 part of the MDM2/p53 complex. As can be seen in **Figure 6B**, all three drugs enhance the stability of p53 as well as its activation (shown by the increase in MDM2 protein). No differences could be observed between control U87MG cells and their TMZ-resistant counterparts. In these experiments, Idasanutlin was the most efficient activator of the p53 pathway even at 0.1 µM (a concentration 10 times lower than for Nutlin-3a and RITA) and RITA the less efficient after 24 hours of treatment. Results suggest that TMZ-resistant cells may benefit from an alternative way to reactivate the p53 tumour suppressor pathway.

6. Impact of integrin antagonists on p53 pathway

We described previously a negative crosstalk between α5β1 integrin and p53 signalling pathways implicated in chemotherapy resistance of glioma cells. We showed that activating p53 concomitantly with inhibiting integrin α5β1 led to an increase in p53 signalling and glioma cell death in α5 integrin subunit overexpressing cells (Janouskova et al., 2012; Renner et al., 2016). We thus wondered if similar results may be obtained in TMZ-resistant cells. We investigated association of p53 activators (Nutlin-3a, RITA and Idasanutlin) with each of the three integrin antagonists on cell confluence. As shown in **Figure 7**, association of Idasanutlin (0.1 µM) with K34c (20 µM) and FR248 (20 µM) for 72 hours in U87MG or U87MG R50 OFF cells led to a significant decrease in cell confluence as compared to each drug alone or no treatment. However, association of Idasanutlin with ATN-161 has no supplementary effect compared to Idasanutlin alone. The summary of all results is given in **Table 3** and shows that all combinations have an impact on cell confluence after 72h of treatment. We also checked Nutlin-3a and RITA combinations with K34c and FR248 in U87MG R50 cells. Results indicated that only Nutlin-3a or RITA association with K34c proved able to significantly affect the confluence over that of either p53 activators alone. The inefficacy of FR248 is in accordance with the low expression of α5 integrin in these cells (data not shown).

We next investigated combination of drugs on p53 and mdm2 expressions after 24h treatment. In U87MG R50 OFF cells, FR248 increased Idasanutlin effects on p53, phosphoser15-p53 and mdm2 expressions although it seems not be the case for U87MG cells (**Figure 8A**). Interestingly, U87MG cells appeared sensitive to the FR248/Idasanutlin or RITA combinations (**Figure 8B and 8C**) which allowed an increase in p53 and mdm2 expression for Idasanutlin but only in p53 expression with RITA.

These experiments must be completed as well as experiments investigating relationships between effects on confluence, p53 signalling and cell death.

Discussion

Glioblastoma remains the most common and most aggressive malignant brain tumour in adult (Geraldo et al., 2019). Despite numerous clinical trials on conventional, targeted, and immunological therapies, no new clear therapeutic options have been proposed these last years (Bush et al., 2017). Failures are in part due to the high molecular and cellular heterogeneity encountered in these tumours as well as to the particular brain microenvironnement. High level of recurrence is a hallmark of GBM linked to tumour cell dissemination in the normal brain but also to mechanisms of resistance to radiotherapy and/or chemotherapy. Although TMZ is currently the only approved chemotherapeutic drug known to significantly improve the overall survival of GBM patients (Stupp et al., 2005), the development of acquired TMZ-resistance leading to treatment failure remains one of the challenge to be resolved. Previous works stressed the role of MGMT which epigenetic regulation (promoter methylation or demethylation) is involved in the clinical response to TMZ. However, both MGMT methylated and MGMT unmethylated GBM can develop resistance to TMZ. Acquired resistance was shown to be linked to loss of DNA mismatch repair (MMR) (McFaline-Figueroa et al., 2015) or activation of the base excision repair (BER) (Bobola et al., 2012). Along with this, strategies to block BER through inhibition of PARP enzymes (Yuan et al., 2020) were proposed to suppress the emergence of TMZ resistance.

In this work, we generated TMZ-resistant cells by subjecting U87MG cells to TMZ 50 µM treatment as an in vitro model of MGMT- negative TMZ resistance. We aimed to compare cells continuously grown in the presence of TMZ (U87MG R50) with resistant cells growing in the absence of TMZ (U87MG R50 OFF), this last model is a reflect of clinical recurrence. We confirmed that U87MG cells were sensitive to TZM, resulting in large population of cell death at the beginning with few cells remaining alive. We showed that the cellular morphology of U87MG R50 cells differed from its parental cells by having a more spread, enlarged, and flattened morphology reminiscent of senescence.

It has already been demonstrated that TMZ induce senescence (Li et al., 2013; Martinkova et al., 2010) which may be associated with senescence-associated β-galactosidase (SA-Bgal) staining (Dimri et al., 1995). In line with this, we demonstrated that the few U87MG cells remaining alive after one-week incubation in 50 µM TMZ were all positive for SA-βGAL staining. A significant proportion of positive cells were maintained in the U87MG R50 cells but largely decreased in U87MG OFF R50 cells further indicating the role of TMZ in this

senescence state. The enlarged morphology of the U87MG R50 cells mirrored that of other studies in which senescent cells were defined as generally enlarge, often doubling in volume, and, if adherent, adopt a flattened morphology (Campisi, 2013). Other studies reported that TMZ-resistant U87MG cells adopt an EMT-like morphology (spindle-cell morphology, loss of intercellular communications, formation of pseudopodia) (Yi et al., 2016). These morphological differences can be attributed to the conditions used to generate the resistant cells, 400 µM TMZ for 6 months versus 50µM TMZ along our study. In fact, several protocols for generating glioma resistant cells were applied with different concentrations of TMZ for various time periods explaining differences in the results (Lee, 2016b). Interestingly, a recent work described a transient state acquired by U251glioma cells during the acquisition of TMZ resistance and defined by slow growth, a distinct morphology and a shift in metabolism (Rabé et al., 2020) indicating that care must be taken when comparing different results. In support of the senescence state, we found a significant increase in p53, p16 and p21 in U87MG R50 cells as compared to the parent cells, whereas an increase in p16 but not in p21 was detected in U87MG R50 OFF cells. In addition, the capacity to fill the culture wells was slightly decreased for U87MG R50 cells as compared to parent and U87MG OFF R50 cells, suggesting a form of cell cycle arrest. Consistent with our finding, the overexpression of p53, p21, or p16INK4a has been demonstrated to be generally sufficient for the initiation and maintenance of senescence growth arrest (Beauséjour et al., 2003; McConnell et al., 1998). Thus, our results showed that TMZ induced a senescence-like phenotype which can persist until the drug is removed from the culture medium. At this time, U87MG cells remains resistant to the drug (U87MG R50 OFF) but recapitulate normal proliferation as would occur in recurrent glioblastoma.

For the first time in our knowledge, an analysis of gene regulation of resistant cells either under the pressure of TMZ or after removal of the drug was done. Interestingly, profound changes were observed between U87MG R50 cells and the non–treated cell whereas U87MGR50 OFF cells showed a more closely related picture to the control cells. Comparison between U87MG R50 and control cells with Reactome indicated that the most affected pathways was Extracellular Matrix Organisation, followed by O-linked glycosylation, Diseases of glycosylation and Integrin cell surface interaction. Interestingly, the heatmap when focused on integrin genes confirmed that profound changes in integrin expressions occurs in the resistant cells as compared to the non-treated cells. Each cell type has a particular set of integrins which is overexpressed as compared to the two others. This may be interesting for specific anti-integrin therapeutic options to be used either concomitantly to TMZ or only at tumour

recurrence. As an example, U87MG R50 OFF cells overexpress α6 and β8 integrins, both known to be glioma stem cell markers (Lathia et al., 2010; Malric et al., 2019). Accordingly, a dedifferentiation of tumour cells towards glioma stem cells has been reported in tumours after radiotherapy or TMZ chemotherapy (Auffinger et al., 2014; Dahan et al., 2014). Specific anti-α6 and/or β8 integrin therapies may be used for recurrent tumors.

In previous studies, we demonstrated that α5β1 integrin is involved in TMZ resistance (Janouskova et al., 2012). As α5 and β1 integrin subunits appears to be decreased at the mRNA level in U87MG R50 cells and thereafter slightly increased in U87MG R50 OFF cells, we focused on this integrin. We found a clear decrease in α5 subunit in U87MG R50 cells at the protein level without significant change in that of the β1 subunit. It is interesting to note that the level of α5 integrin increases after removal of TMZ in the U87MG R50 OFF cells reaching the level seen in non-treated cells and β1 integrin level became slightly higher than in the non-treated cells. We confirmed this results by immunohistochemistry of adherent cells and cells grown as spheres. These findings portray α5β1 integrin as a promising target for recurrent GBM as was proposed in a study examining bevacizumab-treated recurrent glioblastoma (DeLay et al., 2012).

We demonstrated in previous studies that TMZ activate the p53 pathway in U87MG cells (Martinkova et al., 2010; Renner et al., 2016)**.** Here, we compared p53 stabilisation and activation in the 3 cell lines by evaluated the expression of p53 and MDM2 proteins in basal culture conditions. We found that basal p53 is stabilised and its target gene MDM2 is increased in U87MG R50 and U87MG R50 OFF cells, as compared to the parental cell line. Moreover, the mRNA levels of MDM2 and p21 were increased in the presence of TMZ but only MDM2 mRNA remained higher in U87MG R50 OFF cells as compared to control U87MG cells. Results suggest that p53 activation is sustained in the presence of TMZ but that activation of target genes MDM2 and p21 may differ after removal of the drug. As MDM2 level remains high after TMZ removal, it suggests that it may be considered as a therapeutic target in recurrent glioblastoma as well as in primary tumours overexpressing MDM2 (Verreault et al., 2016).

Pharmacological inhibition of α5β1 decrease tumour cell migration, invasion, and pushed TMZ-treated cells from senescence toward apoptosis while modulating the p53 pathway (Martinkova et al., 2010b; Ray et al., 2014). In this study, we compared the effect of the α5β1 integrin antagonists K34c, FR248 and ATN161 on the morphology and confluence of the cells. Our results confirmed that U87MG and U87MG R50 OFF cells may be similarly sensitive to

α5β1 integrin antagonist FR248, the most selective one. K34c was particularly efficient to inhibit cell spreading and to form sphere-like structures in all three cell lines suggesting that it may act not only through inhibition of α5β1 but also through αvβ3 integrin inhibition. ATN161 is unable to affect cell confluence as expected. At this point it must be emphasized that relationships between cell adherence inhibition and cell survival is not clearly established in our experiments precluding definite conclusions on the antagonist's effects on cell viability.

We nevertheless examined the possibility of using these antagonists in combination with several p53 activators including MDM2-targeting molecules.

Restoration of the tumour-suppressor function of p53 by disrupting the MDM2-p53 protein-protein interaction is considered an attractive therapeutic strategy for GBM expressing p53 wild type. Several small molecule inhibitors of the p53-MDM2 complex have been developed with some already in clinical trials. Nutlin-3a, a cis-imidazoline compound is the first selective MDM2 inhibitor developed (Klein and Vassilev, 2004). However, the large hydrophobic protein-protein interaction interface on MDM2 that compromise its potency and pharmacokinetic profiles, led to the discovery of Idasanutlin, a pyrrolidine compound with superior potency and selectivity (Ding et al., 2013). Here, we compared three different p53 activators: Nutlin-3a (Vassilev, 2004) and Idasanutlin (Ding et al., 2013) that bind to the MDM2 part and RITA (Issaeva et al., 2004) that bind to the p53 part of the MDM2/p53 complex to stabilize and activate the p53 pathway. We found that all three drugs enhance the stability of p53 as well as its activation (shown by the increase in MDM2 protein) with Idasanutlin been the most efficient. Results suggest that TMZ-resistant cells may benefit from an alternative way to reactivate the p53 tumour suppressor pathway.

In previous work of the team, a negative crosstalk between α5β1 integrin and p53 signalling pathways implicated in chemotherapy resistance of glioma cells was described. Activating p53 concomitantly with inhibiting integrin α5β1 led to an increase in p53 signalling and glioma cell death in α5 integrin subunit overexpressing cells (Janouskova et al., 2012b; Renner et al., 2016b). We evaluated this strategy on the resistant U87MG cells. All the combinations of integrin antagonists and p53 activators led to a better inhibition of cell confluence than either treatment alone in U87MG and U87MG R50 OFF cells except for combination with ATN161. However, our preliminary data (*which need confirmation*) suggest a dissociation between the impact of combination treatments on cell confluence and on activation of the p53 pathway. In fact, ATN161 which did not alter confluence seems to increase the p53 function in association with Idasanutlin and RITA for U87MG cells but not for U87MG R50 OFF cells. Conversely,

FR248 association with Idasanutlin affects p53 signaling in U87MG R50 OFF cells but not in U87MG cells. These data are not easily explainable at this step but point already to differences in the behaviour of p53 between TMZ naïve cells and resistant cells. Works remain to be done to show if specific combinations may better affect glioma cell viability for each cell type.

Conclusion

In conclusion, our work shows a huge impact of Temozolomide on the integrin repertoire of U87MG cells. The integrin expressions appear highly switchable during temaozolomide treatment. Specific integrins may be particularly targetable at different time points of glioblastoma treatment and combination therapies evaluated according to their expression. Although confirmation in patient-derived cell lines and other preclinical models is needed, our data add new evidence that the α5β1 integrin has a role to play as a therapeutic target in recurrent glioblastoma.

References

Anders, S., Pyl, P.T., and Huber, W. (2015). HTSeq—a Python framework to work with high-throughput sequencing data. Bioinformatics *31*, 166–169.

Auffinger, B., Tobias, A.L., Han, Y., Lee, G., Guo, D., Dey, M., Lesniak, M.S., and Ahmed, A.U. (2014). Conversion of differentiated cancer cells into cancer stem-like cells in a glioblastoma model after primary chemotherapy. Cell Death Differ *21*, 1119–1131.

Beauséjour, C.M., Krtolica, A., Galimi, F., Narita, M., Lowe, S.W., Yaswen, P., and Campisi, J. (2003). Reversal of human cellular senescence: roles of the p53 and p16 pathways. EMBO J *22*, 4212–4222.

Berberich, A., Kessler, T., Thomé, C.M., Pusch, S., Hielscher, T., Sahm, F., Oezen, I., Schmitt, L.-M., Ciprut, S., Hucke, N., et al. (2019). Targeting Resistance against the MDM2 Inhibitor RG7388 in Glioblastoma Cells by the MEK Inhibitor Trametinib. Clin. Cancer Res. *25*, 253–265.

Bobola, M.S., Kolstoe, D.D., Blank, A., Chamberlain, M.C., and Silber, J.R. (2012). Repair of 3-methyladenine and abasic sites by base excision repair mediates glioblastoma resistance to temozolomide. Front Oncol *2*, 176.

Brennan, C.W., Verhaak, R.G.W., McKenna, A., Campos, B., Noushmehr, H., Salama, S.R., Zheng, S., Chakravarty, D., Sanborn, J.Z., Berman, S.H., et al. (2013). The Somatic Genomic Landscape of Glioblastoma. Cell *155*, 462–477.

Bush, N.A.O., Chang, S.M., and Berger, M.S. (2017). Current and future strategies for treatment of glioma. Neurosurg Rev *40*, 1–14.

Campisi, J. (2013). Aging, Cellular Senescence, and Cancer. Annu Rev Physiol *75*, 685–705.

Crespo, I., Vital, A.L., Gonzalez-Tablas, M., Patino, M. del C., Otero, A., Lopes, M.C., de Oliveira, C., Domingues, P., Orfao, A., and Tabernero, M.D. (2015). Molecular and Genomic Alterations in Glioblastoma Multiforme. The American Journal of Pathology *185*, 1820–1833.

Dahan, P., Martinez Gala, J., Delmas, C., Monferran, S., Malric, L., Zentkowski, D., Lubrano, V., Toulas, C., Cohen-Jonathan Moyal, E., and Lemarie, A. (2014). Ionizing radiations sustain glioblastoma cell dedifferentiation to a stem-like phenotype through survivin: possible involvement in radioresistance. Cell Death Dis *5*, e1543.

Ding, Q., Zhang, Z., Liu, J.-J., Jiang, N., Zhang, J., Ross, T.M., Chu, X.-J., Bartkovitz, D., Podlaski, F., Janson, C., et al. (2013). Discovery of RG7388, a Potent and Selective p53–MDM2 Inhibitor in Clinical Development. J. Med. Chem. *56*, 5979–5983.

Dobin, A., Davis, C.A., Schlesinger, F., Drenkow, J., Zaleski, C., Jha, S., Batut, P., Chaisson, M., and Gingeras, T.R. (2013). STAR: ultrafast universal RNA-seq aligner. Bioinformatics *29*, 15–21.

Ellert-Miklaszewska, A., Poleszak, K., Pasierbinska, M., and Kaminska, B. (2020). Integrin Signaling in Glioma Pathogenesis: From Biology to Therapy. Int J Mol Sci *21*.

England, B., Huang, T., and Karsy, M. (2013). Current understanding of the role and targeting of tumor suppressor p53 in glioblastoma multiforme. Tumor Biol. *34*, 2063–2074.

Fishlock, D., Diodone, R., Hildbrand, S., Kuhn, B., Mössner, C., Peters, C., Rege, P.D., Rimmler, G., and Schantz, M. (2018). Efficient Industrial Synthesis of the MDM2 Antagonist Idasanutlin via a Cu(I)-catalyzed [3+2] Asymmetric Cycloaddition. Chimia (Aarau) *72*, 492–500.

Geraldo, L.H.M., Garcia, C., da Fonseca, A.C.C., Dubois, L.G.F., de Sampaio e Spohr, T.C.L., Matias, D., de Camargo Magalhães, E.S., do Amaral, R.F., da Rosa, B.G., Grimaldi, I., et al. (2019). Glioblastoma Therapy in the Age of Molecular Medicine. Trends in Cancer *5*, 46–65.

Grombacher, T., Eichhorn, U., and Kaina, B. (1998). p53 is involved in regulation of the DNA repair gene O6-methylguanine-DNA methyltransferase (MGMT) by DNA damaging agents. Oncogene *17*, 845–851.

Harris, L.C., Remack, J.S., Houghton, P.J., and Brent, T.P. (1996). Wild-Type p53 Suppresses Transcription of the Human O6-Methylguanine-DNA Methyltransferase Gene. 5.

Heckmann, D., Meyer, A., Laufer, B., Zahn, G., Stragies, R., and Kessler, H. (2008). Rational Design of Highly Active and Selective Ligands for the α5β1 Integrin Receptor. ChemBioChem *9*, 1397–1407.

Her, N.-G., Oh, J.-W., Oh, Y.J., Han, S., Cho, H.J., Lee, Y., Ryu, G.H., and Nam, D.-H. (2018). Potent effect of the MDM2 inhibitor AMG232 on suppression of glioblastoma stem cells. Cell Death Dis *9*, 792.

Hombach-Klonisch, S., Mehrpour, M., Shojaei, S., Harlos, C., Pitz, M., Hamai, A., Siemianowicz, K., Likus, W., Wiechec, E., Toyota, B.D., et al. (2018). Glioblastoma and chemoresistance to alkylating agents: Involvement of apoptosis, autophagy, and unfolded protein response. Pharmacol. Ther. *184*, 13–41.

Hynes, R.O. (2002). A reevaluation of integrins as regulators of angiogenesis. Nat Med *8*, 918–921.

Issaeva, N., Bozko, P., Enge, M., Protopopova, M., Verhoef, L.G.G.C., Masucci, M., Pramanik, A., and Selivanova, G. (2004). Small molecule RITA binds to p53, blocks p53–HDM-2 interaction and activates p53 function in tumors. Nat Med *10*, 1321–1328.

Janouskova, H., Maglott, A., Leger, D.Y., Bossert, C., Noulet, F., Guerin, E., Guenot, D., Pinel, S., Chastagner, P., Plenat, F., et al. (2012b). Integrin α5β1 plays a critical role in resistance to temozolomide by interfering with the p53 pathway in high-grade glioma. Cancer Res *72*, 3463–3470.

Khalili, P., Arakelian, A., Chen, G., Plunkett, M.L., Beck, I., Parry, G.C., Doñate, F., Shaw, D.E., Mazar, A.P., and Rabbani, S.A. (2006). A non-RGD-based integrin binding peptide (ATN-161) blocks breast cancer growth and metastasis in vivo. Mol. Cancer Ther. *5*, 2271–2280.

Klein, C., and Vassilev, L.T. (2004). Targeting the p53–MDM2 interaction to treat cancer. Br J Cancer *91*, 1415–1419.

Langmead, B., and Salzberg, S.L. (2012). Fast gapped-read alignment with Bowtie 2. Nat Methods *9*, 357–359.

Lathia, J.D., Gallagher, J., Heddleston, J.M., Wang, J., Eyler, C.E., MacSwords, J., Wu, Q., Vasanji, A., McLendon, R.E., Hjelmeland, A.B., et al. (2010). Integrin alpha 6 regulates glioblastoma stem cells. Cell Stem Cell *6*, 421–432.

Lathia, J.D., Li, M., Sinyuk, M., Alvarado, A.G., Flavahan, W.A., Stoltz, K., Rosager, A.M., Hale, J., Hitomi, M., Gallagher, J., et al. (2014). High-throughput flow cytometry screening reveals a role for junctional adhesion molecule a as a cancer stem cell maintenance factor. Cell Rep *6*, 117–129.

Lee, S.Y. (2016). Temozolomide resistance in glioblastoma multiforme. Genes Dis *3*, 198–210.

Li, L., Hu, Y., Ylivinkka, I., Li, H., Chen, P., Keski-Oja, J., and Hyytiäinen, M. (2013). NETRIN-4 Protects Glioblastoma Cells FROM Temozolomide Induced Senescence. PLoS One *8*.

Love, M.I., Huber, W., and Anders, S. (2014). Moderated estimation of fold change and dispersion for RNA-seq data with DESeq2. Genome Biology *15*, 550.

Malric, L., Monferran, S., Gilhodes, J., Boyrie, S., Dahan, P., Skuli, N., Sesen, J., Filleron, T., Kowalski-Chauvel, A., Moyal, E.C.-J., et al. (2017). Interest of integrins targeting in glioblastoma according to tumor heterogeneity and cancer stem cell paradigm: an update. Oncotarget *8*.

Malric, L., Monferran, S., Delmas, C., Arnauduc, F., Dahan, P., Boyrie, S., Deshors, P., Lubrano, V., Da Mota, D.F., Gilhodes, J., et al. (2019). Inhibiting Integrin β8 to Differentiate and Radiosensitize Glioblastoma-Initiating Cells. Mol Cancer Res *17*, 384–397.

Martin, M. (2011). Cutadapt removes adapter sequences from high-throughput sequencing reads. EMBnet.Journal *17*, 10–12.

Martin, S., Janouskova, H., and Dontenwill, M. (2012). Integrins and p53 pathways in glioblastoma resistance to temozolomide. Front Oncol *2*.

Martinkova, E., Maglott, A., Leger, D.Y., Bonnet, D., Stiborova, M., Takeda, K., Martin, S., and Dontenwill, M. (2010). alpha5beta1 integrin antagonists reduce chemotherapy-induced premature senescence and facilitate apoptosis in human glioblastoma cells. Int J Cancer *127*, 1240–1248.

McConnell, B.B., Starborg, M., Brookes, S., and Peters, G. (1998). Inhibitors of cyclin-dependent kinases induce features of replicative senescence in early passage human diploid fibroblasts. Curr Biol *8*, 351–354.

McFaline-Figueroa, J.L., Braun, C.J., Stanciu, M., Nagel, Z.D., Mazzucato, P., Sangaraju, D., Cerniauskas, E., Barford, K., Vargas, A., Chen, Y., et al. (2015). Minor Changes in Expression of the Mismatch Repair Protein MSH2 Exert a Major Impact on Glioblastoma Response to Temozolomide. Cancer Res. *75*, 3127–3138.

Murphy, P.A., Begum, S., and Hynes, R.O. (2015). Tumor Angiogenesis in the Absence of Fibronectin or Its Cognate Integrin Receptors. PLoS One *10*.

Omuro, A. (2013). Glioblastoma and Other Malignant Gliomas: A Clinical Review. JAMA *310*, 1842.

Park, C.-K., Kim, J.E., Kim, J.Y., Song, S.W., Kim, J.W., Choi, S.H., Kim, T.M., Lee, S.-H., Kim, I.H., and Park, S.-H. (2012). The Changes in MGMT Promoter Methylation Status in Initial and Recurrent Glioblastomas. Translational Oncology *5*, 393-IN19.

Rabé, M., Dumont, S., Álvarez-Arenas, A., Janati, H., Belmonte-Beitia, J., Calvo, G.F., Thibault-Carpentier, C., Séry, Q., Chauvin, C., Joalland, N., et al. (2020). Identification of a transient state during the acquisition of temozolomide resistance in glioblastoma. Cell Death Dis *11*, 19.

Ray, A.-M., Schaffner, F., Janouskova, H., Noulet, F., Rognan, D., Lelong-Rebel, I., Choulier, L., Blandin, A.-F., Lehmann, M., Martin, S., et al. (2014). Single cell tracking assay reveals an opposite effect of selective small non-peptidic α5β1 or αvβ3/β5 integrin antagonists in U87MG glioma cells. Biochim. Biophys. Acta *1840*, 2978–2987.

Reifenberger, G., Liu, L., Ichimura, K., Schmidt, E.E., and Collins, V.P. (1993). Amplification and Overexpression of the MDM2 Gene in a Subset of Human Malignant Gliomas without p53 Mutations. 5.

Renner, G., Janouskova, H., Noulet, F., Koenig, V., Guerin, E., Bär, S., Nuesch, J., Rechenmacher, F., Neubauer, S., Kessler, H., et al. (2016). Integrin α5β1 and p53 convergent pathways in the control of anti-apoptotic proteins PEA-15 and survivin in high-grade glioma. Cell Death Differ. *23*, 640–653.

Stupp, R., Weller, M., Belanger, K., Bogdahn, U., Ludwin, S.K., Lacombe, D., and Mirimanoff, R.O. (2005). Radiotherapy plus Concomitant and Adjuvant Temozolomide for Glioblastoma. The New England Journal of Medicine 10.

Stupp, R., Hegi, M.E., Neyns, B., Goldbrunner, R., Schlegel, U., Clement, P.M.J., Grabenbauer, G.G., Ochsenbein, A.F., Simon, M., Dietrich, P.-Y., et al. (2010). Phase I/IIa study of cilengitide and temozolomide with concomitant radiotherapy followed by cilengitide and temozolomide maintenance therapy in patients with newly diagnosed glioblastoma. J. Clin. Oncol. *28*, 2712–2718.

Stupp, R., Hegi, M.E., Gorlia, T., Erridge, S.C., Perry, J., Hong, Y.-K., Aldape, K.D., Lhermitte, B., Pietsch, T., Grujicic, D., et al. (2014). Cilengitide combined with standard treatment for patients with newly diagnosed glioblastoma with methylated MGMT promoter (CENTRIC EORTC 26071-22072 study): a multicentre, randomised, open-label, phase 3 trial. Lancet Oncol. *15*, 1100–1108.

Tucci, M., Stucci, S., and Silvestris, F. (2014). Does cilengitide deserve another chance? Lancet Oncol *15*, e584–e585.

Vassilev, L.T. (2004). In Vivo Activation of the p53 Pathway by Small-Molecule Antagonists of MDM2. Science *303*, 844–848.

Verhaak, R.G.W., Hoadley, K.A., Purdom, E., Wang, V., Qi, Y., Wilkerson, M.D., Miller, C.R., Ding, L., Golub, T., Mesirov, J.P., et al. (2010). Integrated Genomic Analysis Identifies Clinically Relevant Subtypes of Glioblastoma Characterized by Abnormalities in PDGFRA, IDH1, EGFR, and NF1. Cancer Cell *17*, 98–110.

Verreault, M., Schmitt, C., Goldwirt, L., Pelton, K., Haidar, S., Levasseur, C., Guehennec, J., Knoff, D., Labussiere, M., Marie, Y., et al. (2016). Preclinical Efficacy of the MDM2 Inhibitor RG7112 in MDM2-Amplified and TP53 Wild-type Glioblastomas. Clinical Cancer Research *22*, 1185–1196.

Yi, G.-Z., Liu, Y.-W., Xiang, W., Wang, H., Chen, Z.-Y., Xie, S., and Qi, S.-T. (2016). Akt and β-catenin contribute to TMZ resistance and EMT of MGMT negative malignant glioma cell line. J. Neurol. Sci. *367*, 101–106.

Yi, G.-Z., Huang, G., Guo, M., Zhang, X., Wang, H., Deng, S., Li, Y., Xiang, W., Chen, Z., Pan, J., et al. (2019). Acquired temozolomide resistance in MGMT-deficient glioblastoma cells is associated with regulation of DNA repair by DHC2. Brain *142*, 2352–2366.

Yu, G., and He, Q.-Y. (2016). ReactomePA: an R/Bioconductor package for reactome pathway analysis and visualization. Mol Biosyst *12*, 477–479.

Yuan, A.L., Meode, M., Tan, M., Maxwell, L., Bering, E.A., Pedersen, H., Willms, J., Liao, J., Black, S., Cairncross, J.G., et al. (2020). PARP inhibition suppresses the emergence of temozolomide resistance in a model system. J Neurooncol *148*, 463–472.

Table 1. List of antibodies

Antibody	Reference	Blocking solution	Dilution
Anti-α5 integrin H104(Santa Cruz	SC-10729	5% milk/1xTBS/0.1%Tween -20	1/1000
Anti-β1 integrin Ts2 (Millipore)	AB1952	5% milk/1xTBS/0.1%Tween -20	1/1000
Anti-αv integrin (Millipore)		5% BSA/1xTBS/0.1%Tween -20	1/1000
Anti-p53(BD Bioscience)	554293	5% milk/1xTBS/0.1%Tween -20	1/1000
Anti-pp53ser15(Cell signalling)	9284S	*5% BSA/1xTBS/0.1%Tween -20	1/1000
Anti-GAPDH (Millipore)	MAB374	5% milk/1xTBS/0.1%Tween -20	1/5000
Anti-p21(Cell signalling)	2946S	5% milk/1xTBS/0.1%Tween -20	1/1000
Anti-MDM2 (Calbiochem)	OP466100UG	5% milk/1xPBS/0.1%Tween -20	1/1000
Anti-p16 (Cell signalling)	SC-56330	5% milk/1xPBS/0.1%Tween -20	1/200
Mouse HRP-conjugated secondary antibody (PROMEGA)	W4028	5% milk/1xTBS/0.1%Tween -20	1/10000
Rabbit HRP-conjugated secondary antibody (PROMEGA)	W4018	5% milk/1xTBS/0.1%Tween -20	1/10000
Purified NA/Le mouse anti-human CD49e	555614	3% PBS-BSA	1/100
Purified anti-human CD29	303002	3% PBS-BSA	1/100
Alexa fluoro@647 goat anti-mouse IgG	A21236	3% PBS-BSA	1/200
Alexa fluoro@488 goat anti-mouse IgG	A11029	3% PBS-BSA	1/200

* Membrane was blocked in milk, primary antibody incubated in BSA and secondary antibody in milk.

Table 2. List of primers

Gene	Forward 5'-3'	Reverse 5'-3'
p21	GGCAGACCAGCATGACAGATT	TGTGGGCGGATTAGGGCT
MDM2	AGACCCTGGTTAGACCAA	TGGCCAAGATAAAAAAGAACCTCT
Fas	5CCCTCCTACCTCTGGTTCTTACG	AGTCTTCCTCAATTCCAATCCCTT
Survivin	TGACGACCCCATAGAGGAACA	CGCACTTTCTCCGCAGTTTC
α5 integrin	AGCAAGAGCCGGATAGAGGA	TCAGGGCATTCTTGTCACCC
hGAPDH	GTCACCAGGGCTGCTTTTAACTCT	ACTCAGCCAAGGTTGTGAGG

Table 3. IncuCyte experiments showing the effect of integrin antagonists and p53 activators on U87MG OFF R50 and parental cells.

S/N	Treatment	U87MG Cells	U87MG OFF R50 Cells
1	Ctrl	1,001 ± 0,001	1,0020 ± 0,002
2	TMZ 50 µM	0.5737 ± 0.013	0.9460 ± 0.026
3	Idasanutlin 0.1µM	0,5191 ± 0,050	0,4502 ± 0,018
4	Nutlin-3a µM	0,3490 ± 0,017	0,4254 ± 0,022
5	RITA 1 µM	0,3853 ± 0,012	0,5244 ± 0,025
6	K34c 20 µM	0,4481 ± 0,012	0,5447 ± 0,028
7	Fr248 µM	0,7815 ± 0,041	0,7859 ± 0,048
8	ATN-161 28 µM	0,9337 ± 0,008	0,9728 ± 0,019
9	Idasanutlin + K34c	0,2651 ± 0,005	0,2441 ± 0,007
10	Idasanutlin + Fr248	0,3990 ± 0,005	0,3139 ± 0,009
11	Idasanutlin + ATN-161	0,5351 ± 0,039	0,4613 ± 0,018
12	Nutlin-3a + K34c	0,2132 ± 0,016	0,2474 ± 0,014
12	Nutlin-3a + Fr248	0,2858 ± 0,020	0,3269 ± 0,016
14	Nutlin-3a + ATN-161	0,5280 ± 0,028	0,4292 ± 0,017
15	RITA + K34c	0,2578 ± 0,010	0,3516 ± 0,022
16	RITA + Fr248	0,3585 ± 0,022	0,3863 ± 0,021
17	RITA + ATN-161	0,4705 ± 0,019	0,4165 ± 0,025

Legends to figures

Figure 1. Confirmation of Acquired TMZ Resistance in U87MG GBM Cells. (A) Generation of TMZ-resistant U87MG R50 and U87MG OFF R50 cells, and histograms showing the effect of TMZ (50 µM) on cell confluence of U87MG, U87MG R50 and U87MG OFF R50 cells from 0 to 96 hours of treatment. Results were expressed as the relative area of plate covered after treatment versus the area covered by solvent treated control cells. Histograms represent mean ± S.E.M. of at least three separate experiments. (B) Representative phase contrast images from the IncuCyte showing the cellular morphology of U87MG, U87MG R50 and U87MG OFF R50 cells 72 hrs either non-treated or after treatment with 50µM TMZ. Scale bar, 300µm. Statistical analysis: Student t test (*, $p<0.05$; **, $p<0.01$; ***, $p<0.001$; ns, non-significant).

Figure 2. TMZ induces senescence in U87MG cells. (A) Representative photomicrographs showing cellular senescence after staining with SA-βGal. Scale bars: 10x. (**B**). Representative western blot analysis showing basal expression of p16 and p21 in TMZ resistant cells (U87MG R50 and U87MG OFF R50) compared to the parental cells. Histograms represent the mean ± S.E.M. of three separate experiments and GAPDH expression was used as the loading control. (**C**) Cell confluence was calculated using IncuCyte Zoom software based on phase-contrast images of U87MG, U87MG R50 and U87MG OFF R50 cells from 0 hr to 96hrs. Student t test (*, $p<0.05$; **, $p<0.01$; ***, $p<0.001$; ns, non-significant).

Figure 3. RNAseq analysis of TMZ-resistant and parental cell gene expression. (**A**) Heatmap grouped the nine samples based on the global expresson profiles. Color scale shows high and low expressions as red and green, respectively. Dendogram depicting correlation among different samples based on global expression profiles. (**B**) Top 15 enriched reactome pathway for differentially expressed gene in treated cells versus control. Enrichment map with the inter relation of the top 15 enriched reactome pathway and visualization of DEGs. (**C**) Heatmap visualization comparing expression of genes encoding integrins between samples with dendrogram to show clustering. Color scale shows high and low expressions as red and green, respectively

Figure 4. Modulation of α5, β1 and αv integrin subunits in TMZ-resistant and parental cells. (A) Representative western blot showing basal expression of αv, β1 and α5 integrin in U87MG R50 and U87MG OFF R50 compared to the parental cells. Histograms represent the mean ± S.E.M. of three separate experiments and GAPDH was used as the loading control. (**B**) Representative fluorescence confocal microscopy images and mean gray value of basal α5 and β1 integrin subunits expression in TMZ-resistant U87MG OFF R50 compared to the parental cells. Scale bars: 20µm. Histograms represent mean ± S.E.M. of 10-12 images (4-5 cells per images) from three separate experiments. Statistical analysis: Student t test (*, $p<0.05$; **, $p<0.01$; ***, $p<0.001$; ns, non-significant).

Figure 5. Effect of integrin antagonist on cell confluence and morphology of TMZ-resistant and parental cells. (**A**) Representative phase contrast images from the IncuCyte showing the cellular morphology of U87MG, U87MG R50 and U87MG OFF R50 cells 72 hrs post treatment with solvent, K34c 20µM, Fr248 20µM and ATN-161 28 µM. Scale bar, 300µm. (**B**) Cell confluence was calculated using IncuCyte Zoom software based on phase-contrast images of U87MG, U87MG R50 and U87MG OFF R50 cells from 0 hr to 72 hrs treated with solvent, K34c 20µM, Fr248 20µM and ATN-161 28 µM. Histigrams are expressed as mean±

S.E.M. of at least three independent experiments with *, $p<0.05$; **, $p<0.01$; ***, $p<0.001$; ns, non-significant.

Figure 6. Modulation of the p53 pathway in U87MG, U87MG R50 and U87MG OFF R50 cells. (**A**) Representative western blot and RT-qPCR analysis showing basal expression of MDM2 and p53 in TMZ resistant cells (U87MG R50 and U87MG OFF R50) compared to the parental cells. (**B**) Representative western blot analysis showing p53 stability and expression of MDM2 in TMZ resistant cells (U87MG R50 and U87MG OFF R50) compared to the parental cells 24 hrs post treatment with Nutlin-3a 1 μM, RITA 1μM and Idasanutlin 0.1μM. Histograms represent the mean ± S.E.M. of three separate experiments and GAPDH was used as the loading control. Student t test (*, $p<0.05$; **, $p<0.01$; ***, $p<0.001$; ns, non-significant).

Figure 7. Effect of Idasanutlin and integrin antagonists on TMZ-resistant and parental cells. (**A**) Representative phase contrast images from the IncuCyte showing the cellular morphology of U87MG and U87MG OFF R50 cells 72 hrs post treatment with solvent, Idasanutlin 0.1 μM alone or in combination with K34c 20μM, Fr248 20μM and ATN-161 28 μM. Scale bar, 300μm. (**B**) Cell confluence was calculated using IncuCyte Zoom software based on phase-contrast images of U87MG, U87MG R50 and U87MG OFF R50 cells from 0 hr to 72 hrs treated with solvent, Idasanutlin 0.1 μM alone or in combination with K34c 20μM, Fr248 20μM and ATN-161 28 μM. For all panels: mean± S.E.M. of at least three independent experiments with *, $p<0.05$; **, $p<0.01$; ***, $p<0.001$; ns, non-significant.

Figure 8. Modulation of the p53 pathway in U87MG and U87MG OFF R50 cells by p53 activators and integrin antagonists. Representative western blot showing p53 stability/activity (phosphorylation at ser^{15}) and the expression of MDM2 in TMZ resistant U87MG OFF R50 compared to the parental cells 24 hrs post treatment with (**A**) Idasanutlin 0.1μM and Fr248 20μM each alone or in combination. (**B**) Idasanutlin 0.1μM and ATN-161 28 μM each alone or in combination. (**C**) RITA 1μM and ATN-161 28 μM each alone or in combination. Histograms represent the mean ± S.E.M. of three separate experiments and GAPDH was used as the loading control. Statistical analysis: Student t test (*, $p<0.05$; **, $p<0.01$; ***, $p<0.001$; ns, non-significant).

Figure S1. Dose dependent effect of TMZ on cell confluence of U87MG, U87MG R50 and U87MG OFF R50 cells. Cells were plated in 96-well plate and treated with 12.5 μM, 25 μM, 50μM and 100 μM of TMZ and cell confluence was measured every 2 hours for 72 hours using the IncuCyte live cell analysis system. Results were expressed as the relative area of plate covered versus the area covered by solvent treated control cells. Histograms represent mean ± S.E.M. of at least three separate experiments.

Figure S2. Representative fluorescence confocal microscopy images of basal α5 and β1 integrin subunits expression in TMZ-resistant U87MG OFF R50 compared to the parental cells. Scale bars: 20μm.

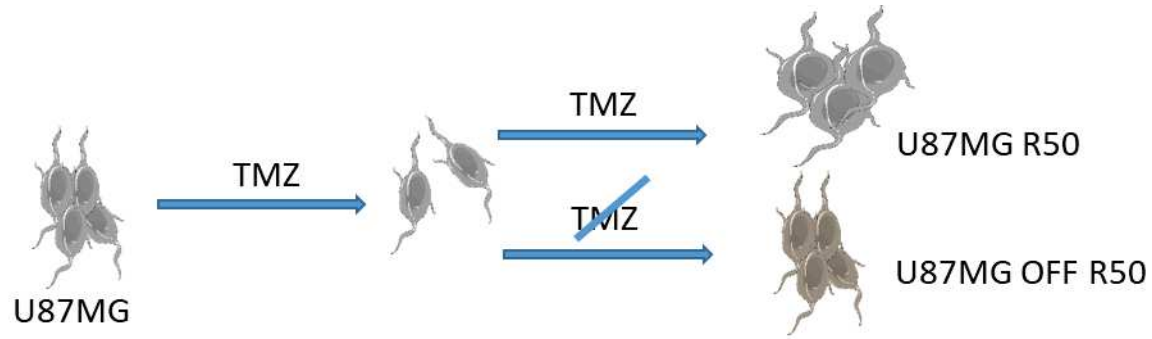

Fig. 1A.

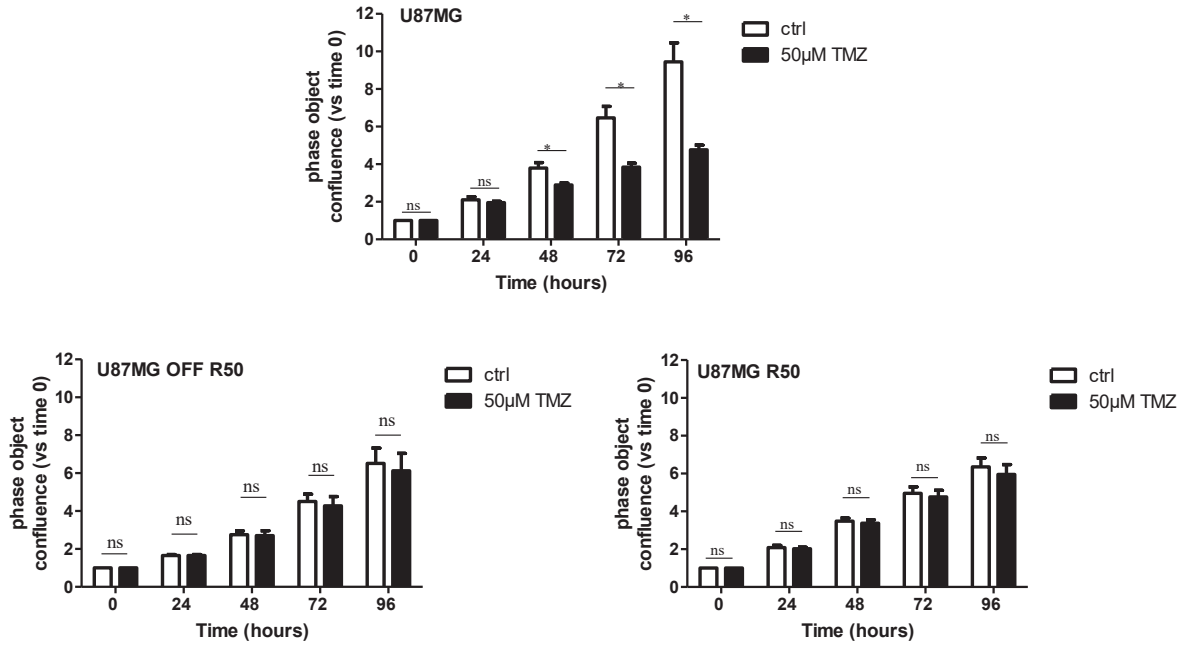

Fig. 1B.

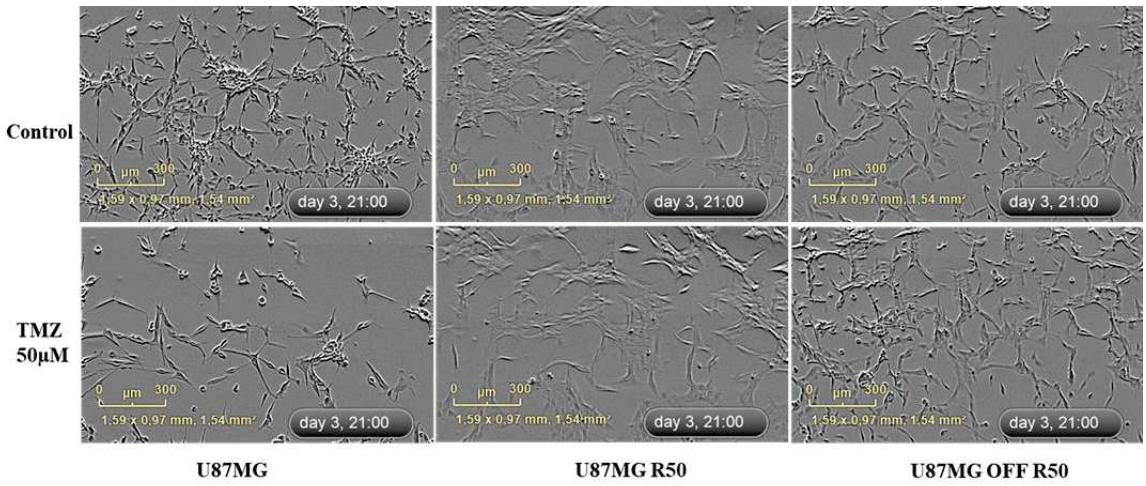

Fig. 1C.

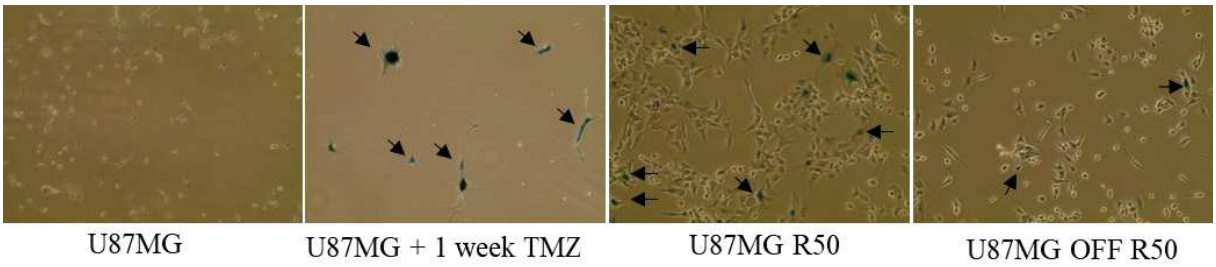

Fig. 2A.

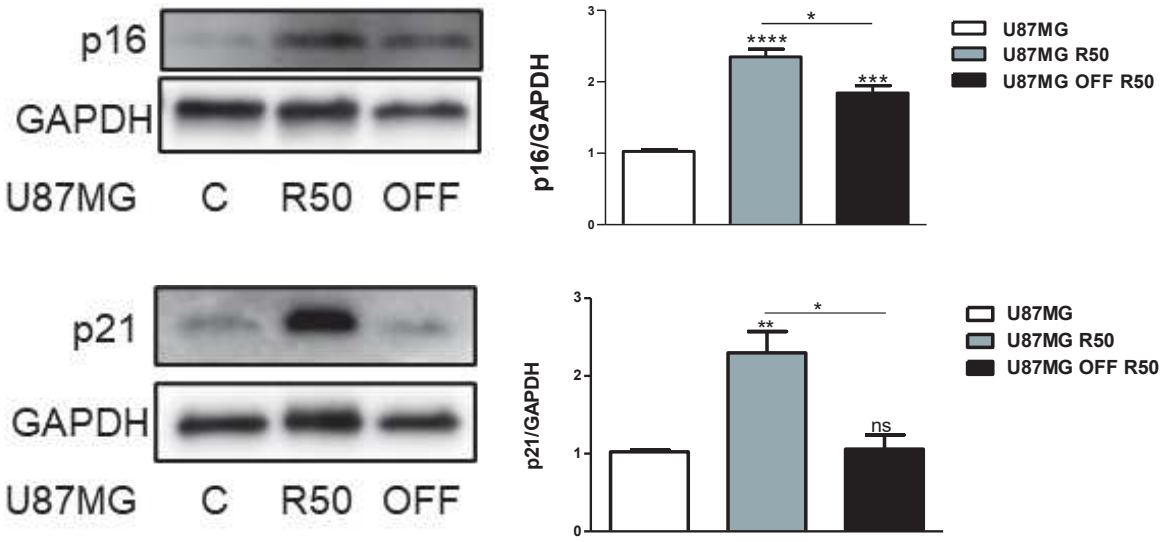

Fig. 2B

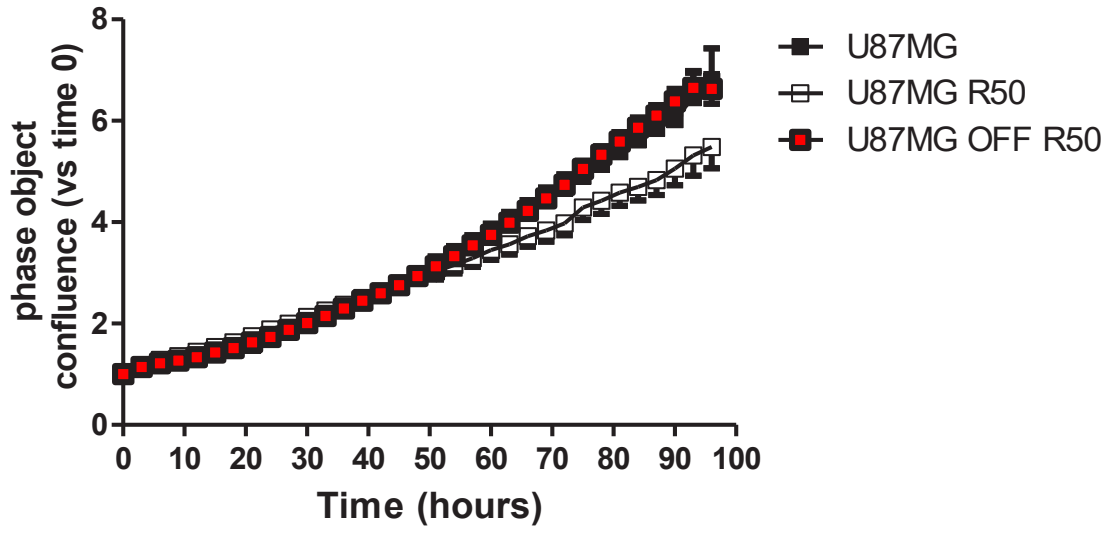

Fig. 2C.

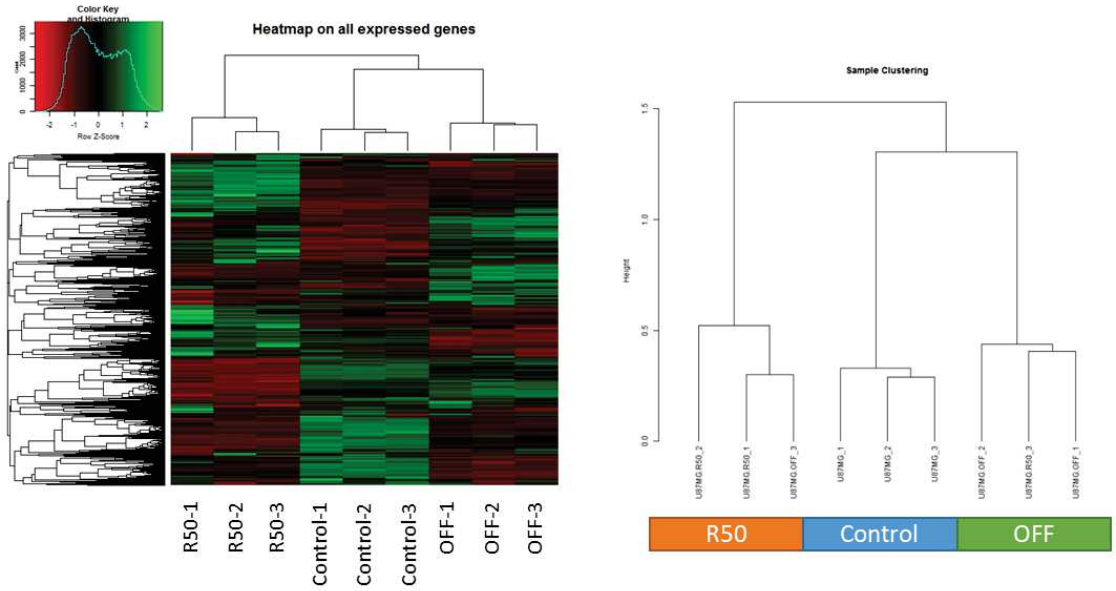
Color Key and Histogram
Heatmap on all expressed genes
Row Z-Score
R50-1
R50-2
R50-3
Control-1
Control-2
Control-3
OFF-1
OFF-2
OFF-3
Sample Clustering
Height
R50
Control
OFF

Fig. 3A.

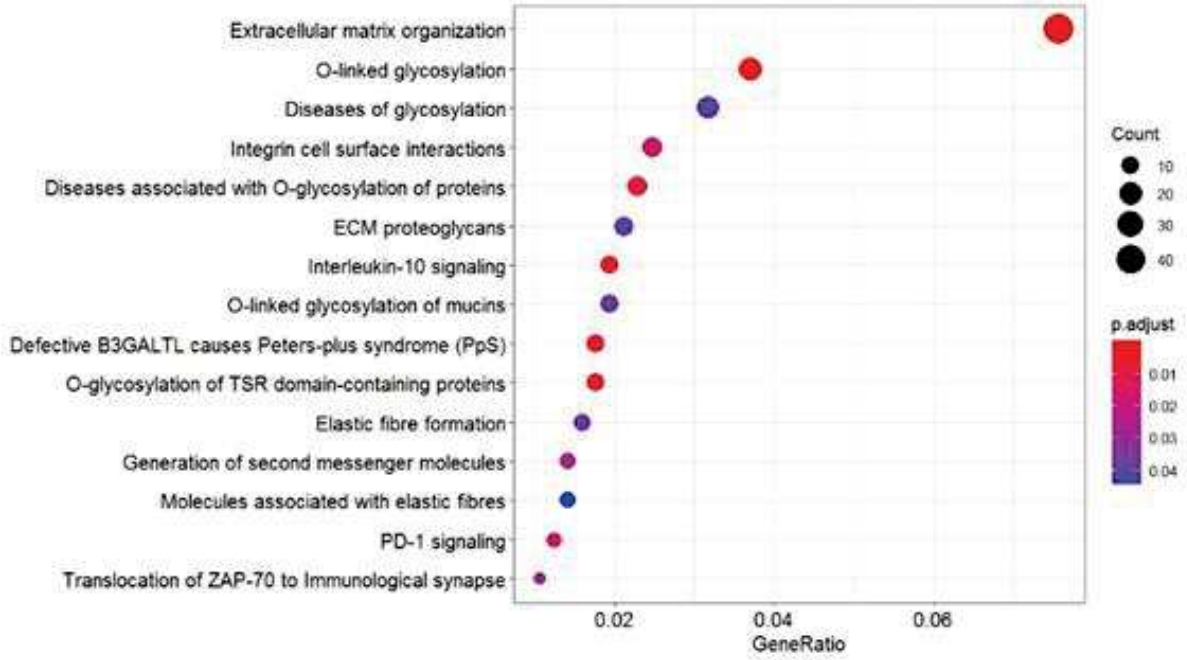
Extracellular matrix organization
O-linked glycosylation
Diseases of glycosylation
Integrin cell surface interactions
Diseases associated with O-glycosylation of proteins
ECM proteoglycans
Interleukin-10 signaling
O-linked glycosylation of mucins
Defective B3GALTL causes Peters-plus syndrome (PpS)
O-glycosylation of TSR domain-containing proteins
Elastic fibre formation
Generation of second messenger molecules
Molecules associated with elastic fibres
PD-1 signaling
Translocation of ZAP-70 to Immunological synapse
0.02
0.04
0.06
GeneRatio
Count
10
20
30
40
p.adjust
0.01
0.02
0.03
0.04

Fig. 3B.

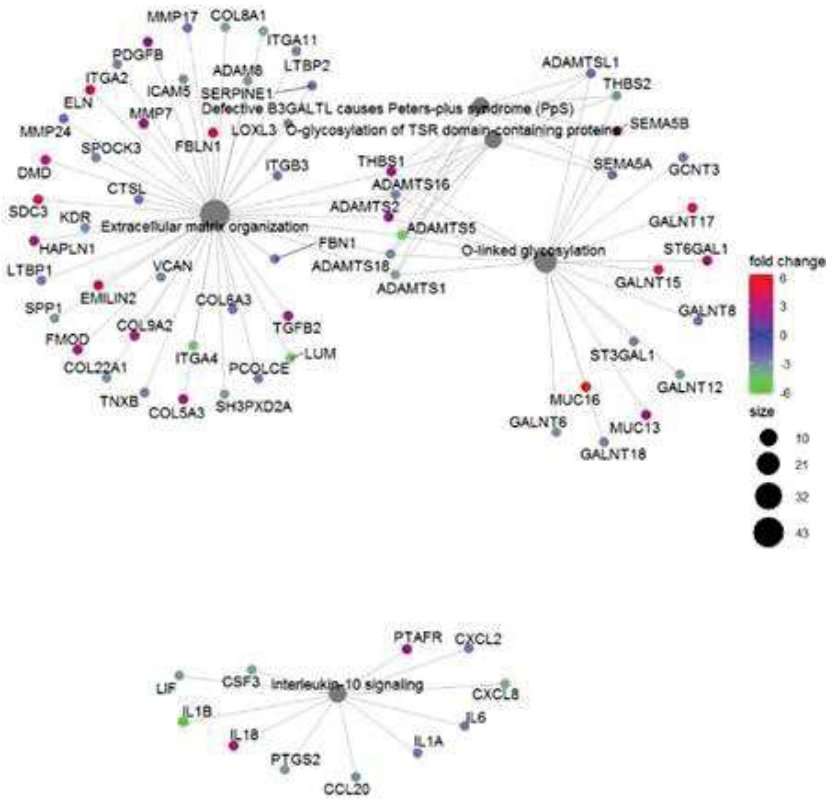
MMP17
COL8A1
ITGA11
PDGFB
ADAM8
LTBP2
ITGA2
ICAM5
SERPINE1
ELN
MMP7
Defective B3GALTL causes Peters-plus syndrome (PpS)
MMP24
LOXL3
O-glycosylation of TSR domain-containing proteins
SPOCK3
FBLN1
DMD
ITGB3
THBS1
CTSL
ADAMTS16
SDC3
KDR
ADAMTS2
Extracellular matrix organization
ADAMTS5
HAPLN1
FBN1
LTBP1
VCAN
ADAMTS18
ADAMTS1
EMILIN2
COL6A3
SPP1
COL9A2
TGFB2
FMOD
ITGA4
LUM
COL22A1
PCOLCE
TNXB
COL5A3
SH3PXD2A
ADAMTSL1
THBS2
SEMA5B
SEMA5A
GCNT3
GALNT17
O-linked glycosylation
ST6GAL1
GALNT15
GALNT8
ST3GAL1
GALNT12
MUC16
GALNT6
MUC13
GALNT18
fold change
size
PTAFR
CXCL2
LIF
CSF3
Interleukin-10 signaling
CXCL8
IL1B
IL6
IL18
IL1A
PTGS2
CCL20

Fig. 3B.

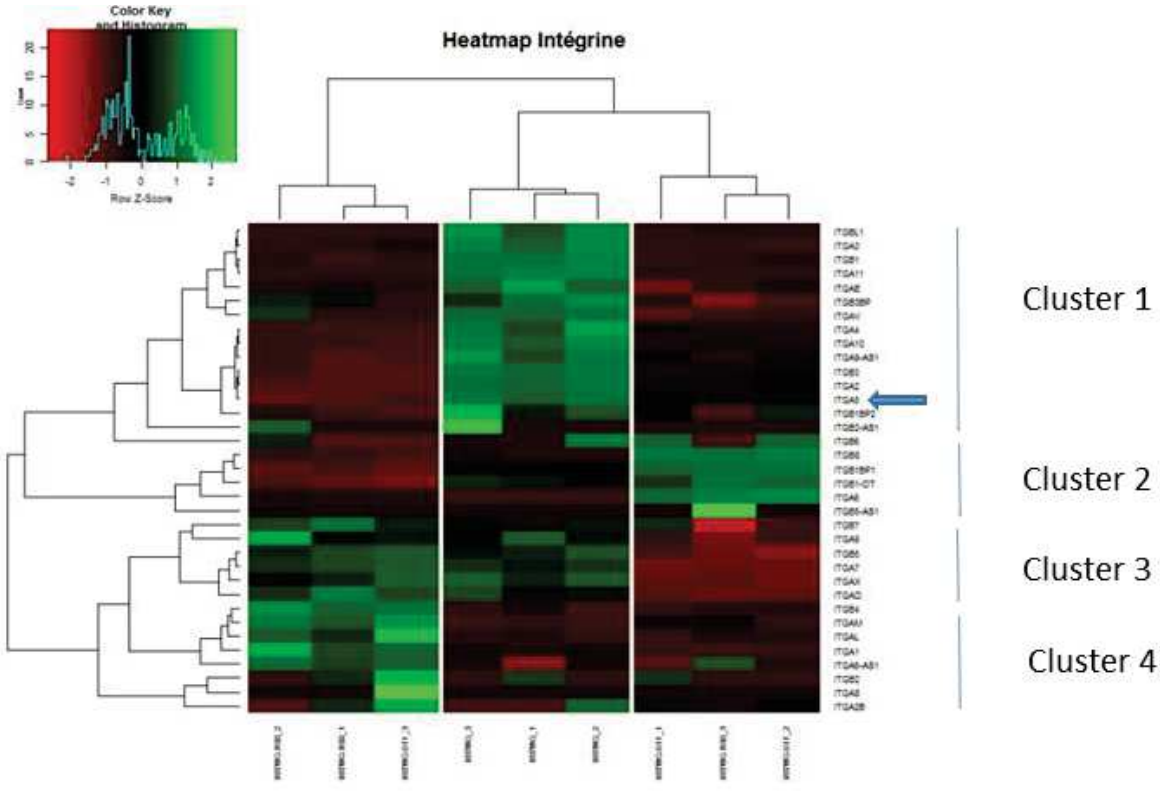
Color Key and Histogram
Heatmap Intégrine
Row Z-Score
Cluster 1
Cluster 2
Cluster 3
Cluster 4

Fig. 3C.

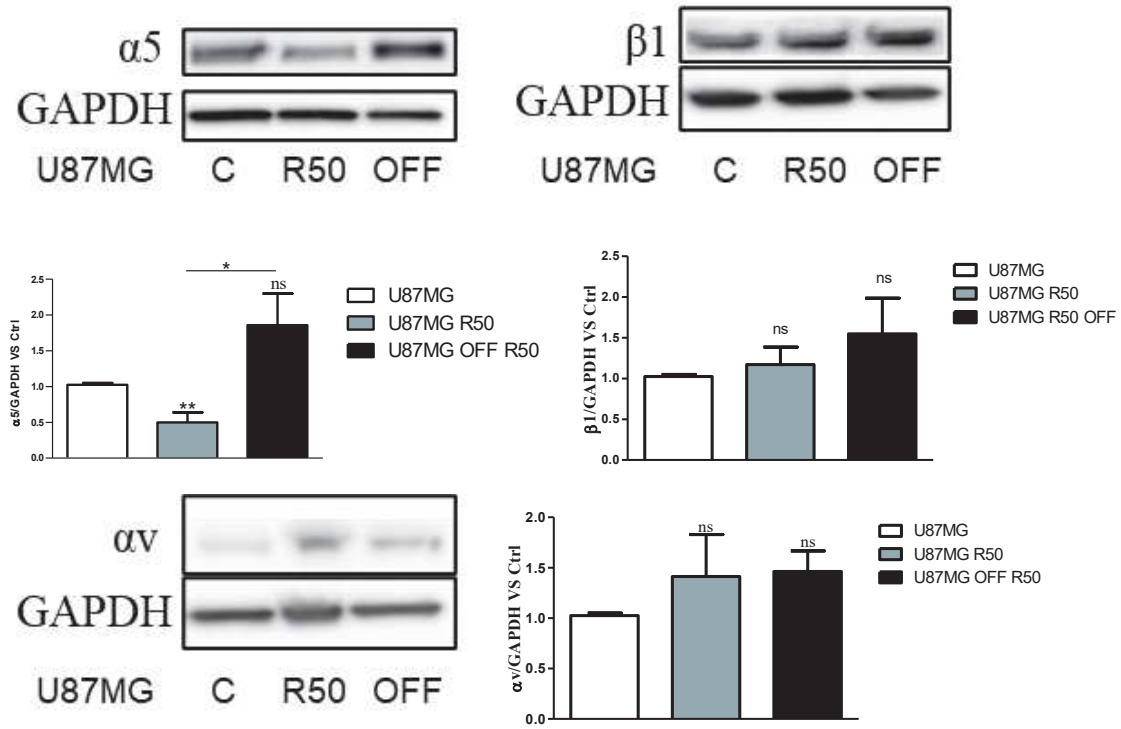
α5
GAPDH
U87MG C R50 OFF
β1
GAPDH
U87MG C R50 OFF
α5/GAPDH VS Ctrl
U87MG
U87MG R50
U87MG OFF R50
β1/GAPDH VS Ctrl
U87MG
U87MG R50
U87MG R50 OFF
αv
GAPDH
U87MG C R50 OFF
αv/GAPDH VS Ctrl
U87MG
U87MG R50
U87MG OFF R50

Fig. 4A.

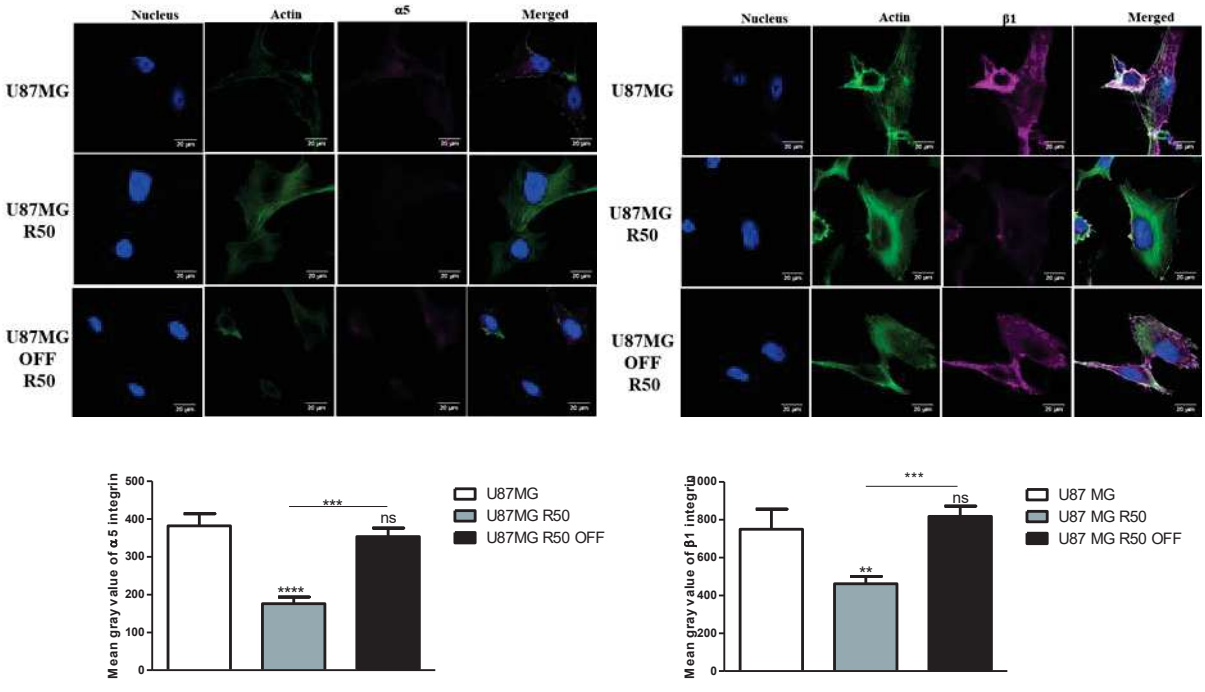
Nucleus
Actin
α5
Merged
U87MG
U87MG R50
U87MG OFF R50
Nucleus
Actin
β1
Merged
U87MG
U87MG R50
U87MG OFF R50
Mean gray value of α5 integrin
U87MG
U87MG R50
U87MG R50 OFF
Mean gray value of β1 integrin
U87 MG
U87 MG R50
U87 MG R50 OFF

Fig. 4B.

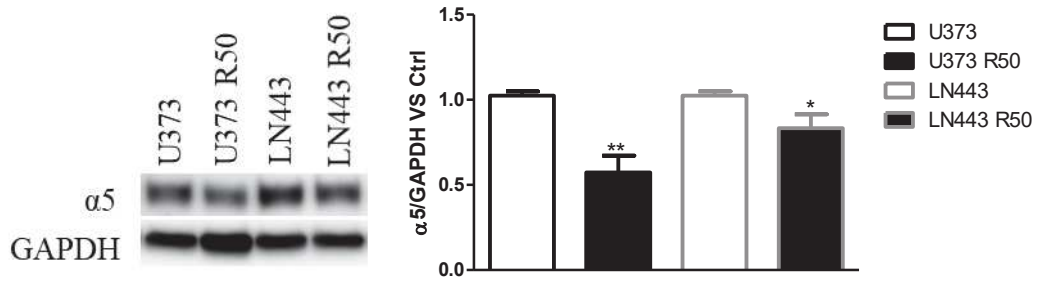
U373
U373 R50
LN443
LN443 R50
α5
GAPDH
α5/GAPDH VS Ctrl
1.5
1.0
0.5
0.0
**
*
U373
U373 R50
LN443
LN443 R50

Fig. 4C

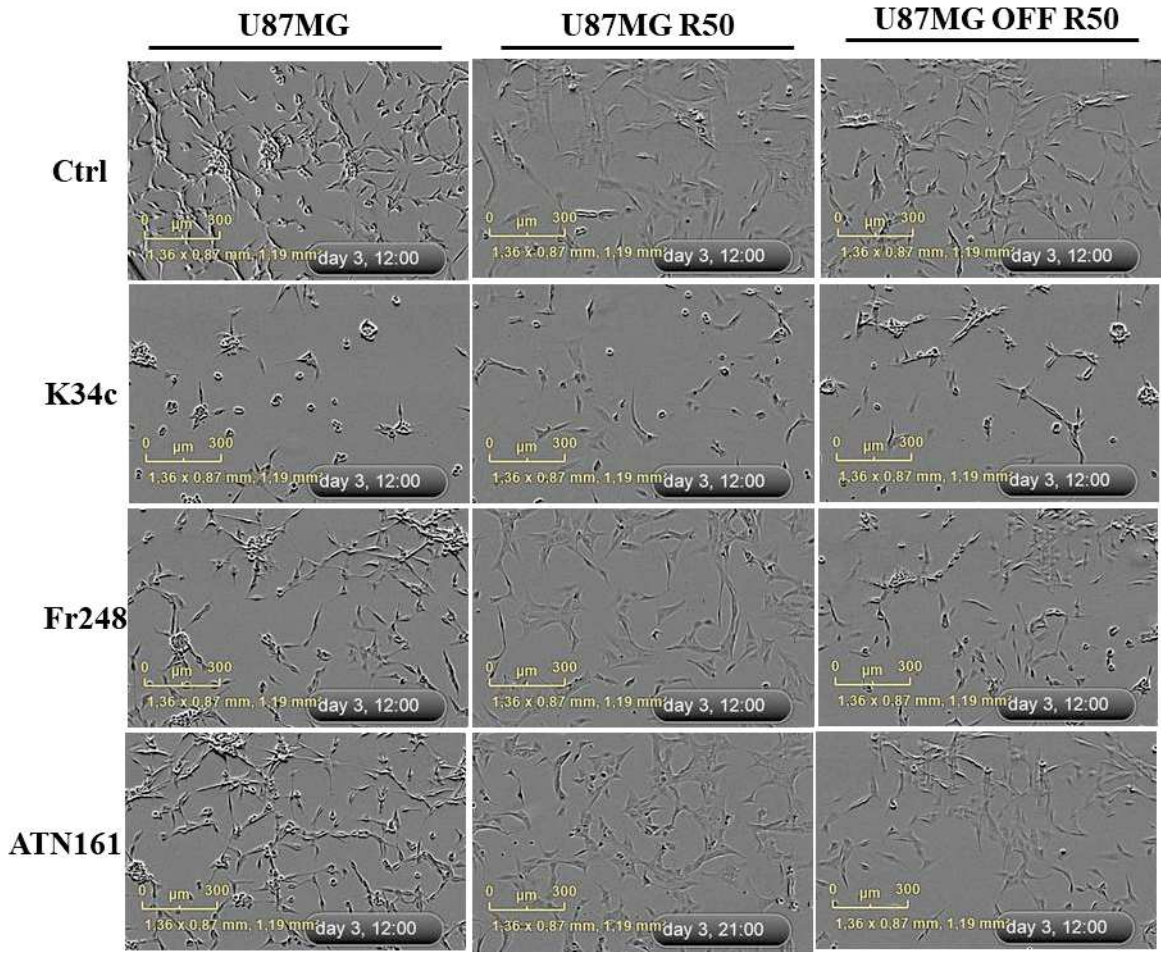
U87MG
U87MG R50
U87MG OFF R50
Ctrl
K34c
Fr248
ATN161
0 µm 300
1,36 x 0,87 mm, 1,19 mm
day 3, 12:00
day 3, 21:00

Fig. 5A.

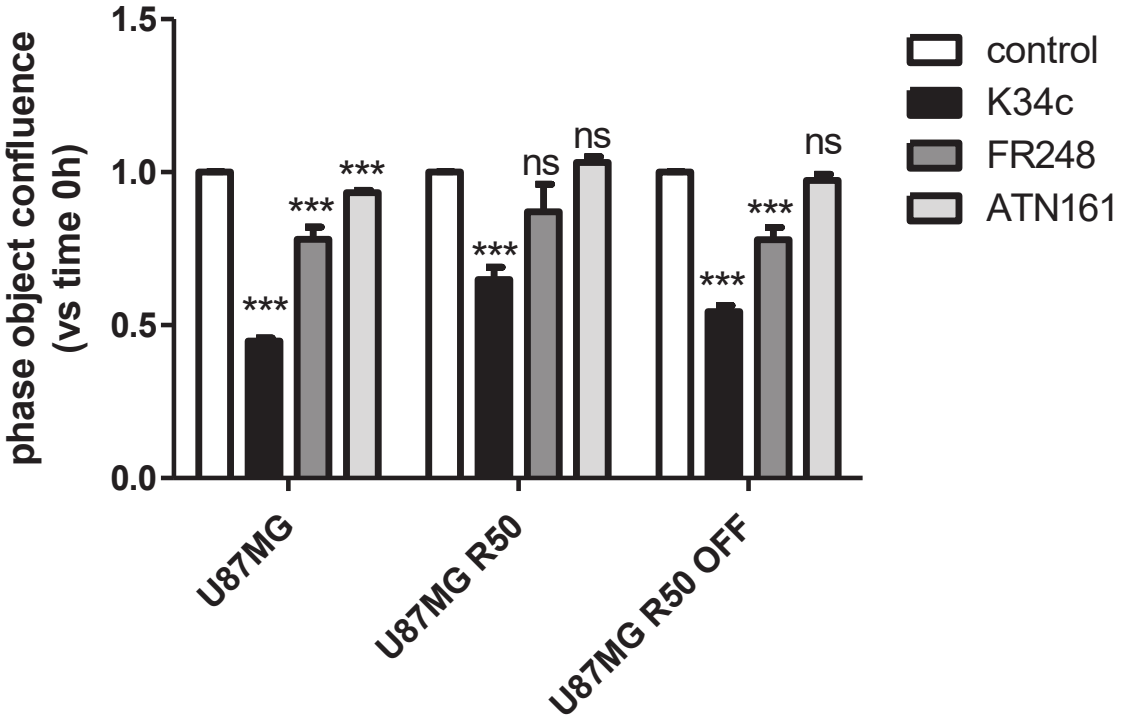
phase object confluence (vs time 0h)
1.5
1.0
0.5
0.0
control
K34c
FR248
ATN161
***
***
***
ns
***
ns
***
ns
U87MG
U87MG R50
U87MG R50 OFF

Fig. 5B.

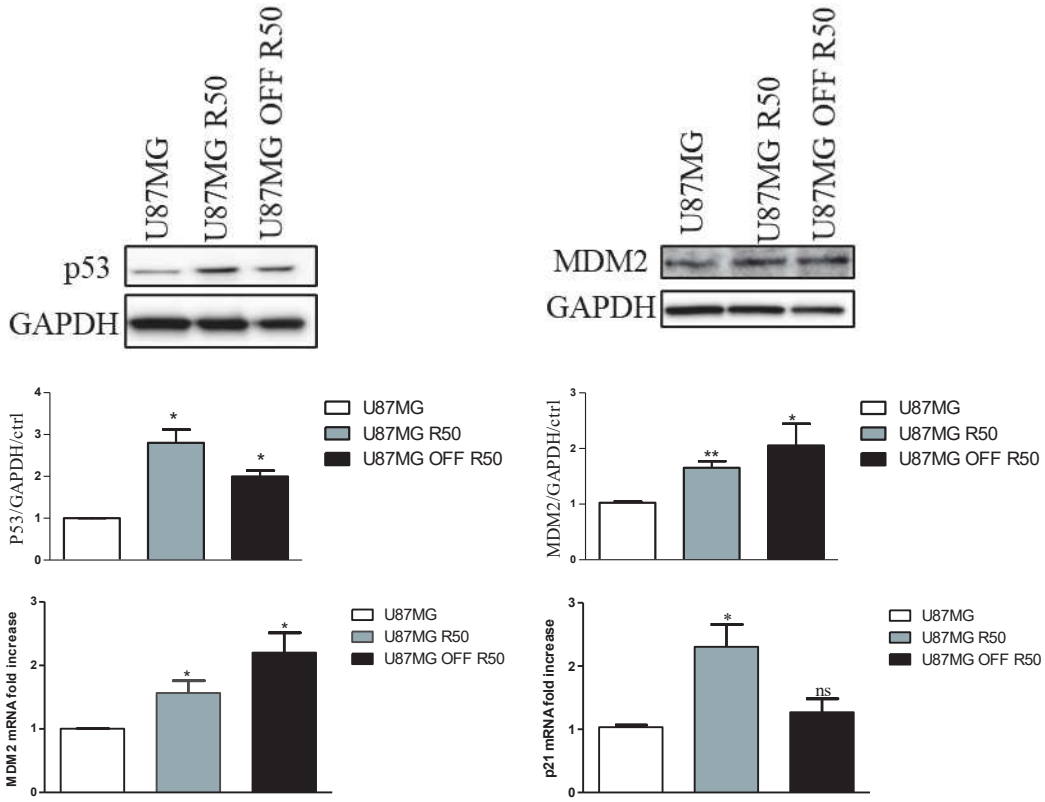
U87MG
U87MG R50
U87MG OFF R50
p53
GAPDH
MDM2
GAPDH
P53/GAPDH/ctrl
MDM2/GAPDH/ctrl
MDM2 mRNA fold increase
p21 mRNA fold increase
ns

Fig. 6A.

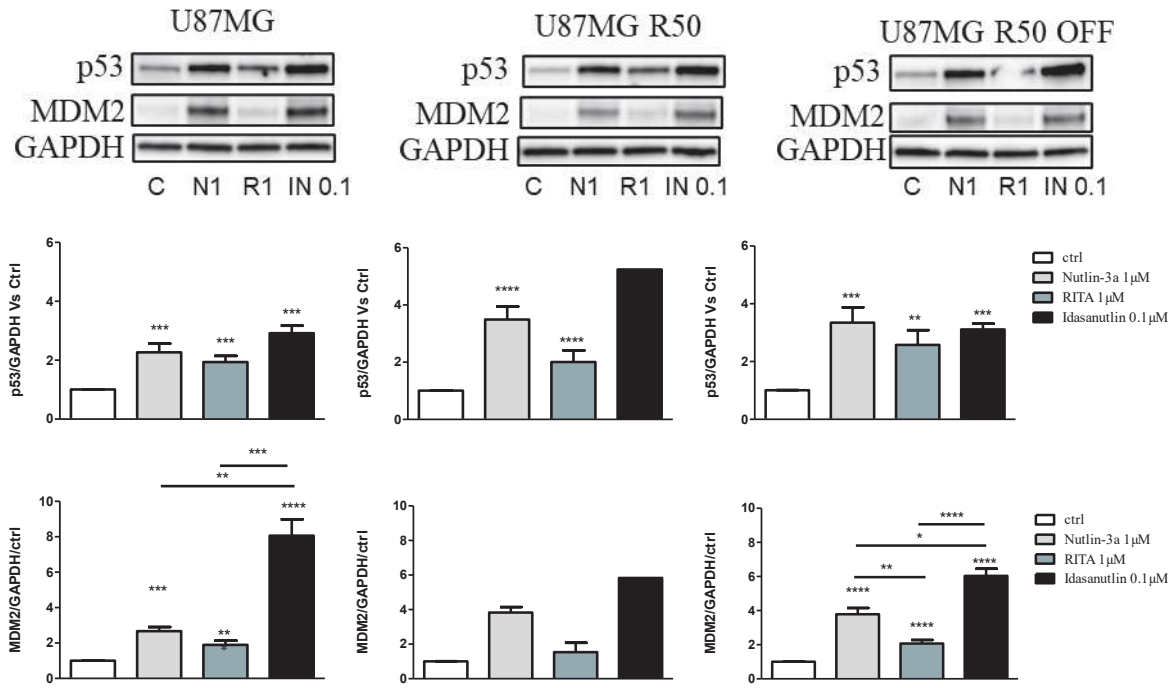
U87MG
U87MG R50
U87MG R50 OFF
p53
MDM2
GAPDH
C N1 R1 IN 0.1
p53/GAPDH Vs Ctrl
MDM2/GAPDH/ctrl
ctrl
Nutlin-3a 1μM
RITA 1μM
Idasanutlin 0.1μM

Fig. 6B

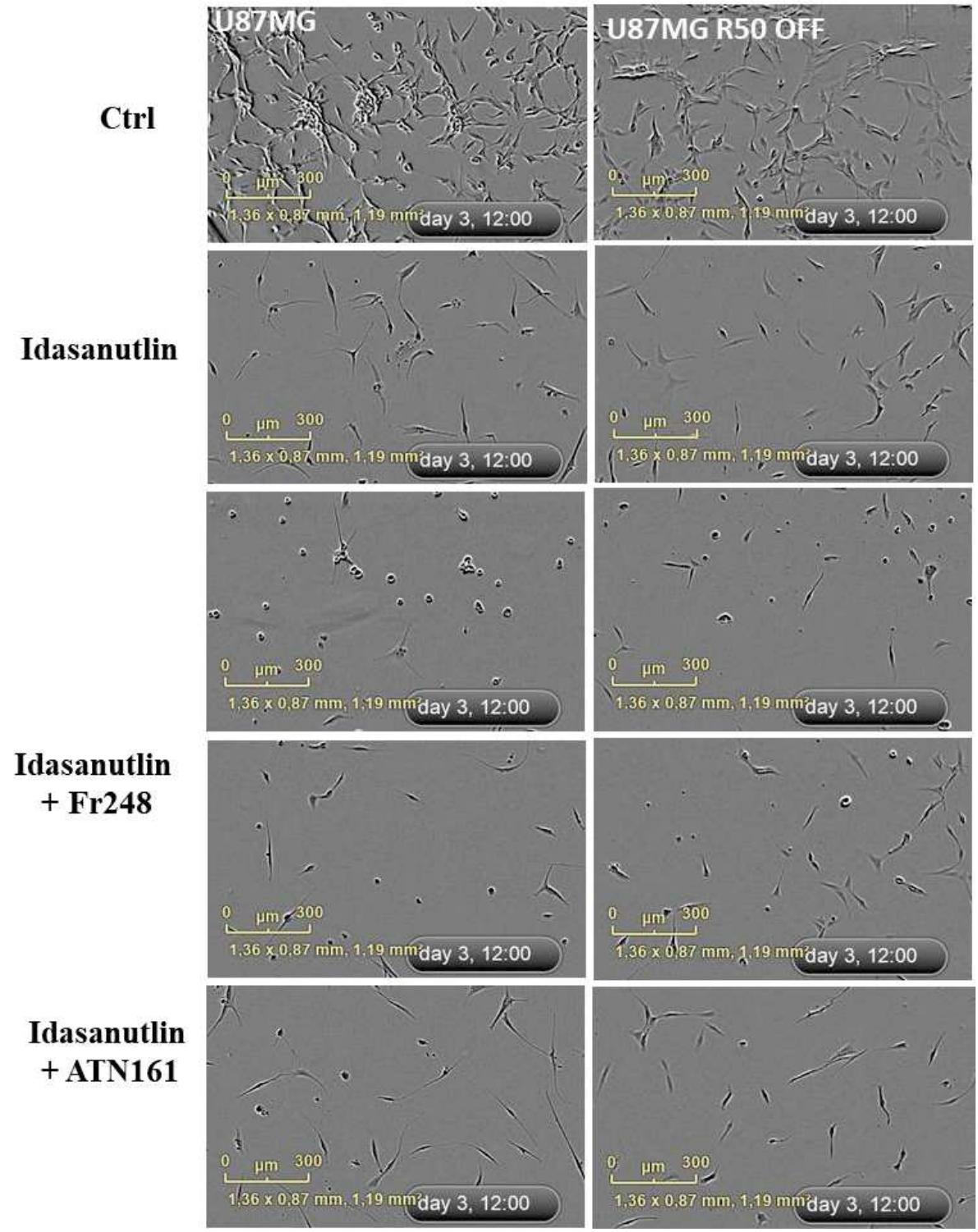
Ctrl
Idasanutlin
Idasanutlin + Fr248
Idasanutlin + ATN161
U87MG
U87MG R50 OFF
0 µm 300
1,36 x 0,87 mm, 1,19 mm
day 3, 12:00

Fig. 7A

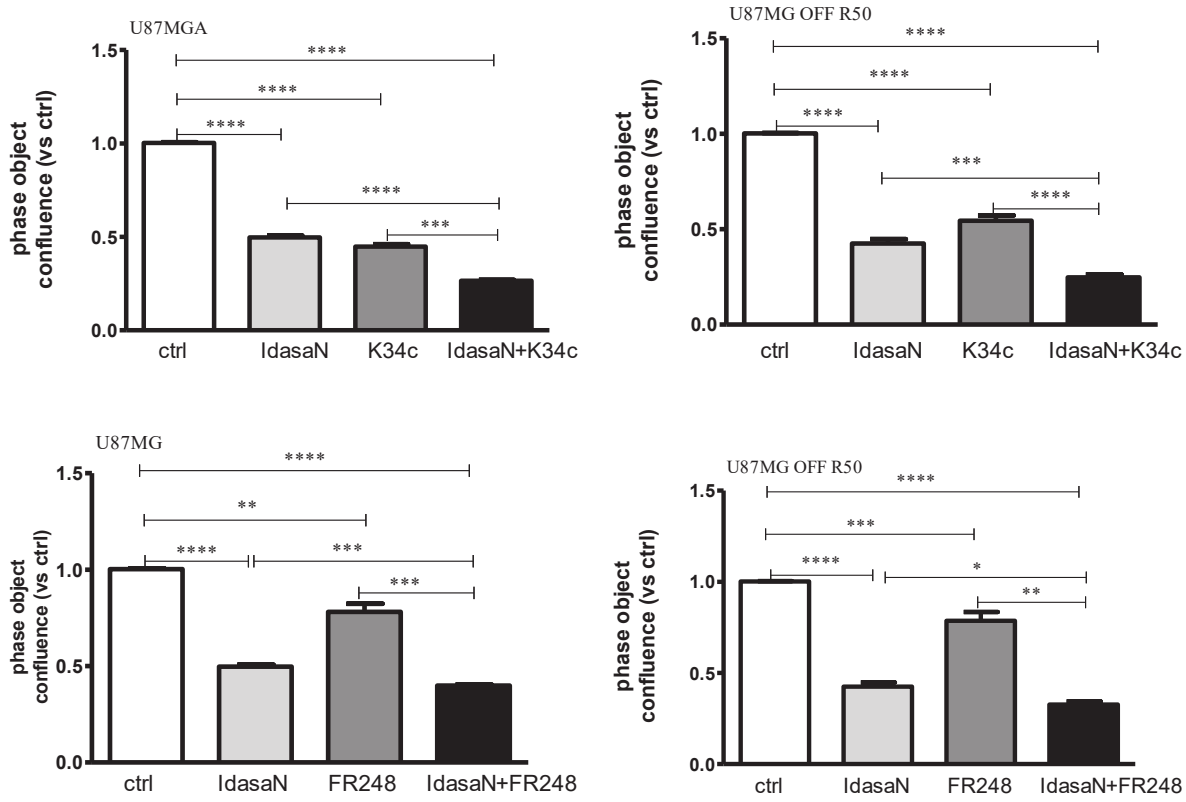

Fig. 35B

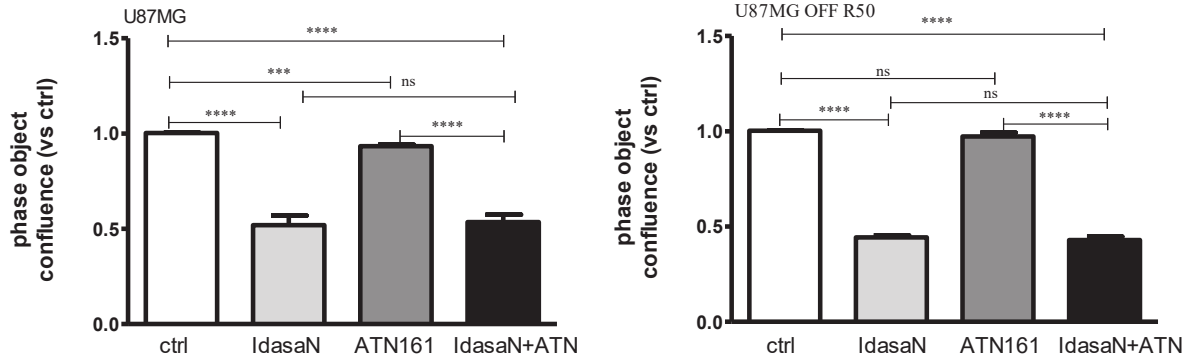

Fig. 7B

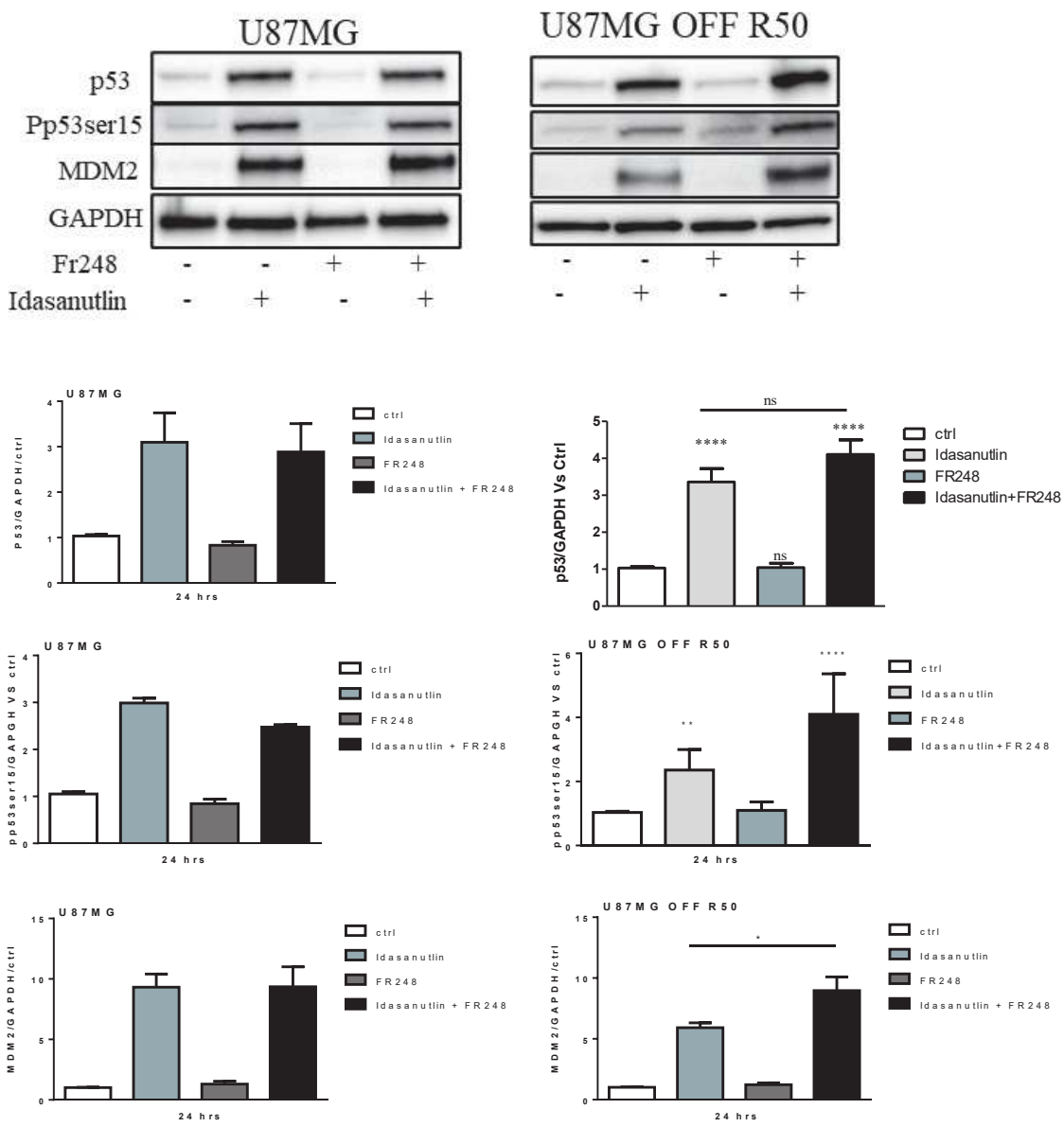
U87MG
U87MG OFF R50
p53
Pp53ser15
MDM2
GAPDH
Fr248
Idasanutlin
U87MG
P53/GAPDH/ctrl
24 hrs
ctrl
Idasanutlin
FR248
Idasanutlin + FR248
p53/GAPDH Vs Ctrl
ns
****
Idasanutlin+FR248
pp53ser15/GAPGH VS ctrl
U87MG OFF R50
**
MDM2/GAPDH/ctrl
*

Fig. 8A

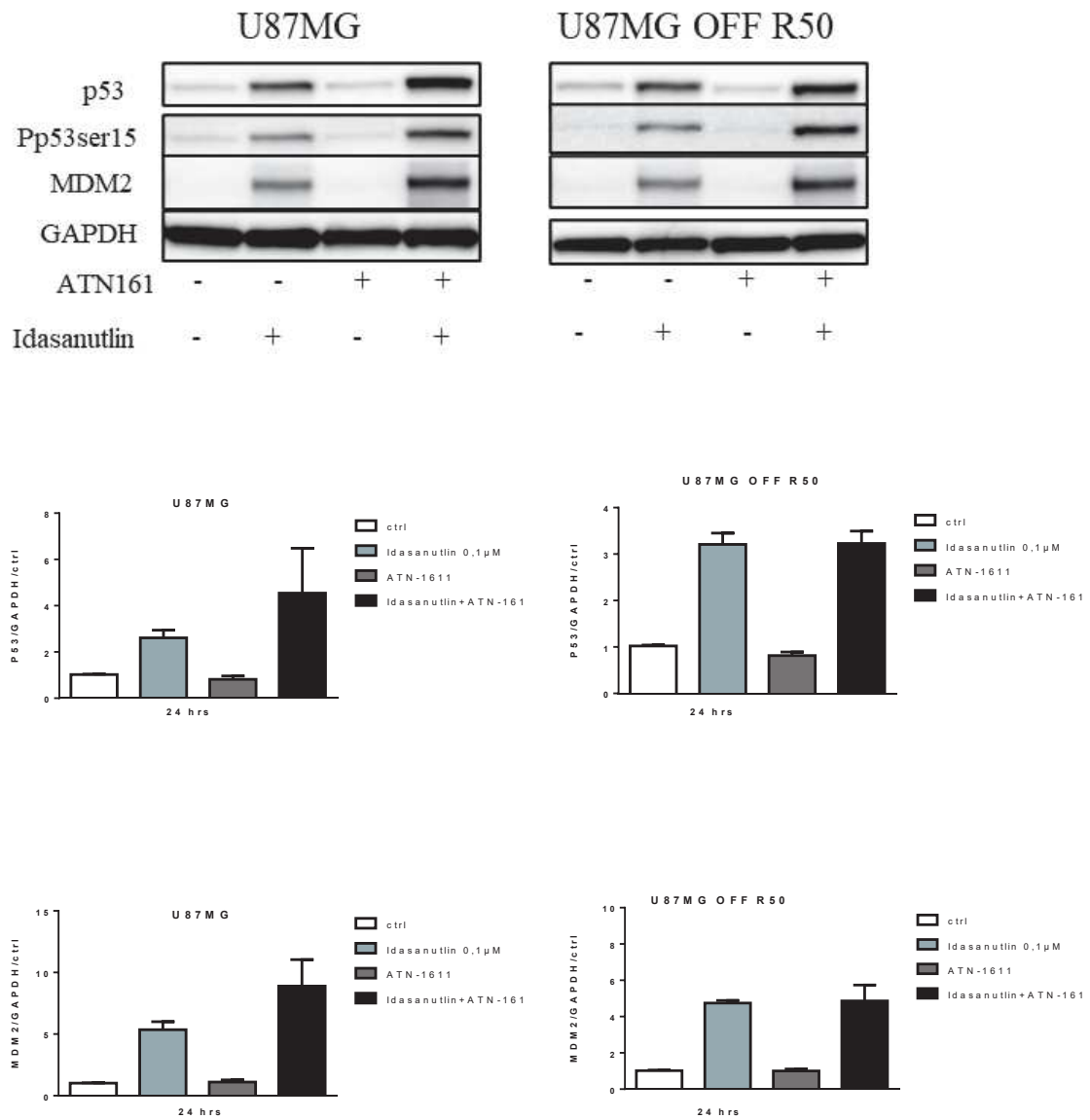
U87MG
U87MG OFF R50
p53
Pp53ser15
MDM2
GAPDH
ATN161
Idasanutlin
U87MG
U87MG OFF R50
P53/GAPDH/ctrl
MDM2/GAPDH/ctrl
24 hrs
ctrl
Idasanutlin 0,1µM
ATN-1611
Idasanutlin+ATN-161

Fig. 8B

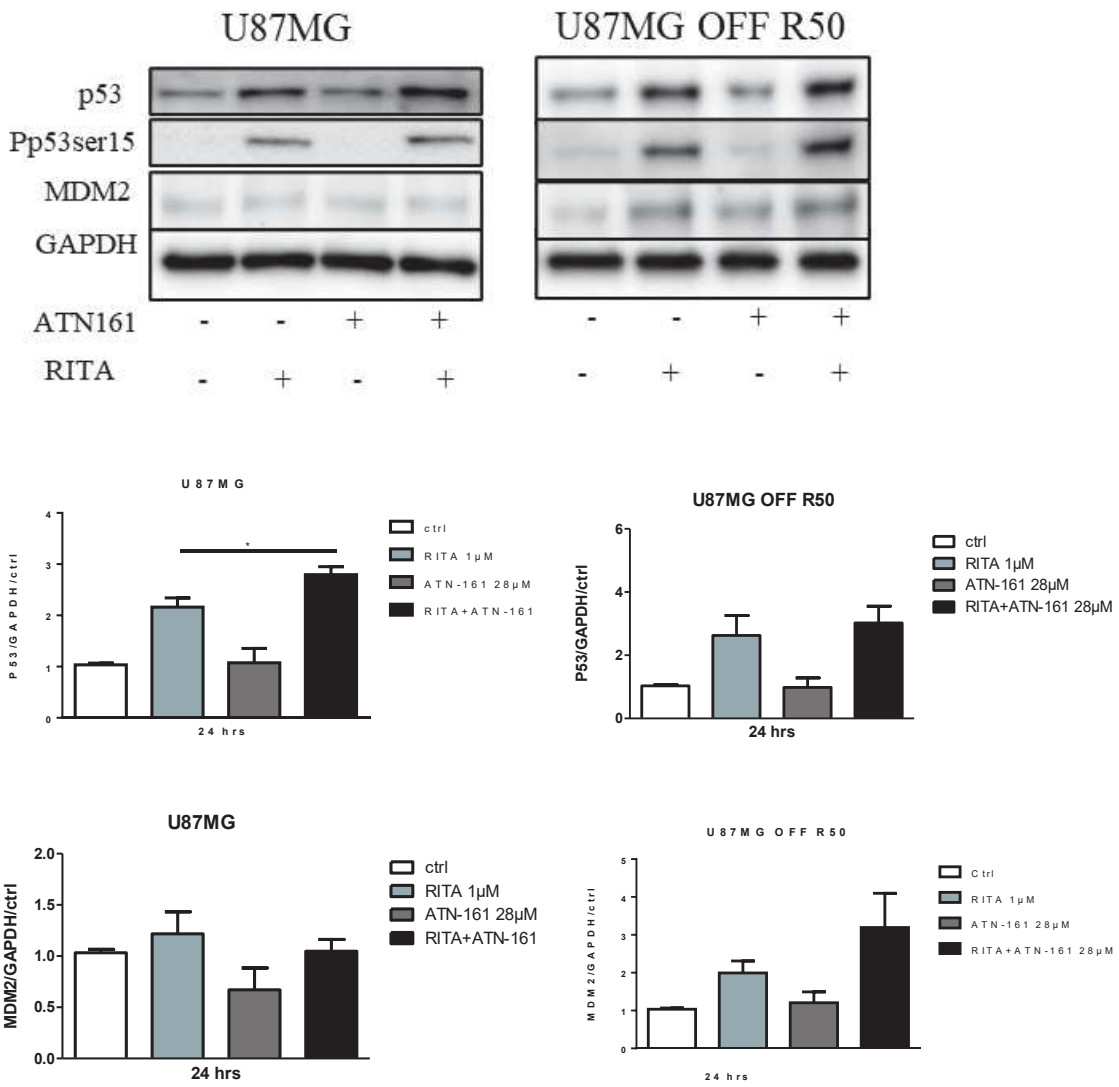
U87MG
U87MG OFF R50
p53
Pp53ser15
MDM2
GAPDH
ATN161
RITA
U87MG
P53/GAPDH/ctrl
ctrl
RITA 1μM
ATN-161 28μM
RITA+ATN-161
24 hrs
U87MG OFF R50
P53/GAPDH/ctrl
ctrl
RITA 1μM
ATN-161 28μM
RITA+ATN-161 28μM
24 hrs
U87MG
MDM2/GAPDH/ctrl
ctrl
RITA 1μM
ATN-161 28μM
RITA+ATN-161
24 hrs
U87MG OFF R50
MDM2/GAPDH/ctrl
Ctrl
RITA 1μM
ATN-161 28μM
RITA+ATN-161 28μM
24 hrs

Fig. 8C

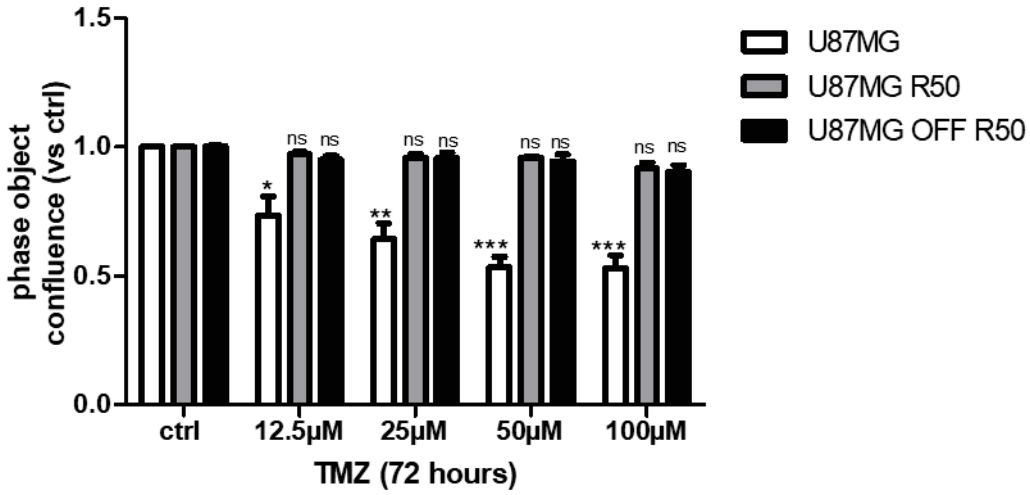

Figure S1

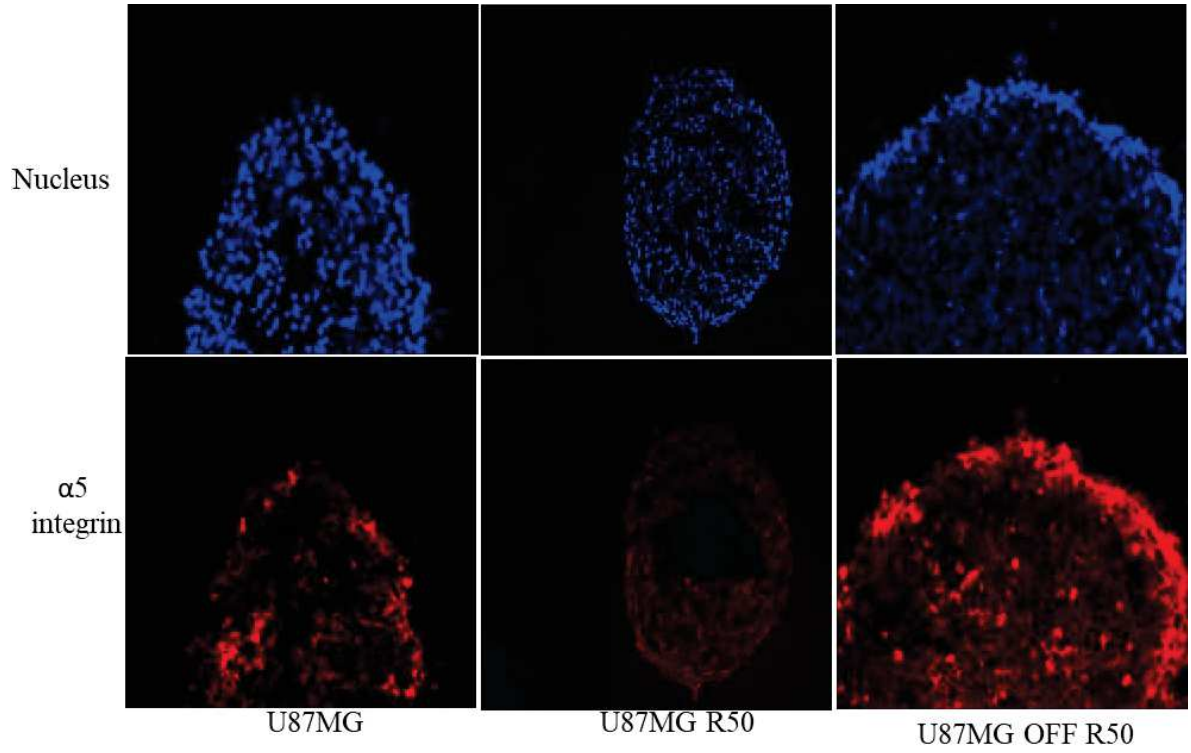

Fig. S2

Results part 3: Effect of Compound 9 as a dual inhibitor of α5β1 integrin and p53/MDM2 complex

In the course of this work, a new compound was described in the literature (Merlino et al., 2018). Compound-9 was described as a potent α5β1 and αvβ3 integrin inhibitor coupled with an inhibitory activity on MDM2 and MDM4 thus combining the effects we were studying. We checked the effect of compound-9 in our cell lines.

1. Effect of Compound-9 on cell confluence

We first evaluated the effect of compound-9 on cell confluence of expressing α5 integrin (U87MG and U87MG OFF R50 cells) and U87MG-α5KO cells in which the gene for α5 integrin was deleted using the CRISPR/Cas 9 technology. We treated U87MG, U87MG-α5KO and U87MG OFF R0 cells with increasing concentrations of compound-9 and the cell confluence was dynamically detected and calculated using IncuCyte Zoom software based on phase-contrast images obtained from the IncuCyte in real time. Compound-9 induced a concentration-dependent decrease in cell confluence in all the cell lines. 50% inhibition was achieved at 0.6μM for U87MG and U87MG OFF R50 cells and 2.5μM for U87MG-α5KO, suggesting that U87MG-α5KO cells lacking α5 integrin are less sensitive to Compound-9 treatment as compared to α5 integrin expressing cells (U87MG and U87MG OFF R50 cells (**Figure 30**).

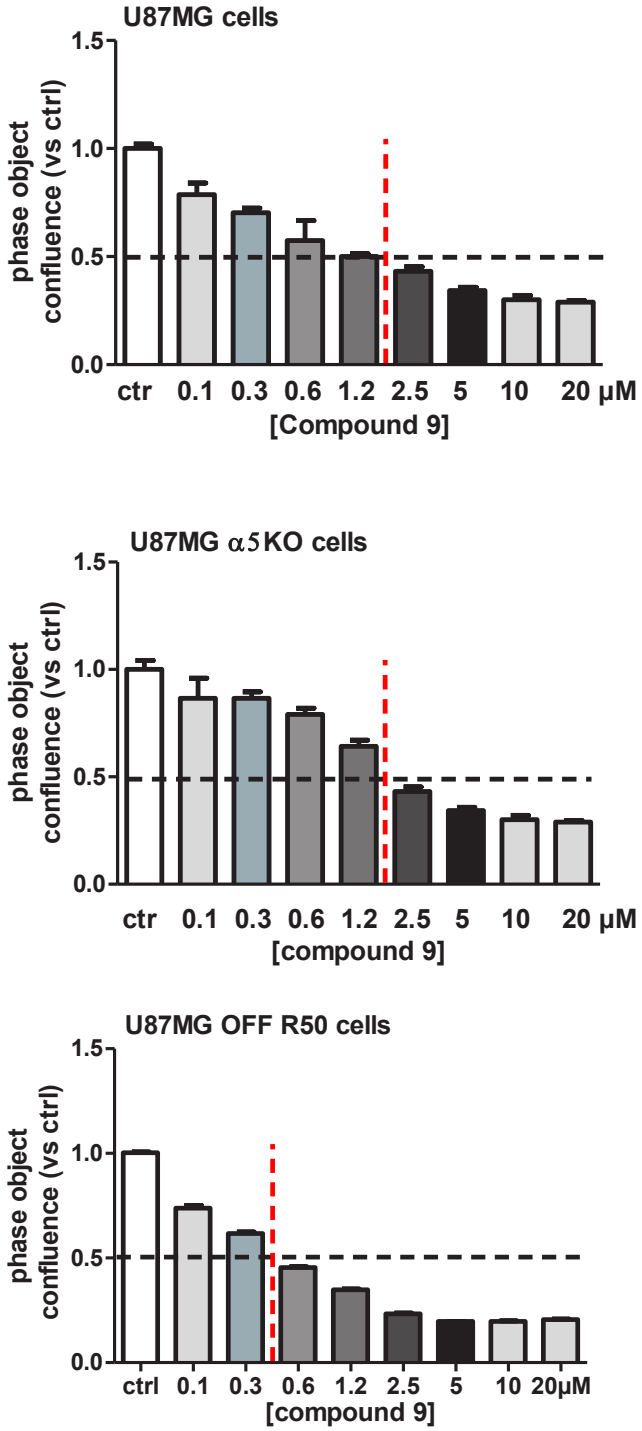

Figure 30. Effect of increasing concentrations of compound-9 on confluence of U87MG, U87MGα5KO and U87MG OFF R50 cells.
Cell confluence was calculated using IncuCyte Zoom software based on phase-contrast images of U87MG, U87MGα5KO and U87MG OFF R50 cells from 0 h to 72 h at increasing concentration of compound-9. Each data point represents mean ± S.E.M. of at least three independent experiments.

We next evaluated the effect of Compound-9 on the morphology of U87MG and U87MG-α5KO cells. Phase contrast images showed that treatment with high concentration of compound-9 (20μM) leads to detachment and rounding up of both U87MG and U87MG-α5KO cells 72hrs post treatment, indicating the effectiveness of compound-9 to interfere with cell adhesion to extracellular matrix that is known to be tightly regulated by integrins. Interestingly, the U87MG-α5KO cells lacking α5 integrin were less sensitive to low concentration of compound (1μM) as compared to the parental U87MG cells, confirming that it recognizes better cells expressing the integrin. However, no differences were observed between the two cell lines when higher concentration of compound 9 was used (**Figure 31**).

These results suggest that compound-9 treatment is more effective at lower concentrations in cells expressing α5 integrin and that higher concentration might possibly act through interaction with αvβ3 integrin.

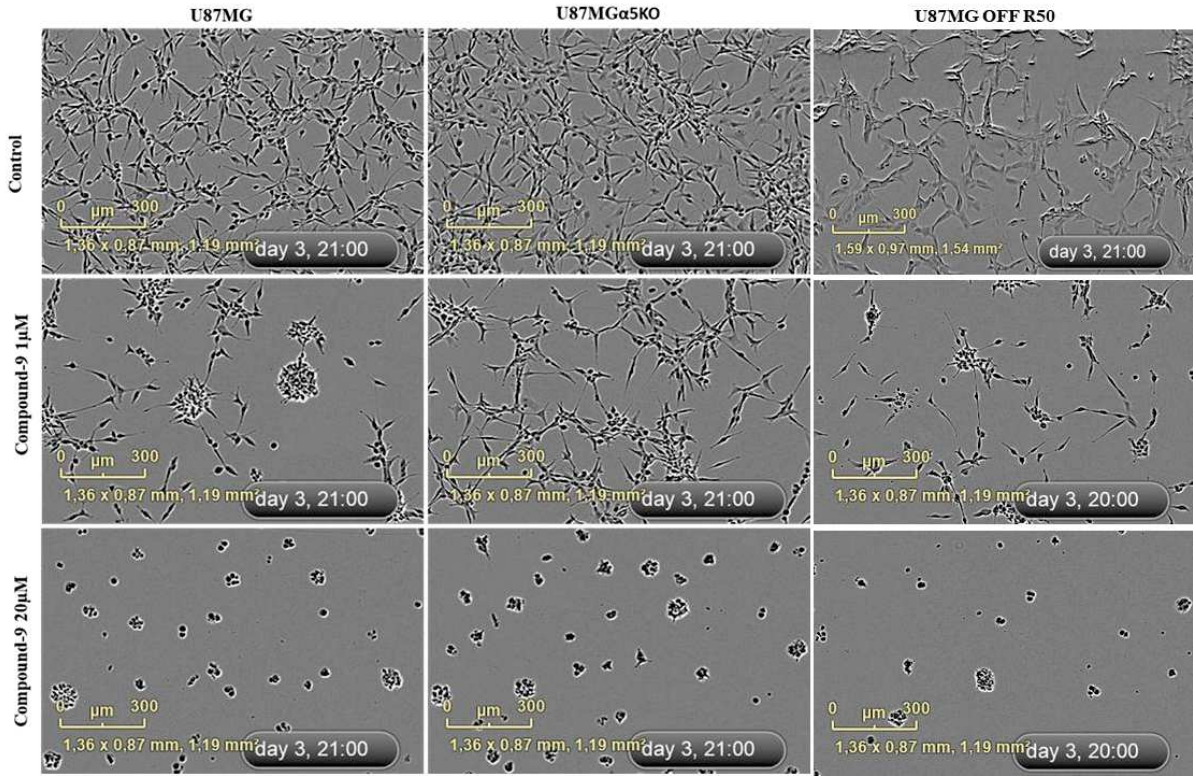

Figure 31. Effect of compound-9 on the cellular morphology of U87MG, U87MGα5KO and U87MG OFF R50 cells.
Representative phase contrast images of U87MG, U87MGα5KO and U87MG OFF R50 cells at 72 hrs post treatment with compound-9 1µM and 20µM. Scale bar, 300µm.

2. Comparison between the effect of Compound-9 as a single agent on cell confluence and combined treatment with Idasanutlin and K34c.

Compound 9 was reported as a potent MDM2/4 and α5β1/αvβ3 blocker (Merlino et al., 2018). To investigate this effect, we evaluated the effect of compound-9 as a single agent in comparison with a combined treatment with the MDM2 inhibitor Idasanutlin and the integrin antagonist K34c. When used at a low concentration (at 1 µM), compound-9 elicited similar effect on confluence than integrin antagonists alone (at 20 µM) and at higher concentration (at 20 µM) it behaves as combined treatment with the integrin antagonists K34c and the p53 activator Idasanutlin in naïve and TMZ-resistant U87MG cells (**Figure 40**). Results thus suggest that this compound may be an interesting way to treat glioma cells.

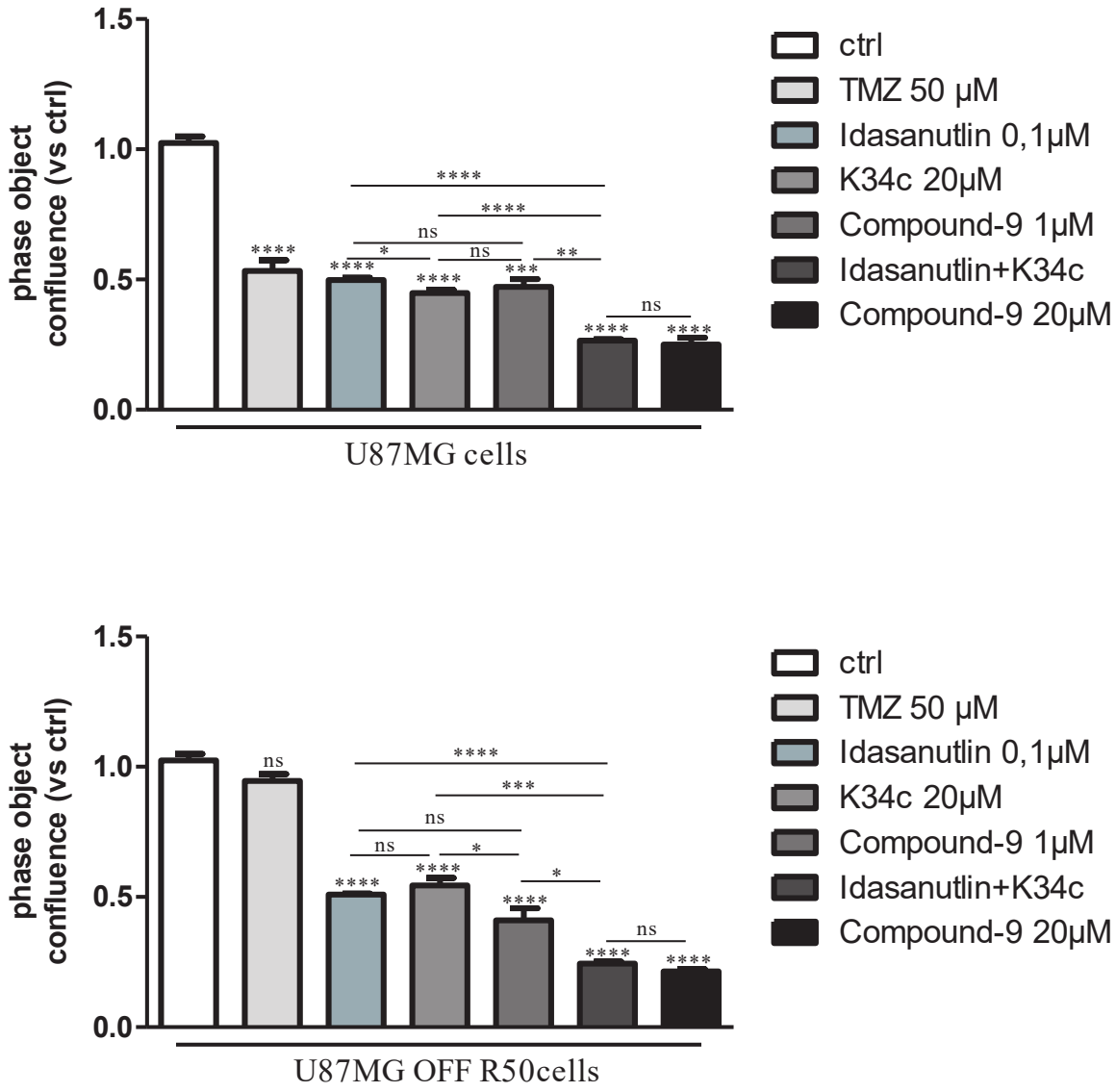

Figure 32.Compound-9 compared to combined treatment with p53 activator and an integrin antagonist.

Cell confluence was calculated using IncuCyte Zoom software based on phase-contrast images of U87MG and U87MG OFF R50 cells from 0 h to 72 hrs post treatment with TMZ, Idasanutlin, K34c and compound-9 each alone or in combination. Each data point represents mean ± S.E.M. of at least three independent experiments with *, $p<0.05$; **, $p<0.01$; ***, $p<0.001$; ns, non-significant.

3. Effect of Compound-9 on the p53 pathway

Based on these results and also on the report that compound-9 stabilized and activates the p53 pathway (Merlino et al., 2018), we further studied the effect of compound-9 on p53 stabilization. We treated U87MG cells with compound-9 under reduced serum condition (2%) and then evaluated p53 protein stability. It can be seen from the western blot results in **Figure 33A** that treatment with Compound-9 did not increase p53 protein stability when compared to the control, 8 hours post treatment. Furthermore, RT-qPCR analysis of p53-repressed target gene mRNA (birc5) and p53-activated target gene mRNAs (fas, p21 and hdm2) showed no detectable increase compared to the control at 6 and 24 hours post treatment with Compound-9 at 1 μM (**Figure 33B**).

These results demonstrated that compound 9 did not stabilize or activate the p53 protein in our cell lines and experimental conditions.

A.

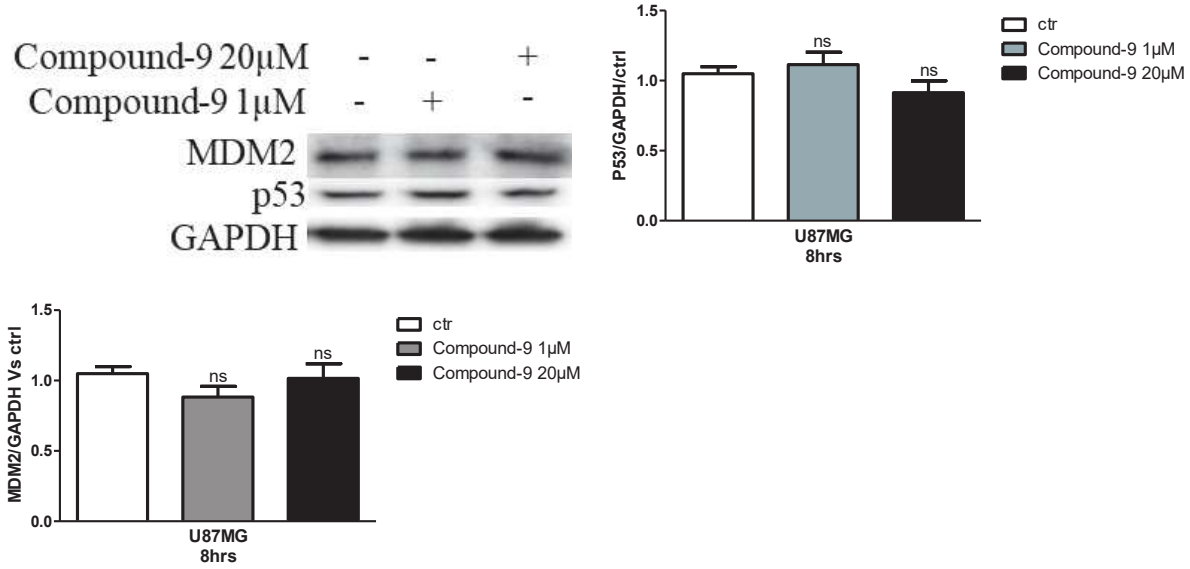

B.

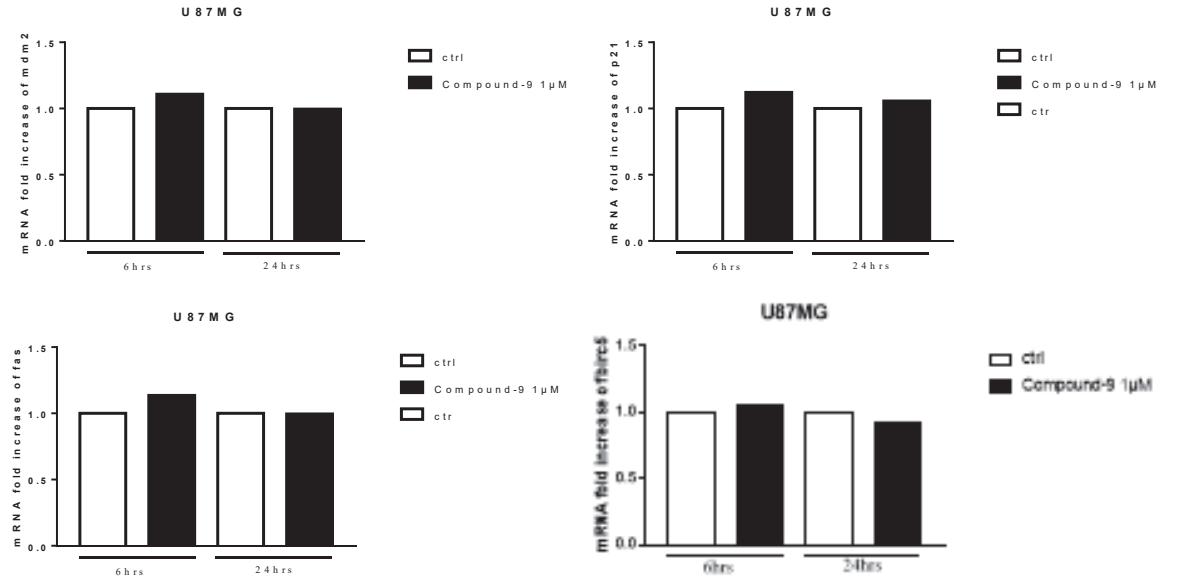

Figure 33. Effect of Compound-9 on the p53 pathway.
(**A**) A representative western blot of p53 stability in U87MG cells treated during 8hrs with Compound-9 (1µM and 20µM). GAPDH was used as the loading control. Histograms represent the mean ± S.E.M. of at least three independent experiments with *, $p<0.05$; **, $p<0.01$; ***, $p<0.001$; ns, non-significant. (**B**) qPCR analysis of the p53 target genes p21, MDM2, Fas and birc5 in U87MG cells 6 and 24hrs post treatment with Compound-9 1 µM. Histograms show the fold increase in mRNA expression normalized to GAPDH. Experiment was made once.

Since Compound-9 was reported to activate the p53 pathway at 0.1µM (Merlino et al., 2018), we next treated U87MG and U87MG-α5KO cells with Compound-9 0.1µM in comparison to the p53 activator Nutlin-3a (1µM) in a kinetic studies and evaluated the stabilization of p53 and MDM2 protein. A comparison of the two results reveals that Nutlin-3a stabilized the p53 and MDM2 protein in both U87MG and U87MG-α5KO cells at all the time points tested (3, 6, 9, 12 and 24hrs) (**Figure 34A**). On the other hand, no detectable increase in p53 protein stability was observed in both U87MG and U87MG-α5KO cells after treatment with compound-9 at all these time points (3, 6, 9, 12 and 24hrs) (**Figure 34A)**.

We wondered whether varying the experimental conditions and concentrations of Compound-9 could have a positive impact on the p53 pathway. We treated U87MG cells with increasing concentration of Compound-9 in medium containing 10% serum and evaluated the stabilization of the p53 protein. No increase in p53 stability was observed at 12 and 24hrs post treatment at all concentration of compound-9 tested (**Figure 34B**).
Overall, Compound-9 did not stabilize or activate the p53 pathway in our cell lines but rather seemed to decrease it with increasing concentration and treatment period.

A.

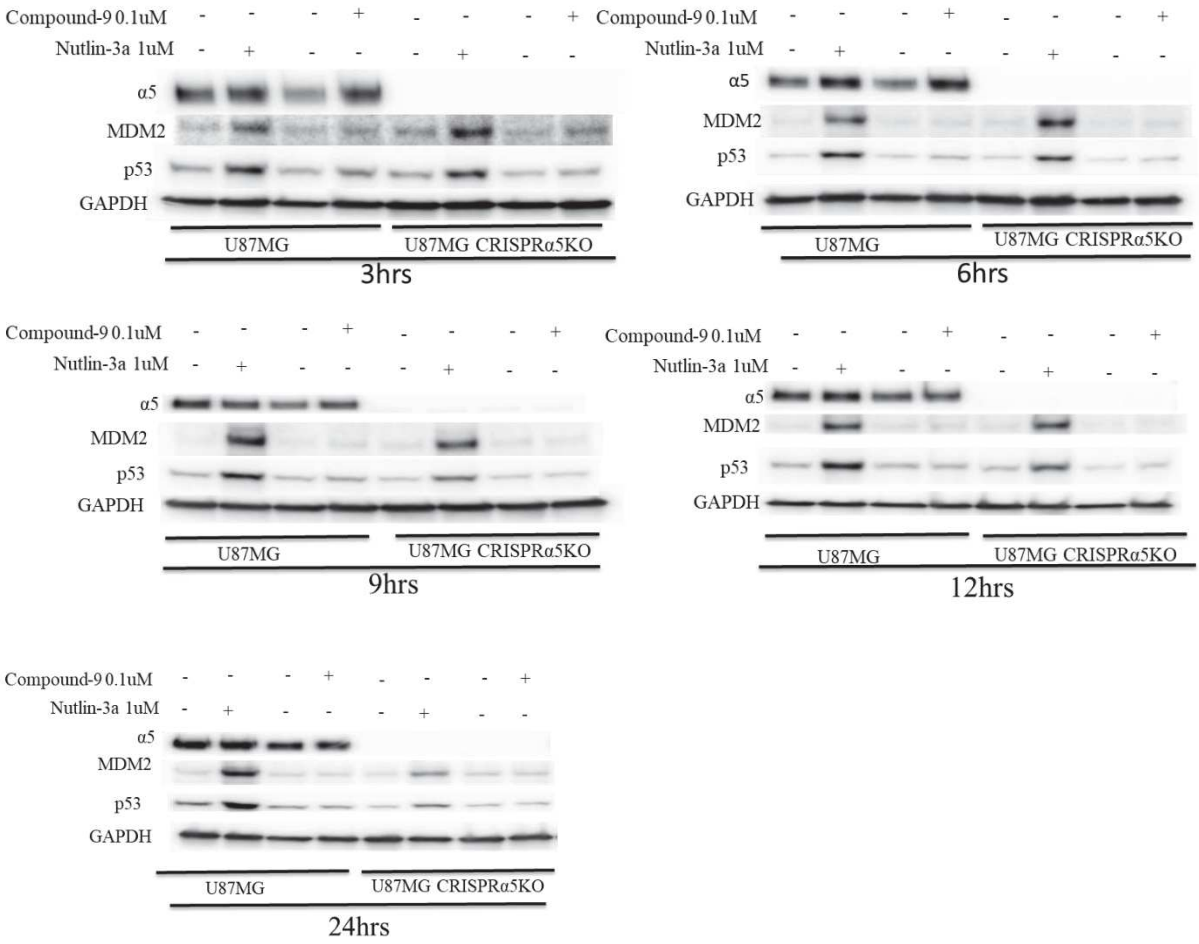

B.

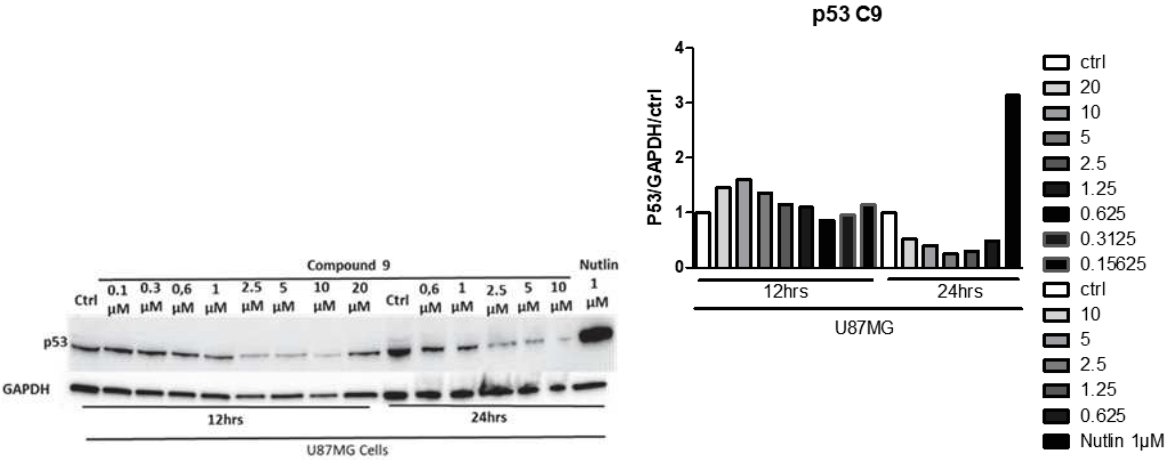

Figure 34. Effect of Nutlin-3a and Compound-9 on p53 and MDM2 protein stability. (**A**) Western blots showing Kinetics of p53 and MDM2 stability in U87MG and U87MG-α5KO cells treated with Compound-9 0.1µM and Nutlin-3a1µM. GAPDH was used as the loading control. (**B**) Western blot of p53 and MDM2 stability and activity in U87MG cells treated during 12 and 24hrs with Nutlin-3a 1µM and increasing concentrations of Compound-9. GAPDH was used as the loading control.

Discussion

Restoration of the tumour suppressor function of wild-type p53 is considered an attractive therapeutic strategy for the treatment of GBM. However, wild-type p53 is often inactivated or degraded by MDM2. The MDM2 proteins is deregulated in GBM (Wade et al., 2013) and its overexpression is correlated with poor clinical prognosis and poor treatment response to current cancer therapies (Momand et al., 1998). To date, several MDM2 inhibitors have been developed. However, studies have demonstrated that activation of the p53 protein by MDM2 inhibitors such as Nutlin-3a (Renner et al., 2016b) or Idasanutlin (Pan et al., 2017) is insufficient to induce apoptosis in cancer cells. Previous data of our Laboratory have identified a convergent pathway involving α5β1 integrin and the p53 protein in the regulation of glioma cell apoptosis(Renner et al., 2016b). This integrin is overexpressed at the mRNA (Ellert-Miklaszewska et al., 2020) and protein (Holmes et al., 2012) levels and its overexpression is associated with decreased survival of patients with GBM (Janouskova et al., 2012). Therefore, α5β1 integrin appeared an interesting target in GBM. In line with these, a Lead optimization carried out on compound 7 (an inhibitor of both MDM2/4 and α5β1/αvβ3 integrins) by Merlino et al. in which its activities on integrins was preserved while improving those on MDM and MDM4 proteins led to the discovery of Compound 9. Compound-9 was described as a potent α5β1 and αvβ3 integrin inhibitor coupled with an inhibitory activity on MDM2 and MDM4. Compound 9 was reported to decrease cell proliferation, stabilized p53 and induced the transcription of the p53 target genes p21, MDM2 and PUMA in a wild-type p53 dependent manner in U87MG cells (Merlino et al., 2018).

It was therefore interesting to test this new compound in our cell lines, as it may combine in one drug the effect of p53 activation and α5β1 integrin antagonism. We demonstrated that Compound-9 induced a concentration-dependent decrease in cell confluence of both U87MG and U87MG-α5KO cells. Moreover, 50% of inhibition was achieved at 0.6µM for U87MG and 2.5µM for U87MG-α5KO, suggesting that U87MG-α5KO cells lacking α5 integrin are less sensitive to Compound-9 treatment as compared to the U87MG parental cells expressing the integrin. This finding agrees with the findings of Merlino et al. in which Compound 9 was described as a potent inhibitor of α5β1 integrin in addition to its capability to inhibit cell proliferation of U87MG. We showed using phase contrast images that treatment with Compound 9 leads to detachment and rounding up of cells indicating the effectiveness of compound-9 to interfere with cell adhesion to extracellular matrix that is known to be tightly

regulated by integrins. We found that U87MG-α5KO cells lacking α5 integrin were less sensitive to low concentration of compound (1μM) as compared to the parental U87MG cells, confirming that it recognizes better cells expressing the integrin. However, no differences were observed between the two cell lines when higher concentration of compound 9 was used. Our data suggest that compound-9 treatment at lower concentrations is more specific for cells expressing α5 integrin and that higher concentration might possibly act through interaction with αvβ3 integrin, MDM2 or MDM4, in addition to α5β1 integrin. Compound 9 appears to be very powerful las an integrin antagonist as 1μM is sufficient to affect cell morphology compared to 20μM for other ligands.This result is in line with the studies in which Merlino et al. demonstrated that compound 9 at lower concentration (0.1μM) functions below the threshold of combined treatment with the MDM2 inhibitor Nutlin-3a and the integrin antagonist Cilengitide, but functions above this threshold at higher concentration (10 μM) (Merlino et al., 2018).

We compared Compound 9 as a single agent with coadministration of the p53 activator Idasanutlin and the integrin antagonist K34c. We found that compound 9 at higher concentration (at 20 μM) elicit an effect on cell confluence that was equivalent to combined treatment with the integrin antagonists K34c and the p53 activator Idasanutlin in both naïve and TMZ-resistant U87MG cells. Consistent with our findings Merlino et al. showed that Compound 9 (10 μM) decreased cell proliferation of U87MG cells to the same extent as combined treatment with Nutlin-3a and the integrin antagonist Cilengitide (Merlino et al., 2018). Results thus suggest that this compound may be an interesting way to treat glioma cells. Moreover, compared to coadministration of different drugs, a single molecule with the ability to simultaneously hit multiple targets could provide several advantages such as lower risk of pharmacokinetic drug-drug interactions and reduced susceptibility to adaptive resistance.

Earlier findings demonstrated that Compound 9 stabilized p53 and enhanced p53 activity via transcriptional induction of the p53 target genes p21, MDM2 and PUMA in a wild-type p53 dependent manner (Merlino et al., 2018). In contrast to these findings, however, no evidence of p53 stabilization or increase in p53 target genes was observed upon treatment with compound 9 in our experimental conditions. To confirm our results, we requested for another batch of compound 9, but no observable increase in p53 stability was obtained. We next modified our experimental conditions using the same concentration of compound 9 (0.1μM), treatment time and serum condition as reported by Merlino et al. (Merlino et al., 2018). No increase in p53 stability was observed despite using this experimental conditions in a kinetic study. These

results are rather disappointing as compound 9 seemed promising based on the cell confluence data obtained in real time but failed to stabilize and activate the p53 protein.

This contrasting results have thrown up many questions in need of further investigation. It would be interesting to assess the cytotoxic effects of compound 9 using techniques such as trypan blue exclusion assay. This would determine if the detached and rounded up cells are dead or alive following compound 9 treatment. If the cells turn out to be dead, it would be interesting do determine the mechanism involved (such as necrosis or autophagy).

Further investigation on compound 9, should be done using other GBM cells and if possible, should be evaluated across a different type of cancer. It would be interesting to further optimize the inhibitory effect of compound 9 on MDM2.

Conclusion

In this investigation, the aim was to assess the effect of Compound 9 on cell confluence and the p53 pathway in GBM. On cell confluence, compound 9 as a single agent elicit equal activity as combined treatment with a p53 activator and an integrin antagonist. However, compound 9 failed to either stabilized or activate the p53 protein in our experimental conditions. Further investigation is necessary to ascertain the role of compound 9 on the p53 pathway or other pathway.

General conclusions and perspectives

Despite advances in science and the use of aggressive treatment approach (Stupp protocol) GBM remain incurable due to the development of acquired resistance to TMZ. therefore, novel therapeutic approach is required to overcome GBM resistance and improve overall survival of patients. With alteration of specific intracellular components contributing to tumour aggressiveness and resistance, targeted therapy towards altered signalling pathways could be promising for recurrent tumours.

We compared Nutlin-3a, RITA and Idasanutlin. We demonstrated that Idasanutlin is the most potent while RITA appeared the least potent. We found that activation of the p53 pathway by Nutlin-3a repressed α5 integrin. Moreover, deletion of the gene for α5 integrin decreased the expression of MDM2 upon p53 activation by Nutlin-3a between 6 to 12 hrs as compared to the parental cells. These results therefore need to be interpreted with caution because both MDM2 and the 53 protein were affected at 6 hrs when Nutlin-3a was combine with the integrin antagonist K34c. Hence, it could conceivably be hypothesised that the crosstalk between α5β1integrin, MDM2 and the p53 would be easier to unravelled using a different model in which the expression of MDM2 due treatment with Nutlin-3a is replaced by the transfection of U87MG cells with cDNA clone of the gene for MDM2 to create a stable cell line overexpressing MDM2. In line with this, an integrin antagonist could be used to monitor the modulation of MDM2 and P53.

We decided to turn our investigations on TMZ-resistant GBM cells, as it was shown in the literature that some recurrent GBM over-express α5 integrin. We thus developed an in vitro model of TMZ-resistant cells. Based on RNAseq analysis, we found that Extracellular matrix organisation, O-linked glycosylation and Integrin cell surface interactions are the Biological pathways mostly impacted by long term TMZ treatment. Moreover, profound rearrangement of integrin subunits expression levels exists between the cell lines. At the protein levels, we found that α5 integrin is repressed in the presence of TMZ but re-expressed in TMZ- resistant cells cultured in the absence of TMZ. Our model of TMZ-resistant cells is consistent with previous work in the literature and could be especially useful in understanding the mechanism of GBM resistance to TMZ and the development of targeted therapies for recurrent GBM. In addition, it could be used for drug repurposing experiments. We are currently in the way of developing TMZ-resistant U373MG and LN443 cells. These would serve as a model for result confirmation. However, this model of TMZ resistant cells has several limitations. For example, the tumour microenvironment in this model is not a true representation of what is obtainable in vivo. However, this could be overcome by generating the resistant cells in nude mice or the

direct use of resistant tumour samples from patients. Developing the TMZ resistant cells as 3D spheroids is another interesting way to mirror the normal tumour microenvironment. Having a model of TMZ-resistant GMB cells that mirrored the normal tumour microenvironment will be especially useful for translational research.

We proposed activation of the p53 pathway and inhibition of α5β1 integrin as a therapeutic strategy to overcome TMZ resistance in U87MG cells. We found that inhibition of α5β1 integrin by an integrin antagonist (K34c or Fr248) concomitant with activation of p53 with a p53 activator (Nutlin-3a, RITA or Idasanutlin) more effectively decreased cell confluence and increased p53 stability and activity than treatment with either drug alone. However, disappointing results on both single and combine treatment were obtained on the apoptotic outcome (either by western blot or FACs analysis). A possible explanation to this outcome could be that the level of α5β1 integrin in both the resistant and parental cells is not sufficient to allow for proper functioning of the integrin antagonist. Since cell confluence assay only measures the surface area covered by cells with no information on cell death, it would be interesting to use cytotoxic assay such as trypan blue exclusion assay to determine if these combinations are cytotoxic to the cells.

Lastly, we found that Compound 9, which combine both p53 activating and α5β1 integrin inhibiting properties showed similar activity on cell confluence as combine treatment using a p53 activator and an integrin antagonist. It seems the α5β1integrin inhibiting property of Compound 9 in our cells overshadows its p53 activating property, as the cells were completely detached and rounded up few hours post treatment even at lower concentration (0.06 μM) but no increase in p53 stability or a positive apoptotic outcome was observed in our experimental conditions. It would be interesting to use trypan blue assay to determine the cytotoxic effect of compound 9 and also to investigate other cell death pathways such as such necrosis and autophagy that are independent of p53, to determine what actually happen to detached and rounded up cells following Compound 9 treatment.

In summary, we developed TMZ-resistant U87MG cells that sowed alteration of α5β1 integrin. We showed that inhibition of this integrin concomitant with activation of p53 may be an effective strategy to overcome TMZ resistance in U87MG cells.

List of publications and oral communications

Publication

Article 1

Saidu SANI, Mélissa MESSE, Quentin FUCHS, Marina PIERREVELCIN, Patrice LAQUERRIERE, Natacha ENTZ-WERLE, Jean Pierre GIES, Damien REITA, Nelly ETIENNE-SELLOUM, Véronique BRUBAN, Sophie FOPPOLO, Laurence CHOULIER, Sophie MARTIN and Monique DONTENWILL (2020). Biological relevance of RGD-integrin subtype-specific ligands in cancer. ChemBioChem 10.1002/cbic.202000626.

Article 2

Ezeddine HARMOUCH, Joseph SEITLINGER, Hassan CHADDAD, Geneviève UBEAUD-SEQUIER, Jochen Barths, **Sani SAIDU**, Laurent DÉSAUBRY, Stéphanie GRANDEMANGE, Thierry MASSFELDER, Guy FUHRMANN, Florence FIORETTI, Monique DONTENWILL, Nadia BENKIRANE-JESSEL & Ysia IDOUX-GILLET (2020). Flavagline synthetic derivative induces senescence in glioblastoma cancer cells without being toxic to healthy astrocytes. Scientific Reports.

Article in preparation for publication

Saidu SANI, Mélissa MESSE, Isabelle LELONG-REBEL, Ezzeddine HARMOUCH, Horst KESSLER, + postdoc kessler, Jean-Pierre GIES, Damien REITA, Lionel THOMAS, Patrice LAQUERRIERE, Sophie FOPPOLO and Monique DONTENWILL. Modulation of integrins in Temozolomide-resistant U87MG glioblastoma cells. Integrin α5β1 as a target.

Poster

Saidu SANI, Isabelle LELONG-REBEL, Fuchs QUENTIN, Luciana MARINELLI and Monique DONTENWILL. New strategies to overcome temozolomide resistance in glioblastoma. Journées du campus d'Illkirch - JCI 2019.

Article 1

Introduction

Integrins are heterodimeric transmembrane cell surface receptors capable of mediating the adhesion of cell to extracellular matrix (ECM) to support cell–cell interactions in different physiological and pathological conditions. In humans there are at least 24 known αβ heterodimers formed by non-covalent combination of 18α and 8β subunits. Integrins are involved in almost all the hallmarks of cancer and those recognizing the Arg-Gly-Asp (RGD) peptide in their natural extracellular matrix ligands represents promising therapeutic targets. The biological relevance of the RGD-integrin subtype-specific ligands in cancer are reviewed in the manuscript (Sani et al., 2020).

- ❖ The rational underlying the need to clearly delineate each RGD-integrin subtype by selective tools was described.
- ❖ The impact of integrins in tumor microenvironment, their involvement in the hallmarks of cancer, and the fundamental control of integrin dependent cell adhesion and signaling was described
- ❖ The need to properly understand the complexity of integrin biology, in order to translate preclinical discoveries with integrin inhibitors into clinical success was discussed.
- ❖ The complex roles of each RGD-integrins (αvβ3 and α5β1 integrins) in tumors and steps towards ligands specificity, selectivity, and activity (antagonism versus agonism) of the three main classes of integrin ligands (antibodies, RGD-derived peptides, and RGD-mimetic small molecules) was described. Also discussed is the use of these ligands tools for tumor diagnosis or tumor targeting markers.

ChemBioChem

Combining Chemistry and Biology

Chemistry Europe

European Chemical Societies Publishing

Accepted Article

Title: Biological relevance of RGD-integrin subtype-specific ligands in cancer

Authors: Saidu SANI, Mélissa MESSE, Quentin FUCHS, Marina PIERREVELCIN, Patrice LAQUERRIERE, Natacha ENTZ-WERLE, Damien REITA, Nelly ETIENNE-SELLOUM, Véronique BRUBAN, Laurence CHOULIER, Sophie MARTIN, and Monique Dontenwill

To be cited as: *ChemBioChem* 10.1002/cbic.202000626

Link to VoR: https://doi.org/10.1002/cbic.202000626

WILEY-VCH

Biological relevance of RGD-integrin subtype-specific ligands in cancer

Saidu SANI[a,b,$], Mélissa MESSE[a,c $], Quentin FUCHS[a], Marina PIERREVELCIN[a], Patrice LAQUERRIERE[c], Natacha ENTZ-WERLE[a,d], Damien REITA[a,e], Nelly ETIENNE-SELLOUM[a,f], Véronique BRUBAN[a], Laurence CHOULIER[a], Sophie MARTIN[a] and Monique DONTENWILL[a,*]

a) Laboratoire de Bioimagerie et Pathologies (LBP), UMR CNRS 7021, Université de Strasbourg, Faculté de Pharmacie, 74 route du Rhin, CS 60024, 67401 Illkirch cedex, France. Institut Thématique Interdisciplinaire InnoVec, Université de Strasbourg.

b) Cancer and Diabetic Research Group, Department of Biochemistry and Molecular Biology, Faculty of Science, Federal University Ndufu-Alike Ikwo, P.M.B 1010, Abakaliki, Ebonyi State. Nigeria.

c) Institut Pluridisciplinaire Hubert Curien (IPHC), UMR CNRS 7178, Université de Strasbourg, 67000 Strasbourg, France.

d) Pediatric Onco-Hematology Department, Pediatrics, University Hospital of Strasbourg, 1 avenue Molière, 67098 Strasbourg, France.

e) Department of Oncobiology, Laboratory of Biochemistry and Molecular Biology, University Hospital of Strasbourg, France

f) Institut du Cancer Strasbourg Europe (ICANS), Service de Pharmacie, Strasbourg, France.

$ equal first authors

* corresponding author; monique.dontenwill@unistra.fr

ABSTRACT

Integrins are heterodimeric transmembrane proteins able to connect the cells with the micro-environment. They represent a family of receptors involved in almost all the hallmarks of cancer. Integrins recognizing the Arg-Gly-Asp (RGD) peptide in their natural extracellular-matrix ligands, have been particularly investigated as tumoral therapeutic targets. In the last 30 years, intense research was dedicated to design specific RGD-like ligands able to discriminate selectively the different RGD-recognizing integrins. Efforts of chemists led to the proposition of modified peptide or peptidomimetic libraries to be used for tumor targeting and/or for tumor imaging. Here we review, from the biological point of view, the rational underlying the need to clearly delineate each RGD-integrin subtype by selective tools. We describe the complex roles of RGD-integrins (mainly the most studied αvβ3 and α5β1 integrins) in tumors, the steps towards selective ligands and the current usefulness of such ligands. Although the impact of integrins in cancer is well acknowledged, the biological characteristics of each integrin subtype in a specific tumor are far from being completely

resolved. Selective ligands may help to reconsider integrins as therapeutic targets in specific clinical settings.

1 INTRODUCTION

Integrins are heterodimeric transmembrane proteins recognized first as adhesion molecules on specific extracellular matrix (ECM) components. They were further assigned to a true receptor family as their ability to initiate intracellular signaling pathways was largely emphasized. In the hallmarks of cancer as defined by Hanahan and Weinberg in 2000 [1], integrins were acknowledged as actors of self-sufficiency growth signaling, as regulators of anti-apoptotic signaling, angiogenesis and adaptation to new environments during invasion and metastasis of tumor cells. New hallmarks were added ten years later [2],in particular, the contribution of the tumor microenvironment (TME) to tumorigenesis. The TME does not only contain ECM but also recruits immune and stromal cells able to facilitate tumor growth. Changes in the repertoire and expression level of integrins in these non tumoral cells were described to support aggressive tumoral phenotypes [3]. Integrins were recognized early as therapeutic targets in cancers [4–6]. The most studied integrins in oncology belong to the RGD-integrin subfamily with αvβ3/β5 and α5β1 integrins in the spotlight for the two last decades [7]. The RGD (Arg-Gly-Asp) peptidic motif is found in ECM proteins (fibronectin, vitronectin, osteopontin, thrombospondin among others) and represents a selective binding site for integrins to ECM. Since activation of integrins by adhesion to their ECM ligands was shown to be essential to non-tumoral adherent cell survival [8,9], similar effect was expected for tumoral cells. Disrupting the interactions between integrins and ECM through RGD-like compounds appeared therefore a valuable strategy to trigger tumor cell apoptosis. Research in the design and characterization of integrin antagonists as cancer drug candidates has expanded rapidly [10]. Cilengitide, a cyclic RGD peptide, was the first αvβ3/β5 integrin antagonist that reached the clinic [11]. Despite numerous preclinical encouraging data, cilengitide failed to improve glioblastoma patient's survival in phase II/III randomized clinical trials [12,13]. No better outcomes were obtained with Volociximab or MINT1526A, both α5β1 integrin inhibitory antibodies, in several clinical settings [14,15]. These disappointing results impeded considerably research on RGD-integrins as therapeutic targets in oncology. However, recent reviews on integrins and cancer emphasize the need to reconsider the topic [6,7,16–20]. In this review we will focus mainly on RGD-integrins αvβ3 and α5β1 as most ligands have been designed for them. We will support the idea that integrins should still be considered as targets for anti-cancer therapies. In addition, ligands specific for definite subtypes of integrins will help in understanding how and where integrins must be targeted and will shed more light on the complexity of the topic.

2 RGD-integrins in cancer

2.1. Integrins in focal adhesion and cell migration

Common rules of integrins have been extensively reviewed elsewhere (for a recent review see [21]). In human, 18 α and 8 β subunits can combine to form heterodimeric transmembrane

proteins with specific ligand recognition properties. They share an architecture comprising an extracellular domain, a transmembrane region, and a generally short intracellular part. If specific adhesion to ligands lies in the composition of the αβ extracellular head, integrins signal inside the cells by structural changes and recruitment of cytoplasmic proteins in complexes named adhesomes [22]. Such complexes contain about 2000 proteins among which a highly dynamic "consensus adhesome" of 60 proteins may control integrin dependent cell adhesion and signaling [23]. Mechanical forces can influence the assembly/disassembly of these macro-molecular structures adding a further level of complexity [24]. Recent work pointed that β3 integrins were more strongly bound to their substrate in adhesion sites submitted to high tension than β1 integrins [25]. The dynamic nanoscale organization of integrins and their regulators within focal adhesion points was shown to differ between β_3- and β1-integrins in the control of signaling during cellular functions [26,27]. Although both integrins recognize fibronectin, striking differences between α5β1 and αvβ3 integrin signaling pathways have been described in normal/tumoral cells. Most data addressed the question of focal adhesion point maturation and cell migration. αvβ3 integrins were associated with persistent migration through activation of Rac-mDia1, whereas α5β1 integrins were linked to RhoA-Rock-MyoDII pathway and random migration [28]. The role of both fibronectin-binding integrin classes can begin with an initial competition followed by a cooperative crosstalk [29]. Alternatively, blocking αvβ3 integrin may activate α5β1 integrin recycling back to membrane and increase cell migration [30]. Distinct mechanisms and/or efficient crosstalk between both integrins have emerged over the years [31]. New insights on focal adhesion maturation have been made possible using ligands specifically designed to target either αvβ3 or α5β1 integrins. It was shown that focal adhesion maturation on α5β1 integrin-selective substrates is dependent on αvβ3 integrin recruitment [32–34]. Most of the above described knowledges were obtained in non-tumoral cells and translation to cancer cells may be even more decisive for their functional behavior as the expression of integrins and the ratio between αvβ3 and α5β1 integrin levels are specifically altered in tumoral tissues as is the case for the expression of their common ECM ligand fibronectin [35].

2.2. Integrins in hallmarks of cancer

Thirty years ago integrin αvβ3 emerged as a marker of tumoral neo-angiogenesis which was inhibited by specific antagonists such as cilengitide in preclinical models [36–38]. These results were challenged as enhanced pathological angiogenesis and increased primary tumor growth were observed in mice lacking β3 or β3/β5 integrins [39]. Specific overexpression of Integrin β3 in tumor cells suppressed tumor growth in a human model of gliomagenesis [40]. Additionally, it was shown that nanomolar concentrations of RGD-mimetic αvβ3/αvβ5 inhibitors can enhance the growth of tumors in vivo by promoting VEGF-mediated angiogenesis [41]. These data may explain in part why the therapies with these inhibitors have failed in humans [12,13]. Other integrins participate in angiogenesis [42] and the proangiogenic function of α5β1 integrin has been clearly demonstrated [43–45]. It was shown that reduced expression of the α5 subunit is associated with reduced blood vessel formation and tumor growth[46] and that α5β1 integrin was overexpressed in tumoral vessels [47]. It will be essential to reconsider and to revisit fundamental biology underlying how these integrins coordinate angiogenesis to successfully target them [48].

Beside their role in angiogenesis, both integrins are overexpressed in many tumoral cells and thought to participate in enhanced survival and resistance to therapies [7,20,49–52]. This overexpression is mainly characterized at the mRNA level but less data exist at the protein level in cohorts of patients. The large transcriptomic databanks available nowadays for different tumor types help not only to define the inter-patient heterogeneity but also to correlate specific gene overexpression in tumor subtypes to patient survival. They have been used for high grade brain tumors (glioblastoma, GBM) for example [53]. In these tumors, α5 and β1 integrin mRNAs are overexpressed in GBM versus normal brain but even more in the GBM mesenchymal subgroup [54]; it was less subgroup dependent for αv and β3 integrin mRNA [55]. α5 and β1 genes are included in the GBM mesenchymal signature so that they represent biomarkers of this aggressive subtype. Interestingly α5 integrin is also overexpressed in subclones of pediatric brain tumors [56]. Extensive evaluation and comparison of integrin gene expression in different tumors and tumor subtypes would be a first step towards efficient anti-integrin therapeutic strategies. Even if determination of integrin proteins in cell lines is a prerequisite to characterize functional implication in vitro, the missing link is however the characterization of integrins at the protein level in clinical studies. Few data on small- to medium-sized patient cohorts are available in the literature. Immunohistochemical analysis of αv or β3 integrin protein expression in such cohorts were recently reported in osteosarcoma [57], hepatocellular carcinoma [58], leukemia [59] and the relationships with patient survival established. A retrospective immunohistochemical analysis of αvβ3, αvβ5 or αvβ8 integrins in the glioblastoma patient cohorts of cilengitide clinical trials was done. It revealed that only αvβ3 integrin expression in tumoral cells may predict benefit from cilengitide inhibition in a subset of patients with glioblastoma lacking *MGMT* promoter methylation [60]. Similarly, high levels of α5 or β1 integrin protein expression corresponded to worse survival in oral carcinoma [61], triple negative breast cancer [62], pancreatic cancer [63], osteosarcoma [64] and colorectal cancer [65]. In the last period, data concerning integrin expressions and functions in non-tumoral cells in the microenvironment of tumors have been increasingly reported. Roles of integrins in Cancer Associated Fibroblasts (CAF) have been reviewed recently [66]. Engineered mice models allowed deletion of integrin gene in specific population of cells. It was shown that acute deletion of β3 integrin in endothelial cells transiently diminished tumor growth and angiogenesis but long term deletion was ineffective [67]. Specific deletion of this gene in myeloid cells resulted in enhanced tumor growth [68] and increase of M2 macrophages at the tumor site thus promoting pro-tumoral functions in the microenvironment [69]. In another work, it was shown that tumor- associated -macrophages (TAM) accumulation correlated with tumor cell expression of αvβ3. This characteristic was used to design an αvβ3 antibody-dependent cellular cytotoxicity (ADCC) against tumoral cells [70]. Two recent works underlined the expression of α5 integrin in the stroma of pancreatic [71] and colorectal tumors [72]. In the former study, inhibition of this integrin in pancreatic stellate cells attenuates tumorigenicity and potentiates efficacy of chemotherapy; in the latter, integrin depletion reduced the ability of CAF to promote cancer cell migration presumably by the down regulation of fibronectin.

All the non-exhaustive recent findings described in the first part of this review suggest that we need to better understand the roles of RGD-integrins in tumors. Encouraging preclinical discoveries with integrin inhibitors did not translate to clinical successes due to the complexity

of integrin biology. We will have to consider not only integrins in tumoral cells and vessels but also in the tumor microenvironment including the immune system (Figure 1). For this point, preclinical modeling of the clinical reality remains a challenge. The overexpression of some integrins in treatment-resistant cells or at metastasic sites must be thoroughly characterized. We will have to refine the positive or negative crosstalk between different integrins and their relationships in specific tumor area or in specific subset of patients. We need to compare different integrin subtypes more systematically to address their respective contribution to tumorigenicity and optimize the use of specific inhibitors. The availability of specific and selective integrin ligands is of great importance to go further on.

3 RGD-integrin ligands

Three main classes of integrin ligands have been proposed: antibodies, RGD-derived peptides and RGD-mimetic small molecules (Figures 2 and 3). More recently, aptamers (short nucleic acid sequences) have been included in this list [73,74]. While antibodies may be highly integrin subtype-specific by nature, RGD-derived ligands may recognize all RGD-binding integrins. Efforts towards achieving high selectivity of RGD-integrin ligands were actively made during the last two decades with, for example, the pioneer works of H. Kessler's group. Although recognizing the same tripeptide sequence in their natural ligands, similarities and differences between RGD-integrins have been highlighted based on their crystal structures. The structures of the extracellular fragment of integrins αvβ3, αIIbβ3 and α5β1 were respectively resolved in 2001 [75,76], 2004 [77] and 2012 [78] helping to understand how ligands fit in the integrin binding sites.

3.1. Specificity, selectivity, and activity of integrin ligands.

Until today, integrin ligands were mainly tested for their capacity to bind integrins and to disrupt their interactions with their preferred natural ligands, using as a readout the role of integrin as adhesion proteins. For the evaluation of large libraries of compounds, tests must be rapid and reliable for lead characterization and optimization. They are based either on cell adhesion assays or on purified soluble integrins adhesion assays on specific ECM substrates. Results (expressed as IC50 values) obtained by both approaches are strongly variable depending on several parameters. Rational design of such tests appears crucial to compare ligands for one integrin or one ligand for different integrins. Recent works give insights in this topic [79,80]. Concerning activity, the notion of integrin antagonism versus agonism is fairly taken into account in the first steps of ligand selection. This point becomes critical in the field of oncology where disruption of cell adherence does not automatically relate to cell death. Moreover, RGD-like compounds may behave as true agonists mimicking the ECM natural ligand-dependent activation of integrins and subsequent pro-tumoral signaling pathways [41]. Very interestingly, recent developments on integrin pure antagonists have been published supporting a new area in integrin ligand research [81–84]. Based on electron microscopy, X-ray chrystallography and receptor priming studies, it was shown that these new classes of integrin antagonists do not induce the integrin conformational changes associated with activation.

3.2 Antibodies

Specific antibodies against RGD-integrins contributed to study integrin activation-state regulation, integrin biology and integrin-based therapeutics. In contrast with peptides or peptide-mimetics acting essentially at the RGD binding domain, they cover a large set of epitopes localized in different structural parts of the α or β integrin subunits [85]. They can be classified into three main groups: stimulatory or activation-specific, inhibitory and non-functional antibodies as largely described by the group of M. Humphries [86–88]. It must be emphasized here that integrin conformations are known to be variable in relation to their functional status which addressed mainly their capacity to adhere to ECM ligands. The bent, the extended closed and the extended open global conformations are likely to be shared by the majority of integrins. Using electron microscopy and biophysical thermodynamic analysis on α5β1 integrin and with the help of specific antibodies, it was shown that only the extended-open conformation mediates adhesion to fibronectin and that intrinsic affinity depends on specific integrin conformational states [89,90]. Antibodies against α5β1 and αvβ3 integrins are thus widely used in preclinical studies to depict fundamental cues, label or inhibit these integrins. Among inhibitory antibodies, some reached early phases clinical trials (volociximab for α5β1 integrin and Intratumumab/CNTO95 or abituzumab for αvβx integrin) [91,92]. But despite being well tolerated, they failed to progress to phase II/III trials.

3.3. RGD-derived peptides

Cilengitide, a cyclic pentapeptide, developed twenty years ago by Horst Kessler and his group, became the prototype of RGD-derived peptides with enhanced selectivity towards αvβ3 integrin. The story of cilengitide is extensively described in [93] explaining the different steps of development from a linear, flexible and non-selective RGD peptide to a cyclic, rigid and selective one. In the search for peptides with increased selectivity either towards αvβ3 or α5β1 integrins, multiple strategies have been explored using isoDGR motifs [94,95], cyclic aza-peptides [96] or di-N- methylation of cilengitide [97]. Cilengitide remains the reference compound in the field and integrin binding characteristics of new integrin ligands are often compared to it. Other groups worked around the cyclic pentapeptide structure. For example, cyclic RGD pseudopentapeptide incorporating bicyclic lactams were described [98] and further optimized leading to potent antagonists of αvβ3/β5 integrins [98–101]. Series of cyclo-octapeptides including RGD have also been described. Based on One-bead One-Compound combinatorial library technology, the lead compound LXW7 was discovered [102] and optimized as LXW64 and LXZ2 [103,104]. These compounds proved able to selectively label tumoral cells expressing αvβ3 in vitro and in vivo. Recently, a novel specific integrin αvβ3 targeting linear pentapeptide, RWrNK, was described [105]. Its development used a structure-based pharmacophore method integrated with molecular docking. Bifunctional diketopiperazines were introduced into cyclic peptidomimetics containing the RGD sequence (DKP-RGD) leading to compounds specific for αvβ3/β5 integrins [106]. Interestingly, these compounds exhibited binding affinities towards α5β1 integrin but always lower than for αvβ3 integrin [107]. Thus using several approaches, numerous peptidic ligands specific/ selective for αvβ3/β5 integrins have been made available unlike those for α5β1 integrin. The isoDGR peptide library [95] was screened to confer to the small lead pentapeptide selectivity towards the fibronectin- binding integrins α5β1 and αvβ6 [94]. Through sequential N-methylation, the biselective c(phg-*iso*DGR-k) was converted to c(phg-isoDGR-(NMe)k) which appeared as a selective α5β1 integrin ligand

[108]. It should be noted that other peptides highly selective for α5β1 integrin have also been proposed without an RGD sequence. The first example is the Cys-Arg-Arg-Glu-Thr-Ala-Trp-Ala-Cys (CRRETAWAC) peptide originally discovered in 1993 from the screening of a phage-display library in which heptapeptides were flanked by cysteine residues, thus making the inserts potentially cyclic [109]. Further investigations showed that residues of the α5 subunit involved in recognition of RRETAWA are predicted to lie close to those involved in RGD binding but do not completely overlap [110]. The second example is ATN161, a capped five amino-acid peptide derived from the synergy region PHSRN of fibronectin (which contributes to high affinity recognition of fibronectin by α5β1 integrin). It was shown to be very selective for α5β1 integrin over αvβ3/β5/β6/β8 integrins in an ELISA test using soluble purified integrins [79]. Compared to other integrin ligands, ATN-161 has the particularity of not competing with the fibronectin binding and thus is unable to detach the cells from the matrix. It was included in two clinical trials (for advanced renal cancer and recurrent glioblastoma) but no results were posted to date.

Panels of selective RGD-derived peptides are available. Few of them have been studied as true antagonists of integrin signaling pathways and pro-tumoral effects. However, knowledge on the mode of binding of RGD-containing peptidomimetics has largely increased with the advent of computer-assisted docking studies in the crystal structure of the integrin binding sites. This helped and will further improve the design of new ligands.

3.4. Small molecules as RGD-mimetics.

In parallel with the design of RGD-derived peptides, search for RGD-mimetics, led to the discovery of selective more stable and bioavailable small molecules as integrin ligands. The first goal of research was to obtain selectivity for αvβ3 versus αIIbβ3 integrins. This latter RGD-integrin is involved in platelets regulation and undesirable antagonist side effects had to be avoided. The second goal was to evaluate the possibility of distinguishing the αvβ3 integrin from the α5β1 in order to have highly selective ligands even though their RGD binding site are highly homologous. Both goals were achieved by pharmaceutical and academic groups. A review recapitulated the αvβ3 antagonists available in 2000 [111]. The field has progressed and began to focus also on α5β1 integrin. The initial series of αvβ3 integrin ligands were generally also recognized by α5β1 integrin. A series of nonpeptide integrin ligands containing spirocyclic scaffolds was described including SJ749 and SJ755, the first highly selective molecules for α5β1 integrin [112,113]. Their biological effects have been characterized : they behave as potential enhancers of antibiotic efficacy by interfering with α5β1 integrin/fibronectin/M1 protein-dependent bacterial entry in epithelial cells [114], as blockers of angiogenesis [115] and as inhibitors of proliferation and migration of glioma cells [116,117]. Docking of SJ749 into a built 3D model of the binding domain of α5β1 integrin has permitted the identification of two potentially important and unique regions of this integrin compared to others [118]. This model was largely used for the rational design of highly active and selective ligands for α5β1 and αvβ3 integrins achieving a selectivity ratio as high as 10000 [119–121]. The differentiation between the α5β1 and αvβ3 integrin-dependent glioma migration modes was possible using such ligands and revealed that αvβ3 integrin antagonists increased single cell migration whereas α5β1 integrin antagonists decreased it [122]. Additionally, we showed that, unlike

αvβ3 integrin antagonists, those selective for α5β1 integrin pushed glioma cells towards apoptosis when combined with chemotherapy or p53 activators [123–125]. Starting from a virtual combinatorial library designed to cover the chemical space specific for RGD-like compounds, Stragies et al synthesized dual α5β1/αvβ3 specific inhibitors [126]. Optimization of one lead gave JSM6427 which exhibits 10000 times more affinity for α5β1 versus αvβ3 and showed inhibitory activity in several models of pathological angiogenesis [127–129]. It was further developed for the treatment of macular degeneration but did not overpass the phase 1 clinical trial.

More recently, new β-lactam derivatives were designed to target integrins. Interestingly, the concept of integrin agonists has gradually emerged since compounds with azetidinone as the only cyclic framework increased integrin-dependent cell adhesion rather than decreasing it [130]. Substituent variations around the β-lactam core led to the discovery of selective compounds for different integrins including α5β1 and αvβ3/β5. Similar selectivity ranges were obtained for these integrins by competitive solid-phase binding assays using purified integrins and cell-adhesion based assays [131,132]. Increase in cell adhesion by integrin "agonists" was corroborated by an increase in integrin-dependent ERK signaling pathway. First characterized as racemic compounds, it was demonstrated that only (S)-enantiomers maintain the agonist activity thus revealing an important stereochemical requirement for integrin recognition and activation [133]. Whether integrin agonists could play a role as therapeutic drugs in oncology remains to be demonstrated [134].

Taking together all the data concerning these RGD-mimetic ligands, structural determinants discriminating different RGD-binding integrins have been characterized based on compound structure-activity relationships and computer-assisted docking on crystallographic integrin models. As is the case for the RGD-derived peptides, few of these original ligands are currently under investigations to check their potential anti-tumoral effects. The main knowledge concerns their ability to inhibit/increase integrin-dependent cell adhesion. Analysis of their roles on integrin signaling pathways has become an urgent need to more clearly decipher the biological cues of specific RGD-integrins in tumoral or surrounding stromal cells.

4 Current applications of RGD-ligands

Huge efforts to get more and more selective RGD-ligands led to interesting libraries of compounds. Due to the failure of the lead cilengitide to improve patient survival in clinical trials, none of them appears to be developed as anti-cancer therapeutics. Currently they are being exploited as useful tools either as tumor diagnostic or tumor targeting markers. They also serve for functionalization of biomaterials helping to solve several selective integrin-dependent cell phenotypes.

4.1. RGD-ligands for tumor diagnostic

As stated above, the input of RGD-integrins in hallmarks of cancer is largely acknowledged. Their heterogeneous expression in patient tumors closed the way to use their antagonists as therapeutics in unselected cohort of patients. Characterization of the integrin expression panel by a noninvasive way may be of importance to delineate patient subpopulations and adapt therapies. From early 2000 to 2015, huge efforts to characterize Positron Emission

Tomography (PET) markers for αvβ3 integrin were made. Radiolabeled cyclic RGD peptides (with ^{18}F, $^{64}Cu/^{68}Ga$ tracers) were thoroughly designed and characterized (for review see [135] and [136]). Several were investigated in the clinic [137–139]. By contrast very few radiotracers specific for α5β1 integrin are available (Table 1) as this integrin moved in the forefront of cancer research more recently, in particular for its unambiguous role in neoangiogenesis. The first α5β1-selective integrin antagonist useful as a PET tracer was described in 2013 by the group of H. Kessler [140]. A selective α5β1 integrin peptidomimetic (described in [119,141]) was functionalized with the NODAGA chelator, labelled with ^{68}Ga and named FR366 [142]. FR366 has a high affinity for α5β1 integrin, a specific integrin uptake in vivo and a good tumor-to-background contrast. A further step was achieved by trimerization of an azide-functionalized pseudopeptide [143] using a 1-pot click chemistry procedure with a TRAP chelator scaffold [144]. The compound ^{68}Ga-Aquibeprin obtained by this way has affinity and selectivity for α5β1 integrins and gave high contrast PET imaging in vivo [145,146]. A similar approach was used with c(phg-isoDGR-(NMe)k peptide (see above) which was conjugated to pentynoic acid on the lysine side chain and then trimerized by the TRAP chelator. In a proof of concept experiment this compound labeled with ^{68}Ga behaved as a potential PET agent for noninvasive imaging of α5β1 expressing tumors [108]. Other PET peptidic radiotracers for α5β1 integrin were proposed (based on CRETTAVAC or KSSPHSRN(SG)5RGDSP linear peptides) but they lack an efficient accumulation in α5β1 integrin-positive tumors in vivo [147,148].

4.2. RGD-ligands for tumor targeting

Integrins appear as valuable entry door for anti-cancer drugs in a tumor selective way. Based on the overexpression of αvβ3 and α5β1 integrins in tumor vasculature and cells and their ability to get internalized through endosomes [149], strategies have been developed to achieve specific transport for therapeutics. RGD-ligands coupled to cytotoxic drugs can serve as direct carriers and are intensively investigated. The drug is coupled to the RGD peptide by a linker which may be cleaved inside the cell to allow the therapeutic effect (for review see [150,151]. Examples of RGD-ligands and cytotoxic drug complexes can be found in two recent reviews ([152,153]. Recent advances in the field included dual-functional complexes that incorporate one fluorophore on one side for imaging and a cytotoxic pro-drug on the other side [154]. But currently intense efforts are mainly directed towards nanocarriers functionalized with RGD-ligands. We will not develop here this topic as recent reviews are available to which readers can refer [155–161].

Although huge literature exists concerning the applications available with RGD-ligands for targeting tumors, they appear, to our knowledge, non-dedicated to address specifically the selectivity of RGD-integrins. The RGD-ligands mainly used in these studies have been designed to target αvβ3 integrins. From a biologist point of view, further improvements will be achieved when tailored systems will be proposed to target specifically either αvβ3 or α5β1 integrin expressing tumors.

5 Summary and outlook

In this review we focused on two RGD-integrins which are important players in oncology, the αvβ3 and α5β1 integrins. It is important to note that other RGD-integrins become under

spotlight as for example the αvβ6 integrin [162]. Selective Inhibitors and PET tracers have been designed [163–167] which will be useful to detect and treat epithelial carcinoma for example. Integrins remain therapeutic targets in oncology (as assessed by 2 recent reviews [168,169]) but we have to reconsider their roles in the area of personalized medicine.

Our goal in this review was to give the biologist point of view regarding the chemical approaches to design selective compounds differentiating RGD-integrins in preclinical and clinical settings. According to the data (even the recent ones), the αvβ3 integrin still remains the gold standard tumoral target. Efforts are however made towards other integrins. This is an important point in order to have a better knowledge of the complex integrin world. To go further, we have to set up a virtuous circle by increasing the knowledge on one particular integrin using selective ligands and inversely to take into account this knowledge to design new ligands with improved efficacy. The biological tests are crucial as are the preclinical models. It is time to progress towards models that better reflect the clinical reality to test integrin antagonists. For example, replacing 2D by 3D sphere cultures and hence by organoids/tumoroids to test integrin antagonists is nowadays accessible steps. In addition, we have to develop high/medium throughput assays aiming to characterize the biological effects of RGD-ligands on not only integrin/cell adhesion but also on oncogenic signaling pathways. We have also to keep in mind that integrin antagonists/agonists may inhibit/activate general mechanisms which are under the control of several players. It will be of great interest to evaluate more thoroughly the benefit of their association with other targeted therapies. Transdisciplinary networks involving biologists, clinicians and chemists will greatly help to go through preclinical investigations towards clinical benefits with integrin ligands.

Acknowledgements

We are thankful for financial support from Institut National du Cancer (grant INCA_11527), Ligue contre le Cancer (CCIR Est), Association pour la Recherche contre le Cancer, CNRS (grant 80 PRIME), the University of Strasbourg (France), the Alex Akwueme Federal University Ndufu-Alike Ikwo (Nigeria), the Association Lyons Club de Niederbronn Les Bains.

Conflict of interest

The authors have no conflict of interest to declare.

Keywords : RGD-integrins, ligand design, inhibitors, peptides, cancer

References

[1] D. Hanahan, R. A. Weinberg, *Cell* **2000**, *100*, 57–70.
[2] D. Hanahan, R. A. Weinberg, *Cell* **2011**, *144*, 646–674.
[3] J. A. Eble, D. Gullberg, *Cancers* **2019**, *11*, DOI 10.3390/cancers11091296.
[4] J. S. Desgrosellier, D. A. Cheresh, *Nat. Rev. Cancer* **2010**, *10*, 9–22.
[5] D. Bianconi, M. Unseld, G. W. Prager, *Int. J. Mol. Sci.* **2016**, *17*, DOI 10.3390/ijms17122037.
[6] S. Raab-Westphal, J. F. Marshall, S. L. Goodman, *Cancers* **2017**, *9*, 110.

[7] M. Nieberler, U. Reuning, F. Reichart, J. Notni, H.-J. Wester, M. Schwaiger, M. Weinmüller, A. Räder, K. Steiger, H. Kessler, *Cancers* **2017**, *9*, 116.
[8] S. M. Frisch, K. Vuori, E. Ruoslahti, P. Y. Chan-Hui, *J. Cell Biol.* **1996**, *134*, 793–799.
[9] D. G. Stupack, X. S. Puente, S. Boutsaboualoy, C. M. Storgard, D. A. Cheresh, *J. Cell Biol.* **2001**, *155*, 459–470.
[10] A. Meyer, J. Auernheimer, A. Modlinger, H. Kessler, *Curr. Pharm. Des.* **2006**, *12*, 2723–2747.
[11] C. Mas-Moruno, F. Rechenmacher, H. Kessler, *Anticancer Agents Med. Chem.* **2010**, *10*, 753–768.
[12] R. Stupp, M. E. Hegi, T. Gorlia, S. C. Erridge, J. Perry, Y.-K. Hong, K. D. Aldape, B. Lhermitte, T. Pietsch, D. Grujicic, J. P. Steinbach, W. Wick, R. Tarnawski, D.-H. Nam, P. Hau, A. Weyerbrock, M. J. B. Taphoorn, C.-C. Shen, N. Rao, L. Thurzo, U. Herrlinger, T. Gupta, R.-D. Kortmann, K. Adamska, C. McBain, A. A. Brandes, J. C. Tonn, O. Schnell, T. Wiegel, C.-Y. Kim, L. B. Nabors, D. A. Reardon, M. J. van den Bent, C. Hicking, A. Markivskyy, M. Picard, M. Weller, *Lancet Oncol.* **2014**, *15*, 1100–1108.
[13] L. B. Nabors, K. L. Fink, T. Mikkelsen, D. Grujicic, R. Tarnawski, D. H. Nam, M. Mazurkiewicz, M. Salacz, L. Ashby, V. Zagonel, R. Depenni, J. R. Perry, C. Hicking, M. Picard, M. E. Hegi, B. Lhermitte, D. A. Reardon, *Neuro-Oncol.* **2015**, *17*, 708–717.
[14] C. D. Weekes, L. S. Rosen, A. Capasso, K. M. Wong, W. Ye, M. Anderson, B. McCall, J. Fredrickson, E. Wakshull, S. Eppler, Q. Shon-Nguyen, R. Desai, M. Huseni, P. S. Hegde, T. Pourmohamad, I. Rhee, A. Bessudo, *Cancer Chemother. Pharmacol.* **2018**, *82*, 339–351.
[15] K. M. Bell-McGuinn, C. M. Matthews, S. N. Ho, M. Barve, L. Gilbert, R. T. Penson, E. Lengyel, R. Palaparthy, K. Gilder, A. Vassos, W. McAuliffe, S. Weymer, J. Barton, R. J. Schilder, *Gynecol. Oncol.* **2011**, *121*, 273–279.
[16] D. Bianconi, M. Unseld, G. W. Prager, *Int. J. Mol. Sci.* **2016**, *17*, 2037.
[17] A. Ellert-Miklaszewska, K. Poleszak, M. Pasierbinska, B. Kaminska, *Int. J. Mol. Sci.* **2020**, *21*, 888.
[18] M. Janiszewska, M. C. Primi, T. Izard, *J. Biol. Chem.* **2020**, *295*, 2495–2505.
[19] H. Hamidi, J. Ivaska, *Nat. Rev. Cancer* **2018**, *18*, 533–548.
[20] A.-F. Blandin, G. Renner, M. Lehmann, I. Lelong-Rebel, S. Martin, M. Dontenwill, *Front. Pharmacol.* **2015**, *6*, 279.
[21] Y. A. Kadry, D. A. Calderwood, *Biochim. Biophys. Acta BBA - Biomembr.* **2020**, *1862*, 183206.
[22] R. O. Hynes, *Cell* **2002**, *110*, 673–687.
[23] E. R. Horton, A. Byron, J. A. Askari, D. H. J. Ng, A. Millon-Frémillon, J. Robertson, E. J. Koper, N. R. Paul, S. Warwood, D. Knight, J. D. Humphries, M. J. Humphries, *Nat. Cell Biol.* **2015**, *17*, 1577–1587.
[24] L. MacKay, A. Khadra, *Comput. Struct. Biotechnol. J.* **2020**, *18*, 393–416.
[25] R. De Mets, I. Wang, M. Balland, C. Oddou, P. Moreau, B. Fourcade, C. Albiges-Rizo, A. Delon, O. Destaing, *Mol. Biol. Cell* **2018**, *30*, 181–190.
[26] O. Rossier, V. Octeau, J.-B. Sibarita, C. Leduc, B. Tessier, D. Nair, V. Gatterdam, O. Destaing, C. Albigès-Rizo, R. Tampé, L. Cognet, D. Choquet, B. Lounis, G. Giannone, *Nat. Cell Biol.* **2012**, *14*, 1057–1067.
[27] N. Strohmeyer, M. Bharadwaj, M. Costell, R. Fässler, D. J. Müller, *Nat. Mater.* **2017**, *16*, 1262–1270.
[28] H. B. Schiller, M.-R. Hermann, J. Polleux, T. Vignaud, S. Zanivan, C. C. Friedel, Z. Sun, A. Raducanu, K.-E. Gottschalk, M. Théry, M. Mann, R. Fässler, *Nat. Cell Biol.* **2013**, *15*, 625–636.

[29] M. Bharadwaj, N. Strohmeyer, G. P. Colo, J. Helenius, N. Beerenwinkel, H. B. Schiller, R. Fässler, D. J. Müller, *Nat. Commun.* **2017**, *8*, 14348.
[30] G. Jacquemet, D. M. Green, R. E. Bridgewater, A. von Kriegsheim, M. J. Humphries, J. C. Norman, P. T. Caswell, *J. Cell Biol.* **2013**, *202*, 917–935.
[31] I. Samaržija, A. Dekanić, J. D. Humphries, M. Paradžik, N. Stojanović, M. J. Humphries, A. Ambriović-Ristov, *Cancers* **2020**, *12*, 1910.
[32] D. Missirlis, T. Haraszti, C. v. C. Scheele, T. Wiegand, C. Diaz, S. Neubauer, F. Rechenmacher, H. Kessler, J. P. Spatz, *Sci. Rep.* **2016**, *6*, 23258.
[33] C. Diaz, S. Neubauer, F. Rechenmacher, H. Kessler, D. Missirlis, *J. Cell Sci.* **2020**, *133*, DOI 10.1242/jcs.232702.
[34] V. Schaufler, H. Czichos-Medda, V. Hirschfeld-Warnecken, S. Neubauer, F. Rechenmacher, R. Medda, H. Kessler, B. Geiger, J. P. Spatz, E. A. Cavalcanti-Adam, *Cell Adhes. Migr.* **2016**, *10*, 505–515.
[35] G. Efthymiou, A. Saint, M. Ruff, Z. Rekad, D. Ciais, E. Van Obberghen-Schilling, *Front. Oncol.* **2020**, *10*, DOI 10.3389/fonc.2020.00641.
[36] P. C. Brooks, R. A. Clark, D. A. Cheresh, *Science* **1994**, *264*, 569–571.
[37] P. C. Brooks, A. M. Montgomery, M. Rosenfeld, R. A. Reisfeld, T. Hu, G. Klier, D. A. Cheresh, *Cell* **1994**, *79*, 1157–1164.
[38] S. Yamada, X.-Y. Bu, V. Khankaldyyan, I. Gonzales-Gomez, J. G. McComb, W. E. Laug, *Neurosurgery* **2006**, *59*, 1304–1312; discussion 1312.
[39] D. Taverna, H. Moher, D. Crowley, L. Borsig, A. Varki, R. O. Hynes, *Proc. Natl. Acad. Sci. U. S. A.* **2004**, *101*, 763–768.
[40] M. Kanamori, S. R. Vanden Berg, G. Bergers, M. S. Berger, R. O. Pieper, *Cancer Res.* **2004**, *64*, 2751–2758.
[41] A. R. Reynolds, I. R. Hart, A. R. Watson, J. C. Welti, R. G. Silva, S. D. Robinson, G. Da Violante, M. Gourlaouen, M. Salih, M. C. Jones, D. T. Jones, G. Saunders, V. Kostourou, F. Perron-Sierra, J. C. Norman, G. C. Tucker, K. M. Hodivala-Dilke, *Nat. Med.* **2009**, *15*, 392–400.
[42] C. J. Avraamides, B. Garmy-Susini, J. A. Varner, *Nat. Rev. Cancer* **2008**, *8*, 604–617.
[43] L. Li, J. Welser-Alves, A. van der Flier, A. Boroujerdi, R. O. Hynes, R. Milner, *Exp. Neurol.* **2012**, *237*, 46–54.
[44] D. Pang, L. Wang, J. Dong, X. Lai, Q. Huang, R. Milner, L. Li, *Exp. Mol. Med.* **2018**, *50*, 117.
[45] S. E. Francis, K. L. Goh, K. Hodivala-Dilke, B. L. Bader, M. Stark, D. Davidson, R. O. Hynes, *Arterioscler. Thromb. Vasc. Biol.* **2002**, *22*, 927–933.
[46] D. Taverna, R. O. Hynes, *Cancer Res.* **2001**, *61*, 5255–5261.
[47] P. Parsons-Wingerter, I. M. Kasman, S. Norberg, A. Magnussen, S. Zanivan, A. Rissone, P. Baluk, C. J. Favre, U. Jeffry, R. Murray, D. M. McDonald, *Am. J. Pathol.* **2005**, *167*, 193–211.
[48] F. Demircioglu, K. Hodivala-Dilke, *Curr. Opin. Cell Biol.* **2016**, *42*, 121–127.
[49] E. Cruz da Silva, M. Dontenwill, L. Choulier, M. Lehmann, *Cancers* **2019**, *11*, DOI 10.3390/cancers11050692.
[50] S. Martin, H. Janouskova, M. Dontenwill, *Front. Oncol.* **2012**, *2*, 157.
[51] F. Schaffner, A. M. Ray, M. Dontenwill, *Cancers* **2013**, *5*, 27–47.
[52] L. Seguin, J. S. Desgrosellier, S. M. Weis, D. A. Cheresh, *Trends Cell Biol.* **2015**, *25*, 234–240.
[53] R. G. W. Verhaak, K. A. Hoadley, E. Purdom, V. Wang, Y. Qi, M. D. Wilkerson, C. R. Miller, L. Ding, T. Golub, J. P. Mesirov, G. Alexe, M. Lawrence, M. O'Kelly, P. Tamayo, B. A. Weir, S. Gabriel, W. Winckler, S. Gupta, L. Jakkula, H. S. Feiler, J. G. Hodgson, C. D. James, J. N. Sarkaria, C. Brennan, A. Kahn, P. T. Spellman, R. K.

Wilson, T. P. Speed, J. W. Gray, M. Meyerson, G. Getz, C. M. Perou, D. N. Hayes, Cancer Genome Atlas Research Network, *Cancer Cell* **2010**, *17*, 98–110.
[54] Y.-B. Pan, S. Wang, B. Yang, Z. Jiang, C. Lenahan, J. Wang, J. Zhang, A. Shao, *J. Cell. Mol. Med.* **2020**, *24*, 3901–3916.
[55] L. Malric, S. Monferran, J. Gilhodes, S. Boyrie, P. Dahan, N. Skuli, J. Sesen, T. Filleron, A. Kowalski-Chauvel, E. Cohen-Jonathan Moyal, C. Toulas, A. Lemarié, *Oncotarget* **2017**, *8*, 86947–86968.
[56] M. Vinci, A. Burford, V. Molinari, K. Kessler, S. Popov, M. Clarke, K. R. Taylor, H. N. Pemberton, C. J. Lord, A. Gutteridge, T. Forshew, D. Carvalho, L. V. Marshall, E. Y. Qin, W. J. Ingram, A. S. Moore, H.-K. Ng, S. Trabelsi, D. H'mida-Ben Brahim, N. Entz-Werle, S. Zacharoulis, S. Vaidya, H. C. Mandeville, L. R. Bridges, A. J. Martin, S. Al-Sarraj, C. Chandler, M. Sunol, J. Mora, C. de Torres, O. Cruz, A. M. Carcaboso, M. Monje, A. Mackay, C. Jones, *Nat. Med.* **2018**, *24*, 1204–1215.
[57] K. Shi, S.-L. Wang, B. Shen, F.-Q. Yu, D.-F. Weng, J.-H. Lin, *World J. Surg. Oncol.* **2019**, *17*, 23.
[58] F. Sun, J. Wang, Q. Sun, F. Li, H. Gao, L. Xu, J. Zhang, X. Sun, Y. Tian, Q. Zhao, H. Shen, K. Zhang, J. Liu, *J. Exp. Clin. Cancer Res.* **2019**, *38*, 449.
[59] S. Johansen, A. K. Brenner, S. Bartaula-Brevik, H. Reikvam, Ø. Bruserud, *Int. J. Mol. Sci.* **2018**, *19*, DOI 10.3390/ijms19010251.
[60] M. Weller, L. B. Nabors, T. Gorlia, H. Leske, E. Rushing, P. Bady, C. Hicking, J. Perry, Y.-K. Hong, P. Roth, W. Wick, S. L. Goodman, M. E. Hegi, M. Picard, H. Moch, J. Straub, R. Stupp, *Oncotarget* **2016**, *7*, 15018–15032.
[61] Y. Deng, Q. Wan, W. Yan, " Integrin α5/ITGA5 Promotes The Proliferation, Migration, Invasion And Progression Of Oral Squamous Carcinoma By Epithelial–Mesenchymal Transition ," can be found under https://www.dovepress.com/integrin-alpha5itga5-promotes-the-proliferation-migration-invasion-and-peer-reviewed-article-CMAR, **2019**.
[62] F. Ou-Yang, M.-R. Pan, S.-J. Chang, C.-C. Wu, S.-Y. Fang, C.-L. Li, M.-F. Hou, C.-W. Luo, *Life Sci.* **2019**, *238*, 116963.
[63] K. Taniuchi, M. Furihata, S. Naganuma, M. Sakaguchi, T. Saibara, *PLOS ONE* **2019**, *14*, e0217920.
[64] R. Li, Y. Shi, S. Zhao, T. Shi, G. Zhang, *Int. J. Biol. Macromol.* **2019**, *123*, 1035–1043.
[65] Z. Niu, P. Xu, D. Zhu, W. Tang, M. Ji, Q. Lin, T. Liu, L. Ren, Y. Wei, J. Xu, *Int. J. Clin. Exp. Pathol.* **2018**, *11*, 4771–4783.
[66] C. Zeltz, I. Primac, P. Erusappan, J. Alam, A. Noel, D. Gullberg, *Semin. Cancer Biol.* **2020**, *62*, 166–181.
[67] V. Steri, T. S. Ellison, A. M. Gontarczyk, K. Weilbaecher, J. G. Schneider, D. Edwards, M. Fruttiger, K. M. Hodivala-Dilke, S. D. Robinson, *Circ. Res.* **2014**, *114*, 79–91.
[68] E. A. Morgan, J. G. Schneider, T. E. Baroni, O. Uluçkan, E. Heller, M. A. Hurchla, H. Deng, D. Floyd, A. Berdy, J. L. Prior, D. Piwnica-Worms, S. L. Teitelbaum, F. Patrick Ross, K. N. Weilbaecher, *FASEB J.* **2010**, *24*, 1117–1127.
[69] X. Su, A. K. Esser, S. R. Amend, J. Xiang, Y. Xu, M. H. Ross, G. C. Fox, T. Kobayashi, V. Steri, K. Roomp, F. Fontana, M. A. Hurchla, B. L. Knolhoff, M. A. Meyer, E. A. Morgan, J. C. Tomasson, J. S. Novack, W. Zou, R. Faccio, D. V. Novack, S. D. Robinson, S. L. Teitelbaum, D. G. DeNardo, J. G. Schneider, K. N. Weilbaecher, *Cancer Res.* **2016**, *76*, 3484–3495.
[70] H. I. Wettersten, S. M. Weis, P. Pathria, T. Von Schalscha, T. Minami, J. A. Varner, D. A. Cheresh, *Cancer Res.* **2019**, *79*, 5048–5059.

[71] P. R. Kuninty, R. Bansal, S. W. L. De Geus, D. F. Mardhian, J. Schnittert, J. van Baarlen, G. Storm, M. F. Bijlsma, H. W. van Laarhoven, J. M. Metselaar, P. J. K. Kuppen, A. L. Vahrmeijer, A. Östman, C. F. M. Sier, J. Prakash, *Sci. Adv.* **2019**, *5*, eaax2770.
[72] L. Lu, R. Xie, R. Wei, C. Cai, D. Bi, D. Yin, H. Liu, J. Zheng, Y. Zhang, F. Song, Y. Gao, L. Tan, Q. Wei, H. Qin, *Mol. Oncol.* **2019**, *13*, 2697–2714.
[73] P. Fechter, E. Cruz Da Silva, M.-C. Mercier, F. Noulet, N. Etienne-Seloum, D. Guenot, M. Lehmann, R. Vauchelles, S. Martin, I. Lelong-Rebel, A.-M. Ray, C. Seguin, M. Dontenwill, L. Choulier, *Mol. Ther. - Nucleic Acids* **2019**, *17*, 63–77.
[74] Marie-Cécile Mercier, Monique Dontenwill, Laurence Choulier, *Cancers* **2017**, *9*, 69.
[75] J.-P. Xiong, *Science* **2001**, *294*, 339–345.
[76] J.-P. Xiong, *Science* **2002**, *296*, 151–155.
[77] T. Xiao, J. Takagi, B. S. Coller, J.-H. Wang, T. A. Springer, *Nature* **2004**, *432*, 59–67.
[78] M. Nagae, S. Re, E. Mihara, T. Nogi, Y. Sugita, J. Takagi, *J. Cell Biol.* **2012**, *197*, 131–140.
[79] T. G. Kapp, F. Rechenmacher, S. Neubauer, O. V. Maltsev, E. A. Cavalcanti-Adam, R. Zarka, U. Reuning, J. Notni, H.-J. Wester, C. Mas-Moruno, J. Spatz, B. Geiger, H. Kessler, *Sci. Rep.* **2017**, *7*, 39805.
[80] R. J. D. Hatley, S. J. F. Macdonald, R. J. Slack, J. Le, S. B. Ludbrook, P. T. Lukey, *Angew. Chem. Int. Ed.* **2018**, *57*, 3298–3321.
[81] J. F. Van Agthoven, J.-P. Xiong, J. L. Alonso, X. Rui, B. D. Adair, S. L. Goodman, M. A. Arnaout, *Nat. Struct. Mol. Biol.* **2014**, *21*, 383–388.
[82] J. Li, Y. Fukase, Y. Shang, W. Zou, J. M. Muñoz-Félix, L. Buitrago, J. van Agthoven, Y. Zhang, R. Hara, Y. Tanaka, R. Okamoto, T. Yasui, T. Nakahata, T. Imaeda, K. Aso, Y. Zhou, C. Locuson, D. Nesic, M. Duggan, J. Takagi, R. D. Vaughan, T. Walz, K. Hodivala-Dilke, S. L. Teitelbaum, M. A. Arnaout, M. Filizola, M. A. Foley, B. S. Coller, *ACS Pharmacol. Transl. Sci.* **2019**, *2*, 387–401.
[83] R. C. Turaga, L. Yin, J. J. Yang, H. Lee, I. Ivanov, C. Yan, H. Yang, H. E. Grossniklaus, S. Wang, C. Ma, L. Sun, Z.-R. Liu, *Nat. Commun.* **2016**, *7*, 11675.
[84] B. D. Adair, J. L. Alonso, J. van Agthoven, V. Hayes, H. S. Ahn, I.-S. Yu, S.-W. Lin, J.-P. Xiong, M. Poncz, M. A. Arnaout, *Nat. Commun.* **2020**, *11*, 398.
[85] A. Byron, J. D. Humphries, J. A. Askari, S. E. Craig, A. P. Mould, M. J. Humphries, *J. Cell Sci.* **2009**, *122*, 4009–4011.
[86] A. P. Mould, M. J. Humphries, *Curr. Opin. Cell Biol.* **2004**, *16*, 544–551.
[87] A. P. Mould, J. A. Askari, A. Byron, Y. Takada, T. A. Jowitt, M. J. Humphries, *J. Biol. Chem.* **2016**, *291*, 20993–21007.
[88] A. P. Mould, S. E. Craig, S. K. Byron, M. J. Humphries, T. A. Jowitt, *Biochem. J.* **2014**, *464*, 301–313.
[89] J. Li, Y. Su, W. Xia, Y. Qin, M. J. Humphries, D. Vestweber, C. Cabañas, C. Lu, T. A. Springer, *EMBO J.* **2017**, *36*, 629–645.
[90] Y. Su, W. Xia, J. Li, T. Walz, M. J. Humphries, D. Vestweber, C. Cabañas, C. Lu, T. A. Springer, *Proc. Natl. Acad. Sci.* **2016**, *113*, E3872–E3881.
[91] S. Almokadem, C. P. Belani, *Expert Opin. Biol. Ther.* **2012**, *12*, 251–257.
[92] M. Hussain, S. Le Moulec, C. Gimmi, R. Bruns, J. Straub, K. Miller, on behalf of the PERSEUS Study Group, *Clin. Cancer Res.* **2016**, *22*, 3192–3200.
[93] M. A. Dechantsreiter, E. Planker, B. Mathä, E. Lohof, G. Hölzemann, A. Jonczyk, S. L. Goodman, H. Kessler, *J. Med. Chem.* **1999**, *42*, 3033–3040.
[94] A. Bochen, U. K. Marelli, E. Otto, D. Pallarola, C. Mas-Moruno, F. S. Di Leva, H. Boehm, J. P. Spatz, E. Novellino, H. Kessler, L. Marinelli, *J. Med. Chem.* **2013**, *56*, 1509–1519.

[95] A. O. Frank, E. Otto, C. Mas-Moruno, H. B. Schiller, L. Marinelli, S. Cosconati, A. Bochen, D. Vossmeyer, G. Zahn, R. Stragies, E. Novellino, H. Kessler, *Angew. Chem. Int. Ed.* **2010**, *49*, 9278–9281.
[96] J. Spiegel, C. Mas-Moruno, H. Kessler, W. D. Lubell, *J. Org. Chem.* **2012**, *77*, 5271–5278.
[97] C. Mas-Moruno, J. G. Beck, L. Doedens, A. O. Frank, L. Marinelli, S. Cosconati, E. Novellino, H. Kessler, *Angew. Chem. Int. Ed.* **2011**, *50*, 9496–9500.
[98] L. Belvisi, A. Bernardi, A. Checchia, L. Manzoni, D. Potenza, C. Scolastico, M. Castorina, A. Cupelli, G. Giannini, P. Carminati, C. Pisano, *Org. Lett.* **2001**, *3*, 1001–1004.
[99] D. Arosio, L. Belvisi, L. Colombo, M. Colombo, D. Invernizzi, L. Manzoni, D. Potenza, M. Serra, M. Castorina, C. Pisano, C. Scolastico, *ChemMedChem* **2008**, *3*, 1589–1603.
[100] L. Belvisi, A. Bernardi, M. Colombo, L. Manzoni, D. Potenza, C. Scolastico, G. Giannini, M. Marcellini, T. Riccioni, M. Castorina, P. LoGiudice, C. Pisano, *Bioorg. Med. Chem.* **2006**, *14*, 169–180.
[101] L. Belvisi, T. Riccioni, M. Marcellini, L. Vesci, I. Chiarucci, D. Efrati, D. Potenza, C. Scolastico, L. Manzoni, K. Lombardo, M. A. Stasi, A. Orlandi, A. Ciucci, B. Nico, D. Ribatti, G. Giannini, M. Presta, P. Carminati, C. Pisano, *Mol. Cancer Ther.* **2005**, *4*, 1670–1680.
[102] W. Xiao, Y. Wang, E. Y. Lau, J. Luo, N. Yao, C. Shi, L. Meza, H. Tseng, Y. Maeda, P. Kumaresan, R. Liu, F. C. Lightstone, Y. Takada, K. S. Lam, *Mol. Cancer Ther.* **2010**, *9*, 2714–2723.
[103] Y. Wang, W. Xiao, Y. Zhang, L. Meza, H. Tseng, Y. Takada, J. B. Ames, K. S. Lam, *Mol. Cancer Ther.* **2016**, *15*, 232–240.
[104] A. Silva, W. Xiao, Y. Wang, W. Wang, H. W. Chang, J. B. Ames, K. S. Lam, Y. Zhang, *Int. J. Mol. Sci.* **2020**, *21*, 3076.
[105] L. Zhang, X. Shan, X. Meng, T. Gu, L. Guo, X. An, Q. Jiang, H. Ge, X. Ning, *Mol. Pharm.* **2019**, *16*, 3977–3984.
[106] A. S. M. da Ressurreição, A. Vidu, M. Civera, L. Belvisi, D. Potenza, L. Manzoni, S. Ongeri, C. Gennari, U. Piarulli, *Chem. - Eur. J.* **2009**, *15*, 12184–12188.
[107] I. Guzzetti, M. Civera, F. Vasile, D. Arosio, C. Tringali, U. Piarulli, C. Gennari, L. Pignataro, L. Belvisi, D. Potenza, *ChemistryOpen* **2017**, *6*, 128–136.
[108] T. G. Kapp, F. S. Di Leva, J. Notni, A. F. B. Räder, M. Fottner, F. Reichart, D. Reich, A. Wurzer, K. Steiger, E. Novellino, U. K. Marelli, H.-J. Wester, L. Marinelli, H. Kessler, *J. Med. Chem.* **2018**, *61*, 2490–2499.
[109] E. Koivunen, B. Wang, E. Ruoslahti, *J. Cell Biol.* **1994**, *124*, 373–380.
[110] A. P. Mould, L. Burrows, M. J. Humphries, *J. Biol. Chem.* **1998**, *273*, 25664–25672.
[111] W. H. Miller, R. M. Keenan, R. N. Willette, M. W. Lark, *Drug Discov. Today* **2000**, *5*, 397–408.
[112] W. J. Pitts, J. Wityak, J. M. Smallheer, A. E. Tobin, J. W. Jetter, J. S. Buynitsky, P. P. Harlow, K. A. Solomon, M. H. Corjay, S. A. Mousa, R. R. Wexler, P. K. Jadhav, *J. Med. Chem.* **2000**, *43*, 27–40.
[113] J. M. Smallheer, C. A. Weigelt, F. J. Woerner, J. S. Wells, W. F. Daneker, S. A. Mousa, R. R. Wexler, P. K. Jadhav, *Bioorg. Med. Chem. Lett.* **2004**, *14*, 383–387.
[114] D. Cue, S. O. Southern, P. J. Southern, J. Prabhakar, W. Lorelli, J. M. Smallheer, S. A. Mousa, P. P. Cleary, *Proc. Natl. Acad. Sci.* **2000**, *97*, 2858–2863.
[115] S. Kim, K. Bell, S. A. Mousa, J. A. Varner, *Am. J. Pathol.* **2000**, *156*, 1345–1362.
[116] A. Maglott, P. Bartik, S. Cosgun, P. Klotz, P. Rondé, G. Fuhrmann, K. Takeda, S. Martin, M. Dontenwill, *Cancer Res.* **2006**, *66*, 6002–6007.

[117] S. Martin, E. C. Cosset, J. Terrand, A. Maglott, K. Takeda, M. Dontenwill, *Biochim. Biophys. Acta BBA - Mol. Cell Res.* **2009**, *1793*, 354–367.
[118] L. Marinelli, A. Meyer, D. Heckmann, A. Lavecchia, E. Novellino, H. Kessler, *J. Med. Chem.* **2005**, *48*, 4204–4207.
[119] D. Heckmann, A. Meyer, L. Marinelli, G. Zahn, R. Stragies, H. Kessler, *Angew. Chem. Int. Ed.* **2007**, *46*, 3571–3574.
[120] N. C. Henderson, T. D. Arnold, Y. Katamura, M. M. Giacomini, J. D. Rodriguez, J. H. McCarty, A. Pellicoro, E. Raschperger, C. Betsholtz, P. G. Ruminski, D. W. Griggs, M. J. Prinsen, J. J. Maher, J. P. Iredale, A. Lacy-Hulbert, R. H. Adams, D. Sheppard, *Nat. Med.* **2013**, *19*, 1617–1624.
[121] S. Neubauer, F. Rechenmacher, R. Brimioulle, F. S. Di Leva, A. Bochen, T. R. Sobahi, M. Schottelius, E. Novellino, C. Mas-Moruno, L. Marinelli, H. Kessler, *J. Med. Chem.* **2014**, *57*, 3410–3417.
[122] A.-M. Ray, F. Schaffner, H. Janouskova, F. Noulet, D. Rognan, I. Lelong-Rebel, L. Choulier, A.-F. Blandin, M. Lehmann, S. Martin, T. Kapp, S. Neubauer, F. Rechenmacher, H. Kessler, M. Dontenwill, *Biochim. Biophys. Acta BBA - Gen. Subj.* **2014**, *1840*, 2978–2987.
[123] H. Janouskova, A.-M. Ray, F. Noulet, I. Lelong-Rebel, L. Choulier, F. Schaffner, M. Lehmann, S. Martin, J. Teisinger, M. Dontenwill, *Cancer Lett.* **2013**, *336*, 307–318.
[124] G. Renner, H. Janouskova, F. Noulet, V. Koenig, E. Guerin, S. Bär, J. Nuesch, F. Rechenmacher, S. Neubauer, H. Kessler, A.-F. Blandin, L. Choulier, N. Etienne-Selloum, M. Lehmann, I. Lelong-Rebel, S. Martin, M. Dontenwill, *Cell Death Differ.* **2016**, *23*, 640–653.
[125] E. Martinkova, A. Maglott, D. Y. Leger, D. Bonnet, M. Stiborova, K. Takeda, S. Martin, M. Dontenwill, *Int. J. Cancer* **2010**, *127*, 1240–1248.
[126] R. Stragies, F. Osterkamp, G. Zischinsky, D. Vossmeyer, H. Kalkhof, U. Reimer, G. Zahn, *J. Med. Chem.* **2007**, *50*, 3786–3794.
[127] G. Zahn, K. Volk, G. P. Lewis, D. Vossmeyer, R. Stragies, J. S. Heier, P. E. Daniel, A. P. Adamis, E. A. Chapin, S. K. Fisher, F. G. Holz, K. U. Löffler, J. Knolle, *Investig. Opthalmology Vis. Sci.* **2010**, *51*, 1028.
[128] G. Zahn, *Arch. Ophthalmol.* **2009**, *127*, 1329.
[129] A.-K. B. Maier, N. Kociok, G. Zahn, D. Vossmeyer, R. Stragies, P. S. Muether, A. M. Joussen, *Curr. Eye Res.* **2007**, *32*, 801–812.
[130] P. Galletti, R. Soldati, M. Pori, M. Durso, A. Tolomelli, L. Gentilucci, S. D. Dattoli, M. Baiula, S. Spampinato, D. Giacomini, *Eur. J. Med. Chem.* **2014**, *83*, 284–293.
[131] M. Baiula, P. Galletti, G. Martelli, R. Soldati, L. Belvisi, M. Civera, S. D. Dattoli, S. M. Spampinato, D. Giacomini, *J. Med. Chem.* **2016**, *59*, 9721–9742.
[132] G. Martelli, M. Baiula, A. Caligiana, P. Galletti, L. Gentilucci, R. Artali, S. Spampinato, D. Giacomini, *J. Med. Chem.* **2019**, *62*, 10156–10166.
[133] G. Martelli, P. Galletti, M. Baiula, L. Calcinari, G. Boschi, D. Giacomini, *Bioorganic Chem.* **2019**, *88*, 102975.
[134] A. Tolomelli, P. Galletti, M. Baiula, D. Giacomini, *Cancers* **2017**, *9*, 78.
[135] H. Cai, P. S. Conti, *J. Label. Compd. Radiopharm.* **2013**, *56*, 264–279.
[136] J. Shi, F. Wang, S. Liu, *Biophys. Rep.* **2016**, *2*, 1–20.
[137] R. Haubner, W. A. Weber, A. J. Beer, E. Vabuliene, D. Reim, M. Sarbia, K.-F. Becker, M. Goebel, R. Hein, H.-J. Wester, H. Kessler, M. Schwaiger, *PLoS Med.* **2005**, *2*, e70.
[138] O. Schnell, B. Krebs, J. Carlsen, I. Miederer, C. Goetz, R. H. Goldbrunner, H.-J. Wester, R. Haubner, G. Pöpperl, M. Holtmannspötter, H. A. Kretzschmar, H. Kessler, J.-C. Tonn, M. Schwaiger, A. J. Beer, *Neuro-Oncol.* **2009**, *11*, 861–870.

[139] N. Withofs, N. Signolle, J. Somja, P. Lovinfosse, E. M. Nzaramba, F. Mievis, F. Giacomelli, D. Waltregny, D. Cataldo, S. S. Gambhir, R. Hustinx, *J. Nucl. Med.* **2015**, *56*, 361–364.
[140] S. Neubauer, F. Rechenmacher, A. J. Beer, F. Curnis, K. Pohle, C. D'Alessandria, H.-J. Wester, U. Reuning, A. Corti, M. Schwaiger, H. Kessler, *Angew. Chem. Int. Ed.* **2013**, *52*, 11656–11659.
[141] D. Heckmann, A. Meyer, B. Laufer, G. Zahn, R. Stragies, H. Kessler, *ChemBioChem* **2008**, *9*, 1397–1407.
[142] C. D'Alessandria, K. Pohle, F. Rechenmacher, S. Neubauer, J. Notni, H.-J. Wester, M. Schwaiger, H. Kessler, A. J. Beer, *Eur. J. Nucl. Med. Mol. Imaging* **2016**, *43*, 953–963.
[143] F. Rechenmacher, S. Neubauer, C. Mas-Moruno, P. M. Dorfner, J. Polleux, J. Guasch, B. Conings, H.-G. Boyen, A. Bochen, T. R. Sobahi, R. Burgkart, J. P. Spatz, R. Fässler, H. Kessler, *Chem. - Eur. J.* **2013**, *19*, 9218–9223.
[144] J. Notni, J. Šimeček, P. Hermann, H.-J. Wester, *Chem. - Eur. J.* **2011**, *17*, 14718–14722.
[145] J. Notni, K. Steiger, F. Hoffmann, D. Reich, T. G. Kapp, F. Rechenmacher, S. Neubauer, H. Kessler, H.-J. Wester, *J. Nucl. Med.* **2016**, *57*, 460–466.
[146] J. Notni, K. Steiger, F. Hoffmann, D. Reich, M. Schwaiger, H. Kessler, H.-J. Wester, *J. Nucl. Med.* **2016**, *57*, 1618–1624.
[147] R. Haubner, S. Maschauer, J. Einsiedel, I. E. Eder, C. Rangger, P. Gmeiner, I. J. Virgolini, O. Prante, *BioMed Res. Int.* **2014**, *2014*, 1–12.
[148] Z.-H. Jin, T. Furukawa, K. Kumata, L. Xie, J. Yui, H. Wakizaka, Y. Fujibayashi, M.-R. Zhang, T. Saga, *Biol. Pharm. Bull.* **2015**, *38*, 1722–1731.
[149] G. Mana, D. Valdembri, G. Serini, *Biochem. Soc. Trans.* **2020**, *48*, 83–93.
[150] A. Dal Corso, L. Pignataro, L. Belvisi, C. Gennari, *Curr. Top. Med. Chem.* **2015**, *16*, 314–329.
[151] A. Dal Corso, L. Pignataro, L. Belvisi, C. Gennari, *Chem. – Eur. J.* **2019**, *25*, 14740–14757.
[152] D. Arosio, L. Manzoni, C. Corno, P. Perego, *Recent Patents Anticancer Drug Discov.* **2017**, *12*, 148–168.
[153] S. Katsamakas, T. Chatzisideri, S. Thysiadis, V. Sarli, *Future Med. Chem.* **2017**, *9*, 579–604.
[154] H.-J. Cho, S.-J. Park, Y.-S. Lee, S. Kim, *J. Controlled Release* **2019**, *300*, 73–80.
[155] K. Ahmad, E. J. Lee, S. Shaikh, A. Kumar, K. M. Rao, S.-Y. Park, J. O. Jin, S. S. Han, I. Choi, *Semin. Cancer Biol.* **2019**, S1044579X19302068.
[156] M. Alipour, M. Baneshi, S. Hosseinkhani, R. Mahmoudi, A. Jabari Arabzadeh, M. Akrami, J. Mehrzad, H. Bardania, *J. Biomed. Mater. Res. A* **2020**, *108*, 839–850.
[157] P.-H. Wu, A. E. Opadele, Y. Onodera, J.-M. Nam, *Cancers* **2019**, *11*, 1783.
[158] Y. Cheng, Y. Ji, *Eur. J. Pharm. Sci.* **2019**, *128*, 8–17.
[159] K. R. Gajbhiye, V. Gajbhiye, I. A. Siddiqui, J. M. Gajbhiye, *J. Drug Target.* **2019**, *27*, 111–124.
[160] S. Fu, X. Xu, Y. Ma, S. Zhang, S. Zhang, *J. Drug Target.* **2019**, *27*, 1–11.
[161] U. K. Marelli, F. Rechenmacher, T. R. A. Sobahi, C. Mas-Moruno, H. Kessler, *Front. Oncol.* **2013**, *3*, DOI 10.3389/fonc.2013.00222.
[162] J. Niu, Z. Li, *Cancer Lett.* **2017**, *403*, 128–137.
[163] F. S. Di Leva, S. Tomassi, S. Di Maro, F. Reichart, J. Notni, A. Dangi, U. K. Marelli, D. Brancaccio, F. Merlino, H.-J. Wester, E. Novellino, H. Kessler, L. Marinelli, *Angew. Chem. Int. Ed.* **2018**, *57*, 14645–14649.

[164] O. V. Maltsev, U. K. Marelli, T. G. Kapp, F. S. Di Leva, S. Di Maro, M. Nieberler, U. Reuning, M. Schwaiger, E. Novellino, L. Marinelli, H. Kessler, *Angew. Chem. Int. Ed.* **2016**, *55*, 1535–1539.
[165] R. H. Kimura, L. Wang, B. Shen, L. Huo, W. Tummers, F. V. Filipp, H. H. Guo, T. Haywood, L. Abou-Elkacem, L. Baratto, F. Habte, R. Devulapally, T. H. Witney, Y. Cheng, S. Tikole, S. Chakraborti, J. Nix, C. A. Bonagura, N. Hatami, J. J. Mooney, T. Desai, S. Turner, R. S. Gaster, A. Otte, B. C. Visser, G. A. Poultsides, J. Norton, W. Park, M. Stolowitz, K. Lau, E. Yang, A. Natarajan, O. Ilovich, S. Srinivas, A. Srinivasan, R. Paulmurugan, J. Willmann, F. T. Chin, Z. Cheng, A. Iagaru, F. Li, S. S. Gambhir, *Nat. Commun.* **2019**, *10*, 4673.
[166] J. Notni, D. Reich, O. V. Maltsev, T. G. Kapp, K. Steiger, F. Hoffmann, I. Esposito, W. Weichert, H. Kessler, H.-J. Wester, *J. Nucl. Med.* **2017**, *58*, 671–677.
[167] Y. Tang, R. Davis, T. Ganguly, J. Sutcliffe, *Molecules* **2019**, *24*, 309.
[168] B. Alday-Parejo, R. Stupp, C. Rüegg, *Cancers* **2019**, *11*, 978.
[169] J. Cooper, F. G. Giancotti, *Cancer Cell* **2019**, *35*, 347–367.

ligand	Cell line	models	references
^{68}Ga-NODAGA-peptidomimetic	Human colon carcinoma (RKO cells) Human melanoma (M21 cells)	Heterotopic xenografts in mice	Neubauer et al, 2013
^{68}Ga-NODAGA-peptidomimetic (FR366)			D'Alessandria et al, 2016
^{68}Ga-TRAP-peptidomimetic (Aquibeprin)			Notni et al, 2016
^{18}F-peptide (CRRETAWAC)	Human prostate carcinoma (DU145 cells)	Heterotopic xenografts in mice	Hauber et al, 2014
^{18}F-NOTA-peptide (KSSPHSRN(SG)$_5$RGDSP)	Murine melanoma (B16-F10 cells) Human colorectal carcinoma (SW48 cells)	Heterotopic xenografts in mice	Jin et al, 2015
^{68}Ga-TRAP-peptide (c(phg-isoDGR-(NMe)k))	Human melanoma (M21 cells)	Heterotopic xenografts in mice	Kapp et al, 2018

Table1: PET radiotracers selective for α5β1 integrin. Different xenografted tumoral cell lines have been used with differential expression of α5β1 and αvβ3 integrins. RKO cells : α5β1 +, αvβ3 -; M21 cells: α5β1 +/- and αvβ3 +; DU145 cells: α5β1 +, αvβ3 -; B16-F10: α5β1+, αvβ3 +/-; SW48 cells: α5β1 -, αvβ3 +/-.

Legends to figures

Figure 1: **Integrins in hallmarks of cancer**. Altered expressions of integrins are detected in tumor cells but also in non tumoral cells in the tumor microenvironment. Integrin-activated signaling pathways have pro-tumoral functions.

Figure 2: RGD-integrin ligands. Integrins αvβ3 and α5β1 both recognize Fibronectin (FN). Ligands able to interfere with FN-integrin complexes have been developed mainly as integrin antagonists of cell adherence (RGD-based peptides, RGD-mimetics). Antibodies recognize epitopes in- or outside the RGD binding sites and are useful to mark integrins in inactivated or activated states. Non-RGD peptides have been developed based on the FN synergy site (PHSRN) recognized by α5β1 integrin.

Figure 3: Chemical structures of some RGD-integrin ligands. Cilengitide was the first RGD-containing cyclic peptide reaching the clinic for glioblastoma treatment [93]. LXW7 is a cyclooctapeptide described in [102]. C(phg-isoDGR-NMe)k) is described in [108]. SJ755 was one of the first small molecule specific for α5β1 integrin [112]. Compound 1 is described in [141] and compound 17 is an α5β1 integrin agonist [131].

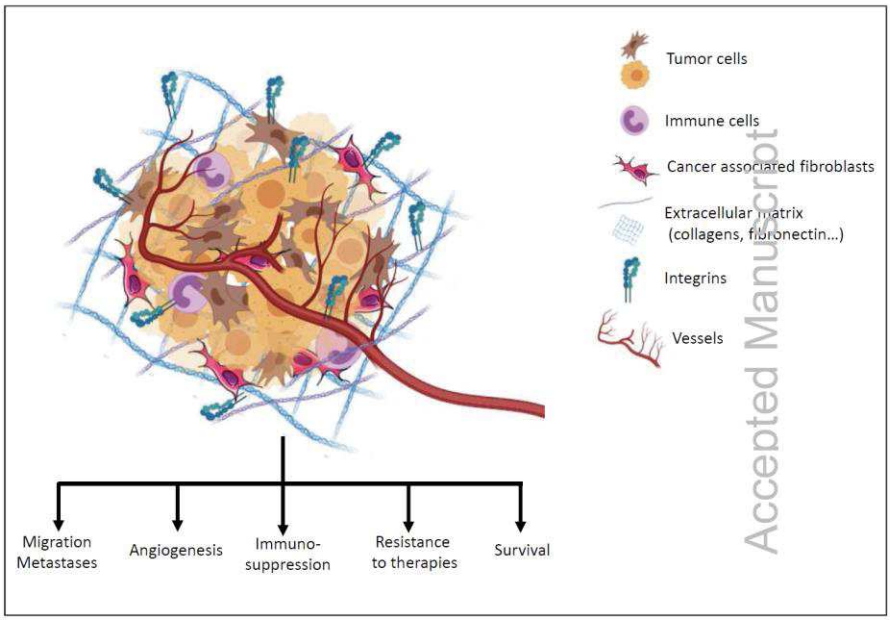

Figure 1

ChemBioChem 10.1002/cbic.202000626

Figure 2

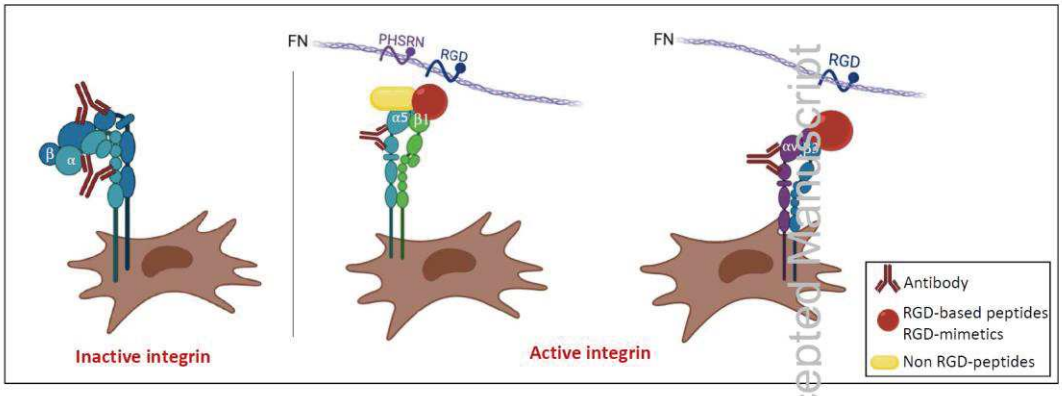

10.1002/cbic.202000626

αvβ3 integrin

α5β1 integrin

Figure 3

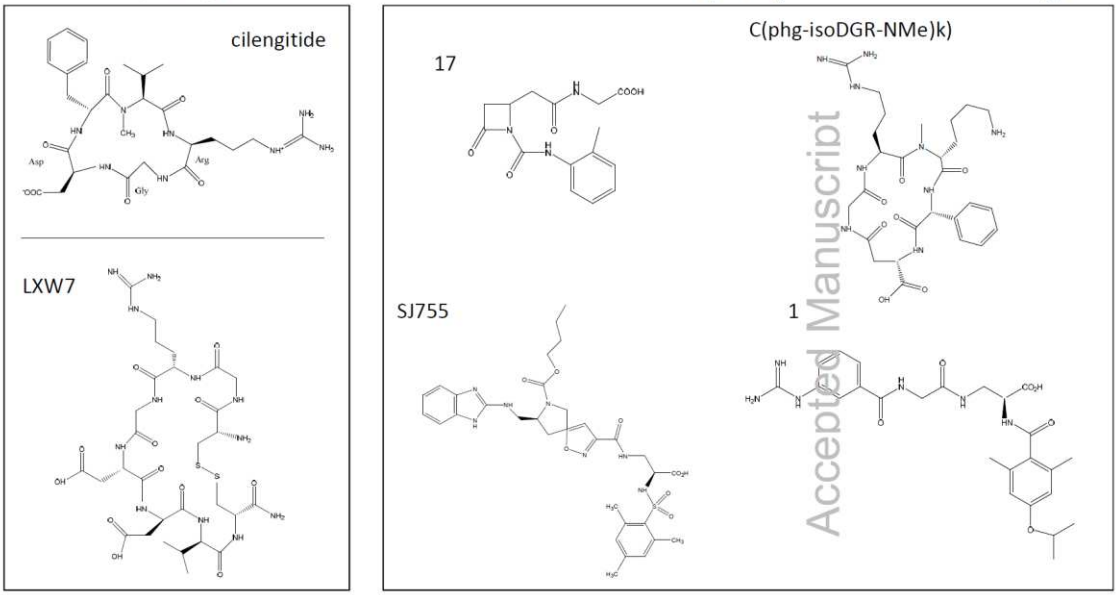

Article 2

Introduction

Flavagline, a natural product first isolated from Aglaia in 1982, is reported to possess strong anti-leukemic activity. The efficacy of the synthetic derivative (FL3) in various type of cancer including lung, breast, and colon cancer is well documented. In urothelial carcinoma cells for example, FL3 inhibited cell cycle progression and induce mitochondria-related apoptosis by directly binding to and preventing the phosphorylation of Prohibitin 1 (PHB) by Akt. However, data are lacking on the effect of FL3 on glioblastoma (GBM), the common and most aggressive malignant primary brain tumor that is characterized with poor prognosis and resistance to therapy. The effect of FL3 in temozolomide (TMZ) sensitive and resistant GBM cells in both normoxic and hypoxic conditions were presented in the manuscript (Harmouch1, Seitlinger, Chaddad, Ubeaud-Sequier, Barths, Sani et al., 2020).

- FL3 inhibit proliferation, induced cell cycle arrest (at the G2 phase) and senescence in U87MG cells but showed no cytotoxic effect on astrocytes.
- The induction of senescence by FL3 was confirmed using LN443 cells expressing p53 wild type. Furthermore, the induction of senescence by FL3 in U373 cells expressing p53 mutant, suggest that its activity is independent of the p53 status of the cells.
- TMZ-resistant cells were generated by subjecting U87MG cells to 50 µM TMZ for 2 months and the development of resistance was confirmed using the IncuCyte live cell analysis system. The resistant cells remained insensitive to TMZ after several weeks of culture in TMZ free medium U87MG TMZ OFF cells. Similar to the parental cells, FL3 decreased proliferation and induced senescence in U87MG TMZ OFF cells.
- Hypoxia was induced by subjecting U87MG cells to 150 µM CoCL2 and was confirmed by western blot (expression of HIF1α) and fluorescence staining.
- Results showed that the effect FL3 on normoxic U87MG cells were similar to those of FL3 on hypoxic U87MG cells. Thus, FL3 induce cell cycle arrest and senescence without inducing apoptosis in both normoxic and hypoxic conditions.

In this collaborative work, we participated in the generation of U87MG TMZ OFF cells and the provision of U373 (pp53 mutant) and LN443 (p53 wild type). Other aspects of this work were carried out by our collaborators.

SCIENTIFIC REPORTS
nature research

Check for updates

OPEN

Flavagline synthetic derivative induces senescence in glioblastoma cancer cells without being toxic to healthy astrocytes

Ezeddine Harmouch[1,2,9], Joseph Seitlinger[1,2,3,9], Hassan Chaddad[1,2,9], Geneviève Ubeaud-Sequier[1,2], Jochen Barths[4], Sani Saidu[5], Laurent Désaubry[6,7], Stéphanie Grandemange[8], Thierry Massfelder[1,2], Guy Fuhrmann[1,2], Florence Fioretti[1,2,3], Monique Dontenwill[5], Nadia Benkirane-Jessel[1,2]✉ & Ysia Idoux-Gillet[1,2]✉

Glioblastoma (GBM) is one of the most aggressive types of cancer, which begins within the brain. It is the most invasive type of glioma developed from astrocytes. Until today, Temozolomide (TMZ) is the only standard chemotherapy for patients with GBM. Even though chemotherapy extends the survival of patients, there are many undesirable side effects, and most cases show resistance to TMZ. FL3 is a synthetic flavagline which displays potent anticancer activities, and is known to inhibit cell proliferation, by provoking cell cycle arrest, and leads to apoptosis in a lot of cancer cell lines. However, the effect of FL3 in glioblastoma cancer cells has not yet been examined. Hypoxia is a major problem for patients with GBM, resulting in tumor resistance and aggressiveness. In this study, we explore the effect of FL3 in glioblastoma cells under normoxia and hypoxia conditions. Our results clearly indicate that this synthetic flavagline inhibits cell proliferation and induced senescence in glioblastoma cells cultured under both conditions. In addition, FL3 treatment had no effect on human brain astrocytes. These findings support the notion that the FL3 molecule could be used in combination with other chemotherapeutic agents or other therapies in glioblastoma treatments.

Flavaglines are natural products isolated from *Aglaia* genus plants possessing unique anticancer properties. One synthetic flavagline, called FL3, is known for its anticancer effects without being toxic to healthy cells[1,2]. Flavaglines were isolated for the first time in 1982 based on their strong anti-leukemic activity[3]. Cytotoxic effects of flavaglines has been reported in a lot of cancer cell lines, such as lung, breast, and colon cancer[4], leading to the inhibition of proliferation and thus inducing cell cycle arrest or apoptosis in tumor cells. Different mechanisms by which FL3 targets cancer cells were reported in the literature. It was shown that in urothelial carcinoma cells, FL3 can directly binds to Prohibitin 1 (PHB) preventing its phosphorylation by Akt, leading to a decrease of PHB in mitochondria, which causes a mitochondria-related apoptosis and cell cycle inhibition[5,6]. PHB is an ubiquitous and evolutionarily conserved protein expressed in different cellular compartments including the nucleus, cytoplasm and mitochondria[7], it is involved in diverse biological processes such as cell proliferation, resistance to apoptosis, maintenance and integrity of mitochondria[7,8]. Also, FL3 was shown to selectively kill cancer stem-like cells through the p38 mitogen-activated protein kinase (MAPK)-dependent caspase-3-dependent pro-apoptotic

[1]INSERM (French National Institute of Health and Medical Research), UMR 1260, Regenerative Nanomedicine (RNM), FMTS, 11 Rue Humann, 67000 Strasbourg, France. [2]Faculté de Chirurgie Dentaire, Université de Strasbourg, 67000 Strasbourg, France. [3]Hôpitaux Universitaire de Strasbourg (HUS), 67000 Strasbourg, France. [4]Core Facility for Flow Cytometry, Cell Sorting and EliSpot, UMR 1110, INSERM, Strasbourg, France. [5]CNRS UMR 7021, Laboratoire de Bioimagerie et Pathologies, Faculté de Pharmacie, Strasbourg, France. [6]Laboratory of Cardio-Oncology and Medicinal Chemistry (FRE 2033), CNRS, Institut Le Bel, Strasbourg, France. [7]Sino-French Joint Lab of Food Nutrition/Safety and Medicinal Chemistry, College of Biotechnology, Tianjin University of Science and Technology, Tianjin, China. [8]CNRS, UMR 7039 CRAN, Université de Lorraine, Campus Sciences, 30 bvd des Aiguillettes, 54505 Vandoeuvre les Nancy Cedex, France. [9]These authors contributed equally: Ezeddine Harmouch, Joseph Seitlinger and Hassan Chaddad. ✉email: nadia.jessel@inserm.fr; yidouxgillet@unistra.fr

pathway, without being toxic to normal stem-like cells[9]. Recently, it has been reported that mitophagy, a process that selectively removes damage or unwanted mitochondria in order to maintain normal cellular physiology, was inhibited by FL3 contributing to the blockage of cancer cell growth[10].

In this study, we used four different glioblastoma cancer cell lines: U87-MG (both TMZ-sensitive and TMZ-resistant cells), U373-MG (p53-mutated) and LN443 (p53 WT) malignant glioma cells. Glioblastoma (GBM) is the most common type of primary brain tumor[11,12], with a rapid growth and aggressive properties leading to an overall survival average of 14 to 18 months[13,14]. This tumor can be found anywhere in the brain and is predominantly composed of abnormal astrocytes but also a mix of different cell types. GBM often benefits from the selective conditions present in the tumor microenvironment. Generation of a hypoxic environment and activation of its main effector, hypoxia-inducible factor-1 (HIF-1), are common features of advanced GBM cancer stages[15]. Low tumor oxygenation promotes tumor cells invasion into the healthy brain tissue[16–18]. Hypoxia is therefore a major problem for patients with GBM, resulting in tumor resistance and aggressiveness. Due to the cellular heterogeneity inside this tumor, the first step of GBM treatment is a surgical removal of the tumor mass. Then radiation therapy and chemotherapy (based on the use of Temozolomide: DNA alkylating agent and the standard chemotherapeutic drug for GBM) are performed in order to kill remaining tumor cells. EGFR amplifications occur in more than 50% of glioblastomas[19]. Drugs targeting the constitutively active form of RTKs (ex: EGFR) and its downstream MAPK/PI3K signalling pathways, are particularly studied as glioblastoma targeted therapies[20]. Afatinib is a well-known drug capable of crossing the blood brain barrier BBB[21] and directly target the EGFR thus limiting the proliferation and invasion of glioblastoma cancer cells. But due to the limited efficacy of this treatment, a new anticancer model has been established combining the Afatinib drug with the TMZ. This new system of anticancer therapy combination significantly reduces the glioblastoma tumor growth both in vitro and in pre-clinical mouse models[22]. All of the new targeted therapies (for example against EGFR) failed in clinical trials and GBM remain a challenge for oncologists.

These conventional therapies target mostly high proliferative and well-oxygenated cells. The challenge consists in targeting hypoxic cancer cells, known to be more aggressive and resistant to anticancer treatments[23].

As FL3 displays potent anticancer activities and is known to inhibit cell proliferation in many cancer cells, we examined its effect on different glioblastoma cell lines and compared normoxic and hypoxic conditions. Also we studied whether FL3 could be toxic for primary human brain astrocytes.

Results

FL3 blocks U87-MG cell proliferation at G2 phase, without inducing apoptosis. First, cell viability was analysed by the Alamar Blue assay at different time points of treatment and using different concentrations of FL3 (chemical structure: Fig. 1A) on U87-MG cells. Our results showed no significant decrease of the Alamar Blue reduction percentage for 20 nM of FL3 after 24 h treatment, but around 50% loss of viability after 48 h and 72 h of treatment (Fig. 1B). A drastic decrease of metabolic activity appeared with a concentration of 200 nM for 24 h of treatment and continued to decrease for 48 h and 72 h. Beyond 200 nM, the loss of cell viability seemed to reach saturation for all treatment time points. To establish a good ratio between the treatment time and the concentration of FL3, we chose to treat the cells for 48 h with 200 nM of FL3. Therefore, the decrease in metabolic activity, cell density associated to microscopic observation (Fig. 1B, C) indicates that FL3 is cytostatic or cytotoxic in U87-MG cells. Cell cycle analysis showed an increased number of cells in the G2 phase after FL3 treatment in a dose dependant manner (Fig. 1D, E). These results were supported by the upregulation of phospho-p38 MAPK protein (Mitogen-activated protein kinases) and the downregulation of Cyclin D expression, known to be involved in the G2 cell cycle arrest (Fig. 1F and G). Interestingly, flow cytometry using Annexin V and Propidium Iodide apoptosis assays revealed that FL3 treatment does not induce cell death in U87-MG cells (Fig. 2A). Moreover, no cleaved-PARP protein has been detected in these treated cells (Fig. 6C). Also live/dead assays showed less cells in treated condition with FL3 compared to the control, and most importantly there were no cells stained in red, corresponding to dead cells, neither in treated nor in control conditions (Fig. 2B).

FL3 induces senescence in glioblastoma cancer cells. As no sign of apoptosis was seen, we aimed to further understand the effect of FL3 on these U87-MG cancer cells. First, by using Hoechst staining, we observed that cells treated with FL3 presented much bigger nuclei compared to the control cells as shown in Fig. 3A, with an average nucleus size of 17 µm for untreated cells and 25 µm for FL3 treated cells (Fig. 3A). Since glioblastoma cells exhibit increased nuclear size with senescence[24], we investigated whether FL3 induces senescence in U87-MG cells. Thus, senescence-associated β-Galactosidase assays have been performed on FL3 treated U87-MG cells, which were maintained for 2, 4, 6 and 8 days post-FL3 treatment. We observed that the majority of cells were positively stained in blue, 6 and 8 days post-FL3 treatment (Figs. 3B, 6E). These results were correlated with the remarkable increase in the transcript levels of the negative cell cycle progression regulators p16, p19 and p21, 6 days post-FL3 treatment (Fig. 6F). Notably, transcript levels of some members of the senescence associated secretory phenotype (SASP; e.g. CXCL1, CXCL2, and CXCL5) were also markedly increased 6 days post-FL3 treatment compared to the control (Fig. 3C). Thus, FL3 eventually induced senescence in U87-MG cells.

In order to confirm the results obtained from U87-MG cells, we tested the effect of FL3 on two other glioblastoma cancer cell lines: U373-MG and LN443 cancer cells. We saw that the metabolic activity of both U373-MG and LN443 cells treated with 200 nM of FL3 was reduced compared to the control (for U373 cells, 45% decrease compared to control, and for LN443 cells, 65% decrease compared to control) (Fig. 4A). Most importantly, both U373-MG and LN443 treated cells with FL3 showed a blue positive staining for the senescence-associated β-Galactosidase assay, 6 days after the treatment (Fig. 4B, C). Thus, FL3 induced also senescence in U373-MG and LN443 glioblastoma cells.

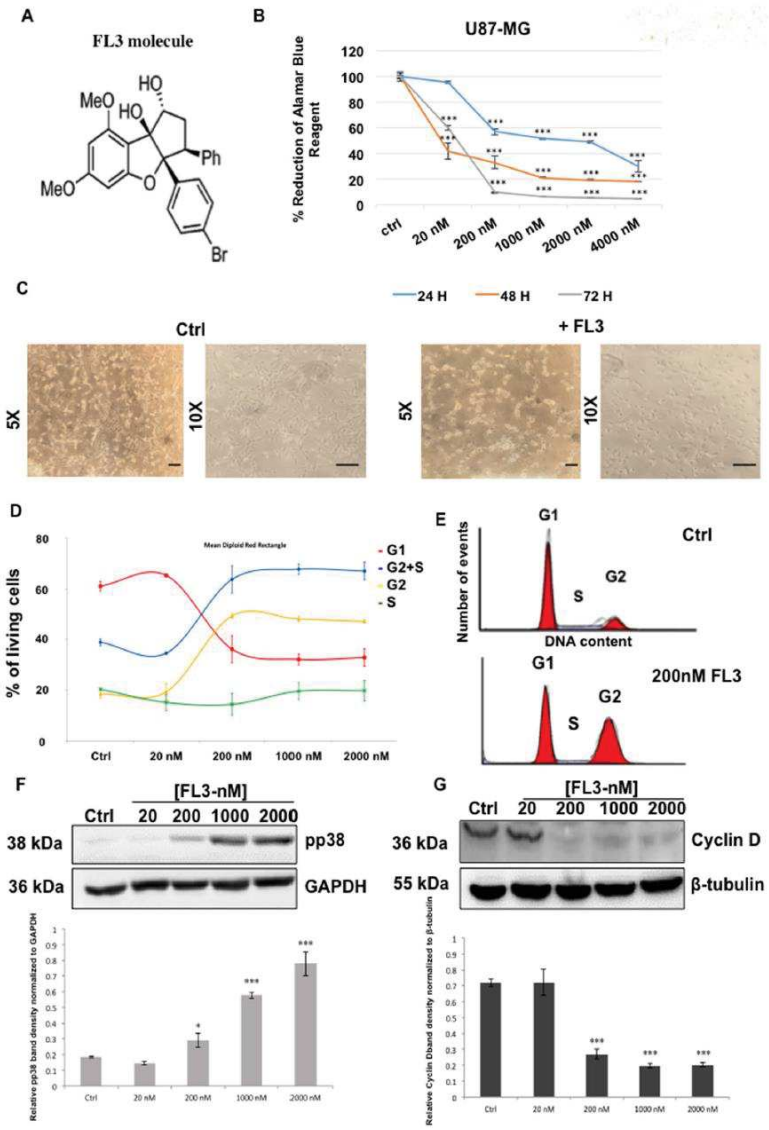

Figure 1. Effect of FL3 on U87-MG glioblastoma cancer cells metabolic activity and proliferation. (**A**) Chemical structure of FL3. (**B**) Analysis of cell viability with the AlamarBlue assay at different time points in U87-MG control cells and U87-MG treated cells with different concentrations of FL3. (**C**) Representative images of control cells and U87-MG cells treated with 200 nM FL3. The scale bar represents 200 µm. (**D**) Distribution of cells in each cell cycle phase in control and treated conditions. (**E**) Representative histogram of cell cycle analysis of U87-MG cells treated with 200 nM FL3. (**F**) Western Blot and quantification of pp38 protein expression in control cells and U87-MG cells treated with different concentrations of FL3. (**G**) Western Blot and quantification of Cyclin D protein expression in control cells and U87-MG cells treated with different concentrations of FL3. Quantification of mean ± SEM from 3 independent experiments, $^{*}P<0.05$, $^{**}P<0.01$, $^{***}P<0.001$ from control. n = 3 for each concentration.

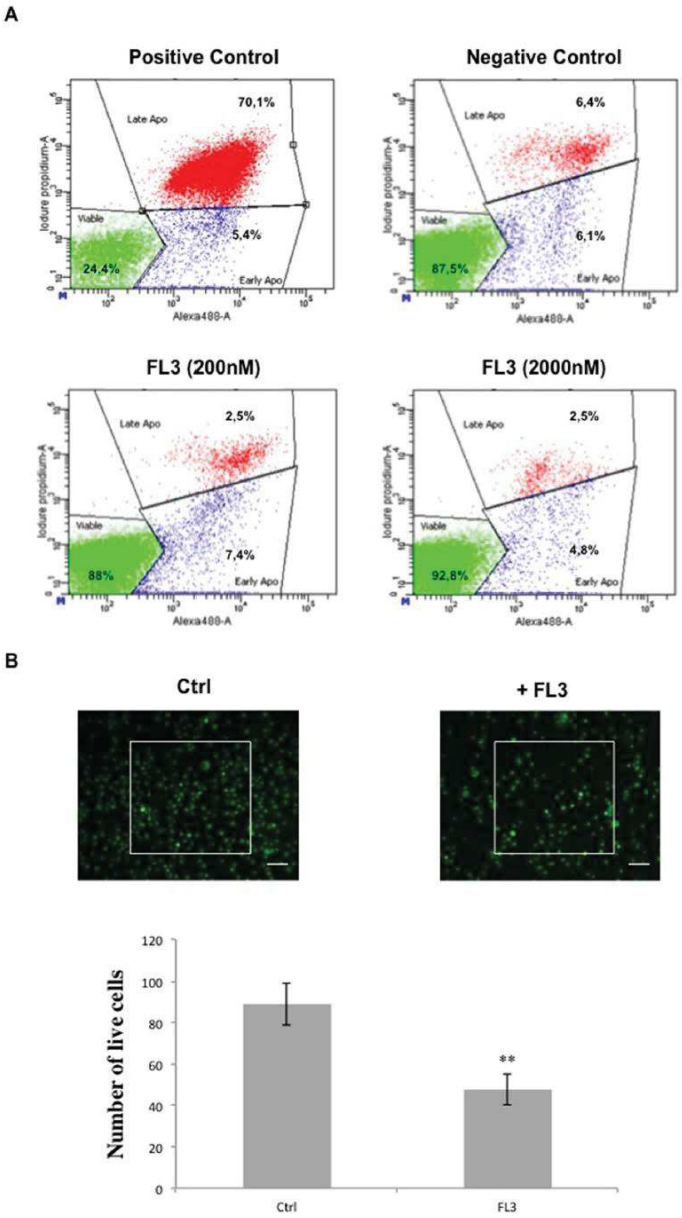

Figure 2. Analysis of the apoptosis in glioblastoma cancer cells. (**A**) Flow cytometry analysis of Annexin V and PI staining in U87-MG cells treated with 200 and 2000 nM FL3 and compared to positive and negative controls. We used an NF-κB inhibitor as positive control. Results are obtained from 3 independent experiments. (**B**) Live/dead assay on U87-MG cells treated or not with 200 nM FL3 and quantification of live cells in each condition. The scale bar represents 20 µm. Cells within white boxes were counted at each time. Quantification of mean ± SEM from 3 independent experiments, $^{**}P < 0.01$ from control. n = 3 for each condition.

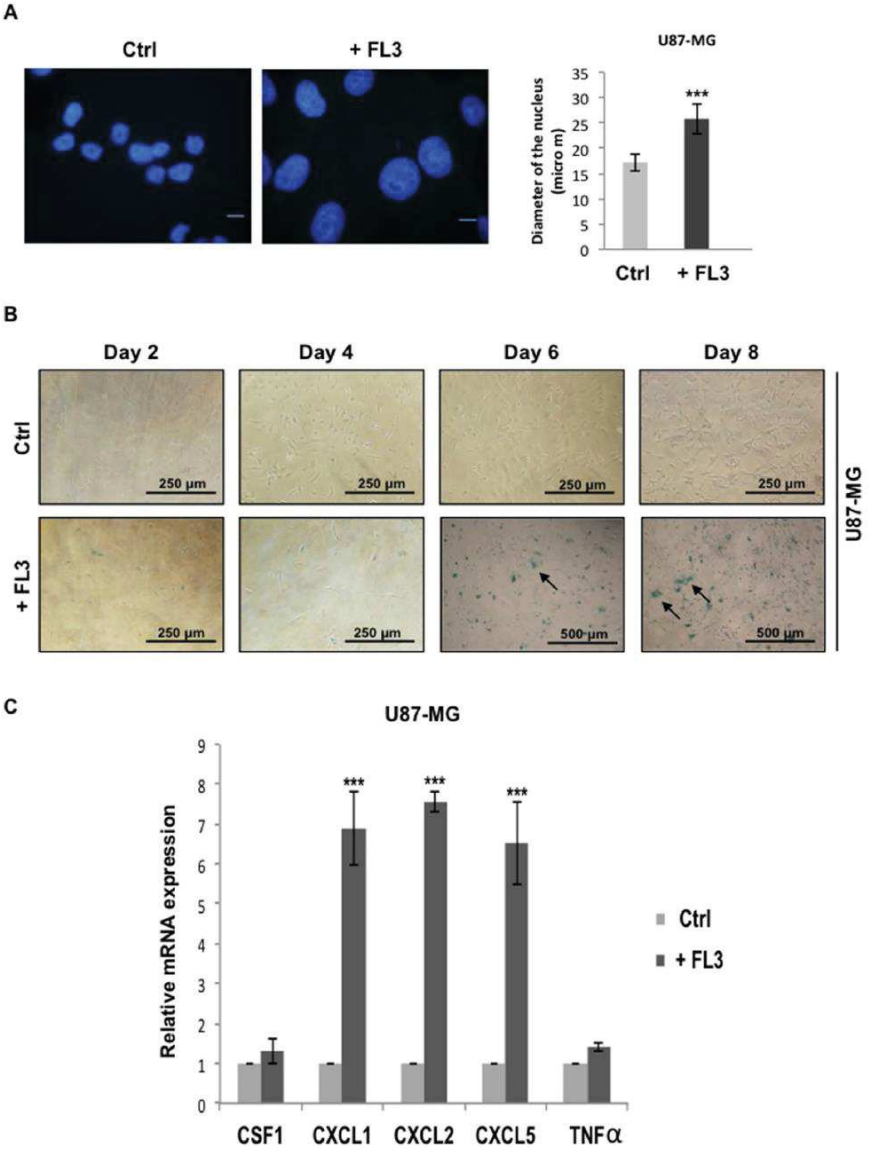

Figure 3. FL3 induced cellular senescence in U373 and LN443 glioblastoma cancer cells. (**A**) Observation and quantification of the nuclear shape and size in U87-MG control and treated cells with 200 nM FL3. 50 nuclei were measured for each condition. The scale bar represents 15 µm. Quantification of mean ± SEM from 3 independent experiments, $^{***}P < 0.001$ from control. (**B**) Representative senescence-associated β-galactosidase (SA β-gal) staining (blue) of control cells and U87-MG cells treated with 200 nM FL3, respectively. Pictures were taken at 2, 4, 6 and 8 days post-FL3 treatment. Black arrows indicate U87-MG positive cells. The scale bar represents: 250 and 500 µm. (**C**) Relative mRNA expression levels of SASP in control and treated U87-MG cells 6 days post treatment with 200 nM FL3. Quantification of mean ± SEM from 3 independent experiments, $^{***}P < 0.001$ from control.

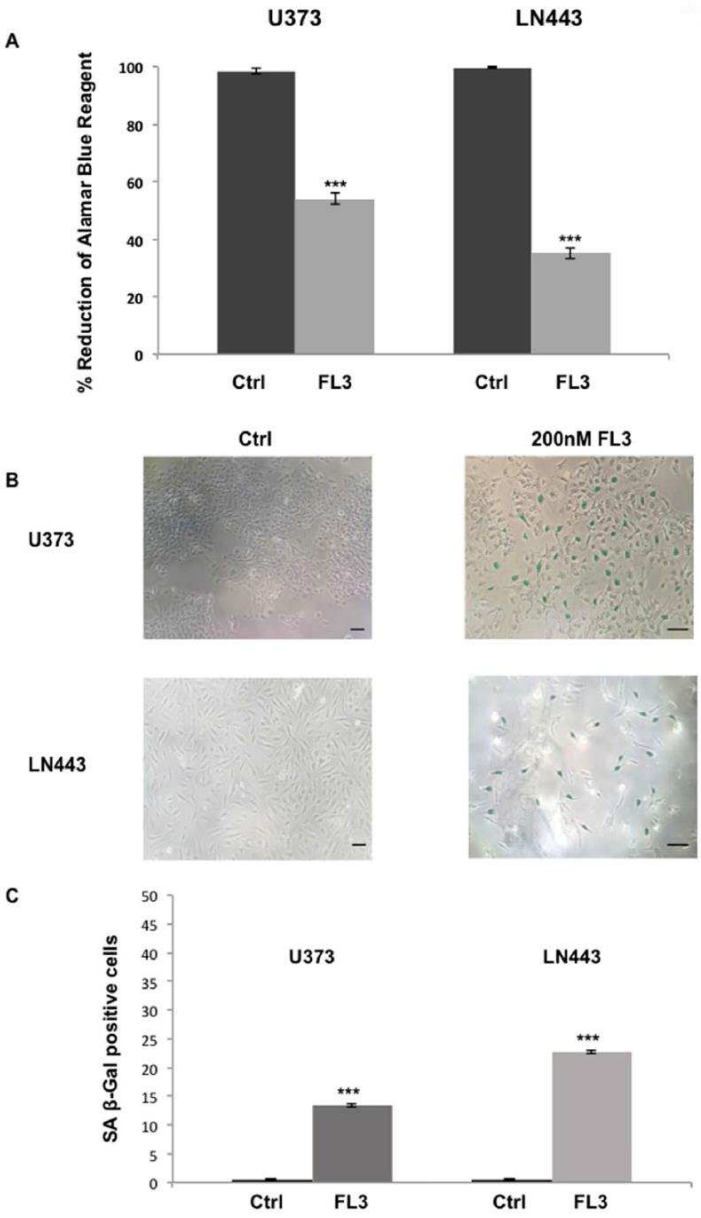

Figure 4. FL3 induced cellular senescence in U373-MG and LN443 glioblastoma cancer cells. (**A**) Analysis of cell viability with the AlamarBlue assay in U373-MG and LN443 control cells and treated cells with 200 nM of FL3, 48 h after the treatment. Quantification mean ± SEM from 3 independent experiments, ***$P < 0.001$ from control. (**B**) Representative senescence-associated β-galactosidase (SA β-gal) staining (blue) of U373 and LN443 control cells and treated cells with 200 nM FL3, 6 days after the treatment. Scale bar represents 150 µm. (**C**) Quantification of SA β-gal positive cells of U373 and LN443 control cells and treated cells with 200 nM of FL3. 50 cells were analysed for each condition. Results for mean ± SEM from 3 independent experiments, ***$P < 0.001$ from control.

Hypoxic conditions do not interfere with FL3 effect. To induce hypoxia in U87-MG cells, we added cobalt chloride (CoCl2) to the regular culture medium. This agent is known to mimic hypoxia via inhibition of the HIF1α protein degradation in these cells[25,26]. Different $CoCl_2$ concentrations were tested, and as expected, our results showed similar transcript levels of HIF1α in controls and CoCl2 treated U87-MG (Fig. 5A), whereas protein levels of HIF1α were increased in U87-MG cells treated with 50 to 200 µM of $CoCl_2$ compared to control ones (Fig. 5B). Moreover, HIF1α target genes such as GLUT1, GLUT3, and VEGF were upregulated inside U87-MG cells treated with all concentrations of $CoCl_2$ compared to control cells. In view of our results we chose to use 150 µM of $CoCl_2$ in our experiments. To confirm that glioblastoma cells are in hypoxia we evaluated the mitochondrial state. Fluorescence staining with an anti-Cytochrome C antibody showed that $CoCl_2$ treated cells presented mitochondrial fission compared to untreated cells exhibiting mitochondrial fusion (Fig. 5C). In 50 counted cells, the ratio between mitochondrial fusion and mitochondrial fission was reversed in U87-MG cells cultured in normoxia and in hypoxia, showing that U87-MG cells treated with 150 µM of $CoCl_2$ were under hypoxic conditions.

To examine the effect of FL3 on U87-MG cells cultured under hypoxic conditions, cells were treated for 24 h with $CoCl_2$ and then incubated with FL3 for 48 h (Fig. 6A), before performing Alamar Blue assays (Fig. 6B). A limited decrease of the metabolic activity of U87-MG cells under hypoxia compared to normoxia was observed. There was no significant difference when we added 20 nM of FL3. However, we observed a drastic decrease in the metabolic activity of U87-MG cells treated with $CoCl_2$ and incubated with 200 nM FL3. These cells did not show any sign of apoptosis, there was no expression of the cleaved PARP at the protein level (Fig. 6C). To understand the effect of FL3 in these U87-MG cells, a SA-beta Galactosidase assay was realized. In these conditions, most of U87-MG cells treated with FL3 were positively stained in blue in both normoxia and hypoxia (Fig. 6D, 6E). Moreover, mRNA expression levels of cell cycle regulators p16, p19 and p21 were increased in $CoCl_2$ + FL3 treated cells, but not when cells were treated only with $CoCl_2$ (Fig. 6F). Taken all together, these results clearly show that FL3 induced senescence in U87-MG cells cultured as well under hypoxia as under normoxia.

FL3 with TMZ combination induces senescence in TMZ resistant GBM cells. In order to test the combination of FL3 molecule with TMZ treatment, we used a TMZ resistant GBM cell line: U87-MG (TMZ off) cells in the next experiment. We saw that FL3 inhibited the metabolic activity of U87-MG (TMZ off) cells (around 45%) compared to the control in contrast with TMZ treatment alone (Fig. 7A). On the other hand, U87-MG (TMZ off) cells were shown to be positive for the SA β-Gal assay 6 days post- FL3 treatment (Fig. 7B, C). Therefore, the use of FL3 molecule in combination with TMZ drug could be used as a treatment to induce senescence in TMZ resistant GBM cells.

Human brain astrocytes are resistant to FL3. Since it has been described that FL3 is not toxic in non-cancer cells, we examined the effect of this molecule on normal human brain astrocytes in order to compare the results we obtained from treated U87-MG glioblastoma cells. When we incubated human brain astrocytes with 200 nM of FL3 for 48 h and by a simple visualization with microscope (Fig. 8A), we did not observe any remarkable difference concerning the number of cells between the control and treated cells. In addition to that and using the Alamar Blue assay, the results showed a slight decrease in the metabolic activity of treated cells (around 20%) with FL3 for 48 h, as compared to the control (Fig. 8B). In U87MG cells, same concentration of FL3 (200 nM) and time point of treatment (48 h), decreased the metabolic activity at about 70%. These results clearly showed that human brain astrocytes are considerably more resistant to the FL3 treatment than glioblastoma cells.

Discussion

In this study, we evaluated the effect of the synthetic derivative of flavagline FL3 on different glioblastoma cell lines and compared normoxia to hypoxia conditions. FL3 is known to have anticancer effects and has been studied in several types of cancer cells but none of these studies was done on brain tumor cells. Here, we showed that FL3 decreases cell metabolic activity and proliferation by provoking cell cycle arrest at G2 phase in these cells (Fig. 1). We showed that FL3 provoked p38 phosphorylation and decreased Cyclin D protein expression as it was reported by Basmadjian et al.[4]. It has also been described that some flavagline derivatives could lead to cell cycle arrest at G0/G1 or G2/M phase in different cancer cell lines such as breast, colon, and prostate cancer cells[27–29]. Moreover, in the literature, these molecules caused apoptosis in cancer cells cultured in 2D models[27,28,30]. In our study, FL3 did not lead to apoptosis in U87-MG cancer cells (Fig. 2), in line with the results of Yuan et al. in bladder cancer cells. They found that FL3 induced cell cycle arrest at G2/M phase, without leading to apoptosis, supporting the fact that FL3 induces cell death in a tumor type-dependent way[31]. That is why it is an interesting perspective to see if the PHB is also implicated in the cell cycle arrest in glioblastoma cells, just like in bladder cancer cells. Indeed, in our study, classical flow cytometry analysis showed approximately the same number of apoptotic cells in treated conditions (with FL3) as compared to the control condition (without FL3), corresponding to the basal number of apoptotic cells. Moreover, PARP polymerase known to be involved in DNA repair, helping cell survival, is normally cleaved by caspase-3 when apoptosis occurs[32], which was not the case in U87-MG glioblastoma cells treated with FL3. The Live/Dead assay results showed less cells when treated with FL3 compared with the control, indicating an inhibition of cell proliferation, but no dead cells were detected (Fig. 2B).

Cellular senescence takes place both in culture and in vivo as a response to excessive extracellular or intracellular stress. In cancer cells, cellular senescence can act as a cell-intrinsic mechanism to suppress tumor growth, by blocking the proliferation of these cells through the activation of p53, p16, p19, p21 tumor suppressor genes[33,34]. It can also act in an extrinsic manner through the development of the senescence-associated secretory phenotype (SASP). Senescent cells secrete cytokines, miRNA, pro-inflammatory mediators, interleukins, chemokines, extracellular proteases, and growth factors that can affect surrounding cells. Chemokines like CXCL1, CXCL2, CXCL5

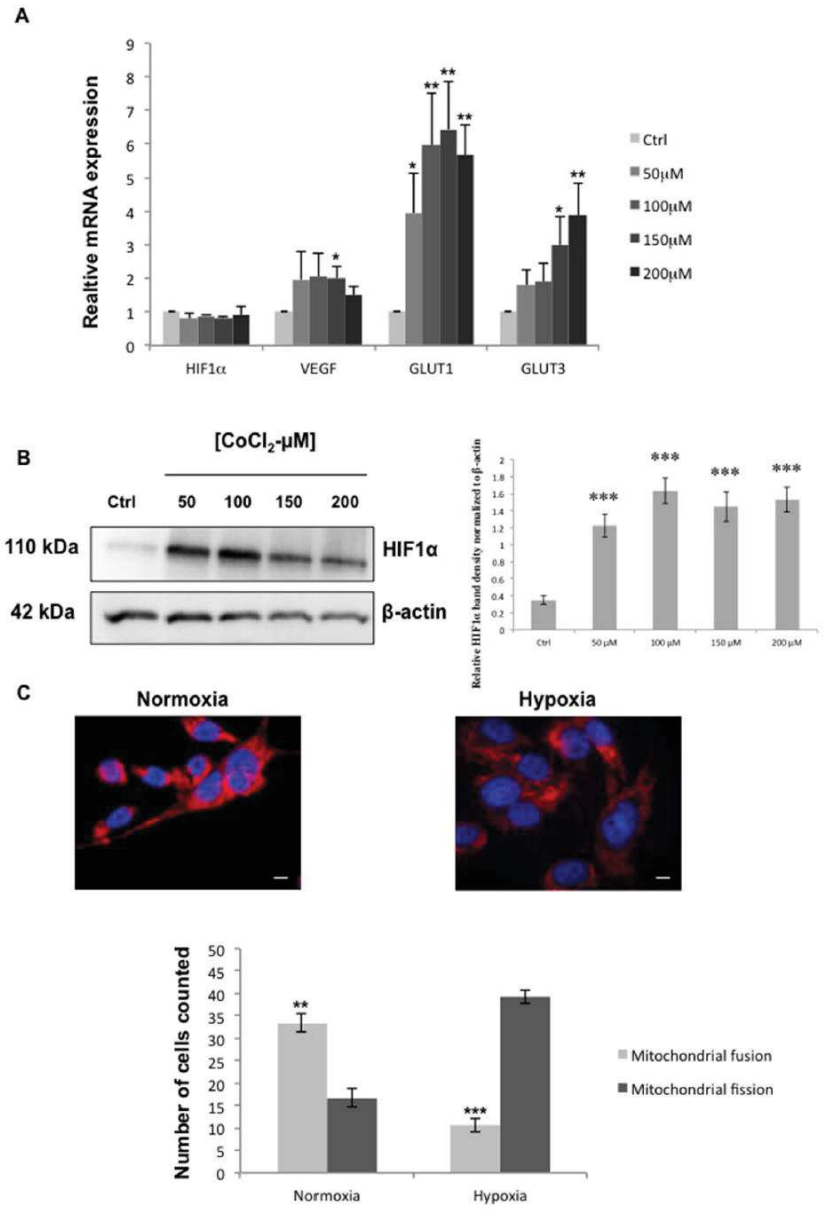

Figure 5. Characterization of the hypoxic model for glioblastoma cancer cells. (A) Relative mRNA expression levels of hypoxia related genes in control cells and U87-MG cells treated with different concentrations of $CoCl_2$ after 24 h of treatment. Quantification of mean ± SEM from 3 independent experiments, $^{*}P<0.05$, $^{**}P<0.01$ from control. (B) Western Blot and quantification of HIF1α protein expression in control cells and U87-MG cells treated with different concentrations of $CoCl_2$ after 24 h of treatment. Quantification of mean ± SEM from 3 independent experiments, $^{***}P<0.001$ from control. (C) Immunofluorescence detection of Cytochrome C (red), in U87-MG cells cultured under normoxia and hypoxia. Blue staining shows the cell nucleus. The scale bar represents 50 μm. ImageJ (1.52a Version, https://imagej.nih.gov/ij/) was used to do our images. Quantification of fusioned and fissioned mitochondria inside U87-MG cells cultured under normoxia and hypoxia. 50 cells were analysed for each condition. Quantification of mean ± SEM from 3 independent experiments, $^{**}P<0.01$, $^{***}P<0.001$ from control.

are known to be upregulated in senescent cells[35,36]. There are few publications concerning the pharmacologically-induced cellular senescence in glioblastoma cancer cells (U87-MG)[37] and it has been shown that U87-MG cells treated with temozolomide (TMZ) presents a G2/M cell cycle arrest, with an increase in p21 gene expression[38,39]. Moreover, these TMZ-treated cells were positively marked with the SA-β-Gal staining. In our study, the results obtained from the SA-β-Gal staining, the increase of nucleus size of glioblastoma U87-MG cancer cells, the significant increase of p16, p19 and p21 gene expression and the appearance of the SASP (CXCL1, 2 and 5 upregulated) (Figs. 3, 5), demonstrate an FL3-dependent induction of senescence in glioblastoma cancer cells. Flavaglines were already known to provoke apoptosis in cancer cells[4]. A recent study showed that these molecules can induce early autophagy in melanoma cells[40], but our results showed for the first time that the flavagline FL3 promotes a cellular senescence in U87-MG glioblastoma cells. In addition, we showed in our study that FL3 provoked the decrease of the metabolic activity of both treated U373-MG and LN443 cancer cells, and that FL3 remarkably induced cellular senescence inside U373 and LN443 treated cells (Fig. 4). Taken together, our results clearly prove that FL3 induces senescence in glioblastoma cancer cells. Interestingly, U373-MG cells express a p53 mutant protein but were pushed towards senescence by FL3 perhaps with less efficacy than in p53WT-expressing U87-MG and LN443 cells. Results suggest that FL3-induced senescence may be partly p53-independent.

Hypoxia plays a key role in tumor progression and metastasis promoting angiogenesis and invasiveness. The resistance of cancer cells to treatment is significantly induced by hypoxia, making it a prime obstacle in anticancer treatments. For example, radiotherapy leads to Reactive Oxygen Species (ROS) production inducing DNA damage under normoxia, but this ROS production is disturbed under hypoxia[41,42]. Chemotherapy faces the same challenge of cancer cell resistance. Due to the abnormal vascularization seen in tumors and the formation of the hypoxic core in the centre of these tumors, chemotherapeutic agents do not reach well this hypoxic region. Moreover, hypoxic cells develop a resistance against chemotherapeutic agents by the overexpression of genes involved in apoptosis, cell proliferation and drug efflux[42,43]. For these reasons, hypoxia remains one of the main barriers blocking an efficient treatment. Here, we chose to mimic hypoxic conditions using $CoCl_2$ agent. The cobalt of $CoCl_2$ agent replaces the iron core (Fe) in prolyhydroxylases making them unable to mark HIF1α thus preventing its degradation. $CoCl_2$ can also inhibit the interaction between HIF1α and von Hippel Lindau (VHL) protein, which is also implicated in the degradation of HIF1α[44,45]. Accordingly, after $CoCl_2$ treatment, we could see an accumulation of HIF1α at the protein level, but not at the RNA level in U87-MG cancer cells (Fig. 5). The accumulation of HIF1α due to a lack of oxygen or an inhibition of protein degradation is reported to lead to the activation of its downstream genes, such as VEGF, GLUT1 and GLUT3[45]. We observed a significant increase in the expression of these three target genes in $CoCl_2$ treated cells, indicating an upregulation of HIF1 transcriptional activity. Mitochondria constantly change shape through cycles of fusion and fission in response to various microenvironmental stimuli such as hypoxia. It has been shown that under hypoxia, mitochondria undergo fission[46] in order to maintain the cellular integrity by decreasing their respiratory activity and keeping ROS production at a physiological low level. Accordingly, the mitochondrial fission is a supplementary marker showing that cells are in hypoxic conditions.

When we treated U87-MG cells with 200 nM of FL3 for 48 h under hypoxia, we observed a decrease of the cell metabolic activity at about 60% compared to the control (Fig. 6). A similar decrease of metabolic activity was found under normoxia with the same conditions for FL3 concentration and time of treatment (Fig. 1). No cleaved-PARP was detected in $CoCl_2$ + FL3 treated cells and cells were positive for the SA-β Gal staining (Fig. 6), meaning that FL3 did not induce apoptosis, but senescence also in hypoxia. Thus, although hypoxia is known to induce resistance to treatments, FL3 is similarly efficient in hypoxia and in normoxia. FL3 therapy may be an interesting way to treat glioblastoma which are highly hypoxic..

The presence of TMZ resistant GBM cells is a major cause of treatment failure, that is why testing the combination of TMZ with other therapeutic molecules would be important to improve treatment outcomes. Our results showed that FL3 is able to trigger a senescence phenotype even in cells resistant to TMZ. The combination of TMZ with FL3 may thus be an interesting way to eliminate both TMZ sensitive and resistant glioma cells. (Fig. 7).

On the clinical level, chemotherapy leads in most cases to intolerable side effects. For this purpose, the discovery and the development of innovative therapeutics must focus on finding a tumor-specific therapy, in order to protect normal cells from the harmful side effects of chemotherapy. In this study, we showed that normal human brain astrocytes were not impacted by FL3 (Fig. 8).

In summary, we showed for the first time that the Flavagline derivative FL3 can induce senescence in glioblastoma cancer cell lines in normoxic or hypoxic conditions. This active molecule could be associated with the standard GBM chemotherapy TMZ or with other therapies to overcome intrinsic or acquired resistance..

Materials and methods

Cell lines and culture conditions. Glioblastoma U87-MG cancer cells were purchased from ATCC (HTB-14), U373 (Uppsala) cells were obtained from ECACC (Sigma Aldrich) and LN443 cells were kindly provided by Pr. M Hegi (Lausanne, Switzerland). All these cells are grown in MEM medium (L0430-500, Dominique Dutscher) with 10 $U.mL^{-1}$ penicillin, 100 µg mL^{-1} streptomycin, 250 U mL^{-1} fungizone, 1 mM Na-pyruvate, 2 mM glutamine and 10% FBS. Human brain astrocytes were purchased from Alphabioregen (HBMP202) and cultured in their adapted medium (AGPM-03, Alphabioregen). Cells were incubated at 37 °C in a humidified atmosphere with 5% CO_2. Cells were cultured and then treated once they reached 70–80% of their confluency inside the plates.

Establishing TMZ resistant GBM cell line. U87-MG cells were treated with 50 µM Temozolomide during 2 months. After this period, TMZ was retrieved from the culture medium and cells U87-MG (TMZ off) were regularly checked for their resistance to the drug by the Incucyte technology.

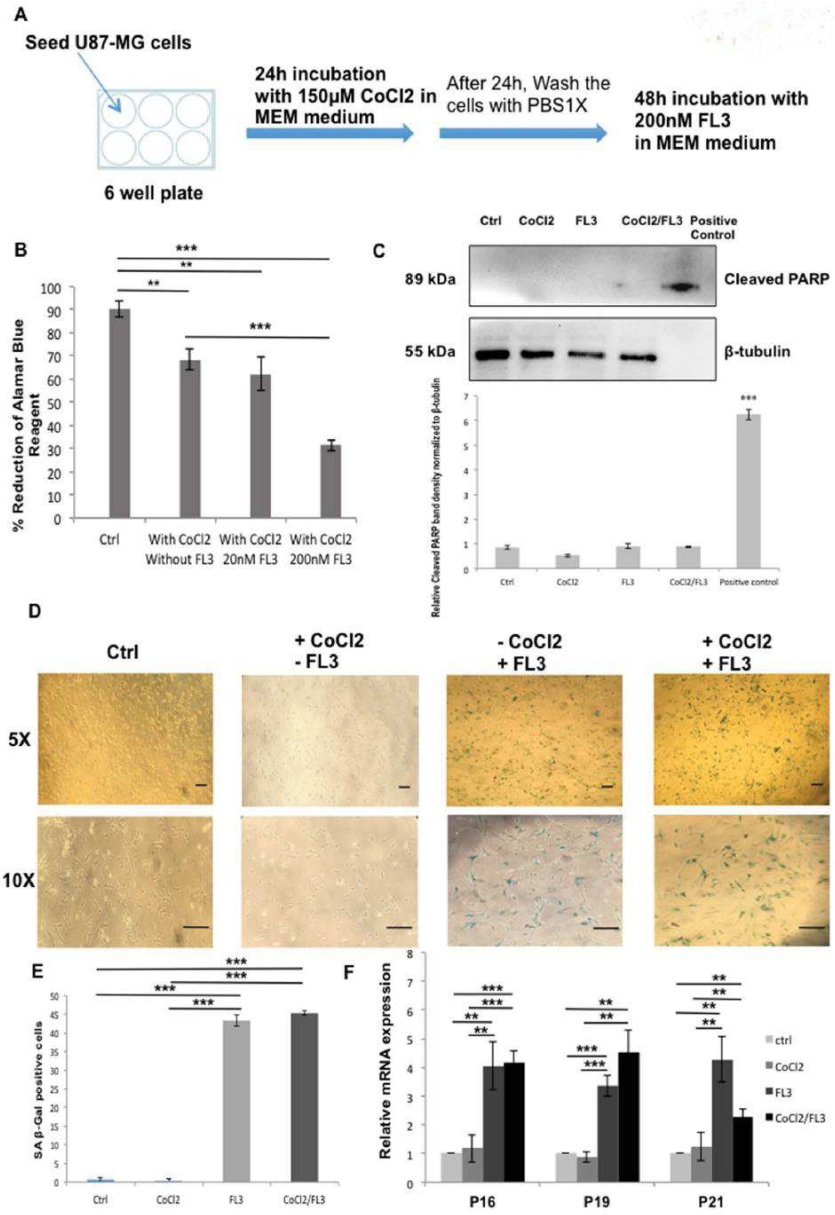
A
Seed U87-MG cells
6 well plate
24h incubation with 150µM CoCl2 in MEM medium
After 24h, Wash the cells with PBS1X
48h incubation with 200nM FL3 in MEM medium
B
% Reduction of Alamar Blue Reagent
Ctrl
With CoCl2 Without FL3
With CoCl2 20nM FL3
With CoCl2 200nM FL3
C
Ctrl
CoCl2
FL3
CoCl2/FL3
Positive Control
89 kDa
Cleaved PARP
55 kDa
β-tubulin
Relative Cleaved PARP band density normalized to β-tubulin
D
Ctrl
+ CoCl2 - FL3
- CoCl2 + FL3
+ CoCl2 + FL3
5X
10X
E
SA β-Gal positive cells
F
Relative mRNA expression
P16
P19
P21
ctrl
CoCl2
FL3
CoCl2/FL3

◂**Figure 6.** Effect of FL3 on hypoxic glioblastoma cancer cells model. (**A**) Representation of the experimental protocol used for the incubation of U87-MG cells with $CoCl_2$ and FL3. (**B**) Analysis of cell viability with the AlamarBlue assay in control cells and U87-MG cells treated with two concentrations of FL3 (20 nM and 200 nM), under hypoxia ($CoCl_2$). Quantification mean ± SEM from 3 independent experiments, $^{**}P < 0.01$, $^{***}P < 0.001$ from control, and from +$CoCl_2$. (**C**) Western Blot and quantification of cleaved PARP protein levels in control cells and U87-MG cells treated with 200 nM FL3 under normoxia and hypoxia ($CoCl_2$). Cleaved PARP protein was used as positive control. Quantification mean ± SEM from 3 independent experiments, $^{***}P < 0.001$ from control. (**D**) Representative senescence associated β-galactosidase staining (blue) of control cells, treated cells with $CoCl_2$ and U87-MG cells treated with 200 nM FL3, under normoxia and hypoxia ($CoCl_2$), 6 days after the FL3 treatment. The scale bar represents 200 µm. (**E**) Quantification of SA β-gal positive cells of control cells, treated cells with CoCl2 and treated U87-MG cells with 200 nM FL3, under normoxia and hypoxia ($CoCl_2$). 50 cells were analysed for each condition. Results for mean ± SEM from 3 independent experiments, $^{***}P < 0.001$ from control, and from +$CoCl_2$. (**F**) Relative mRNA expression levels of cell cycle inhibitors in control cells and U87-MG cells treated with 200 nM FL3 6 days post FL3 treatment, under normoxia and hypoxia ($CoCl_2$). Quantification of mean ± SEM from 3 independent experiments, $^{**}P < 0.01$, $^{***}P < 0.001$ from control, and from +$CoCl_2$.

Treatment of cells. *$CoCl_2$ treatment* 20×10^4 cells per well were seeded into 6 well plates and then treated for 24 h with different concentrations of $CoCl_2$ (50–300 µM) that were prepared from a stock solution of $CoCl_2$ (10 mM) (C8661, MERCK).

FL3 treatment A solution of FL3 in DMSO (10 mM) was graciously given from Dr. Laurent Désaubry (Laboratoire d'Innovation Thérapeutique, UMR 7200, Strasbourg, France). U87-MG cells were treated with FL3 at different concentrations (20–4000 nM) for different time points (24, 48 and 72 h). The highest concentration of DMSO, for treated and non-treated cells, never exceeded 0.002% (v/v) in order to avoid its side effects such as cell toxicity or cell differentiation. In some experiments, cells were kept in culture for 2 to 8 days post-FL3 treatment. Human brain astrocytes were treated with 200 nM of FL3 for 48 h.

FL3 treatment with $CoCl_2$ Cells were first treated with 150 µM of $CoCl_2$ for 24 h, and then washed with PBS 1X and treated with 200 nM of FL3 for additional 48 h. Cells were kept in culture for 2 to 8 days post-FL3 treatment.

TMZ treatment with FL3 Cells were first treated with 100 µM of TMZ for 72 h (we used this TMZ concentration to confirm that the cells are resistant to TMZ), and then washed with PBS 1X and treated with 200 nM of FL3 for additional 48 h. Cells were kept in culture for 6 days post-FL3 treatment.

Metabolic activity. U87-MG cells were seeded into each well of 24 well plates at 5×10^4 cells per well, and then treated with different FL3 concentrations (0, 20, 200, 1000, 2000 and 4000 nM) for 24, 48, and 72 h. AlamarBlue (Invitrogen, Thermo Fisher Scientific, Waltham, MA, USA) was used to assess cell proliferation over time. The AlamarBlue test is a non-toxic, water-soluble, colorimetric redox indicator that changes color in response to the cellular metabolism. At each time point, the cells were washed with PBS 1X and then incubated with 10% AlamarBlue solution diluted in phenol free medium (DMEM medium, BE12-197F, LONZA) for 4 h at 37 °C in a humidified atmosphere of 5% CO_2. Each condition was prepared in triplicate. After 4 h of incubation, 150 µL of incubation medium from each well were transferred to a 96-well plate and the resulting absorbance was measured with a spectrophotometer (Multiskan FC, Thermo Fisher Scientific, Ratastie, Finland), at 570 nm and 595 nm wavelength respectively. Results were shown as the percentage of reduction of AlamarBlue reagent and the percentage of living cells was calculated as the ratio between the OD value of each FL3-treated cell sample and the OD value of the control. The AlamarBlue assay was also done on treated human brain astrocytes with 200 nM of FL3 for 48 h. We did the same protocol of AlamarBlue on U87-MG (TMZ off), U373-MG and LN443 cells.

Cell cycle analysis. U87-MG cells were seeded into 6 well plates at 20×10^4 cells per well, and then treated with FL3 for 48 h. Afterwards, cells were trypsinized and centrifuged to have a unique pellet. The cell pellet is washed with PBS 1X and directly fixed with ethanol 70% for 30 min at 4 °C. The cell pellet was washed with PBS 1X, centrifuged at 850 g, and then treated with 100 µg/ml of ribonuclease (Sigma Aldrich), to finally stain it with 200 µl of Propidium Iodide (PI) (*life technologies*, Sigma Aldrich) at a concentration of 50 µg/ml (prepared from a 5 mg/ml stock solution). After 30 min of incubation at room temperature in the dark, cells were examined using a flow cytometer (MACS Quant, Miltenyi Biotec GmbH, Bergisch Gladbach R. F. A). A minimum of 20×10^3 cells was acquired per sample and data were analyzed using ModFit LT V3.3 software (Verity Software House, Topsahm, Maine, USA, https://www.vsh.com/products/mflt/). The percentage of cells in G0/G1, S and G2/M was determined from DNA content histograms.

Apoptosis analysis. Apoptosis was evaluated by measuring the externalization of phosphatidylserine with Annexin V, and nucleus labelling with propidium iodide (PI). In this context, cultured cells were treated with different concentrations of FL3 for 48 h. Apoptosis rates were assessed using flow cytometry (LSR 2 with Diva 6.2 Software, Becton Dickinson Biosciences, San Jose California, USA, https://www.bdbiosciences.com/en-us/instruments/research-instruments/research-software/flow-cytometry-acquisition/facsdiva-software) using the Annexin V-FITC/PI Apoptosis kit (V13241, Thermo Fisher Scientific) according to the manufacturer's recommendations.

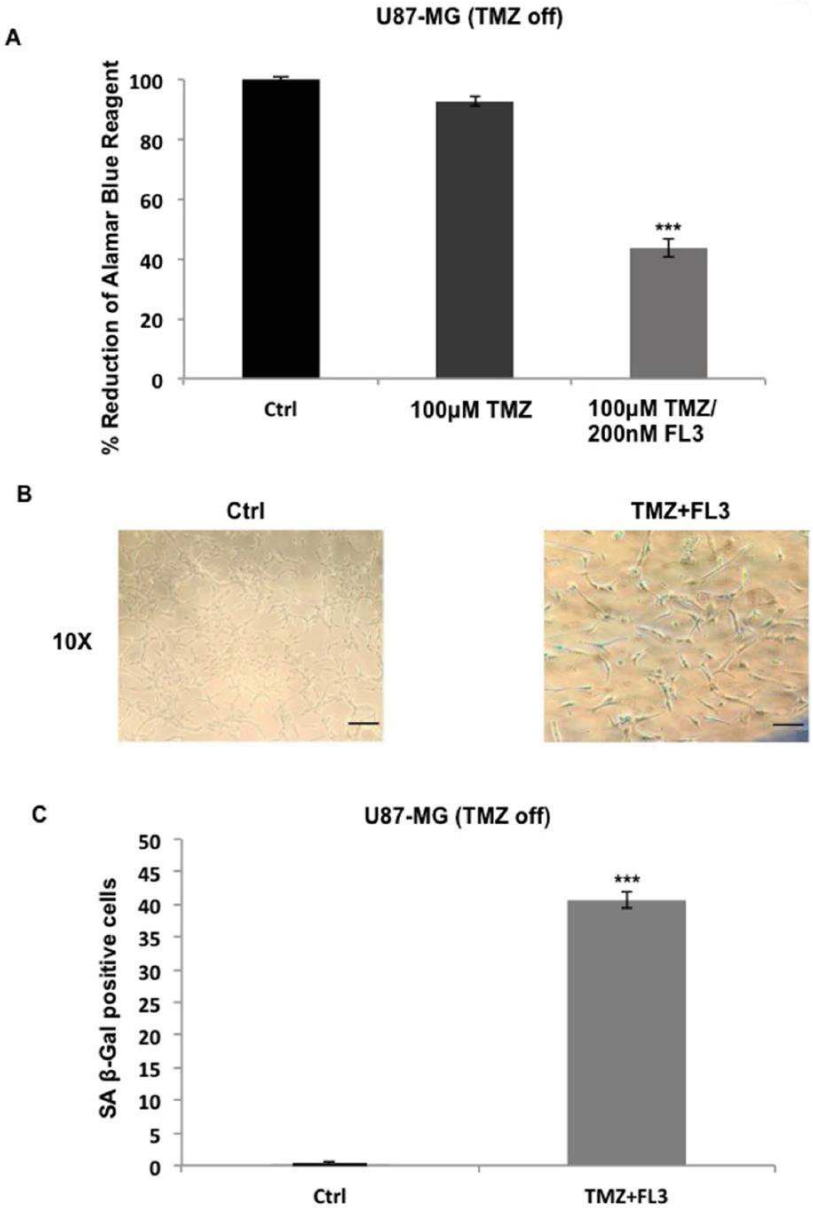

Figure 7. TMZ combination with FL3 induced senescence in U87-MG TMZ resistant cells. (**A**) Analysis of cell viability with the AlamarBlue assay in U87-MG (TMZ off) control cells, treated cells with 100 µM of TMZ and treated cells with 100 µM of TMZ + 200 nM of FL3. Quantification mean ± SEM from 3 independent experiments, ***$P < 0.001$ from control. (**B**) Representative senescence-associated β-galactosidase (SA β-gal) staining (blue) of U87-MG (TMZ off) control cells and treated cells with 100 µM of TMZ + 200 nM of FL3, 6 days after the FL3 treatment. Scale bar represents 100 µm. (**C**) Quantification of SA β-gal positive cells of U87-MG (TMZ off) control cells and treated cells 100 µM of TMZ + 200 nM of FL3. 50 cells were analysed for each condition. Results for mean ± SEM from 3 independent experiments, ***$P < 0.001$ from control.

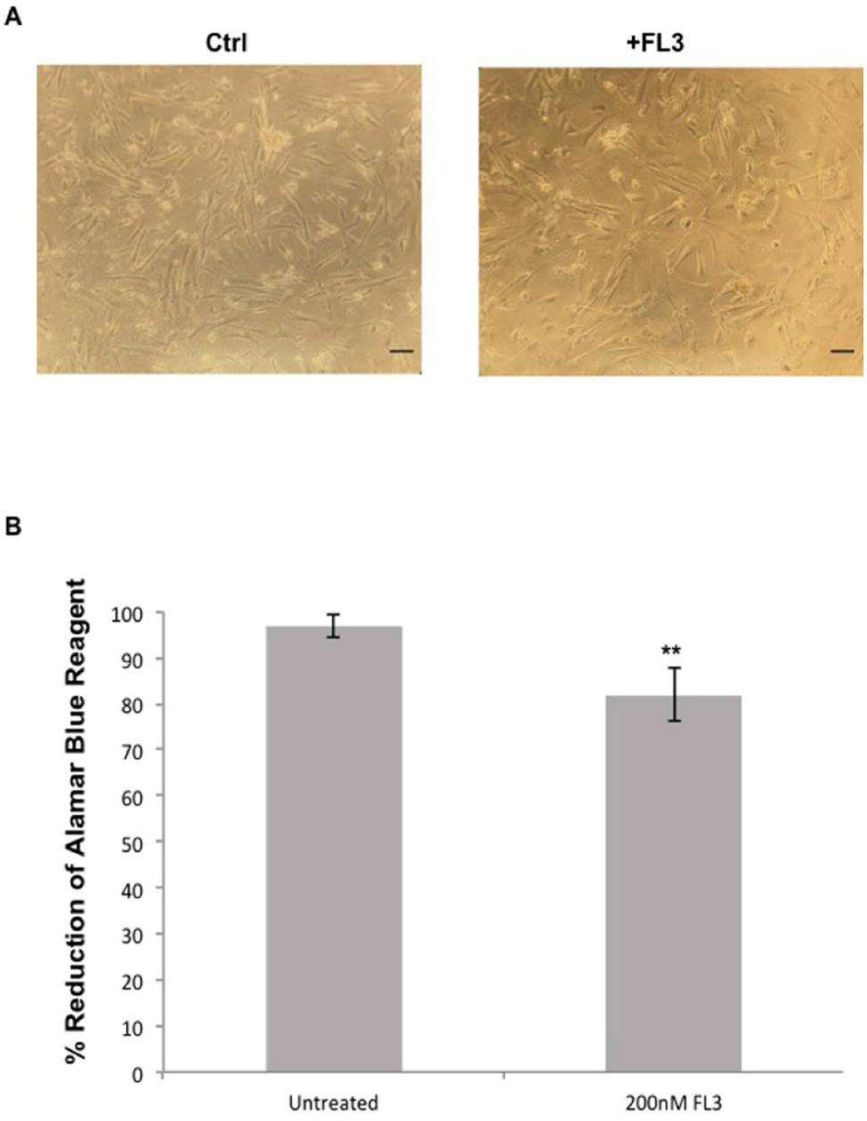

Figure 8. Effect of FL3 on Human brain astrocytes. (**A**) Representative images of control and treated human brain astrocytes with 200 nM FL3. Scale bar represents 100 µm. (**B**) Analysis of cell viability with AlamarBlue assay in human brain astrocytes without treatment and after treatment with 200 nM FL3 respectively. Quantification of mean ± SEM from 3 independent experiments, $^{**}P < 0.01$ from control.

RNA extraction and analysis. Total RNAs were isolated from the U87-MG cell line. 1 µg of RNA was retro-transcribed using the iScript Reverse Transcription Supermix (Bio-Rad Laboratories, Hercules, CA, USA) according to the manufacturer's instructions. Quantitative PCRs of retro-transcribed RNAs were performed and analyzed using the CFX Connect Real Time PCR Detection System (Bio-Rad, Mitry Mory, France). Amplification reactions had been performed using iTaq Universal SYBR Green Supermix (Bio-Rad, France). Actin was used as endogenous control (housekeeping gene) in all cDNA samples (See Table 1 for primers sequences). The

Genes	Forward primer	Reverse primer
Actin	5′-GATGAGATTGGCATGGCTTT-3′	5′-CACCTTCACCGTTCCAGTTT-3′
GLUT1	5′-CTGAAGTCGCACAGTGAATA-3′	5′-TGGGTGGAGTTAATGGAGTA-3′
GLUT3	5′-GACCCAGAGATGCTGTAATGGT-3′	5′-TGGCAAATATCAGAGCTGGGG-3′
HIF1α	5′-CTGCCACCACTGATGAATTA-3′	5′-GTATGTGGGTAGGAGATGGA-3′
VEGF	5′-CCTGGTGGACATCTTCCAGGAGTACC-3′	5′-GAAGCTCATCTCTCCTATGTGCTGGC-3′
p16	5′ CTTCGGCTGACTGGCTGG 3′	5′ TCATCATGACCTGGATCGGC 3′
p19	5′ CGCTGCAGGTCATGATGTTT 3′	5′ GGGTGTCCAGGAATCCAGTG 3′
p21	5′ TGCCGAAGTCAGTTCCTTGT 3′	5′ GTTCTGACATGGCGCCTCC 3′
CSF1	5′ TCCAGCCAAGATGTGGTGAC 3′	5′ TCAGAGTCCTCCCAGGTCAA 3′
CXCL1	5′ CCGAAGTCATAGCCACACTCA 3′	5′ TTCTTAACTATGGGGGATGCAG 3′
CXCL2	5′ GAAAGCTTGTCTCAACCCCG 3′	5′ TGGTCAGTTGGATTTGCCATTTT 3′
CXCL5	5′ CAGACCACGCAAGGAGTTCA 3′	5′ TCTTCAGGGAGGCTACCACT 3′
TNFα	5′ CTTGCGCAATGCCACCCA 3′	5′ TTCATCTTCAGCAGCCGGTC 3′

Table 1. Sequence of primers used for Q-PCR.

mRNA expression levels were calculated using the comparative Ct method ($2^{-\Delta\Delta Ct}$) and normalized to the housekeeping gene. All RT-qPCR assays were performed in triplicate and results were represented by the mean values.

Preparation and analysis of protein extracts. Cells were lysed in ice-cold radioimmunoprecipitation assay buffer (50 mM Tris, pH 7.5, 150 mM NaCl, 0.5% sodium deoxycholate, 0.1% SDS, 1% Triton, supplemented with protease inhibitor cocktail (Sigma-Aldrich). Protein extracts (50 µg) were electrophoresed on 10–15% SDS–polyacrylamide gels and electroblotted to Hybond nitrocellulose membranes (Invitrogen) using iBlot transfer (Invitrogen). Proteins were detected using primary antibodies directed against cleaved PARP 552596 (BD Biosciences), HIF1α (ab17983, Abcam, 1:1000), cyclin-D1 (sc-8396, Santa Cruz, 1:1000), phospho-p38 (9215, Cell Signaling, 1:1000), β-actin (66009-10-Ig, Proteintech, 1:5000), GAPDH (60,004–10-Ig, Proteintech, 1:5000), β-tubulin (10094-1-AP, Proteintech, 1:5000). Membranes were probed with HRP-conjugated mouse (A90-147P, Bethyl Laboratories) and rabbit (sc-2004; Santa Cruz) secondary antibodies, and were detected using ECL chemiluminescence substrate solution (SuperSignal West Pico Plus, Thermo Scientific, USA). Autoradiographic signals were captured on an iBright Imaging System (Invitrogen) and analyzed by the NIH's Image J software (Supplementary Fig. 1).

SA-β gal staining. U87-MG cells were seeded into 24 well plates at 5×10^4 cells per well, and then treated with FL3 for 48 h. Afterwards, the treatment was stopped, cells were washed with PBS, refilled with new fresh medium and incubated for 8 days. Medium was changed every two days. At each time point (2, 4, 6 and 8 days), an aliquot of the cells was fixed and stained with the senescence β-galactosidase staining kit #9860 (Cell Signaling), and then kept in a dry incubator (without CO_2) at 37 °C overnight. Cells were checked under an inverted microscope (Nikon Eclipse TS100, Nikon) for blue color detection and photos were taken using the NIS element software (Nikon). We did the same protocol of SA-β Gal staining on U87-MG (TMZ off), U373-MG and LN443 cells.

Live/dead assay. U87-MG cells were seeded onto coverslips in 24 well plates at 5×10^4 cells per well, and then treated with 200 nM of FL3 for 48 h. After 48 h, the treatment was stopped, and the wells were washed with PBS. The cells were trypsinized and then centrifuged to have a unique pellet. The cell pellet was resuspended in the live/dead assay dye solution for 10 min (Live/dead cell assay kit, Abcam, ab115347), and then visualized under an epifluorescence microscope (Leica DM4000 B).

Immunofluorescence. U87-MG cells were seeded onto coverslips in 24 well plates at 5×10^y cells per well, and then treated with $CoCl_2$ for 24 h. After 24 h, the media was changed, and the wells were washed with PBS. Later, the cells were fixed with PFA 4% for 10 min, rinsed with PBS, permeabilized and saturated with PBS—0.2% Triton—3% BSA solution for 30 min. Then, the cells were incubated with the Cytochrome C 556432 (BD Biosciences) primary antibody diluted at 1/300 for 45 min. After three washes with PBS, cells were incubated for 1 h with anti-mouse secondary antibody (diluted at 1/200) conjugated to Alexa Fluor 594 (A21203, Thermo Fisher Scientific). The cells were washed with PBS and incubated for 5 min with Hoescht 33342 (H3570, Invitorgen, Thermo Fisher Scientific) diluted at 1/10,000 in PBS in order to stain the nucleus in blue. Cells were visualized under a fluorescence microscope (Nikon Eclipse 80i, Nikon).

Statistical analysis. Statistical analyses are performed using *t*-test. All data are presented as mean ± SEM from three independent experiments. $^*P < 0.05$; $^{**}P < 0.01$; $^{***}P < 0.001$.

Received: 24 April 2020; Accepted: 30 July 2020
Published online: 13 August 2020

References

1. Polier, G. *et al.* The natural anticancer compounds rocaglamides inhibit the Raf-MEK-ERK pathway by targeting prohibitin 1 and 2. *Chem. Biol.* **19**(9), 1093–1104 (2012).
2. Qureshi, R. *et al.* FL3, a synthetic flavagline and ligand of prohibitins, protects cardiomyocytes via STAT3 from doxorubicin toxicity. *PLoS ONE* **10**(11), e0141826 (2015).
3. King, M. L. *et al.* X-ray crystal structure of rocaglamide, a novel antileulemic 1 H-cyclopenta [b] benzofuran from Aglaia elliptifolia. *J. Chem. Soc. Chem. Commun.* **20**, 1150–1151 (1982).
4. Basmadjian, C., Thuaud, F., Ribeiro, N. & Désaubry, L. Flavaglines: potent anticancer drugs that target prohibitins and the helicase eIF4A. *Future Med. Chem.* **5**(18), 2185–2197 (2013).
5. Yuan, G. *et al.* Flavagline analog FL3 induces cell cycle arrest in urothelial carcinoma cell of the bladder by inhibiting the Akt/PHB interaction to activate the GADD45α pathway. *J. Exp. Clin. Cancer Res.* **37**(1), 21 (2018).
6. Jiang, L. *et al.* Akt phosphorylates Prohibitin 1 to mediate its mitochondrial localization and promote proliferation of bladder cancer cells. *Cell Death Dis.* **6**(2), e1660–e1660 (2015).
7. Wang, D. *et al.* Prohibitin ligands: a growing armamentarium to tackle cancers, osteoporosis, inflammatory, cardiac and neurological diseases. *Cell. Mol. Life Sci.* **15**, 1–22 (2020).
8. McClung, J. K. *et al.* Isolation of a cDNA that hybrid selects antiproliferative mRNA from rat liver. *Biochem. Biophys. Res. Commun.* **164**(3), 1316–1322 (1989).
9. Emhemmed, F. *et al.* Selective anticancer effects of a synthetic flavagline on human Oct4-expressing cancer stem-like cells via a p38 MAPK-dependent caspase-3-dependent pathway. *Biochem. Pharmacol.* **89**(2), 185–196 (2014).
10. Yan, C. *et al.* PHB2 (prohibitin 2) promotes PINK1-PRKN/Parkin-dependent mitophagy by the PARL-PGAM5-PINK1 axis. *Autophagy* **16**(3), 419–434 (2020).
11. Hanif, F., Muzaffar, K., Perveen, K., Malhi, S. M. & Simjee, S. U. Glioblastoma multiforme: a review of its epidemiology and pathogenesis through clinical presentation and treatment. *Asian Pac. J. Cancer Prev. APJCP* **18**(1), 3 (2017).
12. Perrin, S. L. *et al.* Glioblastoma heterogeneity and the tumour microenvironment: implications for preclinical research and development of new treatments. *Biochem. Soc. Trans.* **47**(2), 625–638 (2019).
13. Rønning, P. A., Helseth, E., Meling, T. R. & Johannesen, T. B. A population-based study on the effect of temozolomide in the treatment of glioblastoma multiforme. *Neuro-oncology* **14**(9), 1178–1184 (2012).
14. Kore, R. A. *et al.* Hypoxia-derived exosomes induce putative altered pathways in biosynthesis and ion regulatory channels in glioblastoma cells. *Biochem. Biophys. Rep.* **14**, 104–113 (2018).
15. Sattiraju, A., Sai, K. K. S. & Mintz, A. Glioblastoma stem cells and their microenvironment. In *Stem Cell Microenvironments and Beyond* (ed. Birbrair, A.) 119–140 (Springer, Cham, 2017).
16. Yang, L., Lin, C., Wang, L., Guo, H. & Wang, X. Hypoxia and hypoxia-inducible factors in glioblastoma multiforme progression and therapeutic implications. *Exp. Cell Res.* **318**(19), 2417–2426 (2012).
17. Kaur, B. *et al.* Hypoxia and the hypoxia-inducible-factor pathway in glioma growth and angiogenesis. *Neuro-oncology* **7**(2), 134–153 (2005).
18. Monteiro, A., Hill, R., Pilkington, G. & Madureira, P. The role of hypoxia in glioblastoma invasion. *Cells* **6**(4), 45 (2017).
19. Xu, H. *et al.* Epidermal growth factor receptor in glioblastoma. *Oncol. Lett.* **14**(1), 512–516 (2017).
20. Pearson, J. R. & Regad, T. Targeting cellular pathways in glioblastoma multiforme. *Signal Transduct. Target. Ther.* **2**(1), 1–11 (2017).
21. Søndergaard, K. L., Hilton, D. A., Penney, M., Ollerenshaw, M. & Demaine, A. G. Expression of hypoxia inducible factor 1α in tumours of patients with glioblastoma. *Neuropathol. Appl. Neurobiol.* **28**(3), 210–217 (2002).
22. Vengoji, R. *et al.* Afatinib and Temozolomide combination inhibits tumorigenesis by targeting EGFRvIII-cMet signaling in glioblastoma cells. *J. Exp. Clin. Cancer Res.* **38**(1), 266 (2019).
23. Saggar, J. K. & Tannock, I. F. Chemotherapy rescues hypoxic tumor cells and induces their reoxygenation and repopulation—an effect that is inhibited by the hypoxia-activated prodrug TH-302. *Clin. Cancer Res.* **21**(9), 2107–2114 (2015).
24. Yoon, K. B., Park, K. R., Kim, S. Y. & Han, S. Y. Induction of nuclear enlargement and senescence by sirtuin inhibitors in glioblastoma cells. *Immune Netw.* **16**(3), 183–188 (2016).
25. Huang, Y. *et al.* Cobalt chloride and low oxygen tension trigger differentiation of acute myeloid leukemic cells: possible mediation of hypoxia-inducible factor-1 α. *Leukemia* **17**, 2065–2073 (2003).
26. Jung, J. Y. & Kim, W. J. Involvement of mitochondrial-and Fas-mediated dual mechanism in $CoCl_2$-induced apoptosis of rat PC12 cells. *Neurosci. Lett.* **371**(2–3), 85–90 (2004).
27. Lee, S. K., Cui, B., Mehta, R. R., Kinghorn, A. D., & Pezzuto, J. M. Cytostatic mechanism and antitumor potential of novel 1H-cyclopenta [b] benzofuran lignans isolated from Aglaiaelliptica. *Chem. Biol. Interact.*, **115**(3), 215–228 (1998).
28. Hausott, B., Greger, H., & Marian, B. Flavaglines: a group of efficient growth inhibitors block cell cycle progression and induce apoptosis in colorectal cancer cells. *Int. J. Cancer*, **109**(6), 933–940 (2004).
29. Cencic, R. *et al.* Antitumor activity and mechanism of action of the cyclopenta [b] benzofuran, silvestrol. *PLoS ONE* **4**(4), e5223 (2009).
30. Thuaud, F. *et al.* Synthetic analogue of rocaglaol displays a potent and selective cytotoxicity in cancer cells: involvement of apoptosis inducing factor and caspase-12. *J. Med. Chem.* **52**(16), 5176–5187 (2009).
31. Park, H. Y. *et al.* Fucoidan inhibits the proliferation of human urinary bladder cancer T24 cells by blocking cell cycle progression and inducing apoptosis. *Molecules* **19**(5), 5981–5998 (2014).
32. Brauns, S. C., Dealtry, G., Milne, P., Naudé, R. & Van de venter, M. A. Caspase-3 activation and induction of PARP cleavage by cyclic dipeptide cyclo (Phe-Pro) in HT-29 cells. *Anticancer Res.* **25**(6B), 4197–4202 (2005).
33. Campisi, J. Aging, cellular senescence, and cancer. *Annu. Rev. Physiol.* **75**, 685–705 (2013).
34. Ritschka, B. *et al.* The senescence-associated secretory phenotype induces cellular plasticity and tissue regeneration. *Genes Dev.* **31**(2), 172–183 (2017).
35. Coppé, J. P., Desprez, P. Y., Krtolica, A. & Campisi, J. The senescence-associated secretory phenotype: the dark side of tumor suppression. *Annu. Revi. Pathol. Mech. Dis.* **5**, 99–118 (2010).
36. He, S. & Sharpless, N. E. Senescence in health and disease. *Cell* **169**(6), 1000–1011 (2017).
37. Aasland, D. *et al.* Temozolomide Induces Senescence and Repression of DNA Repair Pathways in Glioblastoma Cells via Activation of ATR–CHK1, p21, and NF-κB. *Cancer Res.* **79**(1), 99–113 (2019).
38. Hirose, Y., Berger, M. S. & Pieper, R. O. p53 effects both the duration of G2/M arrest and the fate of temozolomide-treated human glioblastoma cells. *Cancer Res.* **61**(5), 1957–1963 (2001).
39. Christmann, M., Aasland, D., Roos, W., Kaina, B. & Tomicic, M. PO-210 anticancer drug-induced senescence in glioblastoma cells is associated with changes in DNA repair capacity. *ESMO Open* **3**, A102.1-A102 (2018).
40. Chen, W. L., Pan, L., Kinghorn, A. D., Swanson, S. M. & Burdette, J. E. Silvestrol induces early autophagy and apoptosis in human melanoma cells. *BMC Cancer* **16**(1), 17 (2016).

41. Valko, M., Izakovic, M., Mazur, M., Rhodes, C. J. & Telser, J. Role of oxygen radicals in DNA damage and cancer incidence. *Mol. Cell. Biochem.* **266**(1–2), 37–56 (2004).
42. Manoochehri Khoshinani, H., Afshar, S. & Najafi, R. Hypoxia: a double-edged sword in cancer therapy. *Cancer Investig.* **34**(10), 536–545 (2016).
43. Rohwer, N. & Cramer, T. Hypoxia-mediated drug resistance: novel insights on the functional interaction of HIFs and cell death pathways. *Drug Resist. Updates* **14**(3), 191–201 (2011).
44. Epstein, A. C. *et al. C. elegans* EGL-9 and mammalian homologs define a family of dioxygenases that regulate HIF by prolyl hydroxylation. *Cell* **107**(1), 43–54 (2001).
45. Lee, H. R., Leslie, F. & Azarin, S. M. A facile in vitro platform to study cancer cell dormancy under hypoxic microenvironments using $CoCl_2$. *J. Biol. Eng.* **12**(1), 12 (2018).
46. Wan, Y. Y. *et al.* Involvement of Drp1 in hypoxia-induced migration of human glioblastoma U251 cells. *Oncol. Rep.* **32**(2), 619–626 (2014).

Author contributions

I-G.Y., B-J.N. and F.F. contributed to the design and the supervision of the study; H.E., S.J. and C.H. performed the experiments; B.J contributed to the acquisition and analysis of flow cytometer results; D.L. provided the synthetic derivative of flavagline FL3; H.E., M.T., U-S.G., B-J.N. and I-G.Y. contributed to the analysis and interpretation of the data; I-G.Y. and H.E. wrote the paper; G.S., U-S.G., F.G., B-J.N. contributed to the corrections.

Competing interests

The authors declare no competing interests.

Additional information

Supplementary information is available for this paper at https://doi.org/10.1038/s41598-020-70820-6.

Correspondence and requests for materials should be addressed to N.B.-J. or Y.I.-G.

Reprints and permissions information is available at www.nature.com/reprints.

Publisher's note Springer Nature remains neutral with regard to jurisdictional claims in published maps and institutional affiliations.

Summary in French

Résistance des glioblastomes au témozolomide : Implication des voies de signalisation α5β1 integrin et p53

Le glioblastome (GBM) est la tumeur cérébrale maligne la plus courante et la plus agressive chez l'adulte, qui se caractérise par une forte prolifération, une invasion dans le tissu cérébral normal et une résistance aux thérapies (Geraldo et al., 2019 ; Omuro, 2013). Il n'existe actuellement aucun traitement efficace à long terme pour cette maladie mortelle, mais la norme de soins est la résection chirurgicale maximale, suivie d'une radiothérapie avec chimiothérapie concomitante et adjuvante au témazolomide (TMZ) (Stupp et al., 2005). Cependant, le pronostic des patients atteints de glioblastome reste faible et ne s'est pas amélioré malgré de nombreux essais cliniques sur de nouvelles propositions thérapeutiques. Il existe donc un besoin urgent de nouvelles stratégies thérapeutiques qui peuvent être soulignées par une compréhension approfondie de la GBM et de la diaphonie du microenvironnement environnant.

La résistance primaire et la résistance acquise sont les principaux défis à relever pour l'utilisation clinique des thérapies standard et ciblées dans le cadre de la GBM (Hombach-Klonisch et al., 2018 ; Yi et al., 2019). Le principal mécanisme de résistance des glioblastomes à la TMZ implique la O6-méthylguanine ADN méthyl transférase (MGMT), une enzyme suicide qui permet la réparation directe de la lésion causée par la TMZ, par l'élimination du groupe méthyle en position O6 de la guanine (Park et al., 2012). Des études antérieures ont montré que l'accumulation cellulaire de la protéine suppresseur de tumeur p53 régule à la baisse l'expression de la MGMT (Grombacher et al., 1998 ; Harris et al., 1996). La protéine p53 est mutée dans environ 30 % des glioblastomes (Brennan et al., 2013), bien qu'un sous-type de glioblastome exprimant principalement le type sauvage p53 ait été identifié dans une analyse génomique intégrée (Verhaak et al., 2010). Mais même si le type sauvage p53 est exprimé dans 70% des GBM, ses fonctions sont fréquemment supprimées par les MDM2/MDM4, les ubiquitines ligases E3 qui marquent et ciblent p53 pour la dégradation protéasomique (Crespo et al., 2015 ; England et al., 2013 ; Vassilev, 2004). La MDM2, une phosphoprotéine nucléaire du doigt de zinc et un régulateur négatif de la protéine p53, est souvent surexprimée dans la GBM et a été impliquée dans la prolifération et la survie des cellules cancéreuses (Her et al., 2018 ; Reifenberger et al., 1993 ; Verreault et al., 2016). L'inhibition de l'interaction p53-MDM2 peut sauver la dégradation de p53 et restaurer l'activité transcriptionnelle de p53, conduisant à l'induction de l'apoptose des cellules tumorales par p53, faisant ainsi du complexe p53-MDM2 une cible prometteuse pour les glioblastomes exprimant le type sauvage p53

(England et al., 2013 ; Vassilev, 2004). La découverte de Nutlin-3a, l'inhibiteur de p53-MDM2, a représenté une percée dans le développement des activateurs de p53 (Vassilev, 2004). Le développement plus récent de RG7388 (Idasanutlin), un inhibiteur de MDM2 de deuxième génération plus puissant, plus sélectif, plus biodisponible et doté d'une capacité efficace d'activation de p53, qui conduit à l'induction de l'apoptose des cellules tumorales par l'intermédiaire de p53, est prometteur pour les cancers, y compris le GBM (Berberich et al., 2019 ; Fishlock et al., 2018).

Les intégrines ont fait l'objet de nombreuses études au cours des 20 dernières années, en raison du rôle essentiel qu'elles jouent dans la progression des tumeurs. Les intégrines sont des récepteurs transmembranaires hétérodimériques de surface cellulaire qui servent de médiateurs pour l'adhésion des cellules à la matrice extracellulaire (MEC) et soutiennent les interactions entre cellules dans de multiples conditions physiologiques et pathologiques (Ellert-Miklaszewska et al., 2020 ; Malric et al., 2017). La dérégulation fréquente des expressions et des voies d'expression des intégrines dans les cellules cancéreuses souligne les contributions majeures des intégrines spécifiques dans la croissance des tumeurs et la résistance aux thérapies. Il a été démontré que la perturbation des voies de signalisation des intégrines par les antagonistes des intégrines inhibe la croissance tumorale et sensibilise les tumeurs aux thérapies dans des contextes précliniques. Le cilengitide a été le premier antagoniste des intégrines αvβ3/β5 à arriver en clinique mais les essais cliniques avec le cilengitide en combinaison avec la norme de soins (protocole Stupp) ont échoué (Stupp et al., 2010, 2014). Plusieurs raisons peuvent expliquer ces échecs, comme indiqué dans (Tucci et al., 2014). Cependant, les connaissances sur les expressions et les fonctions des intégrines dans les glioblastomes méritent d'être approfondies pour adapter les thérapies à base d'intégrines à des sous-populations spécifiques de patients. Ainsi, l'expression de l'intégrine α5 est améliorée dans le sous-groupe mésenchymateux des patients atteints de glioblastome par rapport aux autres (Ellert-Miklaszewska et al., 2020 ; Janouskova et al., 2012), ce qui confère probablement à ces patients une meilleure sensibilité à la thérapie anti-α5 à base d'intégrines.

Nous et d'autres (Janouskova et al., 2012 ; Renner et al., 2016) avons montré précédemment que l'intégrine α5β1 est une cible thérapeutique intéressante pour la GBM. Sa surexpression au niveau de l'ARNm (Lathia et al., 2014) ou de la protéine définit des populations de patients dont le pronostic est moins bon. Des expériences précliniques ont montré que cette intégrine est impliquée dans la survie, la migration, la résistance aux thérapies et la néoangiogénèse, tous étant des signes distinctifs de la GBM (Hynes, 2002 ; Janouskova et al., 2012 ; Murphy et al.,

2015 ; Ray et al., 2014). En particulier, nous avons démontré l'existence d'un croisement négatif entre l'intégrine α5β1 et les voies p53 soutenant une implication dans la résistance des gliomes aux chimiothérapies (Janouskova et al., 2012 ; Martin et al., 2012). Nous avons également montré que l'inhibition de l'intégrine concomitamment à l'activation de p53 avec Nutlin-3a dans les cellules surexprimant α5 a conduit à une augmentation considérable de l'apoptose cellulaire (Renner et al., 2016).

Les expressions d'intégrines dans la GBM varient après les thérapies (Malric et al., 2017). À titre d'exemple, il a été démontré que dans les tumeurs récurrentes après un traitement au bevacizumab, l'intégrine α5β1 était surexprimée dans une sous-population de patients (Delay et al, 2012). Dans cette étude, nous avons cherché à :

I. Comparer l'effet de différents activateurs p53 dans les cellules U87MG

II. Explorer le rôle de l'intégrine α5β1 dans la voie p53/MDM2

III. Déterminer le rôle de l'intégrine α5β1 dans la résistance des GBM à la TMZ

IV. Explorer de nouvelles thérapies combinées pour les cellules GBM résistantes aux TMZ

On a obtenu des cellules U87MG résistantes au témazolomide qui conservent la résistance même après l'élimination du médicament. L'analyse transcriptomique de cellules U87MG non traitées et de cellules résistantes cultivées en présence ou en absence de TMZ a montré une forte variation du niveau des intégrines. Il est intéressant de noter que l'expression des intégrines sur α5β1 diminue en présence mais se rétablit après l'élimination du médicament, ce qui suggère qu'il pourrait représenter une cible thérapeutique pour les glioblastomes récurrents. Nous avons également cherché à savoir si le traitement de ces cellules résistantes aux TMZ récurrentes pouvait être sensible à une combinaison d'antagonistes des intégrines et de réactivants p53. Nos résultats pourraient ajouter de nouvelles perspectives thérapeutiques pour les glioblastomes récurrents exprimant un niveau élevé d'intégrine α5β1.

Résultats partie 1

1. Comparaison des différents modes d'activation de p53 dans les cellules U87MG

La restauration de l'activité de p53 par inhibition de l'interaction p53-MDM2 est considérée comme une approche intéressante pour le traitement du cancer. Nous avons étudié l'impact de la réactivation de p53 par Nutlin-3a, Idasanutlin et RITA. Nutlin-3a est un médicament non génotoxique, connu pour inhiber la boucle de régulation de la rétroaction négative p53-mdm2

en se liant au mdm2 pour empêcher la dégradation de p53 dépendante du mdm2, ce qui entraîne l'activation directe de p53 (Tovar et al., 2013). Comme la Nutlin-3a, l'Idasanutlin se lie également au MDM2 pour perturber l'interaction p53-MDM2, mais cette deuxième génération d'inhibiteur du MDM2 est très puissante et sélective (Ding et al., 2013). RITA est un autre activateur p53 non génotoxique qui a été décrit. Contrairement à Nutlin-3a et Idasanutlin, RITA se lie à p53 pour altérer l'interaction p53-mdm2, ce qui entraîne une stabilisation et une activation de p53 (Issaeva et al., 2004). Les effets de ces activateurs p53 sur la confluence cellulaire, la viabilité et l'activation de la voie de signalisation p53 ont été comparés en utilisant respectivement la technologie Incucyte, le test d'exclusion du bleu de trypan et les Western Blots.

1.1. Effet des activateurs p53 sur la confluence cellulaire et la morphologie des cellules U87MG

Pour déterminer si Nutlin-3a, Idasanutlin et RITA répriment la confluence cellulaire dans les cellules U87MG, nous avons traité les cellules U87MG avec Nutlin-3a 1µM, Idasanutlin 1µM et RITA 1µM et la confluence cellulaire a été détectée et calculée dynamiquement à l'aide du logiciel IncuCyte Zoom basé sur des images à contraste de phase obtenues en temps réel. La Nutlin-3a, l'Idasanutlin et le RITA ont tous diminué de manière significative la confluence cellulaire dans les cellules U87MG. Aucune différence n'a été observée entre le traitement avec Nutlin-3a et RITA. Cependant, l'activateur p53, l'idasanutline, a diminué plus efficacement la confluence cellulaire que les traitements avec Nutlin-3a ou RITA. De plus, les images de contraste de phase obtenues à partir de l'IncuCyte en temps réel ont révélé que le traitement avec Nutlin-3a 1µM, Idasanutlin 1µM et RITA 1µM ont tous diminué le nombre de cellules et la confluence 72 heures après le traitement. Par rapport à Nutlin-3a ou RITA, le traitement à l'Idasanutlin 1µM a permis de réduire plus efficacement le nombre de cellules et la confluence des cellules U87MG.

Ces résultats suggèrent que le traitement avec Nutlin-3a, Idasanutlin et RITA ont tous supprimé la confluence des cellules U87MG. Comparé à Nutlin-3a et RITA, l'Idasanutlin est le plus efficace.

1.2. Effet dose-dépendant des activateurs p53 sur la viabilité et la confluence des cellules U87MG

Pour étudier l'effet de Nutlin-3a et de RITA sur la viabilité cellulaire in vitro, des cellules U87MG ont été traitées avec des concentrations croissantes de Nutlin-3a (1 et 5µM) et de RITA

(0,1, 0,5 et 1µM) pendant 72 heures. A la fin de l'expérience, un test d'exclusion au bleu de trypan a été utilisé pour détecter la survie des cellules. Le test d'exclusion au bleu de trypan a révélé que Nutlin-3a et la dose de RITA diminuaient la viabilité cellulaire des cellules U87MG de manière dépendante. Aucune différence statistiquement significative n'a été observée entre le traitement avec Nutlin-3a (1µM) et RITA (1µM).

Nous avons ensuite traité les cellules U87MG avec des concentrations croissantes d'idasanutline (0,05, 0,1, 0,2, 0,4 et 0,8 µM) et la confluence cellulaire a été détectée et calculée de manière dynamique à l'aide du logiciel IncuCyte Zoom basé sur des images à contraste de phase obtenues en temps réel. Le traitement à l'idasanutline a permis de réduire la confluence cellulaire des cellules U87MG en fonction de la dose, même à la plus faible concentration de 0,05 µM.

Ces résultats suggèrent que le traitement avec Nutlin-3a, Idasanutlin et RITA a supprimé la confluence cellulaire et la viabilité dans les cellules U87MG avec Idasanutlin a été le plus efficace.

2.3. L'effet des activateurs p53 sur la confluence cellulaire dépend du statut p53 des cellules

Nous avons démontré que Nutlin-3a, Idasanutlin et RITA diminuent la confluence cellulaire dans les cellules U87MG exprimant le type sauvage p53. Au cours de ces travaux, nous avons généré des cellules U87MG résistantes aux TMZ (cellules U87MG OFF R50) à partir de cellules U87MG. Nous nous sommes demandé si les activateurs p53 auraient un impact sur ces cellules comme cela a été observé dans les cellules parentales. Pour confirmer ce point, nous avons traité les cellules U87MG OFF R50 résistantes aux TMZ avec Nutlin-3a 1µM, Idasanutlin 1µM et RITA 1µM, et la confluence cellulaire a été détectée dynamiquement et calculée à l'aide du logiciel Incucyte Zoom sur la base d'images à contraste de phase obtenues en temps réel. Comme prévu, Nutlin-3a, Idasanutlin et RITA ont tous diminué de manière significative la confluence cellulaire dans les cellules U87MG OFF R50 résistantes au TMZ. L'idasanutline était la plus efficace, tandis que le RITA semblait être le moins efficace pour diminuer la confluence cellulaire dans ces cellules. De plus, les images en contraste de phase ont révélé que le traitement avec Nutlin-3a 1µM, Idasanutlin 1µM et RITA 1µM diminuaient tous le nombre de cellules et la confluence 72 heures après le traitement. De même, l'idasanutlin était le plus efficace, tandis que le RITA semblait être le moins efficace pour diminuer le nombre de cellules et la confluence de ces cellules.

Sur la base de ces résultats, nous nous sommes demandé si les effets observés des activateurs p53 sur la confluence cellulaire dépendaient de l'état p53 des cellules. Pour confirmer ce point, nous avons traité des cellules U373MG exprimant le p53 mutant avec Nutlin-3a 1µM et Idasanutlin 0.1µM et la confluence cellulaire a été détectée dynamiquement et calculée à l'aide du logiciel IncuCyte Zoom basé sur des images de contraste de phase obtenues en temps réel. Dans ces cellules, le traitement avec Nutlin-3a 1µM et Idasanutlin 0.1µM n'a pas inhibé la confluence cellulaire. Aucune différence observable dans la morphologie cellulaire des cellules U373 MG traitées avec Nutlin-3a ou Idasanutlin par rapport au contrôle n'a été observée.

Ces résultats ont confirmé que la suppression de la confluence cellulaire par les activateurs p53 dépend du statut p53 des cellules et que les cellules mutantes p53 ne seront pas affectées.

2.4. Effet de Nutlin-3a, RITA et Idasanutlin sur la voie p53

Pour étudier l'impact de la réactivation de p53 par Nutlin-3a, RITA et Idasanutlin, nous avons évalué la réactivation de la voie p53 en évaluant la stabilité et l'activité de la protéine p53 dans les cellules U87MG 24 et 48 heures après le traitement avec des concentrations croissantes de Nutlin-3a (1 et 5 µM) et RITA (0,1, 0,5 et 1µM). L'analyse par Western blot a montré que le traitement par Nutlin-3a augmentait significativement et de manière proportionnelle à la dose la stabilité de la protéine p53 dans les cellules U87MG à la fois 24 et 48 heures après le traitement. L'expression de la protéine MDM2 a également été augmentée de manière significative et en fonction de la dose par Nutlin-3a à tous les points de temps testés. En outre, Nutlin-3a à 5µM (mais pas à 1µM) diminue de manière significative les niveaux de protéine de l'intégrine α5 dans ces cellules 24 heures après le traitement. Cette diminution dépendait du temps, car le traitement par Nutlin-3a à 1µM et 5µM a réduit de manière significative les niveaux de protéines de l'intégrine 48 heures après le traitement. Pour justifier l'activation de p53 dans la GBM par Nutlin-3a, nous avons traité des cellules U87MG R50 et U87 MG OF R50, qui sont toutes deux des modèles de GBM résistantes aux TMZ, avec Nulin-3a et évalué les effets sur la stabilité de p53 et l'expression de MDM2 par western blot. Il est intéressant de noter que le traitement avec Nutlin-3a a augmenté de manière dépendante de la dose la stabilité/activité de p53 et l'expression de MDM2 dans les cellules U87MG R50 et U87 MG OF R50. Comme Nutlin-3a, la dose d'idasanutline a augmenté de manière dépendante la stabilité de la protéine p53. En outre, l'idasanutline s'est avérée plus puissante que la Nutlin-3a, car elle stabilise efficacement la protéine p53 à une concentration inférieure de 0,1 µM.

Ensemble, nous avons démontré que Nutlin-3a, RITA et Idasanutlin stabilisaient tous la protéine p53, l'Idasanutlin étant le plus efficace. De plus, la stabilisation de la protéine p53 s'est accompagnée d'une diminution du niveau de l'intégrine α5.

Pour comparer Nutlin-3a (qui se lie à MDM2) et RITA (qui se lie à p53), nous avons traité des cellules U87MG avec des concentrations croissantes de RITA (0,1, 0,5 et 1μM) et évalué les effets sur la voie p53 par western blot. L'analyse par Western blot a montré que le RITA, de manière significative et en fonction de la dose, augmentait la stabilité de la protéine p53 dans les cellules U87MG à la fois 24 et 48 heures après le traitement. Contrairement à Nutlin-3a, RITA n'a eu aucun effet sur la stabilité de la protéine MDM2 et l'expression de l'intégrine α5 dans les cellules U87MG à toutes les concentrations testées à la fois à 24 et 48 heures. De plus, le traitement avec Nutlin-3a (1μM) est plus efficace pour augmenter la stabilité de la protéine p53 que le RITA (1μM).

Nous avons ensuite étudié l'activité transcriptionnelle de p53 en évaluant l'expression des gènes cibles de p53 : MDM2, un inhibiteur physiologique de p53 et sa principale cible transcriptionnelle ; p21, un inhibiteur du cycle cellulaire ; Fas, un produit génique nécessaire à l'apoptose médiée par p53 ; et birc5/survivin, une protéine anti-apoptotique. L'analyse RT-qPCR a montré que la transcription des gènes p21, fas et MDM2 induits par p53 a été significativement augmentée par Nulin-3a et RITA, confirmant l'activation de la voie p53. Le gène cible p53 répressible, birc5, a été significativement diminué après le traitement par Nutlin-3a et RITA. Par rapport à RITA, Nutlin-3a a été plus efficace pour augmenter la transcription de MDM2 et diminuer la transcription de birc 5.

Ces résultats ont confirmé qu'à 1μM, Nutlin-3a est plus efficace que RITA pour réactiver la voie p53 dans les cellules U87MG 24 heures après le traitement.

Des études antérieures ont suggéré que l'expression de l'intégrine α5 inhibait l'activation de p53 en ayant en partie un impact sur la stabilité de la MDM2 (Renner et al., 2016). Pour explorer ce point, nous avons utilisé des cellules U87MG dans lesquelles le gène de l'intégrine α5 a été supprimé grâce à la technologie CRISPR/Cas9 (U87MGα5KO) par rapport aux cellules U87MG exprimant l'intégrine.

Nous avons vérifié les effets de la Nutlin-3a et de la RITA dans une étude cinétique sur la stabilité et l'activité de p53 et sur la stabilité de MDM2. Le traitement avec Nutlin-3a entraîne une induction rapide et forte de la stabilité et de l'activité de p53 déjà 3 heures après le traitement, à la fois dans les cellules U87MG et U87MGα5KO, mais l'induction de la stabilité

et de l'activité de la protéine p53 par RITA a été retardée et n'est apparue qu'après 24 heures après le traitement. Aucune différence n'a pu être constatée entre les deux lignées cellulaires au niveau de la protéine p53.

En ce qui concerne l'expression de la protéine MDM2, les études cinétiques ont révélé qu'à des moments antérieurs, l'expression de l'intégrine α5 a conduit à une stabilisation soutenue de la MDM2 par le traitement Nutlin-3a de 6 à 12 heures alors que dans les cellules U87MG-α5KO son niveau a diminué rapidement. Les résultats suggèrent que cette intégrine pourrait moduler l'expression de la MDM2 dans certaines situations. Pour confirmer ce point, nous avons traité les cellules U87MG d'abord avec Nutlin-3a pour augmenter le niveau de MDM2 et ensuite avec K34c, un antagoniste de l'intégrine. Nous nous attendions à une diminution du niveau de MDM2 avec l'antagoniste sans changement de p53. Cependant, les résultats ont indiqué que les protéines MDM2 et p53 étaient toutes deux affectées par le traitement combiné à 6 heures. Cette partie du projet a été rendue difficile à conclure, car MDM2 semble être diminué par un antagoniste de l'intégrine ; il est également augmenté par l'activation de p53 par Nutlin-3a en tant que gène cible de p53. La partie respective de ces deux effets doit faire l'objet de recherches plus approfondies.

Nous avons décidé d'axer nos recherches sur les cellules GBM résistantes aux TMZ, car il a été démontré dans la littérature que certaines GBM récurrentes surexpriment l'intégrine α5. Nous avons donc décidé de développer un modèle in vitro de cellules résistantes pour explorer si l'activation p53 combinée à des antagonistes des intégrines pourrait être une stratégie valable pour les cibler.

Discussion

La perturbation de l'interaction protéine-protéine MDM2-P53 conduisant à la restauration de la fonction suppresseur de tumeur du type sauvage p53 est considérée comme une stratégie thérapeutique intéressante pour traiter les cancers, y compris le glioblastome. Plusieurs petites molécules inhibitrices du complexe p53-MDM2 ont été mises au point, dont certaines font déjà l'objet d'essais cliniques. Ici, nous avons cherché à comparer les activateurs p53 Nutlin-3a, Idasanutlin et RITA. Nutlin-3a et Idasanutlin ont tous deux pour fonction d'augmenter l'activité de p53 en se liant à MDM2 pour inhiber l'interaction MDM2-p53 protéine-protéine. La Nutlin-3a, un composé de cis-imidazoline, est le premier inhibiteur sélectif de la MDM2 développé (Klein et Vassilev, 2004). Cependant, la grande interface hydrophobe d'interaction protéine-protéine sur la MDM2 qui compromet sa puissance et ses profils pharmacocinétiques, a conduit

à la découverte de l'idasanutline, un composé de pyrrolidine avec une puissance et une sélectivité supérieures (Ding et al., 2013). Nous avons comparé l'effet de la Nutlin-3a et de l'Idasanutlin dans nos lignées cellulaires. Conformément à des résultats antérieurs, nos données ont démontré que l'activateur p53 cliniquement évalué, l'idasanutline, est plus efficace que Nutlin-3a pour réduire la confluence cellulaire et stabiliser la protéine p53. Nous avons démontré que l'effet de Nutlin-3a et de l'idasanutline sur la confluence cellulaire dépend du statut p53 des cellules. Nous avons découvert que les deux médicaments avaient un effet sur les cellules exprimant la protéine p53 de type sauvage mais n'avaient aucun effet sur la confluence des cellules U373MG exprimant la protéine p53 mutante. Nos résultats sont conformes à ceux décrits par Renner et al. et Ding et al., dans lesquels les cellules exprimant le p53 de type sauvage sont sensibles à Nutlin-3a (Renner et al., 2016) et à Idasanutlin (Ding et al., 2013), mais les cellules exprimant le p53 mutant ne sont pas sensibles.

Nous avons en outre comparé Nutlin-3a (qui se lie à mdm2) et RITA (qui se lie à p53) ; ces deux médicaments ont pour fonction d'augmenter l'activité de p53 en inhibant l'interaction MDM2-p53 protéine-protéine. Nous n'avons trouvé aucune différence observable sur la viabilité cellulaire ou la confluence cellulaire entre le traitement avec Nutlin-3a et RITA sur les cellules U87MG. Contrairement à Nutlin-3a, RITA n'a pas diminué l'expression de l'intégrine α5 lorsque les deux ont été testés à concentration égale (1μM), mais l'a fait à une concentration plus élevée, confirmant ainsi d'autres travaux (Janouskova et al., 2012). En outre, une induction moins efficace de p53 sans augmentation de l'expression de MDM2 a été observée avec RITA par rapport à Nutlin-3a. Les résultats observés reflétaient ceux des études précédentes qui comparaient l'effet de Nutlin-3a et de RITA sur le cancer du colon (Janouskova et al., 2012). Il y a plusieurs explications possibles à ces résultats. Par exemple, nos données suggèrent que l'activation de p53 en dessous d'une valeur seuil, telle qu'obtenue avec RITA, est insuffisante pour affecter l'expression de l'intégrine α5. Plus récemment, un mécanisme de seuil similaire a été décrit pour servir de médiateur dans la décision sur le sort des cellules p53 entre l'arrêt du cycle cellulaire et l'apoptose (Kracikova et al., 2013). Une autre explication possible est que la MDM2 est libérée non modifiée lors de la liaison de RITA à p53, alors que la liaison de Nutlin-3a à la MDM2 pourrait entraîner une altération du site de liaison de la MDM2 qui lui permettrait de se lier à d'autres protéines telles que l'intégrine α5 en plus de p53. Ces résultats confirment le rôle important de l'intégrine α5 dans la GBM et la nécessité de poursuivre le développement d'inhibiteurs sélectifs pour cette intégrine.

En ce qui concerne la survie cellulaire et l'induction ou la répression des gènes cibles p53, différents résultats ont été décrits. Par exemple, alors que RITA induisait de préférence l'apoptose, Nutlin-3a pousse plus communément les cellules à l'arrêt du cycle cellulaire (Enge et al., 2009). Nous avons démontré que, par rapport à Nutlin-3a, RITA est moins efficace pour augmenter les gènes cibles p53 ou diminuer la protéine antiapoptotique birc5. Cependant, contrairement aux différences discutées ci-dessus, aucune différence n'a été observée sur l'effet de Nutlin-3a et de RITA sur la survie cellulaire après 72 heures. En conséquence, il est possible que l'activation de p53 par RITA soit supérieure à l'activation par Nutlin-3a sur une période prolongée, puisque le traitement par RITA n'affecte pas de manière significative l'expression de MDM2, le régulateur négatif de p53 par rapport au traitement par Nutlin-3a.

Une interférence négative entre l'intégrine α5β1 et la protéine p53 a été décrite (Janouskova et al., 2012) et il a été démontré que la surexpression de cette intégrine stabilise la protéine MDM2 (Renner et al., 2016b). L'intégrine α5β1 (Janouskova et al., 2012) et la protéine MDM2 (Ene et al., 2020) contribuent toutes deux à l'agressivité de la tumeur et à la résistance au traitement. L'élimination ciblée des principaux facteurs d'agressivité de la tumeur pourrait avoir un impact positif sur le résultat du traitement. Nous avons émis l'hypothèse que lors d'un traitement avec Nutlin-3a, une MDM2 fonctionnelle avec une conformation modifiée pour se lier à d'autres protéines, y compris l'intégrine α5, est exprimée, et que l'inhibition fonctionnelle ou pharmacologique de cette intégrine pourrait inhiber l'expression de la MDM2, empêchant ainsi la dégradation protéasomique de p53, conduisant à une stabilisation et une activation soutenues de p53. Nous avons découvert que le traitement par Nutlin-3a entraînait une augmentation de l'expression de MDM2 dans les cellules U87MG exprimant l'intégrine α5 mais une diminution de la libération de MDM2 dans les cellules dans lesquelles le gène de l'intégrine α5 était supprimé entre 9 et 12 heures. Cette découverte intéressante a ouvert une courte fenêtre thérapeutique dans laquelle un antagoniste de l'intégrine α5 pourrait être utilisé en combinaison avec un activateur p53 pour augmenter la stabilisation/activité de p53 en modulant le niveau de MDM2. Cependant, les résultats obtenus lorsque Nutlin-3a était combiné avec l'antagoniste d'intégrine K34c n'étaient pas très encourageants 6 heures après le traitement, car la MDM2 et la protéine 53 étaient toutes deux affectées. Cette partie du projet a été rendue difficile à conclure, car le MDM2 exprimé par le traitement avec Nutlin-3a est diminué par un antagoniste d'intégrine, en tant que gène cible p53, il est également augmenté par l'activation de p53 par Nutlin-3a. De même, comme p53 est activé par Nurlin-3a, il est dégradé par la MDM2, ce qui correspond à une régulation de rétroaction exercée par un p53 réactivé. La part respective de

ces deux effets doit être étudiée plus en détail. Dans les recherches futures, il pourrait être possible d'utiliser un modèle différent dans lequel l'expression de MDM2 due au traitement par Nutlin-3a est remplacée par la transfection de cellules U87MG avec un clone d'ADNc du gène pour MDM2 afin de créer une lignée cellulaire stable surexprimant MDM2.

Conclusion

Pour revenir à la question posée au début de cette étude, il est maintenant possible d'affirmer qu'Idasanutlin est le plus puissant des activateurs p53 testés. L'une des conclusions les plus significatives qui ressortent de cette étude est que nos données ont ajouté d'autres preuves aux données existantes en soutenant le rôle important de l'intégrine α5β1 dans la MGF. Il a également été démontré que l'inhibition de cette intégrine entraînait une diminution du niveau de la protéine MDM2. Conformément aux résultats précédents de notre laboratoire (Martinkova et al., 2010 ; Renner et al., 2016), cette découverte suggère que l'utilisation de thérapies ciblées pour réprimer l'expression ou inhiber la fonction de cette intégrine pourrait sensibiliser la GBM aux médicaments chimiothérapeutiques conventionnels.

Résultats, partie 2

2.1. L'exposition à long terme des cellules U87MG à la TMZ génère des cellules résistantes persistantes

Pour générer des cellules résistantes à la TMZ, nous avons soumis des cellules U87MG à 50 µM de TMZ pendant plusieurs semaines, ce qui a donné une sous-population de cellules U87MG stables et résistantes à la TMZ. La sous-population de cellules résistantes a été soit cultivée en continu dans un milieu contenant 50 µM de TMZ (U87MG R50), soit, après 2 mois en présence de TMZ, cultivée dans un milieu sans TMZ (U87MG OFF R50). Nous avons confirmé que les cellules parentales étaient sensibles à 50 µM TMZ et que les cellules U87MG R50 étaient insensibles à la TMZ jusqu'à 96 heures. Il est intéressant de noter que la résistance au TMZ a été maintenue dans les cellules U87MG OFF R50. En outre, alors que les cellules parentales étaient sensibles au TMZ en fonction de la dose, les cellules U87MG R50 et U87MG OFF R50 sont restées insensibles à des concentrations variables allant jusqu'à 100 µM TMZ.

Les images en contraste de phase obtenues à partir de l'IncuCyte, ont montré que la morphologie cellulaire des cellules U87MG R50 différait de celle des cellules parentales en ayant une morphologie plus étalée, agrandie et aplatie. Cependant, les cellules U87MG OFF R50

présentaient une morphologie mixte, certaines cellules présentant la morphologie des cellules U87MG R50 tandis que les autres présentaient la morphologie des cellules parentales. Le traitement par TMZ pendant 3 jours a produit un changement profond dans la morphologie des cellules parentales, entraînant une ramification importante, une réduction du nombre total de cellules et une confluence. Au contraire, les cellules U87MG R50 et les cellules U87MG OFF R50 semblaient saines, sans changement morphologique évident, 72 heures après le traitement TMZ. Dans l'ensemble, ces résultats ont démontré qu'une fraction des cellules U87MG qui ont survécu à une exposition prolongée à la TMZ ont développé une résistance à la TMZ acquise qui subsiste même après le retrait de la TMZ.

2.2. La TMZ induit la sénescence dans les cellules U87MG

Comme les cellules résistantes présentaient les caractéristiques morphologiques des cellules sénescentes, nous avons ensuite testé le marqueur de sénescence SA-βGAL. Après une courte incubation dans 50 TMZ μM, les cellules restantes étaient toutes positives pour la coloration SA-βGAL. Les cellules positives ont été maintenues dans les cellules U87MG R50 mais ont largement diminué dans les cellules U87MG OFF R50. En conséquence, une augmentation significative de l'expression des protéines p16 et p21, dont on sait qu'elles sont impliquées dans la sénescence, a été observée dans les cellules U87MG R50 par rapport aux cellules parentales. Une augmentation de p16 mais pas de p21 a été enregistrée dans les cellules U87MG R50 OFF. La capacité à remplir les puits de culture a légèrement diminué pour les cellules U87MG R50 par rapport aux cellules parentales et aux cellules U87MG OFF R50. Dans l'ensemble, les résultats suggèrent que la TMZ déclenche la sénescence dans les cellules U87MG, comme cela a déjà été signalé (Li et al., 2013 ; Martinkova et al., 2010), qui diminue après l'élimination de la TMZ.

2.3. L'organisation de la matrice extracellulaire et les intégrines sont affectées par la TMZ

Nous avons utilisé la RNAseq pour comparer les trois lignées cellulaires. L'analyse des variations génétiques globales par regroupement hiérarchique non supervisé a montré que de profonds changements se produisaient pendant le traitement par TMZ, les différences les plus importantes étant observées entre les cellules U87MG et U87MG R50. Les cellules U7MG R50 OFF étaient plus étroitement liées aux cellules U87MG non traitées. Les gènes les plus importants ont été soumis à une analyse des voies du réactome. Les voies biologiques les plus touchées par le traitement à long terme au témozolomide (cellules R50 par rapport aux cellules témoins) sont l'organisation de la matrice extracellulaire, la glycosylation liée à l'oxygène et les

interactions à la surface des cellules Integrin. En se concentrant sur les gènes des intégrines, de profonds réarrangements des niveaux d'expression des sous-unités d'intégrines ont été observés. Quatre groupes principaux peuvent être soulignés. Le groupe 1 correspond aux intégrines exprimées dans les cellules de contrôle U87MG mais réprimées dans les cellules R50 et avec une expression intermédiaire dans les cellules R50 OFF (Intégrines α2, α3, α4, α5, α10, α11, αv, β1, β3). Le groupe 2 comprend des intégrines surexprimées dans les cellules U87MG R50 OFF par rapport aux deux autres lignées cellulaires (α6, β6 et β8) dont α6 et β8 sont décrites comme des marqueurs de cellules souches de gliome (Lathia et al., 2010 ; Malric et al., 2019). Le groupe 3 correspond aux intégrines réprimées dans les cellules U87MG R50 OFF (α7, α9, αx, αD, β5, β7). Le groupe 4 comprend les intégrines surexprimées dans les cellules U87MG R50 (α1, αL, αM, β2, β4), y compris certaines intégrines spécifiques aux leucocytes. Les données confirment que l'expression des intégrines est soumise à des variations spécifiques au cours de la chimiothérapie au témozolomide.

Comme nous avons démontré précédemment que l'intégrine α5β1 est impliquée dans la résistance aux TMZ (Janouskova et al., 2012), nous nous sommes ensuite concentrés sur cette intégrine et avons examiné son expression au niveau des protéines dans les lignées cellulaires parentales et résistantes aux TMZ. Nous avons observé une nette diminution de la sous-unité α5 dans les cellules U87MG R50 sans changement significatif de celle de la sous-unité β1. Il est intéressant de noter que le niveau d'intégrine de α5 augmente après l'élimination de la TMZ dans les cellules U87MG R50 OFF pour atteindre le niveau observé dans les cellules non traitées et que le niveau d'intégrine de β1 est devenu légèrement plus élevé que dans les cellules non traitées. En revanche, le niveau de l'intégrine de αv (une autre intégrine largement impliquée dans l'agressivité des glioblastomes) n'a pas changé entre les 3 lignées cellulaires. En confirmation, nous avons également abordé les changements d'expression de l'intégrine α5β1 par immunohistochimie. Comme on peut le voir, l'expression de l'intégrine α5 ou β1 est réduite dans les cellules U87MG R50 mais les deux réapparaissent après la suppression de la TMZ dans les cellules U87MG R50 OFF. Ces résultats ont été confirmés dans des cellules cultivées sous forme de sphères. Pour confirmer davantage l'effet de la TMZ sur l'expression de l'intégrine α5β1, nous avons évalué l'effet à long terme de la TMZ sur les cellules de gliome U373 et LN443. Il est intéressant de noter que TMZ a diminué de manière significative l'expression basale de l'intégrine α5 dans la lignée cellulaire U373, mais que la suppression de TMZ n'a pas augmenté son expression. Aucun effet sur l'expression de l'intégrine α5 n'a été observé dans les cellules LN443. Nous avons vérifié l'effet de la TMZ dans les deux lignées

cellulaires et avons observé que les cellules U373 étaient sensibles mais que les cellules LN443 étaient insensibles. Ces résultats suggèrent que l'expression de l'intégrine α5β1 dans la GBM est diminuée sous la pression de la TMZ dans les lignées cellulaires sensibles à la TMZ.

2.4. Effets des antagonistes de α5β1 sur les cellules parentales U87MG et les cellules résistantes aux TMZ.

Nous avons ensuite cherché à comparer les effets de trois antagonistes de α5β1 sur la morphologie et la confluence des cellules par la technologie Incucyte. Nous avons utilisé K34c, FR248 et ATN161. Les deux premiers sont des ligands intégrines de type RGD capables d'inhiber l'adhérence des cellules à la fibronectine, comme le montrent nos travaux précédents (Ray et al., 2014). L'ATN161 a été conçu pour cibler le site de synergie de la fibronectine pour l'intégrine α5β1 et est incapable de perturber l'adhésion cellulaire (Khalili et al., 2006). Le K34c s'est avéré capable de diminuer l'adhésion cellulaire pour les trois lignées cellulaires en inhibant la propagation des cellules et la formation de certaines structures sphériques, en particulier dans les cellules U87MG et U87MG R50 OFF. FR248 est moins efficace pour inhiber la propagation des cellules que K34c et particulièrement inefficace dans les cellules U87MG R50. Enfin, l'ATN161 n'a pas réussi à inhiber l'adhésion cellulaire comme prévu dans toutes les lignées cellulaires. La quantification de la confluence cellulaire après 3 jours de traitements a confirmé ces observations morphologiques. FR248 qui est plus sélectif que K34c pour α5β1 que pour l'intégrine αvβ3 (Heckmann et al., 2008) est inactif dans les cellules U87MG R50 en accord avec le faible niveau d'intégrine α5β1 dans ces cellules. Les données suggèrent que les cellules U87MG et U87MG R50 OFF peuvent être sensibles de manière similaire aux antagonistes de l'intégrine α5β1, au moins pour l'inhibition de l'adhésion et de la confluence cellulaire.

2.5. Voie de signalisation p53 dans les cellules U87MG et TMZ résistantes.

La TMZ est connue pour activer la voie p53 (Martinkova et al., 2010b ; Renner et al., 2016b). Afin de comparer la stabilisation et l'activation de p53 dans les 3 lignées cellulaires, nous avons évalué l'expression des protéines p53 et MDM2 dans des conditions de culture basales. Dans les cellules U87MG R50 ainsi que dans les cellules U87MG R50 OFF, p53 est stabilisé et son gène cible MDM2 est augmenté par rapport à la lignée cellulaire parentale. Les niveaux de MDM2 et d'ARNm de p21 ont montré que les deux étaient augmentés en présence de TMZ mais que seul l'ARNm de MDM2 restait plus élevé dans les cellules U87MG R50 OFF par rapport aux cellules U87MG témoins. Les résultats suggèrent que l'activation de p53 est

maintenue en présence de TMZ mais que l'activation des gènes cibles MDM2 et p21 peut différer après l'élimination du médicament.

Comme la réactivation de p53 par de petites molécules inhibant l'interaction MDM2/p53 et la dégradation de p53 peut représenter une option thérapeutique alternative à la chimiothérapie dans les tumeurs de type sauvage p53 (Renner et al., 2016), nous avons ensuite cherché à savoir si ces médicaments sont capables d'affecter la signalisation p53 dans les cellules témoins et résistantes. Trois activateurs p53 différents ont été utilisés : Nutlin-3a et Idasanutlin qui se lient à la partie MDM2 et RITA qui se lient à la partie p53 du complexe MDM2/p53. Ces trois médicaments renforcent la stabilité de p53 ainsi que son activation (comme le montre l'augmentation de la protéine MDM2). Aucune différence n'a pu être observée entre les cellules U87MG témoins et leurs homologues résistantes aux TMZ. Dans ces expériences, l'idasanutline a été l'activateur le plus efficace de la voie p53 même à 0,1 µM (une concentration 10 fois inférieure à celle de Nutlin-3a et de RITA) et RITA le moins efficace après 24 heures de traitement. Les résultats suggèrent que les cellules résistantes aux TMZ pourraient bénéficier d'un autre moyen de réactiver la voie de suppression des tumeurs p53.

2.6. Impact des antagonistes des intégrines sur la voie p53

Nous avons décrit précédemment une interférence négative entre l'intégrine α5β1 et les voies de signalisation p53 impliquées dans la résistance des cellules de gliome à la chimiothérapie. Nous avons montré que l'activation de p53 en même temps que l'inhibition de l'intégrine α5β1 entraînait une augmentation de la signalisation de p53 et la mort des cellules de gliome dans les cellules surexprimant la sous-unité d'intégrine α5 (Janouskova et al., 2012 ; Renner et al., 2016). Nous nous sommes donc demandé si des résultats similaires pouvaient être obtenus dans les cellules résistantes aux TMZ. Nous avons étudié l'association des activateurs p53 (Nutlin-3a, RITA et Idasanutlin) avec chacun des trois antagonistes des intégrines sur la confluence cellulaire. L'association de l'idasanutline (0,1 µM) avec K34c (20 µM) et FR248 (20 µM) pendant 72 heures dans des cellules U87MG ou U87MG R50 OFF a conduit à une diminution significative de la confluence cellulaire par rapport à chaque médicament seul ou sans traitement. Cependant, l'association de l'idasanutline avec l'ATN-161 n'a pas d'effet supplémentaire par rapport à l'idasanutline seule. Toutes les différentes combinaisons ont un impact sur la confluence cellulaire après 72h de traitement. Nous avons également vérifié les combinaisons Nutlin-3a et RITA avec K34c et FR248 dans les cellules U87MG R50. Les résultats ont indiqué que seule l'association Nutlin-3a ou RITA avec K34c s'est avérée capable d'affecter de manière significative la confluence par rapport à celle des deux activateurs p53

seuls. L'inefficacité de FR248 est en accord avec la faible expression de l'intégrine α5 dans ces cellules (données non montrées).

Nous avons ensuite étudié la combinaison de médicaments sur les expressions p53 et mdm2 après un traitement de 24 heures. Dans les cellules U87MG R50 OFF, FR248 a augmenté les effets de l'idasanutline sur les expressions p53, phosphoser15-p53 et mdm2, bien que cela ne semble pas être le cas pour les cellules U87MG. Il est intéressant de noter que les cellules U87MG sont apparues sensibles aux combinaisons FR248/Idasanutlin ou RITA qui ont permis une augmentation de l'expression de p53 et mdm2 pour l'Idasanutlin mais seulement pour l'expression de p53 avec RITA.

Ces expériences doivent être menées à bien ainsi que les expériences étudiant les relations entre les effets sur la confluence, la signalisation p53 et la mort cellulaire.

Discussion

Le glioblastome reste la tumeur cérébrale maligne la plus courante et la plus agressive chez l'adulte (Geraldo et al., 2019). Malgré de nombreux essais cliniques sur les thérapies conventionnelles, ciblées et immunologiques, aucune nouvelle option thérapeutique claire n'a été proposée ces dernières années (Bush et al., 2017). Les échecs sont en partie dus à la grande hétérogénéité moléculaire et cellulaire rencontrée dans ces tumeurs ainsi qu'au microenvironnement particulier du cerveau. Le niveau élevé de récurrence est une caractéristique de la GBM liée à la dissémination des cellules tumorales dans le cerveau normal mais aussi aux mécanismes de résistance à la radiothérapie et/ou à la chimiothérapie. Bien que la TMZ soit actuellement le seul médicament chimiothérapeutique approuvé connu pour améliorer de manière significative la survie globale des patients atteints de GBM (Stupp et al., 2005), le développement d'une résistance acquise à la TMZ conduisant à un échec du traitement reste l'un des défis à relever. Des travaux antérieurs ont souligné le rôle de la MGMT dont la régulation épigénétique (promoteur de méthylation ou de déméthylation) est impliquée dans la réponse clinique à la TMZ. Cependant, la GBM méthylée et non méthylée par MGMT peut développer une résistance à la TMZ. Il a été démontré que la résistance acquise est liée à la perte de la réparation de l'inadéquation de l'ADN (MMR) (McFaline-Figueroa et al., 2015) ou à l'activation de la réparation par excision de bases (BER) (Bobola et al., 2012). Parallèlement, des stratégies visant à bloquer la BER par l'inhibition des enzymes PARP (Yuan et al., 2020) ont été proposées pour supprimer l'émergence de la résistance aux TMZ.

Dans ce travail, nous avons généré des cellules résistantes aux TMZ en soumettant des cellules U87MG à un traitement TMZ 50 µM comme modèle in vitro de résistance aux TMZ MGMT-négatives. Nous avions pour objectif de comparer des cellules cultivées en continu en présence de TMZ (U87MG R50) avec des cellules résistantes se développant en l'absence de TMZ (U87MG R50 OFF), ce dernier modèle étant un reflet de la récurrence clinique. Nous avons confirmé que les cellules U87MG étaient sensibles à la TZM, ce qui a entraîné une importante population de cellules mortes au début, avec peu de cellules encore vivantes. Nous avons montré que la morphologie cellulaire des cellules U87MG R50 différait de celle de ses cellules parentales en ayant une morphologie plus étendue, élargie et aplatie, rappelant la sénescence.

Il a déjà été démontré que les TMZ induisent la sénescence (Li et al., 2013 ; Martinkova et al., 2010) qui peut être associée à la coloration de la β-galactosidase (SA-Bgal) associée à la sénescence (Dimri et al., 1995). Dans cette optique, nous avons démontré que les quelques cellules U87MG qui restaient en vie après une semaine d'incubation dans 50 µM TMZ étaient toutes positives pour la coloration SA-βGAL. Une proportion significative de cellules positives a été maintenue dans les cellules U87MG R50 mais a largement diminué dans les cellules U87MG OFF R50, ce qui indique encore le rôle de la TMZ dans cet état de sénescence. La morphologie élargie des cellules U87MG R50 reflétait celle d'autres études dans lesquelles les cellules sénescentes étaient définies comme généralement élargies, avec un volume souvent doublé, et, s'il y adhère, adopter une morphologie aplatie (Campisi, 2013). D'autres études ont rapporté que les cellules U87MG résistantes à la TMZ adoptent une morphologie de type EMT (morphologie de cellule fusiforme, perte de communications intercellulaires, formation de pseudopodes) (Yi et al., 2016). Ces différences morphologiques peuvent être attribuées aux conditions utilisées pour générer les cellules résistantes, 400 µM TMZ pendant 6 mois contre 50µM TMZ tout au long de notre étude. En fait, plusieurs protocoles de génération de cellules résistantes aux gliomes ont été appliqués avec différentes concentrations de TMZ pendant des périodes de temps variées, ce qui explique les différences de résultats (Lee, 2016b). Il est intéressant de noter qu'un travail récent a décrit un état transitoire acquis par les cellules de gliome U251 pendant l'acquisition de la résistance à la TMZ et défini par une croissance lente, une morphologie distincte et un changement de métabolisme (Rabé et al., 2020), ce qui indique qu'il faut faire attention en comparant des résultats différents. Pour étayer l'état de sénescence, nous avons constaté une augmentation significative de p53, p16 et p21 dans les cellules U87MG R50 par rapport aux cellules parentales, alors qu'une augmentation de p16 mais pas de p21 a été détectée dans les cellules U87MG R50 OFF. En outre, la capacité de remplissage des puits

de culture a légèrement diminué pour les cellules U87MG R50 par rapport aux cellules parentales et aux cellules U87MG OFF R50, ce qui suggère une forme d'arrêt du cycle cellulaire. Conformément à notre constatation, la surexpression de p53, p21 ou p16INK4a s'est avérée généralement suffisante pour déclencher et maintenir l'arrêt de la croissance de la sénescence (Beauséjour et al., 2003 ; McConnell et al., 1998). Ainsi, nos résultats ont montré que la TMZ induisait un phénotype de type sénescence qui peut persister jusqu'à ce que le médicament soit retiré du milieu de culture. À ce moment, les cellules U87MG restent résistantes au médicament (U87MG R50 OFF) mais reprennent une prolifération normale comme cela se produirait dans un glioblastome récurrent.

Pour la première fois à notre connaissance, une analyse de la régulation des gènes des cellules résistantes a été réalisée, soit sous la pression de la TMZ, soit après le retrait du médicament. Il est intéressant de noter que de profonds changements ont été observés entre les cellules U87MG R50 et la cellule non traitée, alors que les cellules U87MGR50 OFF présentaient une image plus proche de celle des cellules de contrôle. La comparaison entre les cellules U87MG R50 et les cellules témoins avec le Reactome a indiqué que la voie la plus affectée était l'organisation de la matrice extracellulaire, suivie par la glycosylation liée à l'O, les maladies de la glycosylation et l'interaction de la surface des cellules avec l'intégrine. Il est intéressant de noter que la carte thermique, lorsqu'elle a été focalisée sur les gènes des intégrines, a confirmé que des changements profonds dans l'expression des intégrines se produisent dans les cellules résistantes par rapport aux cellules non traitées. Chaque type de cellule possède un ensemble particulier d'intégrines qui est surexprimé par rapport aux deux autres. Cela peut être intéressant pour des options thérapeutiques spécifiques contre les intégrines à utiliser soit en même temps que la ZTM, soit uniquement en cas de récidive de la tumeur. À titre d'exemple, les cellules U87MG R50 OFF surexpriment les intégrines α6 et β8, toutes deux connues pour être des marqueurs de cellules souches de gliome (Lathia et al., 2010 ; Malric et al., 2019). En conséquence, une différenciation des cellules tumorales vers les cellules souches de gliome a été signalée dans des tumeurs après radiothérapie ou chimiothérapie TMZ (Auffinger et al., 2014 ; Dahan et al., 2014). Des thérapies spécifiques anti-α6 et/ou β8 intégrines peuvent être utilisées pour les tumeurs récurrentes.

Dans des études précédentes, nous avons démontré que l'intégrine α5β1 est impliquée dans la résistance aux TMZ (Janouskova et al., 2012). Comme les sous-unités de l'intégrine α5 et β1 semblent être diminuées au niveau de l'ARNm dans les cellules U87MG R50 et ensuite légèrement augmentées dans les cellules U87MG R50 OFF, nous nous sommes concentrés sur

cette intégrine. Nous avons constaté une nette diminution de la sous-unité α5 dans les cellules U87MG R50 au niveau des protéines sans changement significatif de celle de la sous-unité β1. Il est intéressant de noter que le niveau de l'intégrine α5 augmente après l'élimination de la TMZ dans les cellules U87MG R50 OFF pour atteindre le niveau observé dans les cellules non traitées et que le niveau de l'intégrine β1 est devenu légèrement plus élevé que dans les cellules non traitées. Nous avons confirmé ces résultats par immunohistochimie des cellules adhérentes et des cellules cultivées en tant que sphères. Ces résultats montrent que l'intégrine α5β1 est une cible prometteuse pour les GBM récurrentes, comme cela a été proposé dans une étude examinant le glioblastome récurrent traité au bevacizumab (DeLay et al., 2012).

Nous avons démontré dans des études précédentes que les TMZ activent la voie p53 dans les cellules U87MG (Martinkova et al., 2010 ; Renner et al., 2016). Ici, nous avons comparé la stabilisation et l'activation de p53 dans les 3 lignées cellulaires en évaluant l'expression des protéines p53 et MDM2 dans des conditions de culture basale. Nous avons constaté que la p53 basale est stabilisée et que son gène cible MDM2 est augmenté dans les cellules U87MG R50 et U87MG R50 OFF, par rapport à la lignée cellulaire parentale. En outre, les niveaux d'ARNm de MDM2 et de p21 ont augmenté en présence de TMZ, mais seul l'ARNm de MDM2 est resté plus élevé dans les cellules U87MG R50 OFF que dans les cellules U87MG témoins. Les résultats suggèrent que l'activation de p53 est maintenue en présence de TMZ, mais que l'activation des gènes cibles MDM2 et p21 peut différer après l'élimination du médicament. Comme le niveau de MDM2 reste élevé après l'élimination de la TMZ, cela suggère qu'il peut être considéré comme une cible thérapeutique dans les glioblastomes récurrents ainsi que dans les tumeurs primaires surexprimant la MDM2 (Verreault et al., 2016).

L'inhibition pharmacologique de α5β1 diminue la migration des cellules tumorales, l'invasion, et pousse les cellules traitées par la TMZ de la sénescence vers l'apoptose tout en modulant la voie p53 (Martinkova et al., 2010b ; Ray et al., 2014). Dans cette étude, nous avons comparé l'effet des antagonistes des intégrines K34c, FR248 et ATN161 de α5β1 sur la morphologie et la confluence des cellules. Nos résultats ont confirmé que les cellules U87MG et U87MG R50 OFF pourraient être sensibles de la même manière à l'antagoniste de l'intégrine α5β1 FR248, le plus sélectif. Le K34c s'est révélé particulièrement efficace pour inhiber la propagation des cellules et pour former des structures sphériques dans les trois lignées cellulaires, ce qui suggère qu'il pourrait agir non seulement par l'inhibition de α5β1 mais aussi par l'inhibition de l'intégrine αvβ3. L'ATN161 est incapable d'affecter la confluence cellulaire comme prévu. À ce stade, il faut souligner que les relations entre l'inhibition de l'adhérence cellulaire et la survie cellulaire

ne sont pas clairement établies dans nos expériences, ce qui empêche de tirer des conclusions définitives sur les effets de l'antagoniste sur la viabilité cellulaire.

Nous avons néanmoins examiné la possibilité d'utiliser ces antagonistes en combinaison avec plusieurs activateurs p53, y compris des molécules ciblant le MDM2.

La restauration de la fonction suppresseur de tumeur de p53 en perturbant l'interaction MDM2-p53 protéine-protéine est considérée comme une stratégie thérapeutique intéressante pour les GBM exprimant le type sauvage de p53. Plusieurs petites molécules inhibitrices du complexe p53-MDM2 ont été mises au point, dont certaines font déjà l'objet d'essais cliniques. La Nutlin-3a, un composé de cis-imidazoline, est le premier inhibiteur sélectif de la MDM2 développé (Klein et Vassilev, 2004). Cependant, la grande interface d'interaction hydrophobe protéine-protéine sur le MDM2 qui compromet sa puissance et ses profils pharmacocinétiques, a conduit à la découverte de l'idasanutline, un composé de pyrrolidine avec une puissance et une sélectivité supérieures (Ding et al., 2013). Ici, nous avons comparé trois activateurs p53 différents : Nutlin-3a (Vassilev, 2004) et Idasanutlin (Ding et al., 2013) qui se lient à la partie MDM2 et RITA (Issaeva et al., 2004) qui se lient à la partie p53 du complexe MDM2/p53 pour stabiliser et activer la voie p53. Nous avons constaté que ces trois médicaments améliorent la stabilité de p53 ainsi que son activation (démontrée par l'augmentation de la protéine MDM2), l'idasanutline étant le plus efficace. Les résultats suggèrent que les cellules résistantes aux TMZ pourraient bénéficier d'un autre moyen de réactiver la voie de suppression des tumeurs p53.

Dans des travaux antérieurs de l'équipe, une diaphonie négative entre l'intégrine α5β1 et les voies de signalisation p53 impliquées dans la résistance des cellules de gliome à la chimiothérapie a été décrite. L'activation de p53 en même temps que l'inhibition de l'intégrine α5β1 a entraîné une augmentation de la signalisation de p53 et la mort des cellules de gliome dans les cellules surexprimant la sous-unité de l'intégrine α5 (Janouskova et al., 2012b ; Renner et al., 2016b). Nous avons évalué cette stratégie sur les cellules U87MG résistantes. Toutes les combinaisons d'antagonistes des intégrines et d'activateurs p53 ont conduit à une meilleure inhibition de la confluence cellulaire que les deux traitements seuls dans les cellules U87MG et U87MG R50 OFF, sauf pour la combinaison avec l'ATN161. Cependant, nos données préliminaires suggèrent une dissociation entre l'impact des traitements combinés sur la confluence cellulaire et sur l'activation de la voie p53. En fait, l'ATN161 qui n'a pas modifié la confluence semble augmenter la fonction p53 en association avec l'idasanutlin et la RITA pour les cellules U87MG mais pas pour les cellules U87MG R50 OFF. Inversement, l'association de FR248 avec Idasanutlin affecte la signalisation p53 dans les cellules U87MG R50 OFF mais

pas dans les cellules U87MG. Ces données ne sont pas facilement explicables à ce stade, mais indiquent déjà des différences dans le comportement de p53 entre les cellules TMZ naïves et les cellules résistantes. Des travaux restent à faire pour montrer si des combinaisons spécifiques peuvent mieux affecter la viabilité des cellules de gliome pour chaque type de cellule.

Conclusion

En conclusion, notre travail montre un impact énorme du témazolomide sur le répertoire des intégrines des cellules U87MG. Les expressions des intégrines semblent très facilement commutables pendant le traitement au témozolomide. Des intégrines spécifiques peuvent être particulièrement ciblées à différents moments du traitement du glioblastome et des thérapies combinées évaluées en fonction de leur expression. Bien qu'une confirmation dans des lignées cellulaires dérivées de patients et d'autres modèles précliniques soit nécessaire, nos données apportent de nouvelles preuves que l'intégrine α5β1 a un rôle à jouer en tant que cible thérapeutique dans les glioblastomes récurrents.

Résultats, partie 3

3. Effet du composé 9 en tant que double inhibiteur de l'intégrine α5β1 et du complexe p53/MDM2

Au cours de ces travaux, un nouveau composé a été décrit dans la littérature (Merlino et al., 2018). Le composé 9 a été décrit comme un puissant inhibiteur des intégrines α5β1 et αvβ3 couplé à une activité inhibitrice sur la MDM2 et la MDM4, combinant ainsi les effets que nous étudions. Nous avons vérifié l'effet du composé-9 dans nos lignées cellulaires.

3.1. Effet du composé 9 sur la confluence des cellules

Nous avons d'abord évalué l'effet du composé 9 sur la confluence cellulaire de l'expression de l'intégrine α5 (cellules U87MG et U87MG OFF R50) et des cellules U87MG-α5KO dans lesquelles le gène de l'intégrine α5 a été supprimé grâce à la technologie CRISPR/Cas 9. Nous avons traité les cellules U87MG, U87MG-α5KO et U87MG OFF R0 avec des concentrations croissantes de composé-9 et la confluence cellulaire a été détectée et calculée de manière dynamique à l'aide du logiciel IncuCyte Zoom basé sur des images à contraste de phase obtenues à partir de l'IncuCyte en temps réel. Le composé 9 a induit une diminution de la confluence cellulaire en fonction de la concentration dans toutes les lignées cellulaires. Une inhibition de 50 % a été obtenue à 0,6µM pour les cellules U87MG et U87MG OFF R50 et à

2,5µM pour les cellules U87MG-α5KO, ce qui suggère que les cellules U87MG-α5KO dépourvues de l'intégrine α5 sont moins sensibles au traitement par le Compound-9 que les cellules exprimant l'intégrine α5 (cellules U87MG et U87MG OFF R50).

Nous avons ensuite évalué l'effet du Compound-9 sur la morphologie des cellules U87MG et U87MG-α5KO. Des images en contraste de phase ont montré que le traitement avec une forte concentration de composé-9 (20µM) entraîne le détachement et l'arrondissement des cellules U87MG et U87MG-α5KO 72 heures après le traitement, ce qui indique l'efficacité du composé-9 à interférer avec l'adhésion des cellules à la matrice extracellulaire, connue pour être étroitement régulée par les intégrines. Il est intéressant de noter que les cellules U87MG-α5KO dépourvues de l'intégrine α5 étaient moins sensibles à une faible concentration de composé (1µM) que les cellules U87MG parentales, ce qui confirme qu'elles reconnaissent mieux les cellules exprimant l'intégrine. Cependant, aucune différence n'a été observée entre les deux lignées cellulaires lorsque la concentration du composé 9 était plus élevée.

Ces résultats suggèrent que le traitement par le composé 9 est plus efficace à de faibles concentrations dans les cellules exprimant l'intégrine α5 et qu'une concentration plus élevée pourrait éventuellement agir par interaction avec l'intégrine αvβ3.

3.2. Effet du composé 9 sur la voie p53

Sur la base de ces résultats et du rapport selon lequel le composé 9 stabilise et active la voie p53 (Merlino et al., 2018), nous avons étudié plus en détail l'effet du composé 9 sur la stabilisation de la p53. Nous avons traité les cellules U87MG avec le composé 9 dans des conditions sériques réduites (2%) et avons ensuite évalué la stabilité de la protéine p53. Les résultats du Western blot ont montré que le traitement avec le composé-9 n'a pas augmenté la stabilité de la protéine p53 par rapport au contrôle, 8 heures après le traitement. De plus, l'analyse par RT-qPCR de l'ARNm du gène cible réprimé par p53 (birc5) et des ARNm du gène cible activé par p53 (fas, p21 et hdm2) n'a montré aucune augmentation détectable par rapport au contrôle, 6 et 24 heures après le traitement avec le composé 9 à 1 µM.

Ces résultats ont démontré que le composé 9 ne stabilisait ni n'activait la protéine p53 dans nos lignées cellulaires et nos conditions expérimentales.

Comme il a été rapporté que le composé 9 activait la voie p53 à 0,1µM (Merlino et al., 2018), nous avons ensuite traité les cellules U87MG et U87MG-α5KO avec le composé 9 à 0,1µM par rapport à l'activateur p53 Nutlin-3a (1µM) dans une étude cinétique et évalué la stabilisation de

la protéine p53 et MDM2. Une comparaison des deux résultats révèle que Nutlin-3a a stabilisé la protéine p53 et MDM2 dans les cellules U87MG et U87MG-α5KO à tous les points de temps testés (3, 6, 9, 12 et 24 heures). En revanche, aucune augmentation détectable de la stabilité de la protéine p53 n'a été observée dans les cellules U87MG et U87MG-α5KO après traitement avec le composé 9 à tous ces moments (3, 6, 9, 12 et 24 heures).

Nous nous sommes demandé si le fait de varier les conditions expérimentales et les concentrations du composé 9 pouvait avoir un impact positif sur la voie p53. Nous avons traité des cellules U87MG avec une concentration croissante de composé 9 dans un milieu contenant 10 % de sérum et avons évalué la stabilisation de la protéine p53. Aucune augmentation de la stabilité de p53 n'a été observée à 12 et 24 heures après le traitement à toutes les concentrations de composé-9 testées.

Dans l'ensemble, le composé 9 n'a pas stabilisé ou activé la voie p53 dans nos lignées cellulaires mais a plutôt semblé la diminuer avec l'augmentation de la concentration et de la période de traitement.

Discussion

La restauration de la fonction suppressive de la tumeur de type sauvage p53 est considérée comme une stratégie thérapeutique intéressante pour le traitement de la GBM. Cependant, le p53 de type sauvage est souvent inactivé ou dégradé par la MDM2. Les protéines MDM2 sont dérégulées dans la GBM (Wade et al., 2013) et sa surexpression est corrélée à un mauvais pronostic clinique et à une mauvaise réponse aux traitements actuels du cancer (Momand et al., 1998). À ce jour, plusieurs inhibiteurs de la MDM2 ont été mis au point. Cependant, des études ont démontré que l'activation de la protéine p53 par les inhibiteurs MDM2 tels que Nutlin-3a (Renner et al., 2016) ou Idasanutlin (Pan et al., 2017) est insuffisante pour induire l'apoptose dans les cellules cancéreuses. Des données antérieures de notre laboratoire ont identifié une voie convergente impliquant l'intégrine α5β1 et la protéine p53 dans la régulation de l'apoptose des cellules de gliome (Renner et al., 2016b). Cette intégrine est surexprimée au niveau de l'ARNm (Ellert-Miklaszewska et al., 2020) et de la protéine (Holmes et al., 2012) et sa surexpression est associée à une diminution de la survie des patients atteints de GBM (Janouskova et al., 2012). Par conséquent, α5β1 integrin est apparu comme une cible intéressante dans la GBM. Dans le même ordre d'idées, une optimisation du composé 7 (un inhibiteur des intégrines MDM2/4 et αvβ3/αvβ3) réalisée par Merlino et al. dans laquelle ses activités sur les intégrines ont été préservées tout en améliorant celles sur les protéines MDM

et MDM4 a conduit à la découverte du composé 9. Le composé 9 a été décrit comme un puissant inhibiteur des intégrines α5β1 et αvβ3 couplé à une activité inhibitrice sur MDM2 et MDM4. Il a été rapporté que le composé 9 diminuait la prolifération cellulaire, stabilisait p53 et induisait la transcription des gènes cibles p53 p21, MDM2 et PUMA de façon dépendant de p53 de type sauvage dans les cellules U87MG (Merlino et al., 2018).

Il était donc intéressant de tester ce nouveau composé dans nos lignées cellulaires, car il peut combiner en un seul médicament l'effet de l'activation de p53 et l'antagonisme des intégrines α5β1. Nous avons démontré que le composé 9 induisait une diminution de la confluence des cellules U87MG et U87MG-α5KO dépendant de la concentration. De plus, 50 % de l'inhibition a été obtenue à 0,6μM pour U87MG et 2,5μM pour U87MG-α5KO, ce qui suggère que les cellules U87MG-α5KO dépourvues de l'intégrine α5 sont moins sensibles au traitement par le Composé-9 que les cellules parentales U87MG exprimant l'intégrine. Cette conclusion est en accord avec les résultats de Merlino et al. dans lesquels le composé 9 a été décrit comme un puissant inhibiteur de l'intégrine α5β1 en plus de sa capacité à inhiber la prolifération cellulaire de l'U87MG. Nous avons montré, à l'aide d'images de contraste de phase, que le traitement par le composé 9 entraîne le détachement et l'arrondissement des cellules, ce qui indique l'efficacité du composé 9 à interférer avec l'adhésion des cellules à la matrice extracellulaire qui est connue pour être étroitement régulée par les intégrines. Nous avons constaté que les cellules U87MG-α5KO dépourvues de l'intégrine α5 étaient moins sensibles à une faible concentration de composé (1μM) que les cellules U87MG parentales, ce qui confirme qu'elle reconnaît mieux les cellules exprimant l'intégrine. Cependant, aucune différence n'a été observée entre les deux lignées cellulaires lorsque la concentration du composé 9 était plus élevée. Nos données suggèrent que le traitement du composé 9 à des concentrations plus faibles est plus spécifique pour les cellules exprimant l'intégrine α5 et qu'une concentration plus élevée pourrait éventuellement agir par interaction avec l'intégrine αvβ3, MDM2 ou MDM4, en plus de l'intégrine α5β1. Ce résultat est conforme aux études dans lesquelles Merlino et al. ont démontré que le composé 9 à une concentration inférieure (0,1 μM) fonctionne en dessous du seuil de traitement combiné avec l'inhibiteur MDM2 Nutlin-3a et l'antagoniste d'intégrine Cilengitide, mais fonctionne au-dessus de ce seuil à une concentration supérieure (10 μM) (Merlino et al., 2018).

Nous avons comparé le composé 9 en tant qu'agent unique avec la co-administration de l'activateur p53 Idasanutlin et de l'antagoniste des intégrines K34c. Nous avons constaté que le composé 9 à une concentration plus élevée (20 μM) provoque un effet sur la confluence

cellulaire qui est équivalent au traitement combiné avec les antagonistes des intégrines K34c et l'activateur p53 Idasanutlin dans les cellules U87MG naïves et résistantes aux TMZ. Conformément à nos conclusions, Merlino et al. ont montré que le composé 9 (10 μM) diminuait la prolifération cellulaire des cellules U87MG dans la même mesure que le traitement combiné avec Nutlin-3a et l'antagoniste des intégrines Cilengitide (Merlino et al., 2018). Les résultats suggèrent donc que ce composé pourrait être un moyen intéressant de traiter les cellules de gliome. En outre, par rapport à la coadministration de différents médicaments, une seule molécule ayant la capacité d'atteindre simultanément plusieurs cibles pourrait offrir plusieurs avantages, tels qu'un risque moindre d'interactions pharmacocinétiques entre médicaments et une moindre susceptibilité à la résistance adaptative.

Des résultats antérieurs ont démontré que le composé 9 stabilisait p53 et augmentait l'activité de p53 par l'induction transcriptionnelle des gènes cibles p53 p21, MDM2 et PUMA d'une manière dépendant du p53 de type sauvage (Merlino et al., 2018). Contrairement à ces résultats, cependant, aucune preuve de stabilisation de p53 ou d'augmentation des gènes cibles p53 n'a été observée lors du traitement avec le composé 9 dans nos conditions expérimentales. Pour confirmer nos résultats, nous avons demandé un autre lot de composé 9, mais aucune augmentation observable de la stabilité de p53 n'a été obtenue. Nous avons ensuite modifié nos conditions expérimentales en utilisant la même concentration de composé 9 (0,1μM), le même temps de traitement et la même condition sérique que ceux rapportés par Merlino et al. (Merlino et al., 2018). Aucune augmentation de la stabilité de p53 n'a été observée malgré l'utilisation de ces conditions expérimentales dans une étude cinétique. Ces résultats sont plutôt décevants car le composé 9 semblait prometteur sur la base des données de confluence cellulaire obtenues en temps réel mais n'a pas réussi à stabiliser et à activer la protéine p53.

Ces résultats contrastés ont soulevé de nombreuses questions nécessitant des recherches plus approfondies. Il serait intéressant d'évaluer les effets cytotoxiques du composé 9 en utilisant des techniques telles que le test d'exclusion du bleu de trypan. Cela permettrait de déterminer si les cellules détachées et arrondies sont mortes ou vivantes après le traitement du composé 9. Si les cellules s'avèrent mortes, il serait intéressant de déterminer le mécanisme impliqué (comme la nécrose ou l'autophagie).

Des recherches plus approfondies sur le composé 9 devraient être effectuées en utilisant d'autres cellules GBM et, si possible, devraient être évaluées sur un autre type de cancer. Il serait intéressant d'optimiser davantage l'effet inhibiteur du composé 9 sur la MDM2.

Conclusion

Dans cette enquête, l'objectif était d'évaluer l'effet du composé 9 sur la confluence cellulaire et la voie p53 dans la MGF. Sur la confluence cellulaire, le composé 9 en tant qu'agent unique provoque une activité égale à celle d'un traitement combiné avec un activateur p53 et un antagoniste des intégrines. Cependant, le composé 9 n'a pas réussi à stabiliser ou à activer la protéine p53 dans nos conditions expérimentales. Des recherches supplémentaires sont nécessaires pour déterminer le rôle du composé 9 sur la voie p53 ou sur une autre voie.

REFERENCES

Acehan, D., Jiang, X., Morgan, D.G., Heuser, J.E., Wang, X., and Akey, C.W. (2002). Three-dimensional structure of the apoptosome: implications for assembly, procaspase-9 binding, and activation. Mol. Cell *9*, 423–432.

Aguilar, L.K., Arvizu, M., Aguilar-Cordova, E., and Chiocca, E.A. (2012). The Spectrum of Vaccine Therapies for Patients With Glioblastoma Multiforme. Curr. Treat. Options Oncol. *13*, 437–450.

Aldape, K., Zadeh, G., Mansouri, S., Reifenberger, G., and von Deimling, A. (2015). Glioblastoma: pathology, molecular mechanisms and markers. Acta Neuropathol. (Berl.) *129*, 829–848.

Alday-Parejo, B., Stupp, R., and Rüegg, C. (2019). Are Integrins Still Practicable Targets for Anti-Cancer Therapy? Cancers *11*.

Alexandrova, E.M., and Moll, U.M. (2017). Depleting stabilized GOF mutant p53 proteins by inhibiting molecular folding chaperones: a new promise in cancer therapy. Cell Death Differ. *24*, 3–5.

Alexandrova, E.M., Yallowitz, A.R., Li, D., Xu, S., Schulz, R., Proia, D.A., Lozano, G., Dobbelstein, M., and Moll, U.M. (2015). Improving survival by exploiting tumour dependence on stabilized mutant p53 for treatment. Nature *523*, 352–356.

Almeida, K.H., and Sobol, R.W. (2007). A unified view of base excision repair: lesion-dependent protein complexes regulated by post-translational modification. DNA Repair *6*, 695–711.

Almokadem, S., and Belani, C.P. (2012). Volociximab in cancer. Expert Opin. Biol. Ther. *12*, 251–257.

Amirian, E.S., Armstrong, G.N., Zhou, R., Lau, C.C., Claus, E.B., Barnholtz-Sloan, J.S., Il'yasova, D., Schildkraut, J., Ali-Osman, F., Sadetzki, S., et al. (2016). The Glioma International Case-Control Study: A Report From the Genetic Epidemiology of Glioma International Consortium. Am. J. Epidemiol. *183*, 85–91.

Anders, S., Pyl, P.T., and Huber, W. (2015). HTSeq—a Python framework to work with high-throughput sequencing data. Bioinformatics *31*, 166–169.

Anderson, L.R., Owens, T.W., and Naylor, M.J. (2014). Structural and mechanical functions of integrins. Biophys. Rev. *6*, 203–213.

Anthis, N.J., and Campbell, I.D. (2011). The tail of integrin activation. Trends Biochem. Sci. *36*, 191–198.

Anton, K., Baehring, J.M., and Mayer, T. (2012). Glioblastoma multiforme: overview of current treatment and future perspectives. Hematol. Oncol. Clin. North Am. *26*, 825–853.

Arias-Salgado, E.G., Lizano, S., Sarkar, S., Brugge, J.S., Ginsberg, M.H., and Shattil, S.J. (2003). Src kinase activation by direct interaction with the integrin β cytoplasmic domain. Proc. Natl. Acad. Sci. U. S. A. *100*, 13298–13302.

Attardi, L.D., Reczek, E.E., Cosmas, C., Demicco, E.G., McCurrach, M.E., Lowe, S.W., and Jacks, T. (2000). PERP, an apoptosis-associated target of p53, is a novel member of the PMP-22/gas3 family. Genes Dev. *14*, 704–718.

Auffinger, B., Tobias, A.L., Han, Y., Lee, G., Guo, D., Dey, M., Lesniak, M.S., and Ahmed, A.U. (2014). Conversion of differentiated cancer cells into cancer stem-like cells in a glioblastoma model after primary chemotherapy. Cell Death Differ. *21*, 1119–1131.

Auger, N., Thillet, J., Wanherdrick, K., Idbaih, A., Legrier, M.-E., Dutrillaux, B., Sanson, M., and Poupon, M.-F. (2006). Genetic alterations associated with acquired temozolomide resistance in SNB-19, a human glioma cell line. Mol. Cancer Ther. *5*, 2182–2192.

Avraamides, C.J., Garmy-Susini, B., and Varner, J.A. (2008). Integrins in angiogenesis and lymphangiogenesis. Nat. Rev. Cancer *8*, 604–617.

Babashah, S., and Soleimani, M. (2011). The oncogenic and tumour suppressive roles of microRNAs in cancer and apoptosis. Eur. J. Cancer Oxf. Engl. 1990 *47*, 1127–1137.

Baer, J.C., Freeman, A.A., Newlands, E.S., Watson, A.J., Rafferty, J.A., and Margison, G.P. (1993). Depletion of O6-alkylguanine-DNA alkyltransferase correlates with potentiation of temozolomide and CCNU toxicity in human tumour cells. Br. J. Cancer *67*, 1299–1302.

Bai, L., and Zhu, W.-G. (2006). p53: Structure, Function and Therapeutic Applications. 13.

Banelli, B., Carra, E., Barbieri, F., Würth, R., Parodi, F., Pattarozzi, A., Carosio, R., Forlani, A., Allemanni, G., Marubbi, D., et al. (2015). The histone demethylase KDM5A is a key factor for the resistance to temozolomide in glioblastoma. Cell Cycle Georget. Tex *14*, 3418–3429.

Bao, S., Wu, Q., McLendon, R.E., Hao, Y., Shi, Q., Hjelmeland, A.B., Dewhirst, M.W., Bigner, D.D., and Rich, J.N. (2006). Glioma stem cells promote radioresistance by preferential activation of the DNA damage response. Nature *444*, 756–760.

Barani, I.J., and Larson, D.A. (2015). Radiation therapy of glioblastoma. Cancer Treat. Res. *163*, 49–73.

Barczyk, M., Carracedo, S., and Gullberg, D. (2010). Integrins. Cell Tissue Res. *339*, 269–280.

Basu, B., and Ghosh, M.K. (2019). Extracellular Vesicles in Glioma: From Diagnosis to Therapy. BioEssays News Rev. Mol. Cell. Dev. Biol. *41*, e1800245.

Batash, R., Asna, N., Schaffer, P., Francis, N., and Schaffer, M. (2017). Glioblastoma Multiforme, Diagnosis and Treatment; Recent Literature Review. Curr. Med. Chem. *24*, 3002–3009.

Bäuerle, T., Komljenovic, D., Merz, M., Berger, M.R., Goodman, S.L., and Semmler, W. (2011). Cilengitide inhibits progression of experimental breast cancer bone metastases as imaged noninvasively using VCT, MRI and DCE-MRI in a longitudinal in vivo study. Int. J. Cancer *128*, 2453–2462.

Beauséjour, C.M., Krtolica, A., Galimi, F., Narita, M., Lowe, S.W., Yaswen, P., and Campisi, J. (2003). Reversal of human cellular senescence: roles of the p53 and p16 pathways. EMBO J. *22*, 4212–4222.

Becker, A., von Richter, O., Kovar, A., Scheible, H., van Lier, J.J., and Johne, A. (2015). Metabolism and disposition of the αv-integrin ß3/ß5 receptor antagonist cilengitide, a cyclic polypeptide, in humans. J. Clin. Pharmacol. *55*, 815–824.

Bell-McGuinn, K.M., Matthews, C.M., Ho, S.N., Barve, M., Gilbert, L., Penson, R.T., Lengyel, E., Palaparthy, R., Gilder, K., Vassos, A., et al. (2011). A phase II, single-arm study of the anti-α5β1 integrin antibody volociximab as monotherapy in patients with platinum-resistant advanced epithelial ovarian or primary peritoneal cancer. Gynecol. Oncol. *121*, 273–279.

Bennett, M., Macdonald, K., Chan, S.W., Luzio, J.P., Simari, R., and Weissberg, P. (1998). Cell surface trafficking of Fas: a rapid mechanism of p53-mediated apoptosis. Science *282*, 290–293.

Ben-Porath, I., Thomson, M.W., Carey, V.J., Ge, R., Bell, G.W., Regev, A., and Weinberg, R.A. (2008). An embryonic stem cell-like gene expression signature in poorly differentiated aggressive human tumors. Nat. Genet. *40*, 499–507.

Berberich, A., Kessler, T., Thomé, C.M., Pusch, S., Hielscher, T., Sahm, F., Oezen, I., Schmitt, L.-M., Ciprut, S., Hucke, N., et al. (2019). Targeting Resistance against the MDM2 Inhibitor RG7388 in Glioblastoma Cells by the MEK Inhibitor Trametinib. Clin. Cancer Res. Off. J. Am. Assoc. Cancer Res. *25*, 253–265.

Besse, B., Tsao, L.C., Chao, D.T., Fang, Y., Soria, J.-C., Almokadem, S., and Belani, C.P. (2013). Phase Ib safety and pharmacokinetic study of volociximab, an anti-α5β1 integrin antibody, in combination with carboplatin and paclitaxel in advanced non-small-cell lung cancer. Ann. Oncol. Off. J. Eur. Soc. Med. Oncol. *24*, 90–96.

Bhakat, K.K., and Mitra, S. (2003). CpG methylation-dependent repression of the human O6-methylguanine-DNA methyltransferase gene linked to chromatin structure alteration. Carcinogenesis *24*, 1337–1345.

Bhaskar, V., Fox, M., Breinberg, D., Wong, M.H.-L., Wales, P.E., Rhodes, S., DuBridge, R.B., and Ramakrishnan, V. (2008). Volociximab, a chimeric integrin alpha5beta1 antibody, inhibits the growth of VX2 tumors in rabbits. Invest. New Drugs *26*, 7–12.

Bieging, K.T., Mello, S.S., and Attardi, L.D. (2014). Unravelling mechanisms of p53-mediated tumour suppression. Nat. Rev. Cancer *14*, 359–370.

Boatright, K.M., Renatus, M., Scott, F.L., Sperandio, S., Shin, H., Pedersen, I.M., Ricci, J.E., Edris, W.A., Sutherlin, D.P., Green, D.R., et al. (2003). A unified model for apical caspase activation. Mol. Cell *11*, 529–541.

Bobola, M.S., Kolstoe, D.D., Blank, A., Chamberlain, M.C., and Silber, J.R. (2012). Repair of 3-methyladenine and abasic sites by base excision repair mediates glioblastoma resistance to temozolomide. Front. Oncol. *2*, 176.

Boyd, S.D., Tsai, K.Y., and Jacks, T. (2000). An intact HDM2 RING-finger domain is required for nuclear exclusion of p53. Nat. Cell Biol. *2*, 563–568.

Bredel, M., Bredel, C., Juric, D., Duran, G.E., Yu, R.X., Harsh, G.R., Vogel, H., Recht, L.D., Scheck, A.C., and Sikic, B.I. (2006). Tumor necrosis factor-alpha-induced protein 3 as a putative regulator of nuclear factor-kappaB-mediated resistance to O6-alkylating agents in human glioblastomas. J. Clin. Oncol. Off. J. Am. Soc. Clin. Oncol. *24*, 274–287.

Brennan, C.W., Verhaak, R.G.W., McKenna, A., Campos, B., Noushmehr, H., Salama, S.R., Zheng, S., Chakravarty, D., Sanborn, J.Z., Berman, S.H., et al. (2013). The Somatic Genomic Landscape of Glioblastoma. Cell *155*, 462–477.

Brunton, V.G., and Frame, M.C. (2008). Src and focal adhesion kinase as therapeutic targets in cancer. Curr. Opin. Pharmacol. *8*, 427–432.

Buerkle, M.A., Pahernik, S.A., Sutter, A., Jonczyk, A., Messmer, K., and Dellian, M. (2002). Inhibition of the alpha-nu integrins with a cyclic RGD peptide impairs angiogenesis, growth and metastasis of solid tumours in vivo. Br. J. Cancer *86*, 788–795.

Burton, E.C., Lamborn, K.R., Forsyth, P., Scott, J., O'Campo, J., Uyehara-Lock, J., Prados, M., Berger, M., Passe, S., Uhm, J., et al. (2002). Aberrant p53, mdm2, and proliferation differ in glioblastomas from long-term compared with typical survivors. Clin. Cancer Res. Off. J. Am. Assoc. Cancer Res. *8*, 180–187.

Bush, N.A.O., Chang, S.M., and Berger, M.S. (2017). Current and future strategies for treatment of glioma. Neurosurg. Rev. *40*, 1–14.

Cai, H.-Q., Liu, A.-S., Zhang, M.-J., Liu, H.-J., Meng, X.-L., Qian, H.-P., and Wan, J.-H. (2020). Identifying Predictive Gene Expression and Signature Related to Temozolomide Sensitivity of Glioblastomas. Front. Oncol. *10*, 669.

Cain, K., Bratton, S.B., and Cohen, G.M. (2002). The Apaf-1 apoptosome: a large caspase-activating complex. Biochimie *84*, 203–214.

Calderwood, D.A., Tuckwell, D.S., Eble, J., Kühn, K., and Humphries, M.J. (1997). The integrin alpha1 A-domain is a ligand binding site for collagens and laminin. J. Biol. Chem. *272*, 12311–12317.

Campisi, J. (2013). Aging, Cellular Senescence, and Cancer. Annu. Rev. Physiol. *75*, 685–705.

Carlsson, S.K., Brothers, S.P., and Wahlestedt, C. (2014). Emerging treatment strategies for glioblastoma multiforme. EMBO Mol. Med. *6*, 1359–1370.

Cartron, P.-F., Gallenne, T., Bougras, G., Gautier, F., Manero, F., Vusio, P., Meflah, K., Vallette, F.M., and Juin, P. (2004). The first alpha helix of Bax plays a necessary role in its ligand-induced activation by the BH3-only proteins Bid and PUMA. Mol. Cell *16*, 807–818.

Castro-Magdonel, B.E., Orjuela, M., Alvarez-Suarez, D.E., Camacho, J., Cabrera-Muñoz, L., Sadowinski-Pine, S., Medina-Sanson, A., Lara-Molina, C., García-Vega, D., Vázquez, Y., et al. (2020). Circulating miRNome detection analysis reveals 537 miRNAS in plasma, 625 in extracellular vesicles and a discriminant plasma signature of 19 miRNAs in children with retinoblastoma from which 14 are also detected in corresponding primary tumors. PLoS ONE *15*.

Chamberlain, M.C., Cloughsey, T., Reardon, D.A., and Wen, P.Y. (2012). A novel treatment for glioblastoma: integrin inhibition. Expert Rev. Neurother. *12*, 421–435.

Chehab, N.H., Malikzay, A., Appel, M., and Halazonetis, T.D. (2000). Chk2/hCds1 functions as a DNA damage checkpoint in G(1) by stabilizing p53. Genes Dev. *14*, 278–288.

Chen, Q., Manning, C.D., Millar, H., McCabe, F.L., Ferrante, C., Sharp, C., Shahied-Arruda, L., Doshi, P., Nakada, M.T., and Anderson, G.M. (2008). CNTO 95, a fully human anti alphav integrin antibody, inhibits cell signaling, migration, invasion, and spontaneous metastasis of human breast cancer cells. Clin. Exp. Metastasis *25*, 139–148.

Chène, P. (2003). Inhibiting the p53–MDM2 interaction: an important target for cancer therapy. Nat. Rev. Cancer *3*, 102–109.

Cheng, Z.-X., Yin, W.-B., and Wang, Z.-Y. (2017). MicroRNA-132 induces temozolomide resistance and promotes the formation of cancer stem cell phenotypes by targeting tumor suppressor candidate 3 in glioblastoma. Int. J. Mol. Med. *40*, 1307–1314.

Cheresh, D.A., and Stupack, D.G. (2002). Integrin-mediated death: an explanation of the integrin-knockout phenotype? Nat. Med. *8*, 193–194.

Chien, C.-H., Chuang, J.-Y., Yang, S.-T., Yang, W.-B., Chen, P.-Y., Hsu, T.-I., Huang, C.-Y., Lo, W.-L., Yang, K.-Y., Liu, M.-S., et al. (2019). Enrichment of superoxide dismutase 2 in glioblastoma confers to acquisition of temozolomide resistance that is associated with tumor-initiating cell subsets. J. Biomed. Sci. *26*, 77.

Childs, B.G., Durik, M., Baker, D.J., and van Deursen, J.M. (2015). Cellular senescence in aging and age-related disease: from mechanisms to therapy. Nat. Med. *21*, 1424–1435.

Chipuk, J.E., and Green, D.R. (2008). How do BCL-2 proteins induce mitochondrial outer membrane permeabilization? Trends Cell Biol. *18*, 157–164.

Chipuk, J.E., Kuwana, T., Bouchier-Hayes, L., Droin, N.M., Newmeyer, D.D., Schuler, M., and Green, D.R. (2004). Direct activation of Bax by p53 mediates mitochondrial membrane permeabilization and apoptosis. Science *303*, 1010–1014.

Chipuk, J.E., Bouchier-Hayes, L., and Green, D.R. (2006). Mitochondrial outer membrane permeabilization during apoptosis: the innocent bystander scenario. Cell Death Differ. *13*, 1396–1402.

Choy, C.T., Kim, H., Lee, J.-Y., Williams, D.M., Palethorpe, D., Fellows, G., Wright, A.J., Laing, K., Bridges, L.R., Howe, F.A., et al. (2014). Anosmin-1 contributes to brain tumor malignancy through integrin signal pathways. Endocr. Relat. Cancer *21*, 85–99.

Chung, J., Bachelder, R.E., Lipscomb, E.A., Shaw, L.M., and Mercurio, A.M. (2002). Integrin (α6β4) regulation of eIF-4E activity and VEGF translation. J. Cell Biol. *158*, 165–174.

Cianfrocca, M.E., Kimmel, K.A., Gallo, J., Cardoso, T., Brown, M.M., Hudes, G., Lewis, N., Weiner, L., Lam, G.N., Brown, S.C., et al. (2006). Phase 1 trial of the antiangiogenic peptide ATN-161 (Ac-PHSCN-NH2), a beta integrin antagonist, in patients with solid tumours. Br. J. Cancer *94*, 1621–1626.

Cirkel, G.A., Kerklaan, B.M., Vanhoutte, F., der Aa, A.V., Lorenzon, G., Namour, F., Pujuguet, P., Darquenne, S., de Vos, F.Y.F., Snijders, T.J., et al. (2016). A dose escalating phase I study of GLPG0187, a broad spectrum integrin receptor antagonist, in adult patients with progressive high-grade glioma and other advanced solid malignancies. Invest. New Drugs *34*, 184–192.

Cole, S.P.C. (2014). Targeting multidrug resistance protein 1 (MRP1, ABCC1): past, present, and future. Annu. Rev. Pharmacol. Toxicol. *54*, 95–117.

Cooper, J., and Giancotti, F.G. (2019). Integrin Signaling in Cancer: Mechanotransduction, Stemness, Epithelial Plasticity, and Therapeutic Resistance. Cancer Cell *35*, 347–367.

Cordes, N., Seidler, J., Durzok, R., Geinitz, H., and Brakebusch, C. (2006). beta1-integrin-mediated signaling essentially contributes to cell survival after radiation-induced genotoxic injury. Oncogene *25*, 1378–1390.

Crespo, I., Vital, A.L., Gonzalez-Tablas, M., Patino, M. del C., Otero, A., Lopes, M.C., de Oliveira, C., Domingues, P., Orfao, A., and Tabernero, M.D. (2015). Molecular and Genomic Alterations in Glioblastoma Multiforme. Am. J. Pathol. *185*, 1820–1833.

Cristofalo, V.J., Phillips, P.D., Sorger, T., and Gerhard, G. (1989). Alterations in the responsiveness of senescent cells to growth factors. J. Gerontol. *44*, 55–62.

Czabotar, P.E., Lessene, G., Strasser, A., and Adams, J.M. (2014). Control of apoptosis by the BCL-2 protein family: implications for physiology and therapy. Nat. Rev. Mol. Cell Biol. *15*, 49–63.

Dahan, P., Martinez Gala, J., Delmas, C., Monferran, S., Malric, L., Zentkowski, D., Lubrano, V., Toulas, C., Cohen-Jonathan Moyal, E., and Lemarie, A. (2014). Ionizing radiations sustain glioblastoma cell dedifferentiation to a stem-like phenotype through survivin: possible involvement in radioresistance. Cell Death Dis. *5*, e1543.

Dai, C., and Gu, W. (2010). p53 post-translational modification: deregulated in tumorigenesis. Trends Mol. Med. *16*, 528–536.

Dechantsreiter, M.A., Planker, E., Mathä, B., Lohof, E., Hölzemann, G., Jonczyk, A., Goodman, S.L., and Kessler, H. (1999). N-Methylated cyclic RGD peptides as highly active and selective alpha(V)beta(3) integrin antagonists. J. Med. Chem. *42*, 3033–3040.

el-Deiry, W.S. (1998). Regulation of p53 downstream genes. Semin. Cancer Biol. *8*, 345–357.

Delamarre, E., Taboubi, S., Mathieu, S., Bérenguer, C., Rigot, V., Lissitzky, J.-C., Figarella-Branger, D., Ouafik, L., and Luis, J. (2009). Expression of Integrin α6β1 Enhances Tumorigenesis in Glioma Cells. Am. J. Pathol. *175*, 844–855.

DeLay, M., Jahangiri, A., Carbonell, W.S., Hu, Y.-L., Tsao, S., Tom, M.W., Paquette, J., Tokuyasu, T.A., and Aghi, M.K. (2012). Microarray analysis verifies two distinct phenotypes of glioblastomas resistant to antiangiogenic therapy. Clin. Cancer Res. Off. J. Am. Assoc. Cancer Res. *18*, 2930–2942.

Desgrosellier, J.S., and Cheresh, D.A. (2010). Integrins in cancer: biological implications and therapeutic opportunities. Nat. Rev. Cancer *10*, 9–22.

Di Micco, R., Fumagalli, M., Cicalese, A., Piccinin, S., Gasparini, P., Luise, C., Schurra, C., Garre', M., Nuciforo, P.G., Bensimon, A., et al. (2006). Oncogene-induced senescence is a DNA damage response triggered by DNA hyper-replication. Nature *444*, 638–642.

Dickson, D.W. (2004). Apoptotic mechanisms in Alzheimer neurofibrillary degeneration: cause or effect? J. Clin. Invest. *114*, 23–27.

Dimri, G.P., Lee, X., Basile, G., Acosta, M., Scott, G., Roskelley, C., Medrano, E.E., Linskens, M., Rubelj, I., and Pereira-Smith, O. (1995). A biomarker that identifies senescent human cells in culture and in aging skin in vivo. Proc. Natl. Acad. Sci. U. S. A. *92*, 9363–9367.

Ding, Q., Zhang, Z., Liu, J.-J., Jiang, N., Zhang, J., Ross, T.M., Chu, X.-J., Bartkovitz, D., Podlaski, F., Janson, C., et al. (2013). Discovery of RG7388, a Potent and Selective p53–MDM2 Inhibitor in Clinical Development. J. Med. Chem. *56*, 5979–5983.

Dobin, A., Davis, C.A., Schlesinger, F., Drenkow, J., Zaleski, C., Jha, S., Batut, P., Chaisson, M., and Gingeras, T.R. (2013). STAR: ultrafast universal RNA-seq aligner. Bioinformatics *29*, 15–21.

Dolecek, T.A., Propp, J.M., Stroup, N.E., and Kruchko, C. (2012). CBTRUS Statistical Report: Primary Brain and Central Nervous System Tumors Diagnosed in the United States in 2005–2009. Neuro-Oncol. *14*, v1–v49.

Drabløs, F., Feyzi, E., Aas, P.A., Vaagbø, C.B., Kavli, B., Bratlie, M.S., Peña-Diaz, J., Otterlei, M., Slupphaug, G., and Krokan, H.E. (2004). Alkylation damage in DNA and RNA--repair mechanisms and medical significance. DNA Repair *3*, 1389–1407.

Ducassou, A., Uro-Coste, E., Verrelle, P., Filleron, T., Benouaich-Amiel, A., Lubrano, V., Sol, J.-C., Delisle, M.-B., Favre, G., Ken, S., et al. (2013). αvβ3 Integrin and Fibroblast growth factor receptor 1 (FGFR1): Prognostic factors in a phase I-II clinical trial associating continuous administration of Tipifarnib with radiotherapy for patients with newly diagnosed glioblastoma. Eur. J. Cancer Oxf. Engl. 1990 *49*, 2161–2169.

Eke, I., Zscheppang, K., Dickreuter, E., Hickmann, L., Mazzeo, E., Unger, K., Krause, M., and Cordes, N. (2015). Simultaneous β1 integrin-EGFR targeting and radiosensitization of human head and neck cancer. J. Natl. Cancer Inst. *107*.

Ekstrand, A.J., James, C.D., Cavenee, W.K., Seliger, B., Pettersson, R.F., and Collins, V.P. (1991). Genes for epidermal growth factor receptor, transforming growth factor alpha, and epidermal growth factor and their expression in human gliomas in vivo. Cancer Res. *51*, 2164–2172.

Ellert-Miklaszewska, A., Poleszak, K., Pasierbinska, M., and Kaminska, B. (2020). Integrin Signaling in Glioma Pathogenesis: From Biology to Therapy. Int. J. Mol. Sci. *21*.

Elliott, M.R., and Ravichandran, K.S. (2010). Clearance of apoptotic cells: implications in health and disease. J. Cell Biol. *189*, 1059–1070.

Elmore, S. (2007). Apoptosis: a review of programmed cell death. Toxicol. Pathol. *35*, 495–516.

Emsley, J., Knight, C.G., Farndale, R.W., Barnes, M.J., and Liddington, R.C. (2000). Structural basis of collagen recognition by integrin alpha2beta1. Cell *101*, 47–56.

Ene, C.I., Cimino, P.J., Fine, H.A., and Holland, E.C. (2020). Incorporating genomic signatures into surgical and medical decision-making for elderly glioblastoma patients. Neurosurg. Focus *49*, E11.

Enge, M., Bao, W., Hedström, E., Jackson, S.P., Moumen, A., and Selivanova, G. (2009). MDM2-dependent downregulation of p21 and hnRNP K provides a switch between apoptosis and growth arrest induced by pharmacologically activated p53. Cancer Cell *15*, 171–183.

England, B., Huang, T., and Karsy, M. (2013). Current understanding of the role and targeting of tumor suppressor p53 in glioblastoma multiforme. Tumor Biol. *34*, 2063–2074.

Esteller, M., Garcia-Foncillas, J., Andion, E., Goodman, S.N., Hidalgo, O.F., Vanaclocha, V., Baylin, S.B., and Herman, J.G. (2000). Inactivation of the DNA-repair gene MGMT and the clinical response of gliomas to alkylating agents. N. Engl. J. Med. *343*, 1350–1354.

Fishlock, D., Diodone, R., Hildbrand, S., Kuhn, B., Mössner, C., Peters, C., Rege, P.D., Rimmler, G., and Schantz, M. (2018). Efficient Industrial Synthesis of the MDM2 Antagonist Idasanutlin via a Cu(I)-catalyzed [3+2] Asymmetric Cycloaddition. Chimia *72*, 492–500.

Franovic, A., Elliott, K.C., Seguin, L., Camargo, M.F., Weis, S.M., and Cheresh, D.A. (2015). Glioblastomas require integrin αvβ3/PAK4 signaling to escape senescence. Cancer Res. *75*, 4466–4473.

Freedman, D.A., Wu, L., and Levine, A.J. (1999). Functions of the MDM2 oncoprotein. Cell. Mol. Life Sci. CMLS *55*, 96–107.

Fridman, J.S., and Lowe, S.W. (2003). Control of apoptosis by p53. Oncogene *22*, 9030–9040.

Friedlander, M., Brooks, P.C., Shaffer, R.W., Kincaid, C.M., Varner, J.A., and Cheresh, D.A. (1995). Definition of two angiogenic pathways by distinct alpha v integrins. Science *270*, 1500–1502.

Friedman, H.S., Kerby, T., and Calvert, H. (2000). Temozolomide and Treatment of Malignant Glioma. 14.

Fu, D., Calvo, J.A., and Samson, L.D. (2012). SERIES: Genomic instability in cancer Balancing repair and tolerance of DNA damage caused by alkylating agents. Nat. Rev. Cancer *12*, 104–120.

Furnari, F.B., Fenton, T., Bachoo, R.M., Mukasa, A., Stommel, J.M., Stegh, A., Hahn, W.C., Ligon, K.L., Louis, D.N., Brennan, C., et al. (2007). Malignant astrocytic glioma: genetics, biology, and paths to treatment. Genes Dev. *21*, 2683–2710.

Furuta, S., Hidaka, E., Ogata, A., Yokota, S., and Kamata, T. (2004). Ras is involved in the negative control of autophagy through the class I PI3-kinase. Oncogene *23*, 3898–3904.

Gallenne, T., Gautier, F., Oliver, L., Hervouet, E., Noël, B., Hickman, J.A., Geneste, O., Cartron, P.-F., Vallette, F.M., Manon, S., et al. (2009). Bax activation by the BH3-only protein

Puma promotes cell dependence on antiapoptotic Bcl-2 family members. J. Cell Biol. *185*, 279–290.

Gan, Z.R., Gould, R.J., Jacobs, J.W., Friedman, P.A., and Polokoff, M.A. (1988). Echistatin. A potent platelet aggregation inhibitor from the venom of the viper, Echis carinatus. J. Biol. Chem. *263*, 19827–19832.

Garmy-Susini, B., Jin, H., Zhu, Y., Sung, R.-J., Hwang, R., and Varner, J. (2005). Integrin alpha4beta1-VCAM-1-mediated adhesion between endothelial and mural cells is required for blood vessel maturation. J. Clin. Invest. *115*, 1542–1551.

Garros-Regulez, L., Aldaz, P., Arrizabalaga, O., Moncho-Amor, V., Carrasco-Garcia, E., Manterola, L., Moreno-Cugnon, L., Barrena, C., Villanua, J., Ruiz, I., et al. (2016). mTOR inhibition decreases SOX2-SOX9 mediated glioma stem cell activity and temozolomide resistance. Expert Opin. Ther. Targets *20*, 393–405.

Geletina, N.S., Kobelev, V.S., Babayants, E.V., Feng, L., Pustylnyak, V.O., and Gulyaeva, L.F. (2018). PTEN negative correlates with miR-181a in tumour tissues of non-obese endometrial cancer patients. Gene *655*, 20–24.

Geraldo, L.H.M., Garcia, C., da Fonseca, A.C.C., Dubois, L.G.F., de Sampaio e Spohr, T.C.L., Matias, D., de Camargo Magalhães, E.S., do Amaral, R.F., da Rosa, B.G., Grimaldi, I., et al. (2019). Glioblastoma Therapy in the Age of Molecular Medicine. Trends Cancer *5*, 46–65.

Giannakakou, P., Sackett, D.L., Ward, Y., Webster, K.R., Blagosklonny, M.V., and Fojo, T. (2000). p53 is associated with cellular microtubules and is transported to the nucleus by dynein. Nat. Cell Biol. *2*, 709–717.

Gingras, M.C., Roussel, E., Bruner, J.M., Branch, C.D., and Moser, R.P. (1995). Comparison of cell adhesion molecule expression between glioblastoma multiforme and autologous normal brain tissue. J. Neuroimmunol. *57*, 143–153.

Ginsberg, M.H. (2014). Integrin activation. BMB Rep. *47*, 655–659.

Gladson, C.L., Wilcox, J.N., Sanders, L., Gillespie, G.Y., and Cheresh, D.A. (1995). Cerebral microenvironment influences expression of the vitronectin gene in astrocytic tumors. J. Cell Sci. *108 (Pt 3)*, 947–956.

Goldar, S., Khaniani, M.S., Derakhshan, S.M., and Baradaran, B. (2015). Molecular mechanisms of apoptosis and roles in cancer development and treatment. Asian Pac. J. Cancer Prev. APJCP *16*, 2129–2144.

Goligorsky, M.S., and Hirschi, K. (2016). Stress-Induced Premature Senescence of Endothelial and Endothelial Progenitor Cells. Adv. Pharmacol. San Diego Calif *77*, 281–306.

Greaves, W., Xiao, L., Sanchez-Espiridion, B., Kunkalla, K., Dave, K.S., Liang, C.S., Singh, R.R., Younes, A., Medeiros, L.J., and Vega, F. (2012). Detection of ABCC1 expression in classical Hodgkin lymphoma is associated with increased risk of treatment failure using standard chemotherapy protocols. J. Hematol. Oncol.J Hematol Oncol *5*, 47.

Green, D.R. (2005). Apoptotic pathways: ten minutes to dead. Cell *121*, 671–674.

Grombacher, T., Eichhorn, U., and Kaina, B. (1998). p53 is involved in regulation of the DNA repair gene O6-methylguanine-DNA methyltransferase (MGMT) by DNA damaging agents. Oncogene *17*, 845–851.

Gu, W., and Roeder, R.G. (1997). Activation of p53 sequence-specific DNA binding by acetylation of the p53 C-terminal domain. Cell *90*, 595–606.

Guha, A., Feldkamp, M.M., Lau, N., Boss, G., and Pawson, A. (1997). Proliferation of human malignant astrocytomas is dependent on Ras activation. Oncogene *15*, 2755–2765.

Guicciardi, M.E., and Gores, G.J. (2009). Life and death by death receptors. FASEB J. *23*, 1625–1637.

Guo, W., and Giancotti, F.G. (2004). Integrin signalling during tumour progression. Nat. Rev. Mol. Cell Biol. *5*, 816–826.

Gupta, A., Shah, K., Oza, M.J., and Behl, T. (2019). Reactivation of p53 gene by MDM2 inhibitors: A novel therapy for cancer treatment. Biomed. Pharmacother. *109*, 484–492.

Guvenc, H., Pavlyukov, M.S., Joshi, K., Kurt, H., Banasavadi-Siddegowda, Y.K., Mao, P., Hong, C., Yamada, R., Kwon, C.-H., Bhasin, D., et al. (2013). Impairment of glioma stem cell survival and growth by a novel inhibitor for Survivin-Ran protein complex. Clin. Cancer Res. Off. J. Am. Assoc. Cancer Res. *19*, 631–642.

Haas, T.L., Sciuto, M.R., Brunetto, L., Valvo, C., Signore, M., Fiori, M.E., di Martino, S., Giannetti, S., Morgante, L., Boe, A., et al. (2017). Integrin α7 Is a Functional Marker and Potential Therapeutic Target in Glioblastoma. Cell Stem Cell *21*, 35-50.e9.

Hainaut, P., and Hollstein, M. (2000). p53 and human cancer: the first ten thousand mutations. Adv. Cancer Res. *77*, 81–137.

Han, J., Flemington, C., Houghton, A.B., Gu, Z., Zambetti, G.P., Lutz, R.J., Zhu, L., and Chittenden, T. (2001). Expression of bbc3, a pro-apoptotic BH3-only gene, is regulated by diverse cell death and survival signals. Proc. Natl. Acad. Sci. U. S. A. *98*, 11318–11323.

Han, S., Li, Z., Master, L.M., Master, Z.W., and Wu, A. (2014). Exogenous IGFBP-2 promotes proliferation, invasion, and chemoresistance to temozolomide in glioma cells via the integrin β1-ERK pathway. Br. J. Cancer *111*, 1400–1409.

Hanks, S.K., Calalb, M.B., Harper, M.C., and Patel, S.K. (1992). Focal adhesion protein-tyrosine kinase phosphorylated in response to cell attachment to fibronectin. Proc. Natl. Acad. Sci. U. S. A. *89*, 8487–8491.

Hannigan, G.E., Leung-Hagesteijn, C., Fitz-Gibbon, L., Coppolino, M.G., Radeva, G., Filmus, J., Bell, J.C., and Dedhar, S. (1996). Regulation of cell adhesion and anchorage-dependent growth by a new beta 1-integrin-linked protein kinase. Nature *379*, 91–96.

Happold, C., Roth, P., Wick, W., Schmidt, N., Florea, A.-M., Silginer, M., Reifenberger, G., and Weller, M. (2012). Distinct molecular mechanisms of acquired resistance to temozolomide in glioblastoma cells. J. Neurochem. *122*, 444–455.

Hardell, L., Carlberg, M., Söderqvist, F., Mild, K.H., and Morgan, L.L. (2007). Long-term use of cellular phones and brain tumours: increased risk associated with use for > or =10 years. Occup. Environ. Med. *64*, 626–632.

Hardell, L., Carlberg, M., Söderqvist, F., and Hansson Mild, K. (2008). Meta-analysis of long-term mobile phone use and the association with brain tumours. Int. J. Oncol. *32*, 1097–1103.

Harris, L.C., Remack, J.S., Houghton, P.J., and Brent, T.P. (1996). Wild-Type p53 Suppresses Transcription of the Human O6-Methylguanine-DNA Methyltransferase Gene. 5.

Haupt, S., Berger, M., Goldberg, Z., and Haupt, Y. (2003). Apoptosis - the p53 network. J. Cell Sci. *116*, 4077–4085.

Hausmann, C., Temme, A., Cordes, N., and Eke, I. (2015). ILKAP, ILK and PINCH1 control cell survival of p53-wildtype glioblastoma cells after irradiation. Oncotarget *6*, 34592–34605.

Hayflick, L., and Moorhead, P.S. (1961). The serial cultivation of human diploid cell strains. Exp. Cell Res. *25*, 585–621.

He, J., Reifenberger, G., Liu, L., Collins, V.P., and James, C.D. (1994). Analysis of glioma cell lines for amplification and overexpression ofMDM2. Genes. Chromosomes Cancer *11*, 91–96.

Heckmann, D., Meyer, A., Laufer, B., Zahn, G., Stragies, R., and Kessler, H. (2008a). Rational Design of Highly Active and Selective Ligands for the α5β1 Integrin Receptor. ChemBioChem *9*, 1397–1407.

Heckmann, D., Meyer, A., Laufer, B., Zahn, G., Stragies, R., and Kessler, H. (2008b). Rational Design of Highly Active and Selective Ligands for the α5β1 Integrin Receptor. ChemBioChem *9*, 1397–1407.

Hegi, M.E., Diserens, A.-C., Gorlia, T., Hamou, M.-F., de Tribolet, N., Weller, M., Kros, J.M., Hainfellner, J.A., Mason, W., Mariani, L., et al. (2005a). MGMT gene silencing and benefit from temozolomide in glioblastoma. N. Engl. J. Med. *352*, 997–1003.

Hegi, M.E., Hamou, M.-F., de Tribolet, N., Kros, J.M., Mariani, L., Mirimanoff, R.O., and Stupp, R. (2005b). MGMT Gene Silencing and Benefit from Temozolomide in Glioblastoma. N. Engl. J. Med. 7.

Hegi, M.E., Genbrugge, E., Gorlia, T., Stupp, R., Gilbert, M.R., Chinot, O.L., Nabors, L.B., Jones, G., Van Criekinge, W., Straub, J., et al. (2019). MGMT Promoter Methylation Cutoff with Safety Margin for Selecting Glioblastoma Patients into Trials Omitting Temozolomide: A Pooled Analysis of Four Clinical Trials. Clin. Cancer Res. Off. J. Am. Assoc. Cancer Res. *25*, 1809–1816.

Hehlgans, S., Haase, M., and Cordes, N. (2007). Signalling via integrins: implications for cell survival and anticancer strategies. Biochim. Biophys. Acta *1775*, 163–180.

Her, N.-G., Oh, J.-W., Oh, Y.J., Han, S., Cho, H.J., Lee, Y., Ryu, G.H., and Nam, D.-H. (2018). Potent effect of the MDM2 inhibitor AMG232 on suppression of glioblastoma stem cells. Cell Death Dis. *9*, 792.

Hewitt, G., Jurk, D., Marques, F.D.M., Correia-Melo, C., Hardy, T., Gackowska, A., Anderson, R., Taschuk, M., Mann, J., and Passos, J.F. (2012). Telomeres are favoured targets of a persistent DNA damage response in ageing and stress-induced senescence. Nat. Commun. *3*, 708.

Hikawa, T., Mori, T., Abe, T., and Hori, S. (2000). The ability in adhesion and invasion of drug-resistant human glioma cells. J. Exp. Clin. Cancer Res. CR *19*, 357–362.

Hill, V.K., Kim, J.-S., James, C.D., and Waldman, T. (2017). Correction of PTEN mutations in glioblastoma cell lines via AAV-mediated gene editing. PLoS ONE *12*.

Hirose, Y., Berger, M.S., and Pieper, R.O. (2001). p53 effects both the duration of G2/M arrest and the fate of temozolomide-treated human glioblastoma cells. Cancer Res. *61*, 1957–1963.

Hoffman, W.H., Biade, S., Zilfou, J.T., Chen, J., and Murphy, M. (2002). Transcriptional repression of the anti-apoptotic survivin gene by wild type p53. J. Biol. Chem. *277*, 3247–3257.

Hofseth, L.J., Hussain, S.P., and Harris, C.C. (2004). p53: 25 years after its discovery. Trends Pharmacol. Sci. *25*, 177–181.

Holmes, K.M., Annala, M., Chua, C.Y.X., Dunlap, S.M., Liu, Y., Hugen, N., Moore, L.M., Cogdell, D., Hu, L., Nykter, M., et al. (2012). Insulin-like growth factor-binding protein 2-driven glioma progression is prevented by blocking a clinically significant integrin, integrin-linked kinase, and NF-κB network. Proc. Natl. Acad. Sci. U. S. A. *109*, 3475–3480.

Hombach-Klonisch, S., Mehrpour, M., Shojaei, S., Harlos, C., Pitz, M., Hamai, A., Siemianowicz, K., Likus, W., Wiechec, E., Toyota, B.D., et al. (2018). Glioblastoma and chemoresistance to alkylating agents: Involvement of apoptosis, autophagy, and unfolded protein response. Pharmacol. Ther. *184*, 13–41.

Hong, B., van den Heuvel, A.P.J., Prabhu, V.V., Zhang, S., and El-Deiry, W.S. (2014). Targeting tumor suppressor p53 for cancer therapy: strategies, challenges and opportunities. Curr. Drug Targets *15*, 80–89.

Hong, C.-S., Jeong, O., Piao, Z., Guo, C., Jung, M.-R., Choi, C., and Park, Y.-K. (2015). HOXB5 induces invasion and migration through direct transcriptional up-regulation of β-catenin in human gastric carcinoma. Biochem. J. *472*, 393–403.

van der Horst, G., van den Hoogen, C., Buijs, J.T., Cheung, H., Bloys, H., Pelger, R.C., Lorenzon, G., Heckmann, B., Feyen, J., Pujuguet, P., et al. (2011). Targeting of αv-Integrins in Stem/Progenitor Cells and Supportive Microenvironment Impairs Bone Metastasis in Human Prostate Cancer. Neoplasia N. Y. N *13*, 516–525.

Hsieh, J.K., Chan, F.S., O'Connor, D.J., Mittnacht, S., Zhong, S., and Lu, X. (1999). RB regulates the stability and the apoptotic function of p53 via MDM2. Mol. Cell *3*, 181–193.

Hu, P., and Luo, B.-H. (2013). Integrin bi-directional signaling across the plasma membrane. J. Cell. Physiol. *228*, 306–312.

Hu, Y., Ylivinkka, I., Chen, P., Li, L., Hautaniemi, S., Nyman, T.A., Keski-Oja, J., and Hyytiäinen, M. (2012). Netrin-4 Promotes Glioblastoma Cell Proliferation through Integrin β4 Signaling. Neoplasia N. Y. N *14*, 219–227.

Huang, P.H., Xu, A.M., and White, F.M. (2009). Oncogenic EGFR signaling networks in glioma. Sci. Signal. *2*, re6.

Humphries, M.J., Symonds, E.J.H., and Mould, A.P. (2003). Mapping functional residues onto integrin crystal structures. Curr. Opin. Struct. Biol. *13*, 236–243.

Hynes, R.O. (2002). A reevaluation of integrins as regulators of angiogenesis. Nat. Med. *8*, 918–921.

Iacob, G., and Dinca, E. (2009). Current data and strategy in glioblastoma multiforme. J. Med. Life *2*, 386–393.

Irwin, M.S., and Kaelin, W.G. (2001). p53 family update: p73 and p63 develop their own identities. Cell Growth Differ. Mol. Biol. J. Am. Assoc. Cancer Res. *12*, 337–349.

Isobe, M., Emanuel, B.S., Givol, D., Oren, M., and Croce, C.M. (1986). Localization of gene for human p53 tumour antigen to band 17p13. Nature *320*, 84–85.

Issaeva, N., Bozko, P., Enge, M., Protopopova, M., Verhoef, L.G.G.C., Masucci, M., Pramanik, A., and Selivanova, G. (2004). Small molecule RITA binds to p53, blocks p53–HDM-2 interaction and activates p53 function in tumors. Nat. Med. *10*, 1321–1328.

Ito, A., Lai, C.H., Zhao, X., Saito, S., Hamilton, M.H., Appella, E., and Yao, T.P. (2001). p300/CBP-mediated p53 acetylation is commonly induced by p53-activating agents and inhibited by MDM2. EMBO J. *20*, 1331–1340.

Janouskova, H., Maglott, A., Leger, D.Y., Bossert, C., Noulet, F., Guerin, E., Guenot, D., Pinel, S., Chastagner, P., Plenat, F., et al. (2012a). Integrin α5β1 plays a critical role in resistance to temozolomide by interfering with the p53 pathway in high-grade glioma. Cancer Res. *72*, 3463–3470.

Janouskova, H., Maglott, A., Leger, D.Y., Bossert, C., Noulet, F., Guerin, E., Guenot, D., Pinel, S., Chastagner, P., Plenat, F., et al. (2012b). Integrin α5β1 plays a critical role in resistance to temozolomide by interfering with the p53 pathway in high-grade glioma. Cancer Res. *72*, 3463–3470.

Jeffrey, P.D., Gorina, S., and Pavletich, N.P. (1995). Crystal structure of the tetramerization domain of the p53 tumor suppressor at 1.7 angstroms. Science *267*, 1498–1502.

Jiapaer, S., Furuta, T., Tanaka, S., Kitabayashi, T., and Nakada, M. (2018). Potential Strategies Overcoming the Temozolomide Resistance for Glioblastoma. Neurol. Med. Chir. (Tokyo) *58*, 405–421.

Jin, Z., and El-Deiry, W.S. (2005). Overview of cell death signaling pathways. Cancer Biol. Ther. *4*, 139–163.

Kadry, Y.A., and Calderwood, D.A. (2020). Chapter 22: Structural and signaling functions of integrins. Biochim. Biophys. Acta BBA - Biomembr. *1862*, 183206.

Kaghad, M., Bonnet, H., Yang, A., Creancier, L., Biscan, J.C., Valent, A., Minty, A., Chalon, P., Lelias, J.M., Dumont, X., et al. (1997). Monoallelically expressed gene related to p53 at 1p36, a region frequently deleted in neuroblastoma and other human cancers. Cell *90*, 809–819.

Kaina, B., Christmann, M., Naumann, S., and Roos, W.P. (2007). MGMT: Key node in the battle against genotoxicity, carcinogenicity and apoptosis induced by alkylating agents. DNA Repair *6*, 1079–1099.

Kanzawa, T., Germano, I.M., Komata, T., Ito, H., Kondo, Y., and Kondo, S. (2004). Role of autophagy in temozolomide-induced cytotoxicity for malignant glioma cells. Cell Death Differ. *11*, 448–457.

Kapp, T.G., Rechenmacher, F., Neubauer, S., Maltsev, O.V., Cavalcanti-Adam, E.A., Zarka, R., Reuning, U., Notni, J., Wester, H.-J., Mas-Moruno, C., et al. (2017). A Comprehensive Evaluation of the Activity and Selectivity Profile of Ligands for RGD-binding Integrins. Sci. Rep. *7*, 39805.

Kashiwagi, S., Asano, Y., Goto, W., Takada, K., Takahashi, K., Hatano, T., Tanaka, S., Takashima, T., Tomita, S., Motomura, H., et al. (2018). Mesenchymal-epithelial Transition and Tumor Vascular Remodeling in Eribulin Chemotherapy for Breast Cancer. Anticancer Res. *38*, 401–410.

Kastenhuber, E.R., and Lowe, S.W. (2017). Putting p53 in Context. Cell *170*, 1062–1078.

Kato, H., Kato, S., Kumabe, T., Sonoda, Y., Yoshimoto, T., Kato, S., Han, S.Y., Suzuki, T., Shibata, H., Kanamaru, R., et al. (2000). Functional evaluation of p53 and PTEN gene mutations in gliomas. Clin. Cancer Res. Off. J. Am. Assoc. Cancer Res. *6*, 3937–3943.

Ke, B., Tian, M., Li, J., Liu, B., and He, G. (2016). Targeting Programmed Cell Death Using Small-Molecule Compounds to Improve Potential Cancer Therapy. Med. Res. Rev. *36*, 983–1035.

Kerr, J.F., Wyllie, A.H., and Currie, A.R. (1972). Apoptosis: a basic biological phenomenon with wide-ranging implications in tissue kinetics. Br. J. Cancer *26*, 239–257.

Kesanakurti, D., Chetty, C., Dinh, D.H., Gujrati, M., and Rao, J.S. (2013). Role of MMP-2 in the Regulation of IL-6/Stat3 Survival Signaling via Interaction With α5β1 Integrin in glioma. Oncogene *32*, 327–340.

Kesari, S. (2011). Understanding glioblastoma tumor biology: the potential to improve current diagnosis and treatments. Semin. Oncol. *38 Suppl 4*, S2-10.

Khalili, P., Arakelian, A., Chen, G., Plunkett, M.L., Beck, I., Parry, G.C., Doñate, F., Shaw, D.E., Mazar, A.P., and Rabbani, S.A. (2006). A non-RGD-based integrin binding peptide (ATN-161) blocks breast cancer growth and metastasis in vivo. Mol. Cancer Ther. *5*, 2271–2280.

Khosravi-Far, R., and Esposti, M.D. (2004). Death receptor signals to mitochondria. Cancer Biol. Ther. *3*, 1051–1057.

Khurana, A., and Shafer, D.A. (2019). MDM2 antagonists as a novel treatment option for acute myeloid leukemia: perspectives on the therapeutic potential of idasanutlin (RG7388). OncoTargets Ther. *Volume 12*, 2903–2910.

Kim, S., Bell, K., Mousa, S.A., and Varner, J.A. (2000). Regulation of Angiogenesis in Vivo by Ligation of Integrin α5β1 with the Central Cell-Binding Domain of Fibronectin. Am. J. Pathol. *156*, 1345–1362.

Klein, C., and Vassilev, L.T. (2004a). Targeting the p53–MDM2 interaction to treat cancer. Br. J. Cancer *91*, 1415–1419.

Klein, C., and Vassilev, L.T. (2004b). Targeting the p53–MDM2 interaction to treat cancer. Br. J. Cancer *91*, 1415–1419.

Knobbe, C.B., Merlo, A., and Reifenberger, G. (2002). Pten signaling in gliomas. Neuro-Oncol. *4*, 196–211.

Kobet, E., Zeng, X., Zhu, Y., Keller, D., and Lu, H. (2000). MDM2 inhibits p300-mediated p53 acetylation and activation by forming a ternary complex with the two proteins. Proc. Natl. Acad. Sci. U. S. A. *97*, 12547–12552.

Kohsaka, S., Wang, L., Yachi, K., Mahabir, R., Narita, T., Itoh, T., Tanino, M., Kimura, T., Nishihara, H., and Tanaka, S. (2012). STAT3 inhibition overcomes temozolomide resistance in glioblastoma by downregulating MGMT expression. Mol. Cancer Ther. *11*, 1289–1299.

Kracikova, M., Akiri, G., George, A., Sachidanandam, R., and Aaronson, S.A. (2013). A threshold mechanism mediates p53 cell fate decision between growth arrest and apoptosis. Cell Death Differ. *20*, 576–588.

Krex, D., Mohr, B., Appelt, H., Schackert, H.K., and Schackert, G. (2003). Genetic Analysis of a Multifocal Glioblastoma Multiforme: A Suitable Tool to Gain New Aspects in Glioma Development. Neurosurgery *53*, 1377–1384.

Kuwana, T., Bouchier-Hayes, L., Chipuk, J.E., Bonzon, C., Sullivan, B.A., Green, D.R., and Newmeyer, D.D. (2005). BH3 domains of BH3-only proteins differentially regulate Bax-mediated mitochondrial membrane permeabilization both directly and indirectly. Mol. Cell *17*, 525–535.

Kwon, S.M., Kang, S.-H., Park, C.-K., Jung, S., Park, E.S., Lee, J.-S., Kim, S.-H., and Woo, H.G. (2015). Recurrent Glioblastomas Reveal Molecular Subtypes Associated with Mechanistic Implications of Drug-Resistance. PloS One *10*, e0140528.

Lacroix, M., Abi-Said, D., Fourney, D.R., Gokaslan, Z.L., Shi, W., DeMonte, F., Lang, F.F., McCutcheon, I.E., Hassenbusch, S.J., Holland, E., et al. (2001). A multivariate analysis of 416 patients with glioblastoma multiforme: prognosis, extent of resection, and survival. J. Neurosurg. *95*, 190–198.

Lambert, J.M.R., Gorzov, P., Veprintsev, D.B., Söderqvist, M., Segerbäck, D., Bergman, J., Fersht, A.R., Hainaut, P., Wiman, K.G., and Bykov, V.J.N. (2009). PRIMA-1 Reactivates Mutant p53 by Covalent Binding to the Core Domain. Cancer Cell *15*, 376–388.

Lane, D.P., and Benchimol, S. (1990). p53: oncogene or anti-oncogene? Genes Dev. *4*, 1–8.

Langmead, B., and Salzberg, S.L. (2012). Fast gapped-read alignment with Bowtie 2. Nat. Methods *9*, 357–359.

Lanvin, O., Monferran, S., Delmas, C., Couderc, B., Toulas, C., and Cohen-Jonathan-Moyal, E. (2013). Radiation-induced mitotic cell death and glioblastoma radioresistance: a new regulating pathway controlled by integrin-linked kinase, hypoxia-inducible factor 1 alpha and survivin in U87 cells. Eur. J. Cancer Oxf. Engl. 1990 *49*, 2884–2891.

Larson et al., C., A.L.,. Berman, L. and Springer, T. (1989). Primary structure of the leukocyte function-associated molecule-1 alpha subunit: an integrin with an embedded domain defining a protein superfamily. J. Cell Biol. *108*, 703–712.

Lathia, J.D., Gallagher, J., Heddleston, J.M., Wang, J., Eyler, C.E., MacSwords, J., Wu, Q., Vasanji, A., McLendon, R.E., Hjelmeland, A.B., et al. (2010). Integrin alpha 6 regulates glioblastoma stem cells. Cell Stem Cell *6*, 421–432.

Lathia, J.D., Li, M., Sinyuk, M., Alvarado, A.G., Flavahan, W.A., Stoltz, K., Rosager, A.M., Hale, J., Hitomi, M., Gallagher, J., et al. (2014). High-throughput flow cytometry screening reveals a role for junctional adhesion molecule a as a cancer stem cell maintenance factor. Cell Rep. *6*, 117–129.

Lathia, J.D., Mack, S.C., Mulkearns-Hubert, E.E., Valentim, C.L.L., and Rich, J.N. (2015). Cancer stem cells in glioblastoma. Genes Dev. *29*, 1203–1217.

Lau, T.-L., Kim, C., Ginsberg, M.H., and Ulmer, T.S. (2009). The structure of the integrin alphaIIbbeta3 transmembrane complex explains integrin transmembrane signalling. EMBO J. *28*, 1351–1361.

Laws, E.R., Parney, I.F., Huang, W., Anderson, F., Morris, A.M., Asher, A., Lillehei, K.O., Bernstein, M., Brem, H., Sloan, A., et al. (2003). Survival following surgery and prognostic factors for recently diagnosed malignant glioma: data from the Glioma Outcomes Project. J. Neurosurg. *99*, 467–473.

Lawson, C.D., and Burridge, K. (2014). The on-off relationship of Rho and Rac during integrin-mediated adhesion and cell migration. Small GTPases *5*.

Lazzerini Denchi, E., Attwooll, C., Pasini, D., and Helin, K. (2005). Deregulated E2F activity induces hyperplasia and senescence-like features in the mouse pituitary gland. Mol. Cell. Biol. *25*, 2660–2672.

Lee, S.Y. (2016a). Temozolomide resistance in glioblastoma multiforme. Genes Dis. *3*, 198–210.

Lee, S.Y. (2016b). Temozolomide resistance in glioblastoma multiforme. Genes Dis. *3*, 198–210.

Lee, H.S., Oh, S.J., Lee, K.-H., Lee, Y.-S., Ko, E., Kim, K.E., Kim, H., Kim, S., Song, P.H., Kim, Y.-I., et al. (2014). Gln-362 of Angiopoietin-2 Mediates Migration of Tumor and Endothelial Cells through Association with α5β1 Integrin. J. Biol. Chem. *289*, 31330–31340.

Lee, J.O., Bankston, L.A., Arnaout, M.A., and Liddington, R.C. (1995). Two conformations of the integrin A-domain (I-domain): a pathway for activation? Struct. Lond. Engl. 1993 *3*, 1333–1340.

Lee, Y.-R., Chen, M., and Pandolfi, P.P. (2018). The functions and regulation of the PTEN tumour suppressor: new modes and prospects. Nat. Rev. Mol. Cell Biol. *19*, 547–562.

Leroy, B., Fournier, J.L., Ishioka, C., Monti, P., Inga, A., Fronza, G., and Soussi, T. (2013). The TP53 website: an integrative resource centre for the TP53 mutation database and TP53 mutant analysis. Nucleic Acids Res. *41*, D962–D969.

Li, D., Marchenko, N.D., Schulz, R., Fischer, V., Velasco-Hernandez, T., Talos, F., and Moll, U.M. (2011). Functional Inactivation of Endogenous MDM2 and CHIP by HSP90 Causes Aberrant Stabilization of Mutant p53 in Human Cancer Cells. Mol. Cancer Res. *9*, 577–588.

Li, L., Hu, Y., Ylivinkka, I., Li, H., Chen, P., Keski-Oja, J., and Hyytiäinen, M. (2013). NETRIN-4 Protects Glioblastoma Cells FROM Temozolomide Induced Senescence. PLoS ONE *8*.

Li, Y., Drabsch, Y., Pujuguet, P., Ren, J., van Laar, T., Zhang, L., van Dam, H., Clément-Lacroix, P., and Ten Dijke, P. (2015). Genetic depletion and pharmacological targeting of αv integrin in breast cancer cells impairs metastasis in zebrafish and mouse xenograft models. Breast Cancer Res. BCR *17*, 28.

Liddington, R.C. (2014). Structural Aspects of Integrins. In I Domain Integrins, D. Gullberg, ed. (Dordrecht: Springer Netherlands), pp. 111–126.

Lim, S.-T., Chen, X.L., Lim, Y., Hanson, D.A., Vo, T.-T., Howerton, K., Larocque, N., Fisher, S.J., Schlaepfer, D.D., and Ilic, D. (2008). Nuclear FAK promotes cell proliferation and survival through FERM-enhanced p53 degradation. Mol. Cell *29*, 9–22.

Lin, T., Chao, C., Saito, S., Mazur, S.J., Murphy, M.E., Appella, E., and Xu, Y. (2005). p53 induces differentiation of mouse embryonic stem cells by suppressing Nanog expression. Nat. Cell Biol. *7*, 165–171.

Liu, L., Markowitz, S., and Gerson, S.L. (1996). Mismatch repair mutations override alkyltransferase in conferring resistance to temozolomide but not to 1,3-bis(2-chloroethyl)nitrosourea. Cancer Res. *56*, 5375–5379.

Liu, L., Scolnick, D.M., Trievel, R.C., Zhang, H.B., Marmorstein, R., Halazonetis, T.D., and Berger, S.L. (1999). p53 sites acetylated in vitro by PCAF and p300 are acetylated in vivo in response to DNA damage. Mol. Cell. Biol. *19*, 1202–1209.

Liu, Q., Xue, Y., Chen, Q., Chen, H., Zhang, X., Wang, L., Han, C., Que, S., Lou, M., and Lan, J. (2017). PomGnT1 enhances temozolomide resistance by activating epithelial-mesenchymal transition signaling in glioblastoma. Oncol. Rep. *38*, 2911–2918.

Livant, D.L., Brabec, R.K., Pienta, K.J., Allen, D.L., Kurachi, K., Markwart, S., and Upadhyaya, A. (2000). Anti-invasive, Antitumorigenic, and Antimetastatic Activities of the PHSCN Sequence in Prostate Carcinoma. 13.

Lomonaco, S.L., Finniss, S., Xiang, C., Lee, H.K., Jiang, W., Lemke, N., Rempel, S.A., Mikkelsen, T., and Brodie, C. (2011). Cilengitide induces autophagy-mediated cell death in glioma cells. Neuro-Oncol. *13*, 857–865.

Lotti, R., Marconi, A., Truzzi, F., Dallaglio, K., Gemelli, C., Borroni, R.G., Palazzo, E., and Pincelli, C. (2010). A previously unreported function of β(1)B integrin isoform in caspase-8-dependent integrin-mediated keratinocyte death. J. Invest. Dermatol. *130*, 2569–2577.

Louis, D.N., Ohgaki, H., Wiestler, O.D., Cavenee, W.K., Burger, P.C., Jouvet, A., Scheithauer, B.W., and Kleihues, P. (2007). The 2007 WHO Classification of Tumours of the Central Nervous System. Acta Neuropathol. (Berl.) *114*, 97–109.

Louis, D.N., Perry, A., Reifenberger, G., von Deimling, A., Figarella-Branger, D., Cavenee, W.K., Ohgaki, H., Wiestler, O.D., Kleihues, P., and Ellison, D.W. (2016). The 2016 World Health Organization Classification of Tumors of the Central Nervous System: a summary. Acta Neuropathol. (Berl.) *131*, 803–820.

Love, M.I., Huber, W., and Anders, S. (2014). Moderated estimation of fold change and dispersion for RNA-seq data with DESeq2. Genome Biol. *15*, 550.

Lu, W., Pochampally, R., Chen, L., Traidej, M., Wang, Y., and Chen, J. (2000). Nuclear exclusion of p53 in a subset of tumors requires MDM2 function. Oncogene *19*, 232–240.

Lundberg, A.S., Hahn, W.C., Gupta, P., and Weinberg, R.A. (2000). Genes involved in senescence and immortalization. Curr. Opin. Cell Biol. *12*, 705–709.

Luo, B.-H., Carman, C.V., and Springer, T.A. (2007). Structural Basis of Integrin Regulation and Signaling. Annu. Rev. Immunol. *25*, 619–647.

Luo, W., Yan, D., Song, Z., Zhu, X., Liu, X., Li, X., and Zhao, S. (2019). miR-126-3p sensitizes glioblastoma cells to temozolomide by inactivating Wnt/β-catenin signaling via targeting SOX2. Life Sci. *226*, 98–106.

Ma, J., Murphy, M., O'Dwyer, P.J., Berman, E., Reed, K., and Gallo, J.M. (2002). Biochemical changes associated with a multidrug-resistant phenotype of a human glioma cell line with temozolomide-acquired resistance. Biochem. Pharmacol. *63*, 1219–1228.

Ma, Q., Yang, Y., Feng, D., Zheng, S., Meng, R., Fa, P., Zhao, C., Liu, H., Song, R., Tao, T., et al. (2015). MAGI3 negatively regulates Wnt/β-catenin signaling and suppresses malignant phenotypes of glioma cells. Oncotarget *6*, 35851–35865.

MacDonald, T.J., Taga, T., Shimada, H., Tabrizi, P., Zlokovic, B.V., Cheresh, D.A., and Laug, W.E. (2001). Preferential susceptibility of brain tumors to the antiangiogenic effects of an alpha(v) integrin antagonist. Neurosurgery *48*, 151–157.

de Magalhães, J.P., and Passos, J.F. (2018). Stress, cell senescence and organismal ageing. Mech. Ageing Dev. *170*, 2–9.

Maglott, A., Bartik, P., Cosgun, S., Klotz, P., Rondé, P., Fuhrmann, G., Takeda, K., Martin, S., and Dontenwill, M. (2006). The small alpha5beta1 integrin antagonist, SJ749, reduces proliferation and clonogenicity of human astrocytoma cells. Cancer Res. *66*, 6002–6007.

Malanga, M., and Althaus, F.R. (2005). The role of poly(ADP-ribose) in the DNA damage signaling network. Biochem. Cell Biol. *83*, 354–364.

Malric, L., Monferran, S., Gilhodes, J., Boyrie, S., Dahan, P., Skuli, N., Sesen, J., Filleron, T., Kowalski-Chauvel, A., Moyal, E.C.-J., et al. (2017). Interest of integrins targeting in glioblastoma according to tumor heterogeneity and cancer stem cell paradigm: an update. Oncotarget *8*.

Malric, L., Monferran, S., Delmas, C., Arnauduc, F., Dahan, P., Boyrie, S., Deshors, P., Lubrano, V., Da Mota, D.F., Gilhodes, J., et al. (2019). Inhibiting Integrin β8 to Differentiate and Radiosensitize Glioblastoma-Initiating Cells. Mol. Cancer Res. MCR *17*, 384–397.

Marchenko, N.D., Zaika, A., and Moll, U.M. (2000). Death signal-induced localization of p53 protein to mitochondria. A potential role in apoptotic signaling. J. Biol. Chem. *275*, 16202–16212.

Marinelli, L., Meyer, A., Heckmann, D., Lavecchia, A., Novellino, E., and Kessler, H. (2005). Ligand binding analysis for human alpha5beta1 integrin: strategies for designing new alpha5beta1 integrin antagonists. J. Med. Chem. *48*, 4204–4207.

Martens, U.M., Chavez, E.A., Poon, S.S., Schmoor, C., and Lansdorp, P.M. (2000). Accumulation of short telomeres in human fibroblasts prior to replicative senescence. Exp. Cell Res. *256*, 291–299.

Martin, M. (2011). Cutadapt removes adapter sequences from high-throughput sequencing reads. EMBnet.Journal *17*, 10–12.

Martin, S., Cosset, E.C., Terrand, J., Maglott, A., Takeda, K., and Dontenwill, M. (2009). Caveolin-1 regulates glioblastoma aggressiveness through the control of alpha(5)beta(1) integrin expression and modulates glioblastoma responsiveness to SJ749, an alpha(5)beta(1) integrin antagonist. Biochim. Biophys. Acta *1793*, 354–367.

Martin, S., Janouskova, H., and Dontenwill, M. (2012). Integrins and p53 pathways in glioblastoma resistance to temozolomide. Front. Oncol. *2*.

Martinkova, E., Maglott, A., Leger, D.Y., Bonnet, D., Stiborova, M., Takeda, K., Martin, S., and Dontenwill, M. (2010a). α5β1 integrin antagonists reduce chemotherapy-induced premature senescence and facilitate apoptosis in human glioblastoma cells. Int. J. Cancer *127*, 1240–1248.

Martinkova, E., Maglott, A., Leger, D.Y., Bonnet, D., Stiborova, M., Takeda, K., Martin, S., and Dontenwill, M. (2010b). alpha5beta1 integrin antagonists reduce chemotherapy-induced premature senescence and facilitate apoptosis in human glioblastoma cells. Int. J. Cancer *127*, 1240–1248.

Mas-Moruno, C., Rechenmacher, F., and Kessler, H. (2010a). Cilengitide: The First Anti-Angiogenic Small Molecule Drug Candidate. Design, Synthesis and Clinical Evaluation. Anticancer Agents Med. Chem. *10*, 753–768.

Mas-Moruno, C., Rechenmacher, F., and Kessler, H. (2010b). Cilengitide: The First Anti-Angiogenic Small Molecule Drug Candidate. Design, Synthesis and Clinical Evaluation. Anticancer Agents Med. Chem. *10*, 753–768.

Mas-Moruno, C., Beck, J.G., Doedens, L., Frank, A.O., Marinelli, L., Cosconati, S., Novellino, E., and Kessler, H. (2011). Increasing αvβ3 selectivity of the anti-angiogenic drug cilengitide by N-methylation. Angew. Chem. Int. Ed Engl. *50*, 9496–9500.

Matsumura, T., Zerrudo, Z., and Hayflick, L. (1979). Senescent human diploid cells in culture: survival, DNA synthesis and morphology. J. Gerontol. *34*, 328–334.

Matter, M.L., and Ruoslahti, E. (2001). A signaling pathway from the alpha5beta1 and alpha(v)beta3 integrins that elevates bcl-2 transcription. J. Biol. Chem. *276*, 27757–27763.

Mayo, L.D., Dixon, J.E., Durden, D.L., Tonks, N.K., and Donner, D.B. (2002). PTEN protects p53 from Mdm2 and sensitizes cancer cells to chemotherapy. J. Biol. Chem. *277*, 5484–5489.

McConnell, B.B., Starborg, M., Brookes, S., and Peters, G. (1998). Inhibitors of cyclin-dependent kinases induce features of replicative senescence in early passage human diploid fibroblasts. Curr. Biol. CB *8*, 351–354.

McFaline-Figueroa, J.L., Braun, C.J., Stanciu, M., Nagel, Z.D., Mazzucato, P., Sangaraju, D., Cerniauskas, E., Barford, K., Vargas, A., Chen, Y., et al. (2015). Minor Changes in Expression of the Mismatch Repair Protein MSH2 Exert a Major Impact on Glioblastoma Response to Temozolomide. Cancer Res. *75*, 3127–3138.

Meek, D.W. (1999). Mechanisms of switching on p53: a role for covalent modification? Oncogene *18*, 7666–7675.

Merlino, F., Daniele, S., La Pietra, V., Di Maro, S., Di Leva, F.S., Brancaccio, D., Tomassi, S., Giuntini, S., Cerofolini, L., Fragai, M., et al. (2018). Simultaneous Targeting of RGD-Integrins and Dual Murine Double Minute Proteins in Glioblastoma Multiforme. J. Med. Chem. *61*, 4791–4809.

Messaoudi, K., Clavreul, A., and Lagarce, F. (2015). Toward an effective strategy in glioblastoma treatment. Part I: resistance mechanisms and strategies to overcome resistance of glioblastoma to temozolomide. Drug Discov. Today *20*, 899–905.

Meyer, M., Reimand, J., Lan, X., Head, R., Zhu, X., Kushida, M., Bayani, J., Pressey, J.C., Lionel, A.C., Clarke, I.D., et al. (2015). Single cell-derived clonal analysis of human glioblastoma links functional and genomic heterogeneity. Proc. Natl. Acad. Sci. U. S. A. *112*, 851–856.

Mikheev, A.M., Mikheeva, S.A., Trister, A.D., Tokita, M.J., Emerson, S.N., Parada, C.A., Born, D.E., Carnemolla, B., Frankel, S., Kim, D.-H., et al. (2015). Periostin is a novel therapeutic target that predicts and regulates glioma malignancy. Neuro-Oncol. *17*, 372–382.

Mikkelsen, T., Brodie, C., Finniss, S., Berens, M.E., Rennert, J.L., Nelson, K., Lemke, N., Brown, S.L., Hahn, D., Neuteboom, B., et al. (2009). Radiation sensitization of glioblastoma by cilengitide has unanticipated schedule-dependency. Int. J. Cancer *124*, 2719–2727.

Mitjans, F., Meyer, T., Fittschen, C., Goodman, S., Jonczyk, A., Marshall, J.F., Reyes, G., and Piulats, J. (2000). In vivo therapy of malignant melanoma by means of antagonists of alphav integrins. Int. J. Cancer *87*, 716–723.

Miyashita, T., and Reed, J.C. (1995). Tumor suppressor p53 is a direct transcriptional activator of the human bax gene. Cell *80*, 293–299.

Mizoguchi, M., Guan, Y., Yoshimoto, K., Hata, N., Amano, T., Nakamizo, A., and Sasaki, T. (2013). Clinical implications of microRNAs in human glioblastoma. Front. Oncol. *3*.

Momand, J., Jung, D., Wilczynski, S., and Niland, J. (1998). The MDM2 gene amplification database. Nucleic Acids Res. *26*, 3453–3459.

Monferran, S., Skuli, N., Delmas, C., Favre, G., Bonnet, J., Cohen-Jonathan-Moyal, E., and Toulas, C. (2008). Alphavbeta3 and alphavbeta5 integrins control glioma cell response to ionising radiation through ILK and RhoB. Int. J. Cancer *123*, 357–364.

Monian, P., and Jiang, X. (2012). Clearing the final hurdles to mitochondrial apoptosis: regulation post cytochrome C release. Exp. Oncol. *34*, 185–191.

Moroni, M.C., Hickman, E.S., Lazzerini Denchi, E., Caprara, G., Colli, E., Cecconi, F., Müller, H., and Helin, K. (2001). Apaf-1 is a transcriptional target for E2F and p53. Nat. Cell Biol. *3*, 552–558.

Morse, E.M., Brahme, N.N., and Calderwood, D.A. (2014). Integrin Cytoplasmic Tail Interactions. Biochemistry *53*, 810–820.

Moser, M., Nieswandt, B., Ussar, S., Pozgajova, M., and Fässler, R. (2008). Kindlin-3 is essential for integrin activation and platelet aggregation. Nat. Med. *14*, 325–330.

Mould, A.P., and Humphries, M.J. (2004). Cell biology: adhesion articulated. Nature *432*, 27–28.

Mrugala, M.M. (2013). Advances and challenges in the treatment of glioblastoma: a clinician's perspective. Discov. Med. *15*, 221–230.

Mullamitha, S.A., Ton, N.C., Parker, G.J.M., Jackson, A., Julyan, P.J., Roberts, C., Buonaccorsi, G.A., Watson, Y., Davies, K., Cheung, S., et al. (2007). Phase I evaluation of a fully human anti-alphav integrin monoclonal antibody (CNTO 95) in patients with advanced solid tumors. Clin. Cancer Res. Off. J. Am. Assoc. Cancer Res. *13*, 2128–2135.

Muller, P.A.J., and Vousden, K.H. (2014). Mutant p53 in Cancer: New Functions and Therapeutic Opportunities. Cancer Cell *25*, 304–317.

Müller, M., Scaffidi, C.A., Galle, P.R., Stremmel, W., and Krammer, P.H. (1998). The role of p53 and the CD95 (APO-1/Fas) death system in chemotherapy-induced apoptosis. Eur. Cytokine Netw. *9*, 685–686.

Munksgaard Thorén, M., Chmielarska Masoumi, K., Krona, C., Huang, X., Kundu, S., Schmidt, L., Forsberg-Nilsson, K., Floyd Keep, M., Englund, E., Nelander, S., et al. (2019). Integrin α10, a Novel Therapeutic Target in Glioblastoma, Regulates Cell Migration, Proliferation, and Survival. Cancers *11*, 587.

Murphy, M., Ahn, J., Walker, K.K., Hoffman, W.H., Evans, R.M., Levine, A.J., and George, D.L. (1999). Transcriptional repression by wild-type p53 utilizes histone deacetylases, mediated by interaction with mSin3a. Genes Dev. *13*, 2490–2501.

Murphy, P.A., Begum, S., and Hynes, R.O. (2015). Tumor Angiogenesis in the Absence of Fibronectin or Its Cognate Integrin Receptors. PLoS ONE *10*.

Nakada, M., Furuta, T., Hayashi, Y., Minamoto, T., and Hamada, J.-I. (2012). The strategy for enhancing temozolomide against malignant glioma. Front. Oncol. *2*, 98.

Nakamura, S., Roth, J.A., and Mukhopadhyay, T. (2000). Multiple Lysine Mutations in the C-Terminal Domain of p53 Interfere with MDM2-Dependent Protein Degradation and Ubiquitination. Mol. Cell. Biol. *20*, 9391–9398.

Nakano, K., and Vousden, K.H. (2001). PUMA, a novel proapoptotic gene, is induced by p53. Mol. Cell *7*, 683–694.

Nardella, C., Clohessy, J.G., Alimonti, A., and Pandolfi, P.P. (2011). Pro-senescence therapy for cancer treatment. Nat. Rev. Cancer *11*, 503–511.

Narita, M., Nũnez, S., Heard, E., Narita, M., Lin, A.W., Hearn, S.A., Spector, D.L., Hannon, G.J., and Lowe, S.W. (2003). Rb-mediated heterochromatin formation and silencing of E2F target genes during cellular senescence. Cell *113*, 703–716.

Nieberler, M., Reuning, U., Reichart, F., Notni, J., Wester, H.-J., Schwaiger, M., Weinmüller, M., Räder, A., Steiger, K., and Kessler, H. (2017). Exploring the Role of RGD-Recognizing Integrins in Cancer. Cancers *9*.

Noushmehr, H., Weisenberger, D.J., Diefes, K., Phillips, H.S., Pujara, K., Berman, B.P., Pan, F., Pelloski, C.E., Sulman, E.P., Bhat, K.P., et al. (2010). Identification of a CpG Island Methylator Phenotype that Defines a Distinct Subgroup of Glioma. Cancer Cell *17*, 510–522.

Oberstadt, M.C., Bien-Möller, S., Weitmann, K., Herzog, S., Hentschel, K., Rimmbach, C., Vogelgesang, S., Balz, E., Fink, M., Michael, H., et al. (2013). Epigenetic modulation of the drug resistance genes MGMT, ABCB1 and ABCG2 in glioblastoma multiforme. BMC Cancer *13*, 617.

Oda, E., Ohki, R., Murasawa, H., Nemoto, J., Shibue, T., Yamashita, T., Tokino, T., Taniguchi, T., and Tanaka, N. (2000a). Noxa, a BH3-only member of the Bcl-2 family and candidate mediator of p53-induced apoptosis. Science *288*, 1053–1058.

Oda, K., Arakawa, H., Tanaka, T., Matsuda, K., Tanikawa, C., Mori, T., Nishimori, H., Tamai, K., Tokino, T., Nakamura, Y., et al. (2000b). p53AIP1, a potential mediator of p53-dependent apoptosis, and its regulation by Ser-46-phosphorylated p53. Cell *102*, 849–862.

O'Day, S.J., Pavlick, A.C., Albertini, M.R., Hamid, O., Schalch, H., Lang, Z., Ling, J., Mata, M., Reddy, M., and Foster, B. (2012). Clinical and pharmacologic evaluation of two dose levels of intetumumab (CNTO 95) in patients with melanoma or angiosarcoma. Invest. New Drugs *30*, 1074–1081.

Ogier-Denis, E., and Codogno, P. (2003). Autophagy: a barrier or an adaptive response to cancer. Biochim. Biophys. Acta *1603*, 113–128.

Ohgaki, H. (2005). Genetic pathways to glioblastomas. Neuropathol. Off. J. Jpn. Soc. Neuropathol. *25*, 1–7.

Ohgaki, H., and Kleihues, P. (2007). Genetic pathways to primary and secondary glioblastoma. Am. J. Pathol. *170*, 1445–1453.

Ohgaki, H., and Kleihues, P. (2013). The definition of primary and secondary glioblastoma. Clin. Cancer Res. Off. J. Am. Assoc. Cancer Res. *19*, 764–772.

Oliva, C.R., Nozell, S.E., Diers, A., McClugage, S.G., Sarkaria, J.N., Markert, J.M., Darley-Usmar, V.M., Bailey, S.M., Gillespie, G.Y., Landar, A., et al. (2010). Acquisition of temozolomide chemoresistance in gliomas leads to remodeling of mitochondrial electron transport chain. J. Biol. Chem. *285*, 39759–39767.

Omuro, A. (2013). Glioblastoma and Other Malignant Gliomas: A Clinical Review. JAMA *310*, 1842.

Oppenheim, R.W., Flavell, R.A., Vinsant, S., Prevette, D., Kuan, C.Y., and Rakic, P. (2001). Programmed cell death of developing mammalian neurons after genetic deletion of caspases. J. Neurosci. Off. J. Soc. Neurosci. *21*, 4752–4760.

Ostrom, Q.T., Bauchet, L., Davis, F.G., Deltour, I., Fisher, J.L., Langer, C.E., Pekmezci, M., Schwartzbaum, J.A., Turner, M.C., Walsh, K.M., et al. (2014). The epidemiology of glioma in adults: a "state of the science" review. Neuro-Oncol. *16*, 896–913.

Ostrom, Q.T., Gittleman, H., Liao, P., Vecchione-Koval, T., Wolinsky, Y., Kruchko, C., and Barnholtz-Sloan, J.S. (2017). CBTRUS Statistical Report: Primary brain and other central nervous system tumors diagnosed in the United States in 2010–2014. Neuro-Oncol. *19*, v1–v88.

Ouyang, L., Shi, Z., Zhao, S., Wang, F. -T., Zhou, T. -T., Liu, B., and Bao, J. -K. (2012). Programmed cell death pathways in cancer: a review of apoptosis, autophagy and programmed necrosis. Cell Prolif. *45*, 487–498.

Pan, R., Ruvolo, V., Mu, H., Leverson, J.D., Nichols, G., Reed, J.C., Konopleva, M., and Andreeff, M. (2017). Synthetic Lethality of Combined Bcl-2 Inhibition and p53 Activation in AML: Mechanisms and Superior Antileukemic Efficacy. Cancer Cell *32*, 748-760.e6.

Paolillo, M., and Schinelli, S. (2017). Integrins and Exosomes, a Dangerous Liaison in Cancer Progression. Cancers *9*.

Park, C.-K., Kim, J.E., Kim, J.Y., Song, S.W., Kim, J.W., Choi, S.H., Kim, T.M., Lee, S.-H., Kim, I.H., and Park, S.-H. (2012). The Changes in MGMT Promoter Methylation Status in Initial and Recurrent Glioblastomas. Transl. Oncol. *5*, 393-IN19.

Parsons, D.W., Jones, S., Zhang, X., Lin, J.C.-H., Leary, R.J., Angenendt, P., Mankoo, P., Carter, H., Siu, I.-M., Gallia, G.L., et al. (2008). An Integrated Genomic Analysis of Human Glioblastoma Multiforme. Science *321*, 1807.

Patyka, M., Sharifi, Z., Petrecca, K., Mansure, J., Jean-Claude, B., and Sabri, S. (2016). Sensitivity to PRIMA-1^{MET} is associated with decreased MGMT in human glioblastoma cells and glioblastoma stem cells irrespective of p53 status. Oncotarget *7*.

Pawlowska, E., Szczepanska, J., Szatkowska, M., and Blasiak, J. (2018). An Interplay between Senescence, Apoptosis and Autophagy in Glioblastoma Multiforme-Role in Pathogenesis and Therapeutic Perspective. Int. J. Mol. Sci. *19*.

Perry, J., Okamoto, M., Guiou, M., Shirai, K., Errett, A., and Chakravarti, A. (2012). Novel Therapies in Glioblastoma. Neurol. Res. Int. *2012*.

Petitjean, A., Achatz, M.I.W., Borresen-Dale, A.L., Hainaut, P., and Olivier, M. (2007). TP53 mutations in human cancers: functional selection and impact on cancer prognosis and outcomes. Oncogene *26*, 2157–2165.

Pichlmeier, U., Bink, A., Schackert, G., and Stummer, W. (2008). Resection and survival in glioblastoma multiforme: An RTOG recursive partitioning analysis of ALA study patients. Neuro-Oncol. *10*, 1025–1034.

Pierschbacher, M.D., and Ruoslahti, E. (1984). Cell attachment activity of fibronectin can be duplicated by small synthetic fragments of the molecule. Nature *309*, 30–33.

Pietrzak, M., and Puzianowska-Kuznicka, M. (2008). p53-dependent repression of the human MCL-1 gene encoding an anti-apoptotic member of the BCL-2 family: the role of Sp1 and of basic transcription factor binding sites in the MCL-1 promoter. Biol. Chem. *389*, 383–393.

Pitolli, C., Wang, Y., Mancini, M., Shi, Y., Melino, G., and Amelio, I. (2019). Do Mutations Turn p53 into an Oncogene? Int. J. Mol. Sci. *20*, 6241.

Pitts, W.J., Wityak, J., Smallheer, J.M., Tobin, A.E., Jetter, J.W., Buynitsky, J.S., Harlow, P.P., Solomon, K.A., Corjay, M.H., Mousa, S.A., et al. (2000). Isoxazolines as potent antagonists of the integrin alpha(v)beta(3). J. Med. Chem. *43*, 27–40.

Playford, M.P., and Schaller, M.D. (2004). The interplay between Src and integrins in normal and tumor biology. Oncogene *23*, 7928–7946.

Poon, I.K.H., Lucas, C.D., Rossi, A.G., and Ravichandran, K.S. (2014). Apoptotic cell clearance: basic biology and therapeutic potential. Nat. Rev. Immunol. *14*, 166–180.

Rabé, M., Dumont, S., Álvarez-Arenas, A., Janati, H., Belmonte-Beitia, J., Calvo, G.F., Thibault-Carpentier, C., Séry, Q., Chauvin, C., Joalland, N., et al. (2020). Identification of a transient state during the acquisition of temozolomide resistance in glioblastoma. Cell Death Dis. *11*, 19.

Rajagopalan, S., Huang, F., and Fersht, A.R. (2011). Single-Molecule characterization of oligomerization kinetics and equilibria of the tumor suppressor p53. Nucleic Acids Res. *39*, 2294–2303.

Rajaraman, P., Melin, B.S., Wang, Z., McKean-Cowdin, R., Michaud, D., Wang, S.S., Bondy, M., Houlston, R., Jenkins, R.B., Wrensch, M., et al. (2012). Genome-wide Association Study of Glioma and Meta-Analysis. Hum. Genet. *131*, 1877–1888.

Ramakrishnan, V., Bhaskar, V., Law, D.A., Wong, M.H.L., DuBridge, R.B., Breinberg, D., O'Hara, C., Powers, D.B., Liu, G., Grove, J., et al. (2006). Preclinical evaluation of an anti-alpha5beta1 integrin antibody as a novel anti-angiogenic agent. J. Exp. Ther. Oncol. *5*, 273–286.

Ray, A.-M., Schaffner, F., Janouskova, H., Noulet, F., Rognan, D., Lelong-Rebel, I., Choulier, L., Blandin, A.-F., Lehmann, M., Martin, S., et al. (2014). Single cell tracking assay reveals an opposite effect of selective small non-peptidic α5β1 or αvβ3/β5 integrin antagonists in U87MG glioma cells. Biochim. Biophys. Acta *1840*, 2978–2987.

Reeves, K.J., Hurrell, J.E., Cecchini, M., van der Pluijm, G., Down, J.M., Eaton, C.L., Hamdy, F., Clement-Lacroix, P., and Brown, N.J. (2015). Prostate cancer cells home to bone using a novel in vivo model: modulation by the integrin antagonist GLPG0187. Int. J. Cancer *136*, 1731–1740.

Reifenberger, G., Liu, L., Ichimura, K., Schmidt, E.E., and Collins, V.P. (1993). Amplification and Overexpression of the MDM2 Gene in a Subset of Human Malignant Gliomas without p53 Mutations. 5.

Renner, G., Janouskova, H., Noulet, F., Koenig, V., Guerin, E., Bär, S., Nuesch, J., Rechenmacher, F., Neubauer, S., Kessler, H., et al. (2016a). Integrin α5β1 and p53 convergent pathways in the control of anti-apoptotic proteins PEA-15 and survivin in high-grade glioma. Cell Death Differ. *23*, 640–653.

Renner, G., Janouskova, H., Noulet, F., Koenig, V., Guerin, E., Bär, S., Nuesch, J., Rechenmacher, F., Neubauer, S., Kessler, H., et al. (2016b). Integrin α5β1 and p53 convergent pathways in the control of anti-apoptotic proteins PEA-15 and survivin in high-grade glioma. Cell Death Differ. *23*, 640–653.

Reyes, S.B., Narayanan, A.S., Lee, H.S., Tchaicha, J.H., Aldape, K.D., Lang, F.F., Tolias, K.F., and McCarty, J.H. (2013). αvβ8 integrin interacts with RhoGDI1 to regulate Rac1 and Cdc42 activation and drive glioblastoma cell invasion. Mol. Biol. Cell *24*, 474–482.

Ricart, A.D., Tolcher, A.W., Liu, G., Holen, K., Schwartz, G., Albertini, M., Weiss, G., Yazji, S., Ng, C., and Wilding, G. (2008). Volociximab, a chimeric monoclonal antibody that specifically binds alpha5beta1 integrin: a phase I, pharmacokinetic, and biological correlative study. Clin. Cancer Res. Off. J. Am. Assoc. Cancer Res. *14*, 7924–7929.

Riley, K.J.-L., and Maher, L.J. (2007). Analysis of p53-RNA Interactions in Cultured Human Cells. Biochem. Biophys. Res. Commun. *363*, 381–387.

Rodriguez, M.S., Desterro, J.M., Lain, S., Midgley, C.A., Lane, D.P., and Hay, R.T. (1999). SUMO-1 modification activates the transcriptional response of p53. EMBO J. *18*, 6455–6461.

Rodriguez, M.S., Desterro, J.M.P., Lain, S., Lane, D.P., and Hay, R.T. (2000). Multiple C-Terminal Lysine Residues Target p53 for Ubiquitin-Proteasome-Mediated Degradation. Mol. Cell. Biol. *20*, 8458–8467.

Rohle, D., Popovici-Muller, J., Palaskas, N., Turcan, S., Grommes, C., Campos, C., Tsoi, J., Clark, O., Oldrini, B., Komisopoulou, E., et al. (2013). An Inhibitor of Mutant IDH1 Delays Growth and Promotes Differentiation of Glioma Cells. Science *340*, 626–630.

Roth, J., Dobbelstein, M., Freedman, D.A., Shenk, T., and Levine, A.J. (1998). Nucleo-cytoplasmic shuttling of the hdm2 oncoprotein regulates the levels of the p53 protein via a pathway used by the human immunodeficiency virus rev protein. EMBO J. *17*, 554–564.

Roth, P., Silginer, M., Goodman, S.L., Hasenbach, K., Thies, S., Maurer, G., Schraml, P., Tabatabai, G., Moch, H., Tritschler, I., et al. (2013). Integrin control of the transforming growth factor-β pathway in glioblastoma. Brain J. Neurol. *136*, 564–576.

de Rozieres, S., Maya, R., Oren, M., and Lozano, G. (2000). The loss of mdm2 induces p53-mediated apoptosis. Oncogene *19*, 1691–1697.

Ruoslahti, E., and Pierschbacher, M.D. (1987). New perspectives in cell adhesion: RGD and integrins. Science *238*, 491–497.

Russo, M., and Russo, G.L. (2018). Autophagy inducers in cancer. Biochem. Pharmacol. *153*, 51–61.

RUSSO, M.A., PAOLILLO, M., SANCHEZ-HERNANDEZ, Y., CURTI, D., CIUSANI, E., SERRA, M., COLOMBO, L., and SCHINELLI, S. (2012). A small-molecule RGD-integrin antagonist inhibits cell adhesion, cell migration and induces anoikis in glioblastoma cells. Int. J. Oncol. *42*, 83–92.

Ryan, K.M., Ernst, M.K., Rice, N.R., and Vousden, K.H. (2000). Role of NF-kappaB in p53-mediated programmed cell death. Nature *404*, 892–897.

Ryan, K.M., Phillips, A.C., and Vousden, K.H. (2001). Regulation and function of the p53 tumor suppressor protein. Curr. Opin. Cell Biol. *13*, 332–337.

Safa, A.R., Saadatzadeh, M.R., Cohen-Gadol, A.A., Pollok, K.E., and Bijangi-Vishehsaraei, K. (2015). Glioblastoma stem cells (GSCs) epigenetic plasticity and interconversion between differentiated non-GSCs and GSCs. Genes Dis. *2*, 152–163.

Sakaguchi, K., Herrera, J.E., Saito, S., Miki, T., Bustin, M., Vassilev, A., Anderson, C.W., and Appella, E. (1998). DNA damage activates p53 through a phosphorylation-acetylation cascade. Genes Dev. *12*, 2831–2841.

Sanai, N., and Berger, M.S. (2008). Glioma extent of resection and its impact on patient outcome. Neurosurgery *62*, 753–764; discussion 264-266.

Sancar, A., Lindsey-Boltz, L.A., Unsal-Kaçmaz, K., and Linn, S. (2004). Molecular mechanisms of mammalian DNA repair and the DNA damage checkpoints. Annu. Rev. Biochem. *73*, 39–85.

Sanchez, A.M.J., Csibi, A., Raibon, A., Cornille, K., Gay, S., Bernardi, H., and Candau, R. (2012). AMPK promotes skeletal muscle autophagy through activation of forkhead FoxO3a and interaction with Ulk1. J. Cell. Biochem. *113*, 695–710.

Sax, J.K., Fei, P., Murphy, M.E., Bernhard, E., Korsmeyer, S.J., and El-Deiry, W.S. (2002). BID regulation by p53 contributes to chemosensitivity. Nat. Cell Biol. *4*, 842–849.

Sayyah, J., Bartakova, A., Nogal, N., Quilliam, L.A., Stupack, D.G., and Brown, J.H. (2014). The Ras-related Protein, Rap1A, Mediates Thrombin-stimulated, Integrin-dependent Glioblastoma Cell Proliferation and Tumor Growth. J. Biol. Chem. *289*, 17689–17698.

Scaringi, C., Minniti, G., Caporello, P., and Enrici, R.M. (2012). Integrin inhibitor cilengitide for the treatment of glioblastoma: a brief overview of current clinical results. Anticancer Res. *32*, 4213–4223.

Schaller, M.D., Hildebrand, J.D., Shannon, J.D., Fox, J.W., Vines, R.R., and Parsons, J.T. (1994). Autophosphorylation of the focal adhesion kinase, pp125FAK, directs SH2-dependent binding of pp60src. Mol. Cell. Biol. *14*, 1680–1688.

Schittenhelm, J., Schwab, E.I., Sperveslage, J., Tatagiba, M., Meyermann, R., Fend, F., Goodman, S.L., and Sipos, B. (2013). Longitudinal expression analysis of αv integrins in human gliomas reveals upregulation of integrin αvβ3 as a negative prognostic factor. J. Neuropathol. Exp. Neurol. *72*, 194–210.

Schmale, H., and Bamberger, C. (1997). A novel protein with strong homology to the tumor suppressor p53. Oncogene *15*, 1363–1367.

Schnell, O., Romagna, A., Jaehnert, I., Albrecht, V., Eigenbrod, S., Juerchott, K., Kretzschmar, H., Tonn, J.-C., and Schichor, C. (2012). Krüppel-like factor 8 (KLF8) is expressed in gliomas of different WHO grades and is essential for tumor cell proliferation. PloS One *7*, e30429.

Schumacher, T., Bunse, L., Pusch, S., Sahm, F., Wiestler, B., Quandt, J., Menn, O., Osswald, M., Oezen, I., Ott, M., et al. (2014). A vaccine targeting mutant IDH1 induces antitumour immunity. Nature *512*, 324–327.

Sciuscio, D., Diserens, A.-C., van Dommelen, K., Martinet, D., Jones, G., Janzer, R.-C., Pollo, C., Hamou, M.-F., Kaina, B., Stupp, R., et al. (2011). Extent and patterns of MGMT promoter methylation in glioblastoma- and respective glioblastoma-derived spheres. Clin. Cancer Res. Off. J. Am. Assoc. Cancer Res. *17*, 255–266.

Scott, J., Tsai, Y.-Y., Chinnaiyan, P., and Yu, H.-H.M. (2011). Effectiveness of radiotherapy for elderly patients with glioblastoma. Int. J. Radiat. Oncol. Biol. Phys. *81*, 206–210.

Sedelnikova, O.A., Horikawa, I., Zimonjic, D.B., Popescu, N.C., Bonner, W.M., and Barrett, J.C. (2004). Senescing human cells and ageing mice accumulate DNA lesions with unrepairable double-strand breaks. Nat. Cell Biol. *6*, 168–170.

Sengupta, S., Vonesch, J.-L., Waltzinger, C., Zheng, H., and Wasylyk, B. (2000). Negative cross-talk between p53 and the glucocorticoid receptor and its role in neuroblastoma cells. EMBO J. *19*, 6051–6064.

Serres, E., Debarbieux, F., Stanchi, F., Maggiorella, L., Grall, D., Turchi, L., Burel-Vandenbos, F., Figarella-Branger, D., Virolle, T., Rougon, G., et al. (2014). Fibronectin expression in glioblastomas promotes cell cohesion, collective invasion of basement membrane in vitro and orthotopic tumor growth in mice. Oncogene *33*, 3451–3462.

Shamma, A., Takegami, Y., Miki, T., Kitajima, S., Noda, M., Obara, T., Okamoto, T., and Takahashi, C. (2009). Rb Regulates DNA damage response and cellular senescence through E2F-dependent suppression of N-ras isoprenylation. Cancer Cell *15*, 255–269.

Shangary, S., and Wang, S. (2009). Small-Molecule Inhibitors of the MDM2-p53 Protein-Protein Interaction to Reactivate p53 Function: A Novel Approach for Cancer Therapy. Annu. Rev. Pharmacol. Toxicol. *49*, 223–241.

Shattil, S.J., Kim, C., and Ginsberg, M.H. (2010). The final steps of integrin activation: the end game. Nat. Rev. Mol. Cell Biol. *11*, 288–300.

Shchors, K., Persson, A.I., Rostker, F., Tihan, T., Lyubynska, N., Li, N., Swigart, L.B., Berger, M.S., Hanahan, D., Weiss, W.A., et al. (2013). Using a preclinical mouse model of high-grade astrocytoma to optimize p53 restoration therapy. Proc. Natl. Acad. Sci. U. S. A. *110*, E1480–E1489.

Shi, L., Chen, J., Yang, J., Pan, T., Zhang, S., and Wang, Z. (2010). MiR-21 protected human glioblastoma U87MG cells from chemotherapeutic drug temozolomide induced apoptosis by decreasing Bax/Bcl-2 ratio and caspase-3 activity. Brain Res. *1352*, 255–264.

Shieh, S.-Y., Ahn, J., Tamai, K., Taya, Y., and Prives, C. (2000). The human homologs of checkpoint kinases Chk1 and Cds1 (Chk2) phosphorylate p53 at multiple DNA damage-inducible sites. Genes Dev. *14*, 289–300.

Shikama, N., Lee, C.W., France, S., Delavaine, L., Lyon, J., Krstic-Demonacos, M., and La Thangue, N.B. (1999). A novel cofactor for p300 that regulates the p53 response. Mol. Cell *4*, 365–376.

Siebzehnrubl, F.A., Silver, D.J., Tugertimur, B., Deleyrolle, L.P., Siebzehnrubl, D., Sarkisian, M.R., Devers, K.G., Yachnis, A.T., Kupper, M.D., Neal, D., et al. (2013). The ZEB1 pathway links glioblastoma initiation, invasion and chemoresistance. EMBO Mol. Med. *5*, 1196–1212.

Silber, J.R., Bobola, M.S., Blank, A., and Chamberlain, M.C. (2012). O6-methylguanine-DNA methyltransferase in glioma therapy: Promise and problems. Biochim. Biophys. Acta *1826*, 71–82.

Silginer, M., Weller, M., Ziegler, U., and Roth, P. (2014). Integrin inhibition promotes atypical anoikis in glioma cells. Cell Death Dis. *5*, e1012.

Silginer, M., Burghardt, I., Gramatzki, D., Bunse, L., Leske, H., Rushing, E.J., Hao, N., Platten, M., Weller, M., and Roth, P. (2016). The aryl hydrocarbon receptor links integrin signaling to the TGF-β pathway. Oncogene *35*, 3260–3271.

Skuli, N., Monferran, S., Delmas, C., Favre, G., Bonnet, J., Toulas, C., and Cohen-Jonathan Moyal, E. (2009). Alphavbeta3/alphavbeta5 integrins-FAK-RhoB: a novel pathway for hypoxia regulation in glioblastoma. Cancer Res. *69*, 3308–3316.

Slee, E.A., O'Connor, D.J., and Lu, X. (2004). To die or not to die: how does p53 decide? Oncogene *23*, 2809–2818.

Smallheer, J.M., Weigelt, C.A., Woerner, F.J., Wells, J.S., Daneker, W.F., Mousa, S.A., Wexler, R.R., and Jadhav, P.K. (2004). Synthesis and biological evaluation of nonpeptide integrin antagonists containing spirocyclic scaffolds. Bioorg. Med. Chem. Lett. *14*, 383–387.

Song, D., Zhao, J., Su, C., Jiang, Y., and Hou, J. (2018). Etoposide induced NMI promotes cell apoptosis by activating the ARF-p53 signaling pathway in lung carcinoma. Biochem. Biophys. Res. Commun. *495*, 368–374.

Stambolic, V., MacPherson, D., Sas, D., Lin, Y., Snow, B., Jang, Y., Benchimol, S., and Mak, T.W. (2001). Regulation of PTEN transcription by p53. Mol. Cell *8*, 317–325.

St-Coeur, P.-D., Poitras, J.J., Cuperlovic-Culf, M., Touaibia, M., and Morin, P. (2015). Investigating a signature of temozolomide resistance in GBM cell lines using metabolomics. J. Neurooncol. *125*, 91–102.

Stoeltzing, O., Liu, W., Reinmuth, N., Fan, F., Parry, G.C., Parikh, A.A., McCarty, M.F., Bucana, C.D., Mazar, A.P., and Ellis, L.M. (2003). Inhibition of integrin alpha5beta1 function with a small peptide (ATN-161) plus continuous 5-FU infusion reduces colorectal liver metastases and improves survival in mice. Int. J. Cancer *104*, 496–503.

Strobel, H., Baisch, T., Fitzel, R., Schilberg, K., Siegelin, M.D., Karpel-Massler, G., Debatin, K.-M., and Westhoff, M.-A. (2019). Temozolomide and Other Alkylating Agents in Glioblastoma Therapy. Biomedicines *7*, 69.

Stupp, R., Mason, W.P., van den Bent, M.J., Weller, M., Fisher, B., Taphoorn, M.J.B., Belanger, K., Brandes, A.A., Marosi, C., Bogdahn, U., et al. (2005a). Radiotherapy plus concomitant and adjuvant temozolomide for glioblastoma. N. Engl. J. Med. *352*, 987–996.

Stupp, R., Weller, M., Belanger, K., Bogdahn, U., Ludwin, S.K., Lacombe, D., and Mirimanoff, R.O. (2005b). Radiotherapy plus Concomitant and Adjuvant Temozolomide for Glioblastoma. N. Engl. J. Med. 10.

Stupp, R., Hegi, M.E., and Mason, W.P. (2009). Effects of radiotherapy with concomitant and adjuvant temozolomide versus radiotherapy alone on survival in glioblastoma in a randomised phase III study: 5-year analysis of the EORTC-NCIC trial. *10*, 8.

Stupp, R., Hegi, M.E., Neyns, B., Goldbrunner, R., Schlegel, U., Clement, P.M.J., Grabenbauer, G.G., Ochsenbein, A.F., Simon, M., Dietrich, P.-Y., et al. (2010). Phase I/IIa study of cilengitide and temozolomide with concomitant radiotherapy followed by cilengitide and temozolomide maintenance therapy in patients with newly diagnosed glioblastoma. J. Clin. Oncol. Off. J. Am. Soc. Clin. Oncol. *28*, 2712–2718.

Stupp, R., Hegi, M.E., Gorlia, T., Erridge, S.C., Perry, J., Hong, Y.-K., Aldape, K.D., Lhermitte, B., Pietsch, T., Grujicic, D., et al. (2014a). Cilengitide combined with standard treatment for patients with newly diagnosed glioblastoma with methylated MGMT promoter (CENTRIC EORTC 26071-22072 study): a multicentre, randomised, open-label, phase 3 trial. Lancet Oncol. *15*, 1100–1108.

Stupp, R., Hegi, M.E., Gorlia, T., Erridge, S.C., Perry, J., Hong, Y.-K., Aldape, K.D., Lhermitte, B., Pietsch, T., Grujicic, D., et al. (2014b). Cilengitide combined with standard treatment for patients with newly diagnosed glioblastoma with methylated MGMT promoter (CENTRIC EORTC 26071-22072 study): a multicentre, randomised, open-label, phase 3 trial. Lancet Oncol. *15*, 1100–1108.

Sui, X., Chen, R., Wang, Z., Huang, Z., Kong, N., Zhang, M., Han, W., Lou, F., Yang, J., Zhang, Q., et al. (2013). Autophagy and chemotherapy resistance: a promising therapeutic target for cancer treatment. Cell Death Dis. *4*, e838.

Sumihito, N., Joel, L., Anne, W., Young Ho, K., Jian, H., Catherine, L., Paul, K., and Hiroko, O. (2010). Intratumoral patterns of genomic imbalance in glioblastoma. Brain Pathol.

Taga, T., Suzuki, A., Gonzalez-Gomez, I., Gilles, F.H., Stins, M., Shimada, H., Barsky, L., Weinberg, K.I., and Laug, W.E. (2002). alpha v-Integrin antagonist EMD 121974 induces apoptosis in brain tumor cells growing on vitronectin and tenascin. Int. J. Cancer *98*, 690–697.

Takada, Y., Ye, X., and Simon, S. (2007). The integrins. Genome Biol. *8*, 215.

Takekawa, M., Adachi, M., Nakahata, A., Nakayama, I., Itoh, F., Tsukuda, H., Taya, Y., and Imai, K. (2000). p53-inducible wip1 phosphatase mediates a negative feedback regulation of p38 MAPK-p53 signaling in response to UV radiation. EMBO J. *19*, 6517–6526.

Tal, P., Eizenberger, S., Cohen, E., Goldfinger, N., Pietrokovski, S., Oren, M., and Rotter, V. (2016). Cancer therapeutic approach based on conformational stabilization of mutant p53 protein by small peptides. Oncotarget *7*.

Tamkun, J.W., DeSimone, D.W., Fonda, D., Patel, R.S., Buck, C., Horwitz, A.F., and Hynes, R.O. (1986). Structure of integrin, a glycoprotein involved in the transmembrane linkage between fibronectin and actin. Cell *46*, 271–282.

Tanaka, M., Koul, D., Davies, M.A., Liebert, M., Steck, P.A., and Grossman, H.B. (2000). MMAC1/PTEN inhibits cell growth and induces chemosensitivity to doxorubicin in human bladder cancer cells. Oncogene *19*, 5406–5412.

Tchaicha, J.H., Reyes, S.B., Shin, J., Hossain, M.G., Lang, F.F., and McCarty, J.H. (2011). Glioblastoma angiogenesis and tumor cell invasiveness are differentially regulated by β8 integrin. Cancer Res. *71*, 6371–6381.

Thorburn, A., Thamm, D.H., and Gustafson, D.L. (2014). Autophagy and cancer therapy. Mol. Pharmacol. *85*, 830–838.

Tivnan, A., Zakaria, Z., O'Leary, C., Kögel, D., Pokorny, J.L., Sarkaria, J.N., and Prehn, J.H.M. (2015). Inhibition of multidrug resistance protein 1 (MRP1) improves chemotherapy drug response in primary and recurrent glioblastoma multiforme. Front. Neurosci. *9*, 218.

Tome, Y., Kimura, H., Kiyuna, T., Sugimoto, N., Tsuchiya, H., Kanaya, F., Bouvet, M., and Hoffman, R.M. (2016a). Disintegrin targeting of an αvβ3 integrin-over-expressing high-metastatic human osteosarcoma with echistatin inhibits cell proliferation, migration, invasion and adhesion in vitro. Oncotarget *7*, 46315–46320.

Tome, Y., Kimura, H., Sugimoto, N., Tsuchiya, H., Kanaya, F., Bouvet, M., and Hoffman, R.M. (2016b). The disintegrin echistatin in combination with doxorubicin targets high-metastatic human osteosarcoma overexpressing αvβ3 integrin in chick embryo and nude mouse models. Oncotarget *7*, 87031–87036.

Tournillon, A.-S., López, I., Malbert-Colas, L., Findakly, S., Naski, N., Olivares-Illana, V., Karakostis, K., Vojtesek, B., Nylander, K., and Fåhraeus, R. (2017). p53 binds the mdmx mRNA and controls its translation. Oncogene *36*, 723–730.

Tovar, C., Graves, B., Packman, K., Filipovic, Z., Xia, B.H.M., Tardell, C., Garrido, R., Lee, E., Kolinsky, K., To, K.-H., et al. (2013). MDM2 Small-Molecule Antagonist RG7112 Activates p53 Signaling and Regresses Human Tumors in Preclinical Cancer Models. Cancer Res. *73*, 2587–2597.

Trikha, M., Zhou, Z., Nemeth, J.A., Chen, Q., Sharp, C., Emmell, E., Giles-Komar, J., and Nakada, M.T. (2004). CNTO 95, a fully human monoclonal antibody that inhibits alphav integrins, has antitumor and antiangiogenic activity in vivo. Int. J. Cancer *110*, 326–335.

Tsai, Y.-T., Wu, A.-C., Yang, W.-B., Kao, T.-J., Chuang, J.-Y., Chang, W.-C., and Hsu, T.-I. (2019). ANGPTL4 Induces TMZ Resistance of Glioblastoma by Promoting Cancer Stemness Enrichment via the EGFR/AKT/4E-BP1 Cascade. Int. J. Mol. Sci. *20*.

Tsang, L.L., Farmer, P.B., Gescher, A., and Slack, J.A. (1990). Characterisation of urinary metabolites of temozolomide in humans and mice and evaluation of their cytotoxicity. Cancer Chemother. Pharmacol. *26*, 429–436.

Tubbs, J.L., Pegg, A.E., and Tainer, J.A. (2007). DNA binding, nucleotide flipping, and the helix-turn-helix motif in base repair by O6-alkylguanine-DNA alkyltransferase and its implications for cancer chemotherapy. DNA Repair *6*, 1100–1115.

Tucci, M., Stucci, S., and Silvestris, F. (2014). Does cilengitide deserve another chance? Lancet Oncol. *15*, e584–e585.

Uchida, N., Buck, D.W., He, D., Reitsma, M.J., Masek, M., Phan, T.V., Tsukamoto, A.S., Gage, F.H., and Weissman, I.L. (2000). Direct isolation of human central nervous system stem cells. Proc. Natl. Acad. Sci. U. S. A. *97*, 14720–14725.

Ueno, H., Tomiyama, A., Yamaguchi, H., Uekita, T., Shirakihara, T., Nakashima, K., Otani, N., Wada, K., Sakai, R., Arai, H., et al. (2015). Augmentation of invadopodia formation in temozolomide-resistant or adopted glioma is regulated by c-Jun terminal kinase-paxillin axis. Biochem. Biophys. Res. Commun. *468*, 240–247.

Ujifuku, K., Mitsutake, N., Takakura, S., Matsuse, M., Saenko, V., Suzuki, K., Hayashi, K., Matsuo, T., Kamada, K., Nagata, I., et al. (2010). miR-195, miR-455-3p and miR-10a∗ are implicated in acquired temozolomide resistance in glioblastoma multiforme cells. Cancer Lett. *296*, 241–248.

Van Meir, E.G., Hadjipanayis, C.G., Norden, A.D., Shu, H.-K., Wen, P.Y., and Olson, J.J. (2010). Exciting new advances in neuro-oncology: the avenue to a cure for malignant glioma. CA. Cancer J. Clin. *60*, 166–193.

Vassilev, L.T. (2004). In Vivo Activation of the p53 Pathway by Small-Molecule Antagonists of MDM2. Science *303*, 844–848.

Vehlow, A., Klapproth, E., Storch, K., Dickreuter, E., Seifert, M., Dietrich, A., Bütof, R., Temme, A., and Cordes, N. (2017). Adhesion- and stress-related adaptation of glioma radiochemoresistance is circumvented by β1 integrin/JNK co-targeting. Oncotarget *8*, 49224–49237.

Velpula, K.K., Rehman, A.A., Chelluboina, B., Dasari, V.R., Gondi, C.S., Rao, J.S., and Veeravalli, K.K. (2012). Glioma stem cell invasion through regulation of the interconnected ERK, integrin α6 and N-cadherin signaling pathway. Cell. Signal. *24*, 2076–2084.

Verhaak, R.G.W., Hoadley, K.A., Purdom, E., Wang, V., Qi, Y., Wilkerson, M.D., Miller, C.R., Ding, L., Golub, T., Mesirov, J.P., et al. (2010). Integrated Genomic Analysis Identifies

Clinically Relevant Subtypes of Glioblastoma Characterized by Abnormalities in PDGFRA, IDH1, EGFR, and NF1. Cancer Cell *17*, 98–110.

Verreault, M., Schmitt, C., Goldwirt, L., Pelton, K., Haidar, S., Levasseur, C., Guehennec, J., Knoff, D., Labussiere, M., Marie, Y., et al. (2016). Preclinical Efficacy of the MDM2 Inhibitor RG7112 in MDM2-Amplified and TP53 Wild-type Glioblastomas. Clin. Cancer Res. *22*, 1185–1196.

Visvader, J.E. (2011). Cells of origin in cancer. Nature *469*, 314–322.

Vogelstein, B., Lane, D., and Levine, A.J. (2000). Surfing the p53 network. Nature *408*, 307–310.

Vousden, K.H., and Lu, X. (2002). Live or let die: the cell's response to p53. Nat. Rev. Cancer *2*, 594–604.

Vousden, K.H., and Vande Woude, G.F. (2000). The ins and outs of p53. Nat. Cell Biol. *2*, E178-180.

Vu, B., Wovkulich, P., Pizzolato, G., Lovey, A., Ding, Q., Jiang, N., Liu, J.-J., Zhao, C., Glenn, K., Wen, Y., et al. (2013). Discovery of RG7112: A Small-Molecule MDM2 Inhibitor in Clinical Development. ACS Med. Chem. Lett. *4*, 466–469.

Wade, M., Li, Y.-C., and Wahl, G.M. (2013). MDM2, MDMX and p53 in oncogenesis and cancer therapy. Nat. Rev. Cancer *13*, 83–96.

Walsh, E.M., Kim, R., Del Valle, L., Weaver, M., Sheffield, J., Lazarovici, P., and Marcinkiewicz, C. (2012). Importance of interaction between nerve growth factor and α9β1 integrin in glial tumor angiogenesis. Neuro-Oncol. *14*, 890–901.

Wang, E. (1995). Senescent human fibroblasts resist programmed cell death, and failure to suppress bcl2 is involved. Cancer Res. *55*, 2284–2292.

Wang, J., Zhou, F., Li, Y., Li, Q., Wu, Z., Yu, L., Yuan, F., Liu, J., Tian, Y., Cao, Y., et al. (2017). Cdc20 overexpression is involved in temozolomide-resistant glioma cells with epithelial-mesenchymal transition. Cell Cycle Georget. Tex *16*, 2355–2365.

Wang, W., Wang, F., Lu, F., Xu, S., Hu, W., Huang, J., Gu, Q., and Sun, X. (2011). The antiangiogenic effects of integrin alpha5beta1 inhibitor (ATN-161) in vitro and in vivo. Invest. Ophthalmol. Vis. Sci. *52*, 7213–7220.

Wang, Z., Gao, J., Zhou, J., Liu, H., and Xu, C. (2019). Olaparib induced senescence under P16 or P53 dependent manner in ovarian cancer. J. Gynecol. Oncol. *30*, e26.

Weathers, S.-P., and Gilbert, M.R. (2015). Current challenges in designing GBM trials for immunotherapy. J. Neurooncol. *123*, 331–337.

Weilbacher, A., Gutekunst, M., Oren, M., Aulitzky, W.E., and van der Kuip, H. (2014). RITA can induce cell death in p53-defective cells independently of p53 function via activation of JNK/SAPK and p38. Cell Death Dis. *5*, e1318–e1318.

Weiner, L.M., Surana, R., and Wang, S. (2010). Antibodies and cancer therapy: versatile platforms for cancer immunotherapy. Nat. Rev. Immunol. *10*, 317–327.

Weissmueller, S., Manchado, E., Saborowski, M., Morris, J.P., Wagenblast, E., Davis, C.A., Moon, S.-H., Pfister, N.T., Tschaharganeh, D.F., Kitzing, T., et al. (2014). Mutant p53 Drives Pancreatic Cancer Metastasis through Cell-Autonomous PDGF Receptor β Signaling. Cell *157*, 382–394.

Weller, M., van den Bent, M., Hopkins, K., Tonn, J.C., Stupp, R., Falini, A., Cohen-Jonathan-Moyal, E., Frappaz, D., Henriksson, R., Balana, C., et al. (2014). EANO guideline for the diagnosis and treatment of anaplastic gliomas and glioblastoma. Lancet Oncol. *15*, e395-403.

Wen, Y.-T., Wu, A.T., Bamodu, O.A., Wei, L., Lin, C.-M., Yen, Y., Chao, T.-Y., Mukhopadhyay, D., Hsiao, M., and Huang, H.-S. (2019). A Novel Multi-Target Small Molecule, LCC-09, Inhibits Stemness and Therapy-Resistant Phenotypes of Glioblastoma Cells by Increasing miR-34a and Deregulating the DRD4/Akt/mTOR Signaling Axis. Cancers *11*.

Wickström, M., Dyberg, C., Milosevic, J., Einvik, C., Calero, R., Sveinbjörnsson, B., Sandén, E., Darabi, A., Siesjö, P., Kool, M., et al. (2015). Wnt/β-catenin pathway regulates MGMT gene expression in cancer and inhibition of Wnt signalling prevents chemoresistance. Nat. Commun. *6*.

Wilson, T., Karajannis, M., and Harter, D. (2014). Glioblastoma multiforme: State of the art and future therapeutics. Surg. Neurol. Int. *5*, 64.

Wood, R.D., Mitchell, M., and Lindahl, T. (2005). Human DNA repair genes, 2005. Mutat. Res. *577*, 275–283.

Woods, D.B., and Vousden, K.H. (2001). Regulation of p53 function. Exp. Cell Res. *264*, 56–66.

Wu, G.-J., Yang, S.-T., and Chen, R.-M. (2020). Major Contribution of Caspase-9 to Honokiol-Induced Apoptotic Insults to Human Drug-Resistant Glioblastoma Cells. Mol. Basel Switz. *25*.

Wu, L., Bernard-Trifilo, J.A., Lim, Y., Lim, S.-T., Mitra, S.K., Uryu, S., Chen, M., Pallen, C.J., Cheung, N.-K., Mikolon, D., et al. (2008). Distinct FAK-Src activation events promote alpha5beta1 and alpha4beta1 integrin-stimulated neuroblastoma cell motility. Oncogene *27*, 1439–1448.

Wu, Y., Mehew, J.W., Heckman, C.A., Arcinas, M., and Boxer, L.M. (2001). Negative regulation of bcl-2 expression by p53 in hematopoietic cells. Oncogene *20*, 240–251.

Xiong, J.-P., Mahalingham, B., Alonso, J.L., Borrelli, L.A., Rui, X., Anand, S., Hyman, B.T., Rysiok, T., Müller-Pompalla, D., Goodman, S.L., et al. (2009). Crystal structure of the complete integrin alphaVbeta3 ectodomain plus an alpha/beta transmembrane fragment. J. Cell Biol. *186*, 589–600.

Xu, J.-X., Yang, Y., Zhang, X., and Luan, X.-P. (2020). MicroRNA-29b promotes cell sensitivity to Temozolomide by targeting STAT3 in glioma. Eur. Rev. Med. Pharmacol. Sci. *24*, 1922–1931.

Xu, K., Zhang, Z., Pei, H., Wang, H., Li, L., and Xia, Q. (2017). FoxO3a induces temozolomide resistance in glioblastoma cells via the regulation of β-catenin nuclear accumulation. Oncol. Rep. *37*, 2391–2397.

Xu-Welliver, M., and Pegg, A.E. (2002). Degradation of the alkylated form of the DNA repair protein, O(6)-alkylguanine-DNA alkyltransferase. Carcinogenesis *23*, 823–830.

Yamada, K., and Yoshida, K. (2019). Mechanical insights into the regulation of programmed cell death by p53 via mitochondria. Biochim. Biophys. Acta Mol. Cell Res. *1866*, 839–848.

Yamada, R., and Nakano, I. (2012). Glioma stem cells: their role in chemoresistance. World Neurosurg. *77*, 237–240.

Yamashiro, K., Nakao, K., Ohba, S., and Hirose, Y. (2020). Human Glioma Cells Acquire Temozolomide Resistance After Repeated Drug Exposure Via DNA Mismatch Repair Dysfunction. Anticancer Res. *40*, 1315–1323.

Yang, J., Ma, Y.-Q., Page, R.C., Misra, S., Plow, E.F., and Qin, J. (2009). Structure of an integrin alphaIIb beta3 transmembrane-cytoplasmic heterocomplex provides insight into integrin activation. Proc. Natl. Acad. Sci. U. S. A. *106*, 17729–17734.

Yang, Y.-P., Chien, Y., Chiou, G.-Y., Cherng, J.-Y., Wang, M.-L., Lo, W.-L., Chang, Y.-L., Huang, P.-I., Chen, Y.-W., Shih, Y.-H., et al. (2012). Inhibition of cancer stem cell-like properties and reduced chemoradioresistance of glioblastoma using microRNA145 with cationic polyurethane-short branch PEI. Biomaterials *33*, 1462–1476.

Yi, G.-Z., Liu, Y.-W., Xiang, W., Wang, H., Chen, Z.-Y., Xie, S., and Qi, S.-T. (2016). Akt and β-catenin contribute to TMZ resistance and EMT of MGMT negative malignant glioma cell line. J. Neurol. Sci. *367*, 101–106.

Yi, G.-Z., Xiang, W., Feng, W.-Y., Chen, Z.-Y., Li, Y.-M., Deng, S.-Z., Guo, M.-L., Zhao, L., Sun, X.-G., He, M.-Y., et al. (2018). Identification of Key Candidate Proteins and Pathways Associated with Temozolomide Resistance in Glioblastoma Based on Subcellular Proteomics and Bioinformatical Analysis. BioMed Res. Int. *2018*, 5238760.

Yi, G.-Z., Huang, G., Guo, M., Zhang, X., Wang, H., Deng, S., Li, Y., Xiang, W., Chen, Z., Pan, J., et al. (2019). Acquired temozolomide resistance in MGMT-deficient glioblastoma cells is associated with regulation of DNA repair by DHC2. Brain J. Neurol. *142*, 2352–2366.

Yip, S., Miao, J., Cahill, D.P., Iafrate, A.J., Aldape, K., Nutt, C.L., and Louis, D.N. (2009). MSH6 Mutations Arise in Glioblastomas during Temozolomide Therapy and Mediate Temozolomide Resistance. Clin. Cancer Res. *15*, 4622–4629.

Youle, R.J., and Strasser, A. (2008). The BCL-2 protein family: opposing activities that mediate cell death. Nat. Rev. Mol. Cell Biol. *9*, 47–59.

Yu, G., and He, Q.-Y. (2016). ReactomePA: an R/Bioconductor package for reactome pathway analysis and visualization. Mol. Biosyst. *12*, 477–479.

Yu, G., Wu, F., and Wang, E. (2016). KLF8 Promotes Temozolomide Resistance in Glioma Cells via β-Catenin Activation. Cell. Physiol. Biochem. Int. J. Exp. Cell. Physiol. Biochem. Pharmacol. *38*, 1596–1604.

Yu, Z.K., Geyer, R.K., and Maki, C.G. (2000). MDM2-dependent ubiquitination of nuclear and cytoplasmic P53. Oncogene *19*, 5892–5897.

Yuan, A.L., Meode, M., Tan, M., Maxwell, L., Bering, E.A., Pedersen, H., Willms, J., Liao, J., Black, S., Cairncross, J.G., et al. (2020). PARP inhibition suppresses the emergence of temozolomide resistance in a model system. J. Neurooncol. *148*, 463–472.

Yuen, C.A., Asuthkar, S., Guda, M.R., Tsung, A.J., and Velpula, K.K. (2016). Cancer stem cell molecular reprogramming of the Warburg effect in glioblastomas: a new target gleaned from an old concept. CNS Oncol. *5*, 101–108.

Zache, N., Lambert, J.M.R., Wiman, K.G., and Bykov, V.J.N. (2008). PRIMA-1MET inhibits growth of mouse tumors carrying mutant p53. Anal. Cell. Pathol. 411–418.

Zeisberg, M., and Neilson, E.G. (2009). Biomarkers for epithelial-mesenchymal transitions. J. Clin. Invest. *119*, 1429–1437.

Zeng, H., Xu, N., Liu, Y., Liu, B., Yang, Z., Fu, Z., Lian, C., and Guo, H. (2017). Genomic profiling of long non-coding RNA and mRNA expression associated with acquired temozolomide resistance in glioblastoma cells. Int. J. Oncol. *51*, 445–455.

von Zglinicki, T. (2002). Oxidative stress shortens telomeres. Trends Biochem. Sci. *27*, 339–344.

Zhang, H., Wang, R., Yu, Y., Liu, J., Luo, T., and Fan, F. (2019). Glioblastoma Treatment Modalities besides Surgery. J. Cancer *10*, 4793–4806.

Zhang, J., Stevens, M.F.G., Laughton, C.A., Madhusudan, S., and Bradshaw, T.D. (2010). Acquired resistance to temozolomide in glioma cell lines: molecular mechanisms and potential translational applications. Oncology *78*, 103–114.

Zhang, J., Stevens, M.F.G., and Bradshaw, T.D. (2012). Temozolomide: Mechanisms of Action, Repair and Resistance. 13.

Zhang, Y., Dube, C., Gibert, M., Cruickshanks, N., Wang, B., Coughlan, M., Yang, Y., Setiady, I., Deveau, C., Saoud, K., et al. (2018). The p53 Pathway in Glioblastoma. Cancers *10*, 297.

Zheng, H., Ying, H., Yan, H., Kimmelman, A.C., Hiller, D.J., Chen, A.-J., Perry, S.R., Tonon, G., Chu, G.C., Ding, Z., et al. (2008). p53 and Pten control neural and glioma stem/progenitor cell renewal and differentiation. Nature *455*, 1129–1133.

Zhou, P., Erfani, S., Liu, Z., Jia, C., Chen, Y., Xu, B., Deng, X., Alfáro, J.E., Chen, L., Napier, D., et al. (2015). CD151-α3β1 integrin complexes are prognostic markers of glioblastoma and cooperate with EGFR to drive tumor cell motility and invasion. Oncotarget *6*, 29675–29693.

Zhu, W.-G. (2017). Regulation of p53 acetylation. Sci. China Life Sci. *60*, 321–323.

Zou, Y., Wang, Q., Li, B., Xie, B., and Wang, W. (2014). Temozolomide induces autophagy via ATM-AMPK-ULK1 pathways in glioma. Mol. Med. Rep. *10*, 411–416.

Zouaoui, S., Rigau, V., Mathieu-Daudé, H., Darlix, A., Bessaoud, F., Fabbro-Peray, P., Bauchet, F., Kerr, C., Fabbro, M., Figarella-Branger, D., et al. (2012). [French brain tumor

database: general results on 40,000 cases, main current applications and future prospects]. Neurochirurgie. *58*, 4–13.

Zutter, M.M. (2007). Integrin-mediated adhesion: tipping the balance between chemosensitivity and chemoresistance. Adv. Exp. Med. Biol. *608*, 87–100.